Effect of Backbone Structure on Membrane Properties of Poly(arylene ether) Random and Multiblock Copolymers

By

Jarrett Robert Rowlett

Dissertation submitted to the Faculty of Virginia Polytechnic Institute and State University in partial fulfillment of the requirements for the degree of

DOCTOR OF PHILOSOPHY

In

Macromolecular Science and Engineering

James E. McGrath, Chair
Judy S. Riffle, Co-Chair
S. Richard Turner
Donald G. Baird
Sue J. Mecham
John Matson

September 3, 2014

Blacksburg, VA

Keywords: Poly(arylene ether), membrane, multiblock copolymer, structure-property relationship

Effect of Backbone Structure on Membrane Properties of Poly(arylene ether) Random and Multiblock Copolymers

Jarrett Robert Rowlett

Abstract

Poly(arylene ether)s are a well-established class of thermoplastics that are known for their mechanical toughness, thermal stability, and fabrication into membranes. These materials can undergo a myriad of modifications including backbone structure variability, sulfonation, and crosslinking. In this dissertation, structure-property relationships are considered for poly(arylene ether)s with regard to membrane applications for proton exchange and gas separation membranes.

All of the proton exchange membranes in this dissertation focus on a disulfonated poly(arylene ether sulfone) based hydrophilic structure to produce hydrophilic-hydrophobic multiblock copolymers. The hydrophobic segments were based upon poly(arylene ether benzonitrile) polymers and copolymers. The oligomers were synthesized and isolated separately, then reacted under mild conditions to form the alternating multiblock copolymers. Structure-property relationships were considered for two different proton exchange membrane applications. One multiblock copolymer system was for H_2/air fuel cells, and the other for direct methanol fuel cells (DMFCs). The H_2/air fuel cells operate under harsh conditions and varying levels of relative humidity, while the DMFCs operate in an aqueous environment with a methanol-water mixture (typically 0.5-1 M MeOH). Thus two different approaches were taken for the multiblock copolymers. All of the multiblock copolymers were cast into membranes and after annealing resulted in drastically reduced water uptake as compared to random and non-

annealed systems. The membranes were characterized with regard to composition, mechanical properties, morphology, water uptake, proton conductivity, and molecular weight. Membranes were also sent to collaborators to elicit the fuel cell performance of the proton exchange membranes.

In H_2/air fuel cells the approach was to increase charge density by bisphenol choice in the hydrophilic phase. This was performed by switching to a lower molecular weight monomer, hydroquinone, and a monosulfonated hydroquinone. This produced higher charge density in the hydrophilic phase, and the corresponding multiblock copolymer. With increased hydrophilicity the multiblock copolymers showed increased phase separation, proton conductivity, and better performance under relative humidity testing. In the second system for DMFCs, the primary goal was to reduce methanol permeability by bisphenol selection in the hydrophobic phase. This was done with by replacing fifty mole percent of the fluorinated monomer with a series of increasing hydrophobicity bisphenols. Addition of benzylic methyl groups on the bisphenols, was the method undertaken to increase the hydrophobicity. The combination of reduced fluorine content along with the addition of methyl groups resulted in multiblock copolymers with extremely low water uptake and methanol permeability. This allowed for a PEM with better performance than Nafion® in 1M MeOH in DMFC testing.

The gas separation membranes presented in this dissertation are based upon poly(arylene ether ketone)s. Two systems were presented: one with a polymer directly synthesized with a bisphenol containing benzylic methyl groups and 4,4'-difluorobenzophenone, and the other a difunctional poly(phenylene oxide) oligomer polymerized with 4,4'-difluorobenzophenone. These systems were crosslinked via UV light through excitation of the ketone group to the triplet state and then hydrogen abstraction from the benzylic methyl. Confirmation of crosslinking was

performed via differential scanning calorimetry and infrared spectroscopy. Changes in the glass transitions between crosslinked and non-crosslinked materials were characterized with respect to the concentration of ketones to elicit the effects of crosslink density on the polymers and copolymers. Gas transport properties showed a strong dependence on the ketone percentage as the selectivity was much higher for the homopolymer, while the permeability was higher for the PPO copolymer in the CO_2/CH_4 and O_2/N_2 gas pairs.

Acknowledgments

I would like to express my greatest gratitude to my late advisor Dr. James E. McGrath for all of the continuous support, help, guidance, and opportunities he provided along my graduate student career. The experience and knowledge I gained under his tutelage is invaluable and I will carry it with myself pridefully. It was an honor to be one of his last graduate students. I would also like to especially thank Dr. Riffle who helped oversee my transition and the finishing of my PhD after the unfortunate passing of Dr. McGrath. Furthermore, I would like to thank my current and former committee members, Dr. Sue J. Mecham, Dr. John Matson, Dr. Richard Turner, Dr. Donald G. Baird, and Dr. Webster Santos who have been invaluable and continually giving in their advice and support.

My seamless experience in graduate school would also not have been possible without the tireless work of the administrative assistants in the Macromolecules and Interfaces Institute. Most specifically I want to thank Laurie Good, Cyndy Graham, and Tammy Jo Hiner for their help in scheduling, organizing, and navigating the academic requirements for my PhD. And of course I need to thank Yu Chen, Benjamin Sundell, and my fellow lab members who provided countless discussions and helpful advice for further direction and problem solving in my research. For mechanical testing, thermal analysis, proton conduction, and many other membrane characterization measurements I owe my thanks to Andrew Shaver. I am also grateful to Ozma Lane for TEM and AFM imaging, Mingqiang Zhang and Gregory Fahs from Dr. Moore's group for providing SAXS analysis, and Mark Flynn for SEC testing. I am also very grateful for the many outside collaborators in my dissertation research, which include Dr. Freeman's group from the University of Texas, Giner Inc., and Los Alamos National Laboratory. Without their help and

collaboration in these projects many of the results in this dissertation would not have been possible.

Lastly I want to thank my friends and family who have never wavered in their encouragement and enthusiasm. You may never know how important you have been to my success and motivation. To my mother and father who have provided any assistance without question and always been there during the ups and down I cannot thank you enough. I would have never accomplished any of this without all of your support.

Table of Contents

List of Figures

List of Tables

Attributions

Chapter 2:

Yu Chen: This coauthor is from Virginia Tech in the department of Macromolecular Science and Engineering. Yu Chen helped in the development of the outline of the research project. Additionally, he provided help in the preparation and the synthesis of the polymers presented in chapter 2.

Andrew Shaver: This coauthor is from Virginia Tech in the department of Macromolecular Science and Engineering. Andrew preformed the conductivity experiments which are shown in Table 2.1 and the conductivities as a function of relative humidity that are shown in Figures 2.11 -2.13. Additionally, Andrew performed the mechanical testing which is shown in Figure 2.8.

Ozma Lane: This coauthor is from the Virginia Tech in the department of Macromolecular Science and Engineering. Ozma coauthor preformed the imaging of the polymers shown in this chapter. These images are shown in Figure 2.10 of Chapter 2.

Hui Xu: This coauthor is from Giner Incorporated. Hui and Giner Incorporated assembled the membrane electrode assembly of the membranes shown in Chapter 2. Also Hui and Giner oversaw the fuel cell testing of the membranes shown in Figure 2.14.

Cortney Mittelsteadt: This coauthor is from Giner Incorporated. Cortney oversaw the project at Giner Incorporated which included the formation of the MEA and the single cell testing

Mingqiang Zhang: This coauthor is in the Chemistry department at Virginia Tech. Mingqinag preformed the SAXS experiments which the results of are shown in Figure 2.9. Also the coauthor helped to write a portion of SAXS section 2.3.4.

Robert Moore: This coauthor is a professor in the Chemistry department at Virginia Tech. Dr. Moore was the advisor of Mingqiang and oversaw the SAXS experiments.

Sue Mecham: This coauthor is from Virginia Tech in the department of Macromolecular Science and Engineering. Sue oversaw and ran the SEC experiments of the polymers presented in Chapter 2. The molecular weights obtained from those experiments are shown in Table 2.1.

James McGrath: This coauthor is a professor in the Chemistry department at Virginia Tech. Dr. McGrath was the author's advisor and oversaw the project.

Chapter 3:

Yu Chen: This coauthor is from Virginia Tech in the department of Macromolecular Science and Engineering. Yu Chen helped in the development of the outline of the research project. Additionally, he provided help in the preparation and the synthesis of the polymers presented in chapter 3.

Andrew Shaver: This coauthor is from Virginia Tech in the department of Macromolecular Science and Engineering. Andrew preformed the DSC experiments of the polymers shown in Figure 3.6 and the proton conductivities of the membranes shown in Table 3.1 of Chapter 3.

Gregory Fahs: This coauthor is in the Chemistry department at Virginia Tech. Gregory preformed the SAXS experiments which the results of are shown in Figure 3.8. Also Gregory preformed the calculations for the data presented in Table 3.3 and the coauthor helped to write a portion of SAXS section 3.3.3.

Robert Moore: This coauthor is a professor in the Chemistry department at Virginia Tech. Dr. Moore was the advisor of Gregory and oversaw the SAXS experiments.

Benjamin Sundell: This coauthor is from Virginia Tech in the department of Macromolecular Science and Engineering. Benjamin provided help in the preparation and the synthesis of the polymers presented in chapter 3.

Qing Li: This coauthor is from Los Alamos National Laboratory. Qing assembled the MEAs of the membranes presented in Chapter 3 along with the testing of the membranes. This testing included the methanol permeability shown in Table 3.1 and all of the values shown in Table 3.2. The polarization curves shown in Figure 3.9 were also performed by the coauthor.

Yu Sueng Kim: This coauthor is from Los Alamos National Laboratory and was the primary contact for the collaborative project between Los Alamos and Virginia Tech. Yu Sueng designed and oversaw the experiments performed by Qing in Chapter 3.

Piotr Zelenay: This coauthor is from Los Alamos National Laboratory. This coauthor was the manager of the project and was responsible for the work done by Yu Sueng and Qing.

Sue Mecham: This coauthor is from Virginia Tech in the department of Macromolecular Science and Engineering. Sue oversaw and ran the SEC experiments of the polymers presented in Chapter 3. The molecular weights obtained from those experiments are shown in Table 3.1.

James McGrath: This coauthor is a professor in the Chemistry department at Virginia Tech. Dr. McGrath was the author's advisor and oversaw the project.

Chapter 1: Literature Review

1.1 Introduction to Polymer Membranes

Polymer membranes over the last several decades have become important materials in industrial and commercial applications. The applications for polymer membranes and other membrane systems include: separation processes, electronics, dialysis, and alternative energy. The materials can function as gas separation, water purification, capacitor, semiconductor, and fuel cell membranes in these processes. Membranes are desirable in dialysis, batteries, and fuel cells due to their high transport of ions and high permeability. Their semipermeable nature and high-energy efficiency make these materials very desirable for water purification and gas separation membranes. Large scale production of membranes and hollow fibers has made these materials even more attractive, because of the ease of scale up and the low manufacturing cost.[1-2] Two applications, fuel cell and gas separation membranes, will be discussed with a focus on poly(arylene ether)s as membranes for these processes.

1.1.1 Fuel cells

1.1.1.1 Discovery and brief history of fuel cells

The basic principles of fuel cells, were discovered by the German scientist Christian Friedrich Schonbein and published in 1838 and still hold true for modern day fuel cells.[3] A year later in 1839, William Grove used these principles to create an electrochemical device that generated electricity from the combination of hydrogen and oxygen gases. When this device was first invented, this fuel cell precursor was called a "gaseous voltaic battery" and consisted of a relatively simple design with platinum electrodes, sulfuric acid as the electrolyte, and oxygen and hydrogen gases as the reactants. Grove's device required twenty-six cells connected in series

in order to successfully electrolyze the water, and eventually was expanded to fifty cells. Further modifications and discoveries to the "gaseous voltaic battery" were made by Lord Rayleigh (1882), Ludwig Mond and Carl Langer (1889), and Alder Wright Thompson (1889). In the years after the discovery of the first fuel cell, many different designs and applications were proposed, including some using coal as the fuel source. However, it wasn't until 1932 with the creation of the alkaline fuel cell by Francis T. Bacon that modern fuel cells began to be developed.[3]

In 1959 Bacon was able to develop a large "battery" that consisted of forty fuel cell stacks and produced 6 kW of power. This was sufficient to power most construction equipment, including a forklift. One early application for fuel cells was for the Apollo space missions in 1965. The fuel cells used on the spacecraft for the Apollo and Gemini missions were based on Bacon's design and were used to provide power and clean drinking water for the trips. Because of the current rise in demand of fossil fuels and the limited supply of those sources, the need to develop alternative energy sources is becoming increasingly important. Fuel cells offer an attractive alternative because of their high energy efficiency, low emissions (byproduct is water), high power density, quiet operation, and temperature flexibility. However, the current costs of the fuel cell components (more specifically the electrolyte membrane and the electrode catalysts) are much too high and the need to develop cheaper and more efficient materials is a major focus of current fuel cell research.[4-6]

1.1.1.2 Principles and types of fuel cells

Fuel cells are electrochemical cells that convert chemical energy into electrical energy. A basic fuel cell design is shown in Figure 1.1.[7]

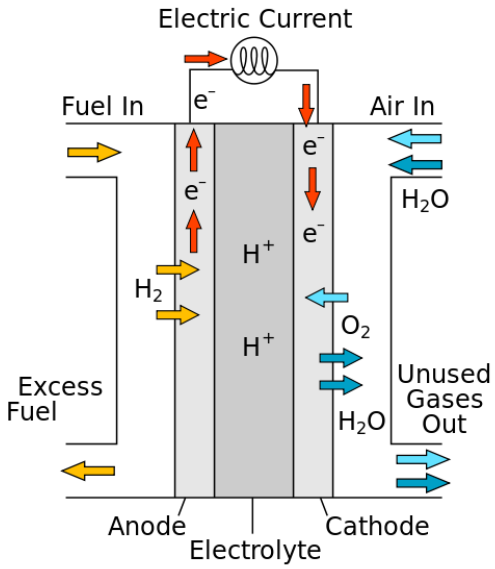

Figure 1.1: Basic Design of a Fuel Cell. http://en.wikipedia.org/wiki/Fuel_cell, Public Domain

Similar to Grove's original design, a fuel cell is comprised of two electrodes (an anode and cathode which contain the catalyst), an electrolyte, and a fuel source. The hydrogen gas (or other fuel sources) is oxidized at the anode, while the protons pass through the electrolyte and combine with reduced oxygen at the cathode to form water. The electrons pass through the bridge between the anode and cathode and this creates the electric current. Thus, unlike alkaline batteries which run on a sealed internal fuel source, fuel cells can be used continuously as long as the external fuel source is supplied. The general efficiency of a fuel is typically observed to be around 40-60% using only electricity obtained from oxidation of the fuel source. However, heat is generated when the protons (oxidized hydrogen) are combined with the reduced oxygen. If captured, the efficiency of this process can be greatly increased (values are higher than 85%).[5,7] Because of the energy potential and advantages of these devices many possible applications exist which include large power sources such as transportation vehicles, and smaller electronic devices such as computers and cell phones. Thus, different types of fuel cells are needed in order to satisfy the vastly different energy requirements.[3,8]

The major types of fuel cells currently used and scientifically studied are alkaline fuel cells, polymer electrolyte membrane fuel cells (PEMFCs), phosphoric acid fuel cells, molten carbonate fuel cells, and solid oxide fuel cells. A general breakdown and description of the different types of fuel cells are shown in Table 1.1.[9] Differences among the classes of fuel cells depend on the type of electrolyte used in the fuel cell assembly. Different electrolytes allow for a wide range of operating temperatures and conditions; however, each different type of fuel cell has its own advantages and shortcomings. One advantage of polymer electrolyte membrane fuel cells is that they operate at a relatively low temperature and avoid the harsh conditions that are associated with a liquid electrolyte, unlike the alkaline, phosphoric acid, and molten carbonate fuel cells. The electrolyte feature of some fuel cells can create management problems for the liquid matrix and lead to corrosion and premature failure. However, the PEMFCs require an expensive catalyst at the cathode and anode (platinum) and are sensitive to fuel impurities. Both the solid oxide and molten carbonate fuel cells exhibit high efficiency and fuel and catalyst flexibility, but also require extremely high temperatures for operation (>600^{o}C), thus limiting their energy applications. In addition, the high temperatures in these systems can lead to increased mechanical failure.[9] Alkaline fuel cells have a relatively low cost and like the PEMFCs can operate at reasonable temperatures and conditions, but the only current applications for these systems are for spacecraft and aerospace power.[5] This is primarily because of the severe CO_2 that the fuel cells experience, thus in an atmosphere rich in CO_2 this would be a major obstacle to overcome.

Table 1.1: Major types of fuel cells. Reprinted via permission of public domain

Fuel Cell Type	Common Electrolyte	Operating Temperature	Typical Stack Size	Efficiency	Applications
Polymer Electrolyte Membrane (PEM)	Perfluoro sulfonic acid	50-100°C 122-212° typically 80°C	< 1kW–100kW	60% transpor-tation 35% stationary	• Backup power • Portable power • Distributed generation • Transporation • Specialty vehicles
Alkaline (AFC)	Aqueous solution of potassium hydroxide soaked in a matrix	90-100°C 194-212°F	10–100 kW	60%	• Military • Space
Phosphoric Acid (PAFC)	Phosphoric acid soaked in a matrix	150-200°C 302-392°F	400 kW 100 kW module	40%	• Distributed generation
Molten Carbonate (MCFC)	Solution of lithium, sodium, and/ or potassium carbonates, soaked in a matrix	600-700°C 1112-1292°F	300 kW-3 MW 300 kW module	45-50%	• Electric utility • Distributed generation
Solid Oxide (SOFC)	Yttria stabi-lized zirconia	700-1000°C 1202-1832°F	1 kW–2 MW	60%	• Auxiliary power • Electric utility • Distributed generation

1.1.1.3 Polymer electrolyte membrane fuel cells (PEMFCs)

PEMFCs use a solid polymer membrane as the electrolyte for the fuel cell and can be further divided into two categories, direct methanol fuel cells (DMFCs) which use methanol/water solutions as the fuel source, and proton exchange membrane fuel cells which use hydrogen as the fuel source. These systems operate under the same principles with the fuel source oxidized at the anode and protons combining with reduced oxygen from air at the cathode

to form the water byproduct (DMFCs also form CO_2).[6] The reactions are depicted below in Figures 1.2 and 1.3.

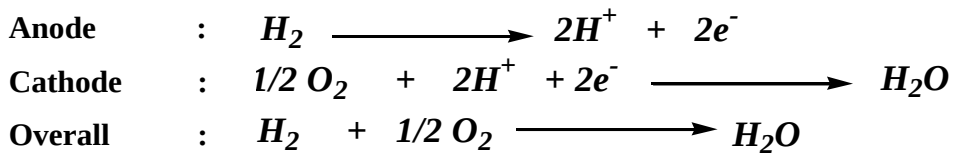

Figure 1.2: Half reactions at anode and cathode and overall reaction for hydrogen fuel source

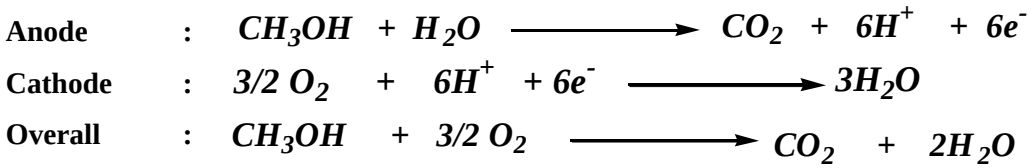

Figure 1.3: Half reactions at anode and cathode and overall reaction for methanol fuel source

PEMFCs offer many appealing advantages for fuel cell applications, and a critical aspect for their performance is the membrane electrode assembly. The membrane electrode assembly consists of the proton exchange membrane sealed in between the two electrodes to form a single electric cell. This assembly is the heart of the fuel cell with the polymer membrane responsible for the transport of protons, forming a gas/fuel barrier between the electrodes, and electronic insulation. The anode and cathode electrodes are coated with a platinum catalyst which oxidizes the fuel source (generating the protons and electric current), and reduces the oxygen to allow for recombination with the transported protons.[8] A schematic of the membrane electrode assembly is shown in Figure 1.4.[6]

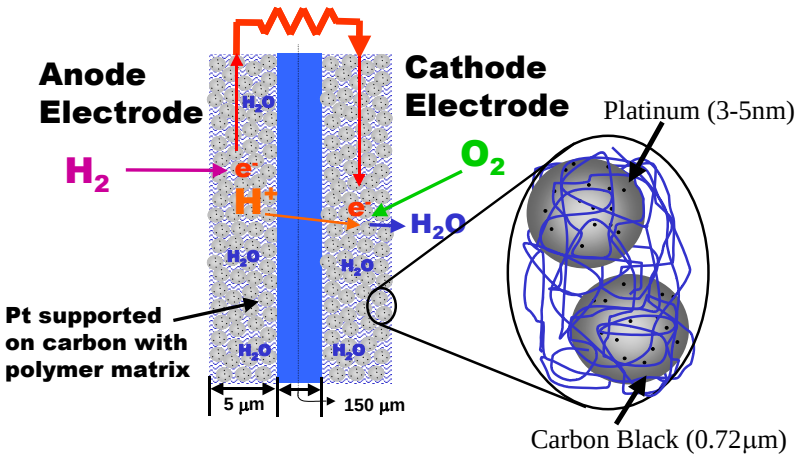

Figure 1.4: An example of the membrane electrode assembly for PEMFCs. "Hickner, M. A.; Ghassemi, H.; Kim, Y. S.; Einsla, B. R.; McGrath, J. E., Chemical Reviews 2004, 104, 4587" Used with permission of American Chemical Society, 2014, Copyright "2004" American Chemical Society.

In a review article by Hickner and McGrath,[6] the critical characteristics for proton exchange membranes were defined as: (1) high proton conductivity, (2) low electronic conductivity, (3) low permeability to fuel and oxidant, (4) low water transport through diffusion and electro-osmosis, (5) oxidative and hydrolytic stability, (6) good mechanical properties in the fully and partially hydrated states, (7) low cost, (8) and processability (ability to be cast into the membrane electrode assembly). Because almost all of the current materials and polymers rely on water to provide the transport for the protons in the fuel cell, water retention and management is an important aspect of these materials. Thus, because of the water management problem associated with current PEMFCs, their operation temperature is generally limited to 70-80^{o}C. However fuel cells need to operate between 120^{o}C and 150^{o}C in order to be applicable for automotive and other transportation applications.[5] At these higher temperatures the heat removal

becomes more efficient and the tolerance to CO impurities is increased.[5] In addition, at higher temperatures less of the platinum catalyst on the electrodes would be required for the membrane electrode assembly. This would be desirable since it could significantly reduce the cost of the membrane electrode assembly and the fuel cell as a whole.[4] In order to make fuel cells more practical, current research is being examined by the McGrath group and others to meet these criteria and critical characteristics necessary for proton exchange membranes.

1.1.1.4 Current proton exchange membrane and research into new materials

The current state-of-the-art PEM is Nafion®, a perfluorinated sulfonic acid polymer developed by DuPont in the late 1960's (shown in Figure 1.5).[3,10] Nafion® has a poly(tetrafluoroethylene) (Teflon) backbone with fluorinated ether side chains that contain sulfonic acid groups. The sulfonic acid groups promote the transport of cations. The poly(tetrafluoroethylene) backbone provides a small amount of crystallinity for the ionomer which provides a very unique morphology and strong solvent/chemical resistance. Additionally, the fluorine containing backbone also provides good thermal and mechanical stability for the membrane. Nafion® has very good proton conductivity when the concentration of water in the membrane is high. However, when the amount of water is reduced such as in lower humidity conditions, the conductivity drops dramatically. Because of Nafion's® relatively low glass transition temperature (around 110^{o}C) higher temperatures cause a large decrease in the fuel cell performance. The hydrogen gas fuel source is humidified in order to keep the relative humidity levels high in the fuel cell. Unfortunately, this is a rather expensive process and even with humidified hydrogen the practical limit of the fuel cell operation is about 80^{o}C. In order for PEMFCs to be applicable towards transportation purposes an operating temperature between 120^{o}C and 150^{o}C is desired. Thus, efforts have been made to develop new proton exchange

membrane materials that could operate efficiently in this temperature range and at lower relative humidity levels. It also should be noted that Nafion® is an expensive material to produce, so a cheaper proton exchange membrane would be desirable for PEMFCs to be practical.[8,10]

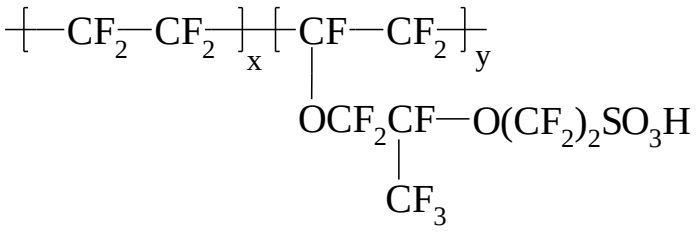

Figure 1.5: Chemical structure of Nafion®

Currently the research into new PEMs has been focused into five general areas which are: poly(perfluorosulfonic acid) copolymers, sulfonated branched and crosslinked polymers, high performance materials based on polybenzimidazoles and polyimides, sulfonic acid containing linear polymers and copolymers, and hydrophilic-hydrophobic block copolymers. The sulfonated linear polymers and block copolymers have been concentrated on both aliphatic and aromatic backbone containing polymers. The work in the McGrath group in the last few years has been focused on making hydrophilic-hydrophobic disulfonated polysulfone block copolymers based on aromatic backbones for use as proton exchange membranes in polyelectrolyte membrane fuel cells.[11-13]

1.1.2 Gas Separation Membranes

1.1.2.1 Techniques for gas separation and history of gas separation membranes

Currently there are five general techniques that are employed for gas separation processes. These are pressure swing adsorption, vacuum swing adsorption, temperature swing adsorption, cryogenic distillation, and membrane gas separation. The adsorption techniques rely

on an adsorbent material such as a zeolite, molecular sieve, activated carbon, or silica gel to collect the desired gas from the rest of the gaseous mixture. This first step is performed at a high temperature or pressure, then to collect the gas trapped in the absorbent, the system is swung to a separate low temperature or low pressure chamber to desorb the gas from the material. This process is then repeated to obtain the desired gas and purity. Cryogenic distillation is also done by lowering the temperature, but this process requires a phase transition of the gaseous mixture to the liquid state, then the pure gases are separated by distillation using their differences in boiling points. This process requires extremely cold temperatures and very precise distillation methods. Gas separation membranes use a solid polymer membrane to separate gas pairs and are generally conducted at ambient temperatures. The polymers can either be used as dense polymer films or spun into hollow fibers for the gas separation modules. They function by using the differences in the solubility and diffusivity between gases in order to isolate a gas mixture that is enriched in one of the components. The permeate is gas flow that goes through the membrane module while the retentate is the gas flow that is rejected. The gaseous species of interest that is collected can be either the retentate or the permeate. This technique requires high gas pressures, and requires synthetic membranes that are highly selective and can withstand the high pressures.[14-17]

While the gas separation market is still dominated by pressure swing adsorption and cryogenic distillation, gas separation membranes are competing against these techniques and are projected to have a strong future growth. As is the case for water purification, membrane separations could reduce cost significantly. Membrane-based gas separations do not require extremely low temperatures or rapid changes in pressure. Costs for membrane-based gas separations have been projected to be nearly half of that of pressure swing adsorption and a third

of the cost of cryogenic distillation (Fig. 1.6).[18] Additionally, the infrastructure for membrane-based separations has already been established due to the commercial success of water purification membranes which dominate the ultrafiltration and desalination markets. These factors, combined with advances in synthetic membrane materials, make membrane-based separations an attractive alternative to the current processes used in gas separation. However, improvements in gas selectivity of membranes are needed for applications that require ultrahigh purity single gases, which currently are only achieved by cryogenic distillation. Similarly, improvements in membrane stability are also needed for membranes to be applicable in separations with harsh feed conditions.[17]

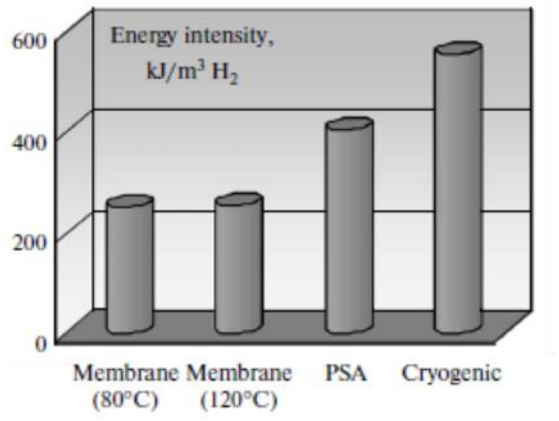

Figure 1.6: Energy cost for recovery of H_2 for membrane-based gas separations versus pressure swing adsorption and distillation. "Bernardo, P.; Drioli, E., *Petroleum Chemistry* **2010,** *50*, 271" Reprinted with permission of Springer, 2014, Copyright "2010" Springer.

The first observations of gas separation via membranes were made by J.K. Mitchell in the early 1830's, when he observed that rubber balloons filled at different rates with different gases. He observed that CO_2 absorbed relatively quickly, and he attributed this to expansion of the

rubber creating greater porosity. Later in 1866 these experiments were expanded on by Thomas Graham, who obtained oxygen-enriched air using rubber membranes. Over the next several decades more observations and advances were made, eventually leading to defining the permeability coefficient as the product of both the diffusivity and solubility of the gases through the membranes. These were derived from Fick's laws of diffusion and formed the basis for the measurement of permeation.[19]

While most of the early work utilized rubbery polymers for the membranes, many newer materials were investigated as polymer science advanced. One such example was the investigation into polyolefins after the discovery of Ziegler-Natta synthesis and catalysts.[19] However, by the 1970's and 1980's it became apparent that amorphous glassy polymers with high glass transition temperatures (T_g's) were more desirable for use as gas separation membranes. This was attributed to the increased free volume associated with amorphous glassy polymers, which resulted in much more permeable membranes. In order to directly compare the many different types of polymers that had been studied in the literature, permeability and selectivity values of the membranes were plotted against one another by Roberson, revealing trends for gas separation membranes.[20] This established a famous trade-off relationship with these materials, with higher membrane permeabilities resulting in lower membrane selectivities, and vice versa. Why this fundamental relationship exists, and how to "surpass" the upper bound has been a major focus of research in gas separation membranes.[21-22]

1.1.2.2 Mechanism and equations defining gas separation membrane properties

Permeation of gases through dense membranes is understood to occur by the solution diffusion model. Unlike many other membrane separation techniques, most gas pairs are too small and close in size to separate based on pore size. As shown in Figure 1.7, in membranes that

operate by the solution-diffusion mechanism, gases dissolve into the membrane and diffuse through to the other side.[23] In order to separate species, gas separation membranes rely on the difference in solubility (S) and diffusivity (D) of the gases in the membrane. These two coefficients make up the permeability coefficient (P) shown in equation 1.1. [2,14-15,19,21]

(1.1) $$P = S * D$$

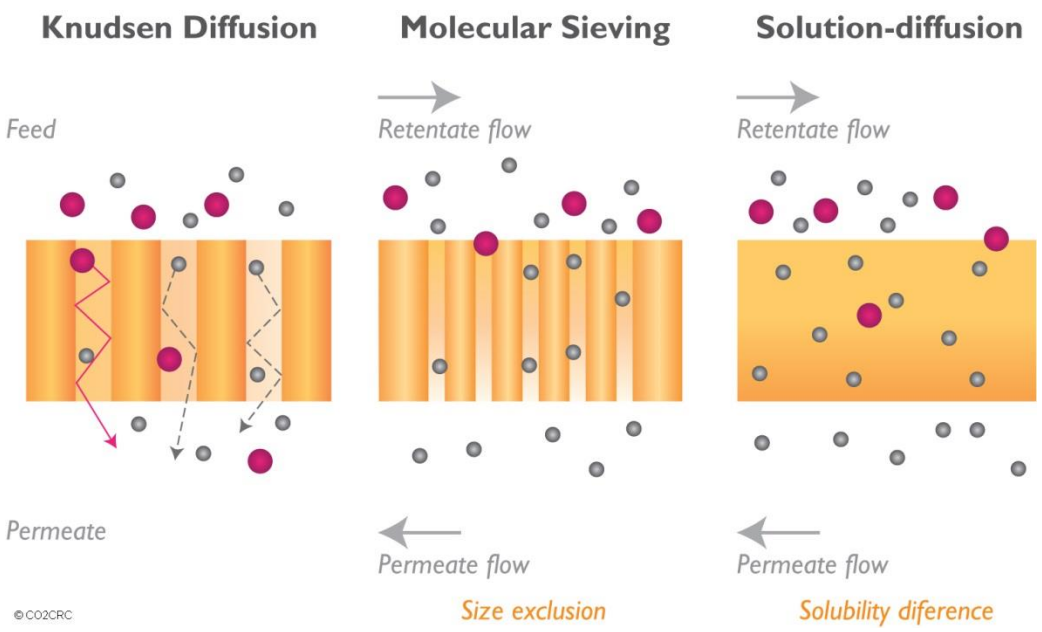

Figure 1.7: Differences between mechanisms for gas separation.

http://www.co2crc.com.au/aboutccs/cap_membranes.html, Public Domain.

The separation ability of a polymeric membrane is defined as the selectivity (α), which is the ratio of the permeability of gas A over gas B. Since permeability is the product of solubility and diffusivity, selectivity is the ratio of solubility and diffusivity of gas A over solubility and diffusivity of gas B. Equation 1.2 shows this ratio, with gas A as the more permeable species.

(1.2) $$\alpha_{A/B} = \frac{P_A}{P_B} = \frac{S_A}{S_B}\frac{D_A}{D_B}$$

As stated before, Roberson found that as the selectivity of a gas pair increases, the permeability consequently decreases. This was characterized by an empirical relationship, displayed in equation 1.3, between selectivity and permeability for gas A where $\beta_{A/B}$ and $\lambda_{A/B}$ are constants for common gas pairs.[20]

(1.3) $$\alpha_{A/B} = \beta_{A/B}/P_A^{\lambda_{A/B}}$$

Freeman expanded on this relationship, relating it to polymeric backbone structure. This validated many of the observations made for gas separation membranes, with glassy high T_g materials having better performance with regard to the upper bound for gas pairs. Dr. Freeman attributed this result to increased backbone stiffness and increased free volume by disruption of interchain packing. It was also proposed that diffusivity would have a stronger effect on upper bound performance than solubility.[21] Therefore high glass transition and amorphous polymers, such as poly(arylene ether)s and other partially aromatic polymers, make excellent candidates for gas separation membranes and hollow fibers.

1.2 Non poly(arylene ether) based membranes

1.2.1 Membranes for use as PEMs

1.2.1.1 Poly(perfluorosulfonic acid) copolymers

Poly(perfluorosulfonic acid) membranes have become the state of the art and the standard PEM used in low and medium temperature fuel cells. This is due to their unique morphological properties which allow for excellent thermal/chemical resistance and high proton conductivity.[24] Nafion® was the first of these materials, produced by Dupont in 1966, and is still commercially available today. The fuel cell performance of this material inspired exploration of similar tetrafluoroethylene copolymers with sulfonic acid side chains.[25] Some common and

commercialized poly(perfluorosulfonic acid) membranes which are similar to that of Nafion® are Aquivision™ (developed by Dow Chemical but no longer produced), the 3M ionomer, Flemion® (AGC), and Acipex® (Asahi Chemical) (Fig. 1.8).[8]

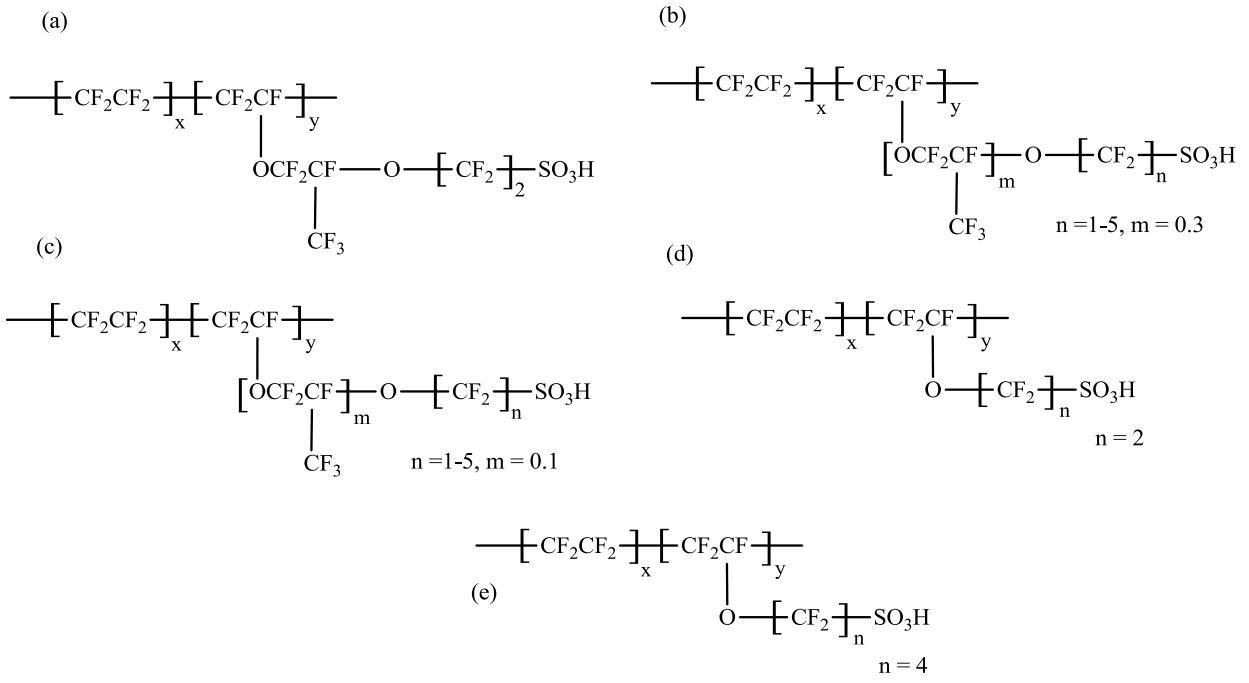

Figure 1.8: Structures of different poly(perfluorosulfonic acid)s (PFSAs): (a) Nafion®. (b) Flemion®. (c) Acipex®. (d) Aquivision™. (e) The 3M ionomer.

These polymers are all produced via a copolymerization of tetrafluoroethylene and a sulfonyl fluoride containing vinyl ether comonomer with varying side chain lengths. The comonomers are prepared using various synthetic chain extension methods from the base tetrafluoroethylene monomer, (synthetic scheme shown in Figure 1.9).[8]

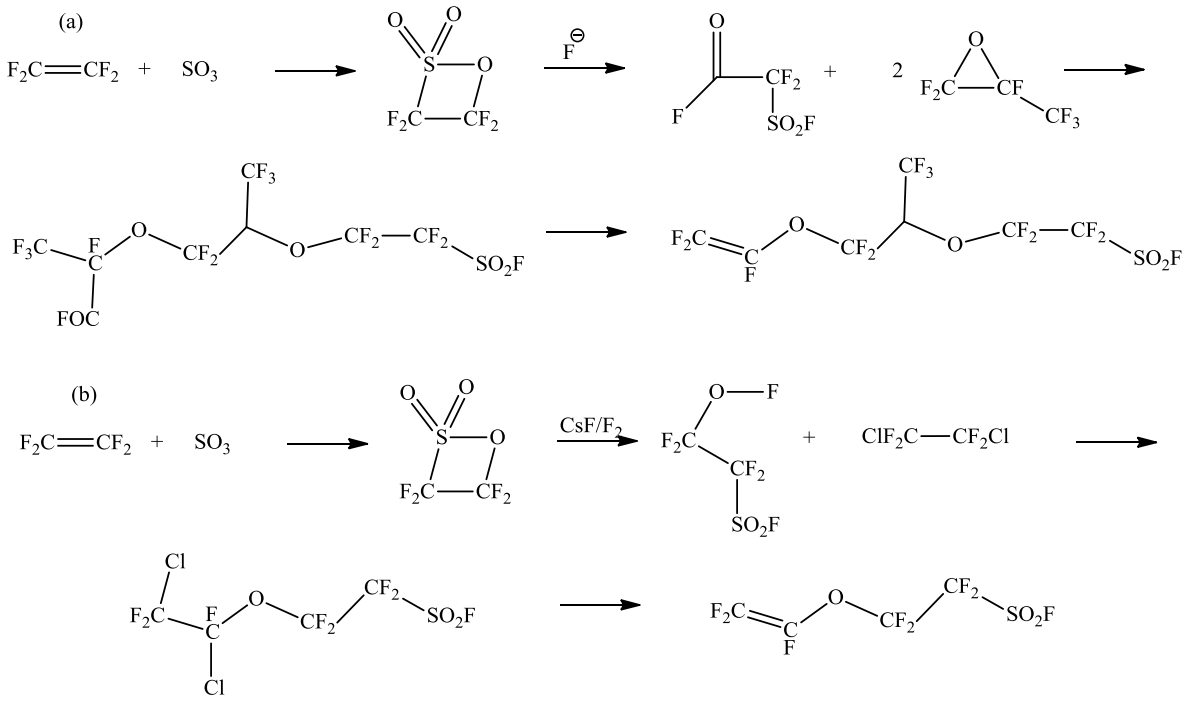

Figure 1.9: Synthetic schemes for the synthesis of the sulfonated side chain: (a) Nafion® vinyl ether monomer, (b) Aquivision™ vinyl ether monomer.

The two monomers are then used in a free radical copolymerization to synthesize the targeted poly(perfluorosulfonic acid) copolymers. The sulfonated monomer is usually kept in low concentration in the copolymer, typically around 5-10 mol%, in order to maintain the semi-crystalline morphology of the polytetrafluoroethylene backbone. This semi-crystallinity prevents the membrane from undergoing excessive swelling due to the sulfonic acid groups, and also provides the chemical and mechanical resistance for the PEM in the fuel cell. Because of these unique properties, the poly(perfluorosulfonic acid) copolymers are extremely difficult to process and cast into films. Thus the poly(perfluorosulfonic acid)s are not actually dissolved and cast into films, but are dispersed into (PFSAs can be in acid or salt form) a water/alcohol solution.[26]

The dispersion is then heated to remove the solvent and produce the copolymer membrane. Based on the concentration and the volume of dispersion, the thickness of the membranes can be varied to make either a thin or thick film. This film preparation method was first described in a patent by Grot.[27]

Equivalent weight (EW) is used to denote the approximate amount of sulfonic acid content in a given membrane. The EW is equal to the number of grams of the dry poly(perfluorosulfonic acid) copolymer per moles of sulfonic acid groups in the material (g/meq). Thus the lower the EW, the more sulfonic acid groups are present in the material. This is fairly equivalent to ion exchange capacity (IEC). The equation for IEC is defined as the moles of ionic groups capable of ionic exchange per gram of polymer (meq/g), in which a higher number would correspond to greater concentrations of acid groups. Concentration of acid groups can be quantified by either term, though EW is typically used for poly(perfluorosulfonic acid)s and IEC is used for most other charged polymers. However, poly(perfluorosulfonic acid)s have a lower limit for EW because of the low reactivity of the sulfonated side chain monomer. The sulfonated commoner will not self-propagate and therefore reactions that have high mol% of the sulfonated commoner will only produce low molecular weight copolymers. For Nafion® the EW that is typically used and found to have the best tradeoff between mechanical stability and acid group concentration, is between 1000-1100 EW. In fact the Nafion® 112, 117 and 212 membranes all have equivalent weights of 1100 g/mol, with the differences being in the thickness of the membranes.[10,26] The charge density/sulfonation level is typically higher for sulfonated hydrocarbon PEMs. However, the sulfonic acid groups have a lower pKa in the poly(perfluorosulfonic acid)s due to the presence of the highly fluorinated and electron withdrawing carbons. The stronger acid groups in the poly(perfluorosulfonic acid)s is believed to

be the cause of the increased conductivity over similar EW hydrocarbon PEMs.[28] However, the conductivity values are low in reduced relative humidity conditions for the poly(perfluorosulfonic acid)s membranes. This is one of the most significant problems that all proton exchange membranes must address for fuel cells based on H_2/air fuel sources. Another issue for poly(perfluorosulfonic acid)s membranes (especially in direct methanol fuel cells) is high fuel permeability, which drastically reduces the efficiency and performance of the PEMFCs.[28] Furthermore, the synthesis of monomers, the processing required, and the large fluorine content contained in these copolymers, make these membranes very expensive to produce. Prices for poly(perfluorosulfonic acid)s membranes are typically around $600-700 per square meter of film.

Other variations on PFSAs include grafted copolymers, which have been used to either reduce cost of PSFAs or to alter the morphology and properties of the membranes. Grafting of these types of copolymers has been designed using both pre-irradiation and irradiation techniques on both fully and partial poly(tetrafluoroethylene) backbones.[10] By using grafting methods to create sulfonation on the polymers, the poly(perfluorosulfonic acid)s could take advantage of the phase separation morphology characteristic of grafted copolymer systems.[8]

In the branched PFSA membranes, polystyrene is typically grafted onto the base polymer chain and then post-sulfonated to provide the sulfonic acid groups necessary for proton conductivity. The base polymer is typically a commercial fluoropolymer such as PTFE, PVDF, poly(tetrafluoroethylene-*co*-hexafluoropropolyene) (FEP), etc., which is irradiated with either γ-rays or an electron-beam to provide the radical sites that initiate polymerization of the co-monomer onto the main polymer chain backbone.[29] The base polymer and the co-monomer can either be mixed together and then irradiated (direct radiation), or the pre-polymer can be

irradiated and then combined with the desired monomer (pre-irradiation) to form the grafted copolymer. Performance of these materials typically suffer from shorter lifetimes compared to the linear PFSA membranes. However when divinyl benzene is used as a crosslinking agent values have been reported as high as 7900 h for H_2/O_2 fuel cells.[30] The chemical structures of some representative radiation-grafted sulfonated copolymers are provided in Figure 1.10 and a general scheme for preparation of the irradiated PEMs is shown in Figure 1.11.[8,30]

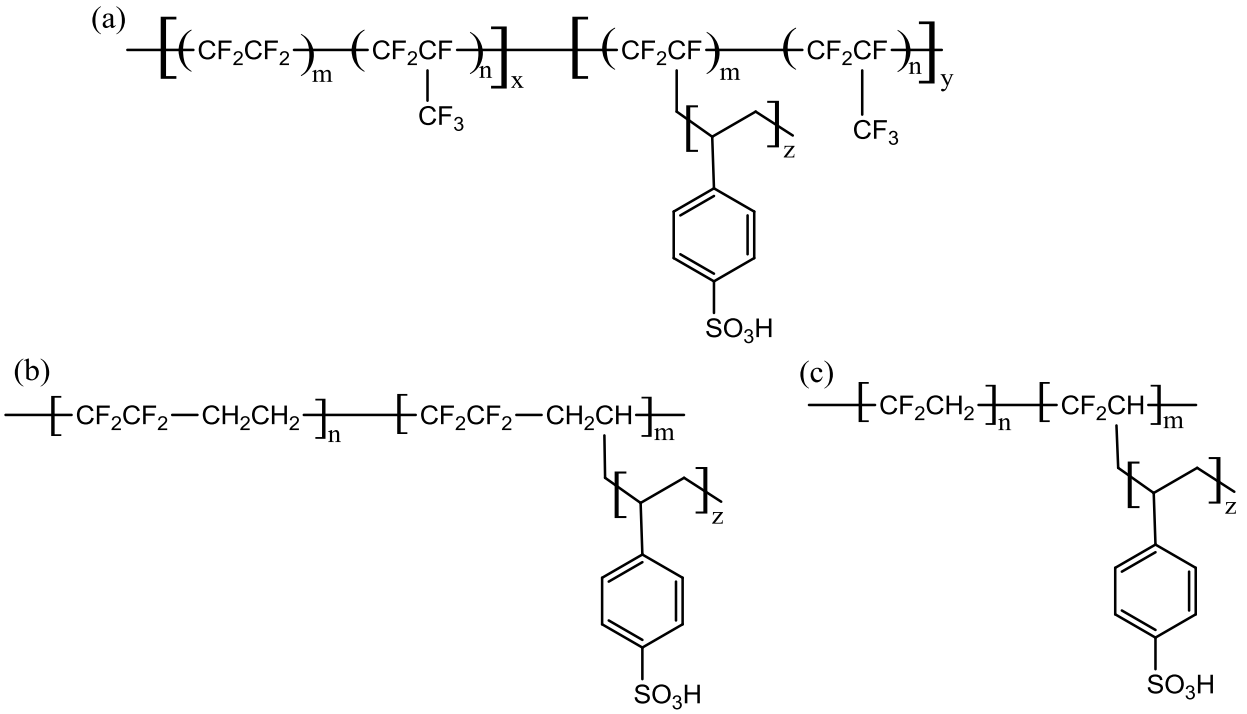

Figure 1.10: Chemical structures of some radiation-grafted fluoropolymer PEMs: (a) poly(tetrafluoroethylene-co-hexafluoropropylene)-g-poly(styrene sulfonic acid) (FEP-g-PSSA); (b) poly(ethylene-alt-tetrafluoroethylene)-g-PSSA (ETFE-g-PSSA); (c) PVDF-g-PSSA.

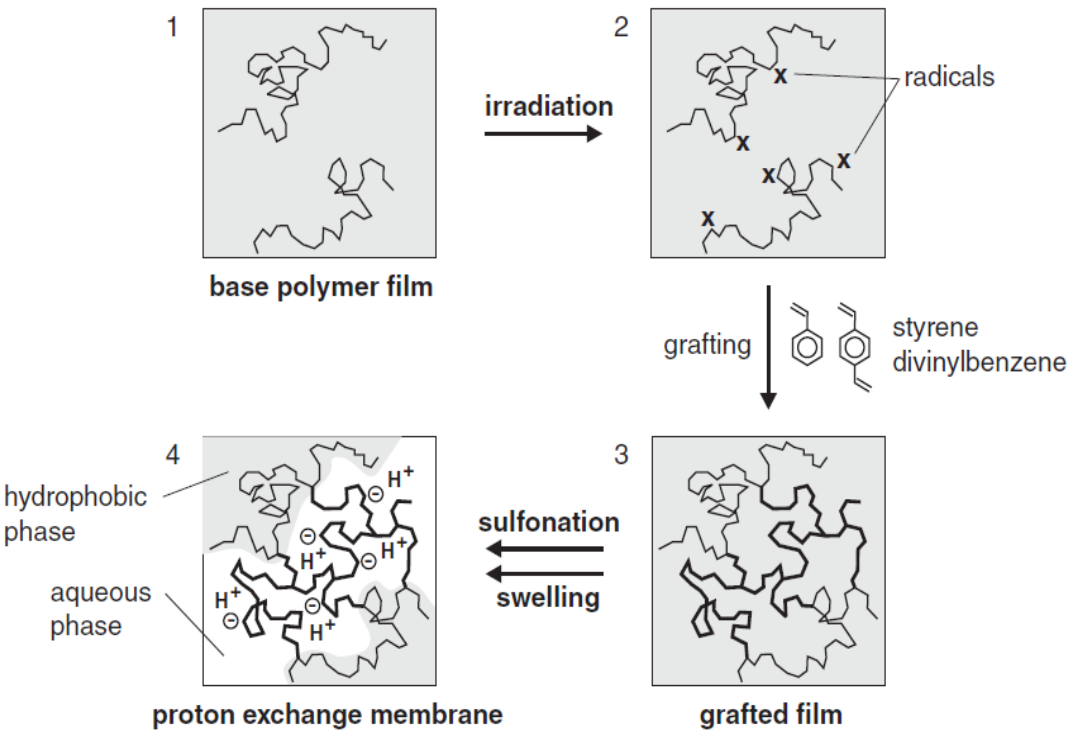

Figure 1.11: General preparation of a grafted copolymer PEM using pre-irradiation and divinyl benzene as a cross-linker. "L.Gubler; Kuhn, H.; Scherer, G. G.; Brack, H. P.; Simbeck, K., *Fuel Cells* **2004,** *4*, 196" Reprinted with permission of John Wiley and Sons, 2014, Copyright "2004" John Wiley and Sons.

In this grafting process typically the base polymer is already in film form and the co-monomer is polymerized onto the film, which is then sulfonated to form the PEM. PEMs are not homogeneous due to the random growth of polystyrene on the base polymer film. An example system is shown in Figure 1.12 b, which shows the HAADF-STEM images of PVDF-*g*-PSSA (a polyvinylidene backbone with grafted sulfonated polystyrene side chains). Three domains can generally be observed in the grafted poly(perfluorosulfonic acid) copolymers. In Figure 1.12 b the fluoropolymer PVDF matrix is associated with the dark areas, sulfonated polystyrene corresponding to the grey regions, and the bright white specks belonging to the sulfonic ion

clusters.[31] This differs from the commercial PFSAs (e.g. Nafion), which appear to have relatively uniform distribution of ionic aggregates upon imaging (Fig. 1.12 a).

Lu et al. reported an alternate grafting procedure in which pre-irradiated was performed on the PVDF powder.[29] After polymerization of the polystyrene side chain, the polymer was cast into a film and sulfonated to form the PEM. By performing the branching step before the film was formed, the non-homogeneity exhibited by other grafted copolymer PEMs was avoided and uniformly distributed domains were observed. The degree of grafting leveled off after 6 h for this process, however a grafting percent as high as 35% was achieved. Although higher levels of grafting were achieved, only copolymers with degrees of grafting lower than 30% were soluble in NMP. As the degree of branching increased for the PEM, increases in IEC, water uptake, and conductivity were also observed. This was consistent with other grafted PFSAs. However, the PEMs had very low proton conductivity (less than ~ 10^{-3} S/cm).

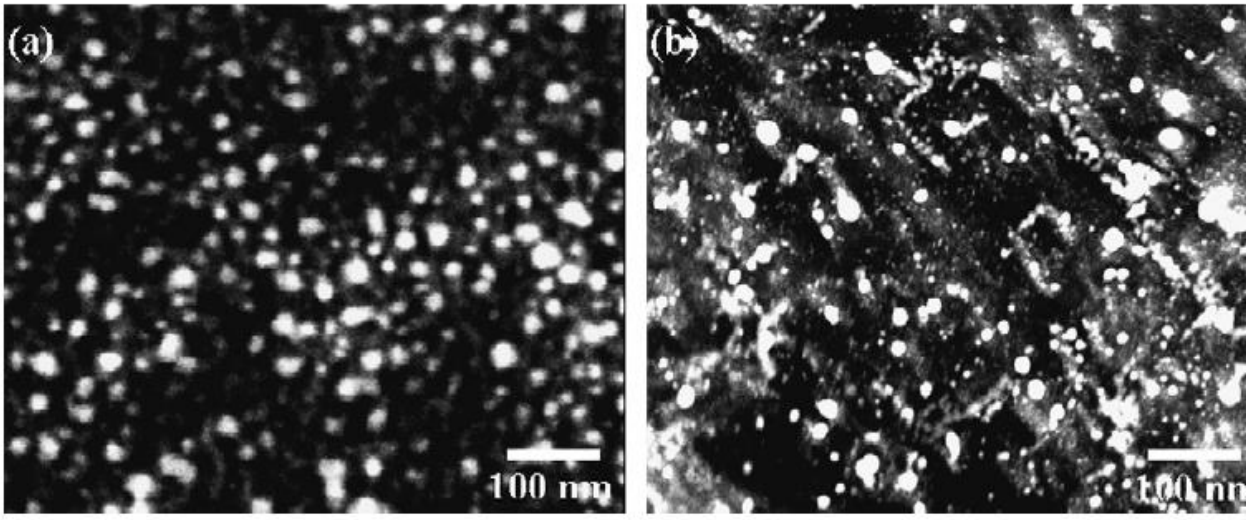

Figure 1.12: HAADF-STEM images stained with Ag+ after 5 days of immersion in 50% methanol solution of (a) Nafion® 117 and (b) PVDF-g-PSSA. "Huang, H. S.; Chen, C. Y.; Lo, S.

C.; Lin, C. J.; Chen, S. J.; Lin, L. J., *Applied Surface Science* **2006,** *253*, 2685" Reprinted with permission of Elsevier, 2014, Copyright "2006" Elsevier.

Holdcraft et al.[32-33] reported a controlled synthesis grafting technique using a different approach to address the non-homogeneity issue. First, a fluoropolymer macroinitiator with pendent chlorine groups was created by copolymerizing vinylidene difluoride and chlorotrifluoroethylene. The macroinitiator was then used as the base polymer for the controlled synthesis technique atom transfer reversible polymerization (ATRP). Styrene was grafted onto the main fluoropolymer chain in a controlled process and then post-sulfonated. By controlling the time of the grafting process, a series of increasing charge density/degree of sulfonation (DS) PEMs were made with IECs ranging from 0.64-2.53 meq/g. Morphology characterization by TEM showed that all of those membranes exhibited a phase-separated morphology with interconnected ionic aggregates. The number and size of the ionic clusters depended on both the molecular weight of the grafted polystyrene chain, and the degree of sulfonation. For the copolymer PEMs with shorter sulfonated polystyrene chains, as the DS increased, the size of the aggregates increased but the number of clusters remained constant. Conversely, the opposite was true for the longer grafted sulfonated polystyrene chains. The grafted copolymer membranes had high conductivities, with the copolymer having the longer sulfonated polystyrene graft segments having the highest conductivity. Additionally, the longer chain sulfonated polystyrene copolymers had comparable or less water uptake than the copolymers with shorter segments. For all branch lengths the water content and conductivity increased with higher IECs, until the IEC reached > 2.3 meq/g. Upon this sulfonation level the membranes excessively swelled, leading to a loss in conductivity and mechanical strength. A general scheme of the synthesis process is shown in Figure 1.13 while a similar synthesis approach is shown in Figure 1.14.[33-34]

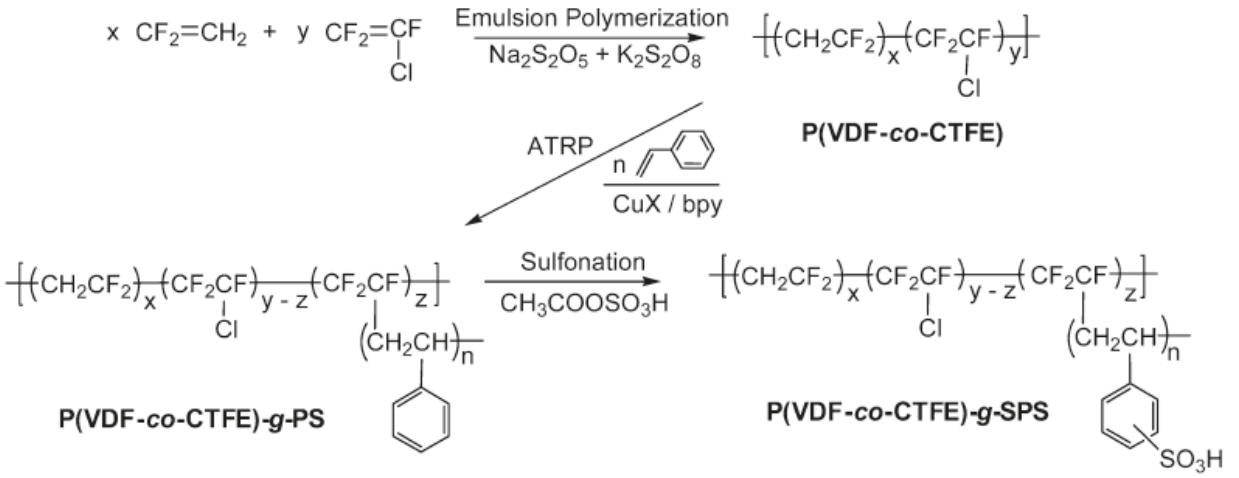

Figure 1.13: General synthesis scheme for poly((vinylidene difluoride)-*co*-chlorotrifluoroethylene)-g-sulfonated styrene) (P(VDF-co-CTFE)-g-PS)[33]

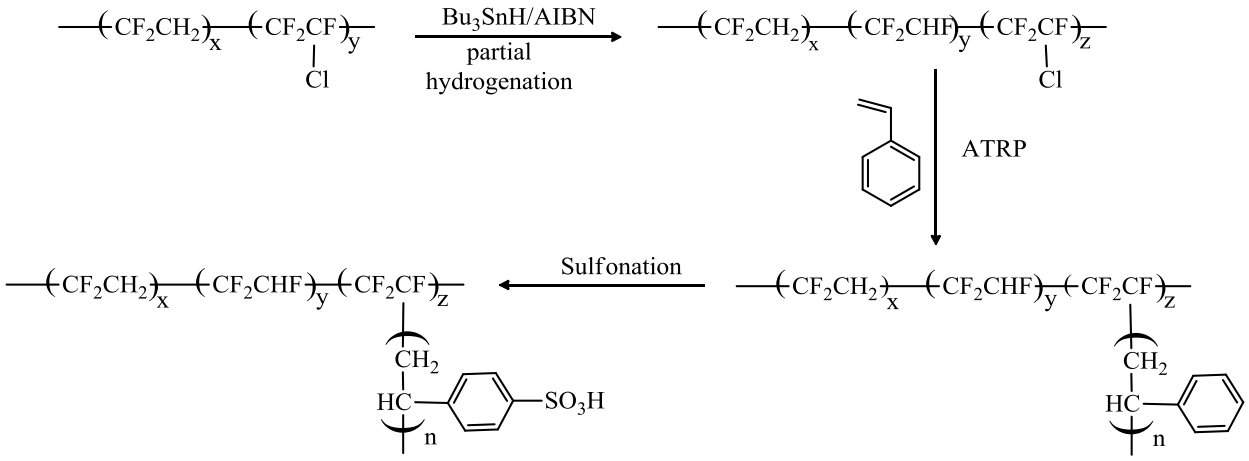

Figure 1.14: Synthetic scheme for PVDF-g-SPS

1.2.1.2 High performance materials based on polybenzimidazoles

Over the past few years, polybenzimidazole (PBI) membranes have become an interesting alternative to the poly(perfluorosulfonic acid) polymers and other sulfonated PEMs. Polybenzimidazole membranes are highly thermally stable, and exhibit unique properties desirable for high temperature fuel cells.[35-36] Operating at higher temperatures would provide many benefits for fuel cell construction and performance. Most notably, higher operation temperatures would reduce or eliminate the need to humidify the fuel cell and allow for a greater tolerance to impurities. These improvements would widen the selection for fuel sources, improve conductivities and kinetics at the anode/cathode, and reduce the required amount of catalyst.[37] The first reported synthesis of a fully aromatic polybenzimidazole was in 1961 by Vogel and Marvel. They reacted 3,3',4,4'-tetraaminobiphenyl with diphenylisophthalate in a two-step melt polymerization process to form the polymer *m*-PBI.[35]

This synthesis approach has led to a commercial process and is used to make many different textiles and fabrics that, exhibit desirable properties such as high temperature resistance, chemical and thermal stability. Because of these excellent mechanical and thermal properties, PBI's are considered a promising potential material for high temperature fuel cells. However, by itself *m*-PBI has a very low proton conductivity with reported values only as high as 10^{-6} S/cm. However, an interesting feature of PBI's is that they can be doped with acids to increase the conductivity of the membranes.[38]

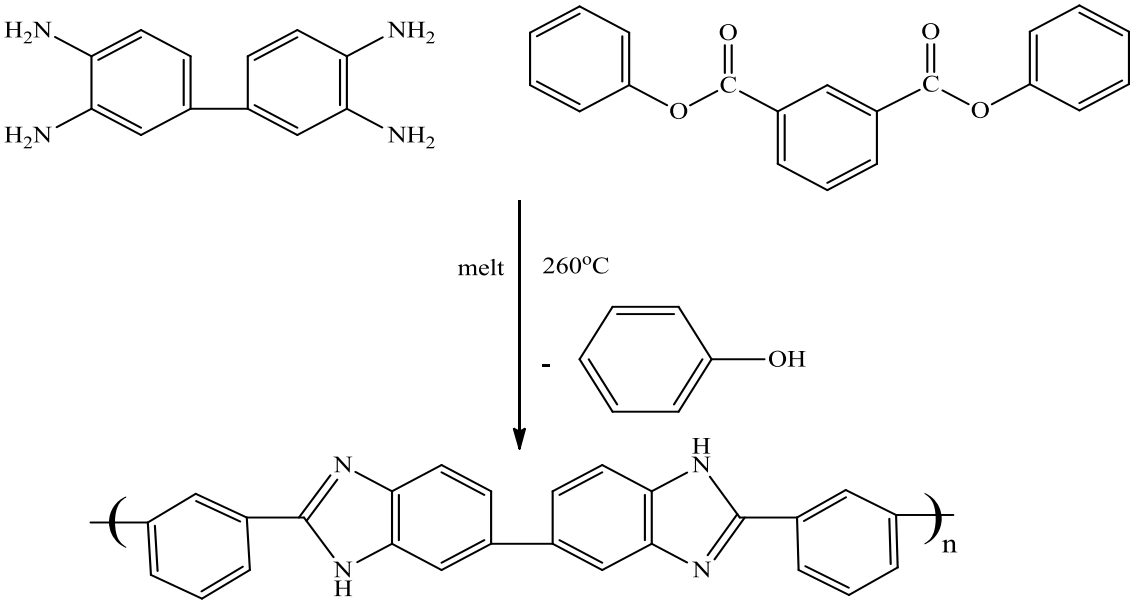

Figure 1.15: Polymerization scheme of *m*-PBI from 3,3,4,4'-tetraaminobiphenyl and diphenylisophthalate

Savinell et al. reported the doping of commercialized Celanese PBI films with phosphoric acid, and tested the conductivity and thermal properties of the polymer-acid complexes.[36,38-39] The films were cast from a solution of DMAc and a commercial PBI polymer from Celanese, and then doped by immersing the film into an 11 M solution of phosphoric acid for 24 h. The resulting membrane contained approximately five phosphoric acid molecules per repeat unit of PBI and had a conductivity in the range of 10^{-3} – 0.04 S/cm. Further research was conducted by other groups with comparable PBIs to form phosphoric acid doped PEMs. They showed that these types of membranes exhibited high ionic conductivity at elevated temperatures, high chemical and thermal stability, minimal water drag coefficient, and low gas/fuel permeability (Fig. 1.16).[40-41] Proton conductivity and performance (current and power density curves) of these membranes were found to correlate closely to the doping level and the doping agent that was used for the membrane.

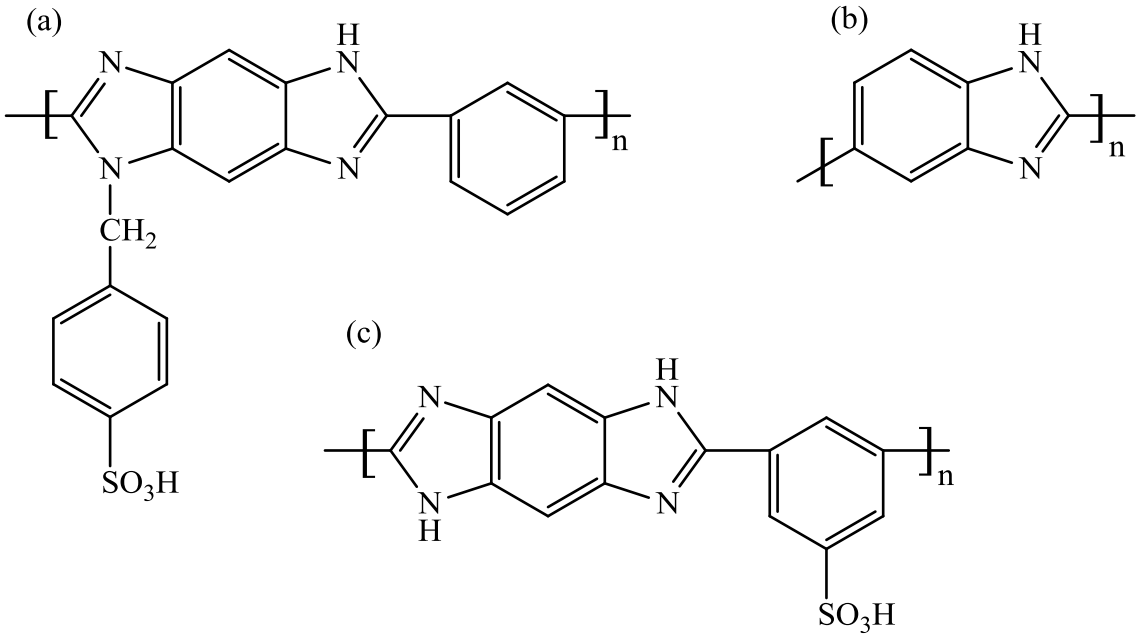

Figure 1.16: Chemical structures of acid-doped PBI's: (a) side chain sulfonated PBI. (b) AB-PBI. (c) sulfonated PBI.

A study done by Rozier and Jones compared the conductivities of a PBI film when immersed in different acids. Sulfuric and phosphoric acid produced the results for the polymer-acid complex with values much higher than the other tested acids.[42-43] When the doping level was kept between 6-10 moles of phosphoric acid per repeat unit of polymer the measured conductivity was between 10^{-4} – 10^{-2} S/cm, with no water or humidification present or necessary for the PEMs. In addition, these phosphoric acid-doped membranes were thermally stable and had long performance lifetimes (>2000 h).[44] However, the conductivity was still rather low for these systems even at higher temperatures. Bjerrum et al. attempted to increase the ionic conductivity by increasing the doping level to 16 moles per repeat unit for the membrane-acid complex (equal to 1600 mol percent doping level).[44] At 160^{o}C the conductivity was found to reach as high as 0.13 S/cm, which slightly exceeded that of the perfluorosulfonic acid membrane Nafion®. Unfortunately, at this high doping level, the mechanical properties of the PEM were

very poor, and the complex became unstable. The tensile strength was near zero at 150^{o}C for the membrane with a 1600 mol percent doping level. When considering the mechanical strength, Bjerrum concluded that only a doping level between 350-750 mol percent of phosphoric could be used to produce mechanically stable membranes. However, the conductivities of the polymers with these doping levels were only 0.02-0.06 S/cm at 150^{o}C. Thus, in order for the highly conductive PBI membranes to be applicable, the mechanical strength of the membranes will need to be maintained for high doping levels.

Sulfonation of PBIs has also been used to enhance proton conductivity and eliminate the need to acid dope the resulting membranes. Yan et al. used this approach to create several different thermally stable sulfonated polybenzimidazoles. The synthesis schemes for two different approaches are shown in Figures 1.17 and 1.18.[45-46]

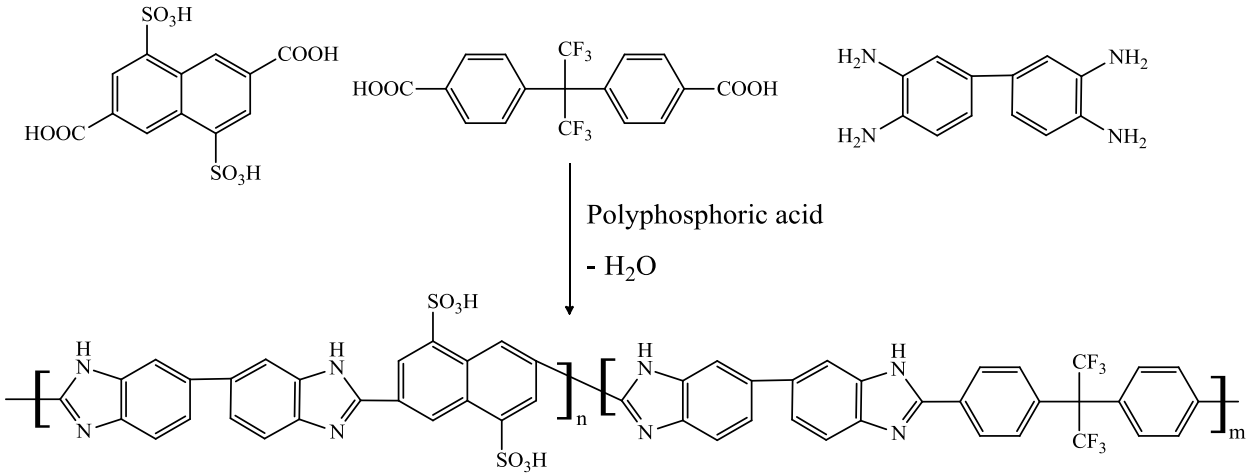

Figure 1.17: Synthesis of sulfonated polybenzimidazole sPBI-NF

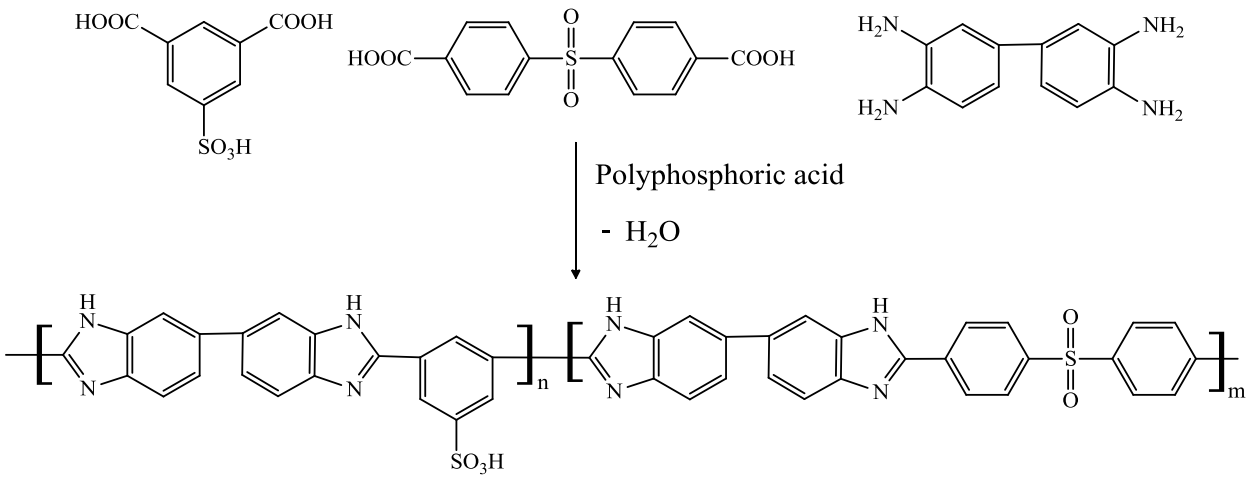

Figure 1.18: Synthesis of a sulfonated random PBI polymer (sPBI-IS)

The polymers were co-polymerized with two different difunctional carboxylic acid-containing monomers and a tetraamine monomer. The resultant copolymers showed excellent thermal properties with no degradation occurring before 300^{o}C in the acid form, and a thermal stability near 500^{o}C in the salt form. The membranes prepared from the PBI copolymers produced tough and transparent films, and were able to be cast from polar aprotic solvents. Unfortunately, although these PEMs displayed strong mechanical and thermal properties, the conductivities were very low with values only reported as high as 3.0 x 10^{-3} S/cm at 90^{o}C. In addition, these films still required humidification and water to enhance proton transport.

A major breakthrough in the PBI PEMs for high temperature fuel cells was discovered by Benicewicz et al., who developed a sol-gel synthesis process to produce a phosphoric acid-doped polybenzimidazole film (a general diagram for the sol-gel process is shown in Figure 1.19).[47] For this sol-gel process, PBI was polymerized in polyphosphoric acid (PPA), which was used as both the solvent for the reaction and the polycondensation agent. The polyphosphoric acid reacted with water produced from the PBI polymerization and formed phosphoric acid during the synthesis. The resultant polymers had high molecular weights and films could be directly cast

from the polymerization solution. The films were cast at 200 – 220^{o}C with no purification or isolation necessary. Because of the hygroscopic properties of both the PPA and PBI, water is absorbed from the atmosphere and hydrolyzes the PPA into phosphoric acid "*in-situ"* during drying of the membrane, thus producing an acid-doped membrane in one step. The membranes acquired after the drying process were gel-like in structure, and contained around 32 moles of phosphoric acid per repeat unit of polymer. The doping level of these membranes were significantly higher than the doping levels reported by Bjerrum et al., which produced membranes with 13-16 moles of phosphoric acid per repeat unit.[44] However, unlike the membranes reported by Bjerrum et al., the membranes produced by via the polyphosphoric acid process had extremely high doping levels, yet maintained strong properties. Tensile strengths ranged from 1.0 and 3.5 MPa, with elongations at break ranging from 150-390%. In addition, the good mechanical properties depended on the inherent viscosity of the PBI base polymer. These PEMs had remarkably high conductivities at elevated temperatures, with values as high as 0.26 S/cm at 200^{o}C. The combined conductivity and mechanical performance for the PEMs fabricated via the sol-gel process were significantly higher than previously reported doping methods for high temperature PEMs. However, the conductivity values only reached such high conductivity values at elevated temperatures. Thus the optimal operating temperature for these films would be greater than 150^{o}C. Lifetimes of the films were found to be >1000 h, even with temperatures in excess of 150^{o}C and the harsh phosphoric acid environment present in the fuel cell.

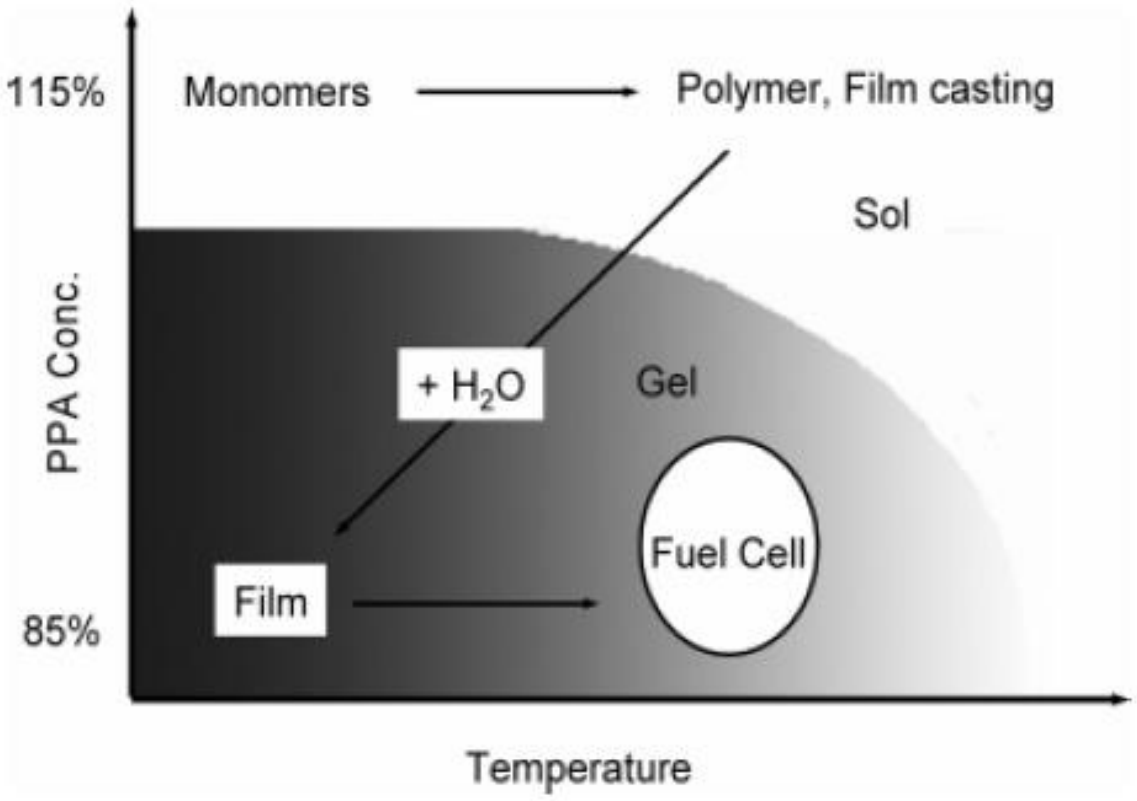

Figure 1.19: Sol-gel PBI acid-doping process. "Xiao, L.; Zhang, H.; Scanlon, E.; Ramanathan, L. S.; Choe, E. W.; Rogers, D.; Apple, T.; Benicewicz, B. C., *Chemistry of Materials* **2005,** *17*, 5328" Reprinted with permission of American Chemical Society, 2014, Copyright "2005" American Chemical Society.

Benicewicz et al. further expanded the direct casting method to other PBI derivatives in order to further increase the performance and stability of the membranes.[37,48-50] A partially crosslinked PBI film (2OH-PBI) was made by incorporating two phenol groups per repeat unit of the polymer, which reacted with the polyphosphoric acid as a polycondensation agent to form a covalent crosslink between chains. The phenol groups were introduced via 2,5-dihydroxyterephthalic acid (Fig. 1.20 a), and the acid-doped film was made in the one step direct casting method similarly to the procedure for the previous PBI polymers using PPA as the solvent for the reaction. Although the crosslinked 2OH-PBI membrane had higher conductivity

when compared to the PBI acid-doped membrane without the hydroxyl groups (*para*-PBI), the PEM did not show much of an increase in performance. This was attributed to limitations of the platinum catalyst used in the electrodes of the membrane electrode assembly. Specifically, the oxygen reduction rate at the cathode was significantly slower than the hydrogen oxidation. However, the authors added that the mechanism by which the hydroxyl groups increased the proton conductivity was unclear and needed to be further investigated. Similar high conductivity results were found for a sulfonated PBI (Fig. 1.20 b) membrane that had been synthesized in PPA and cast using the direct method. Both PEMs had comparable mechanical strength to the unsubstituted PBI acid-doped complex, with the sulfonated PBI having a lifetime of nearly 3000 h.

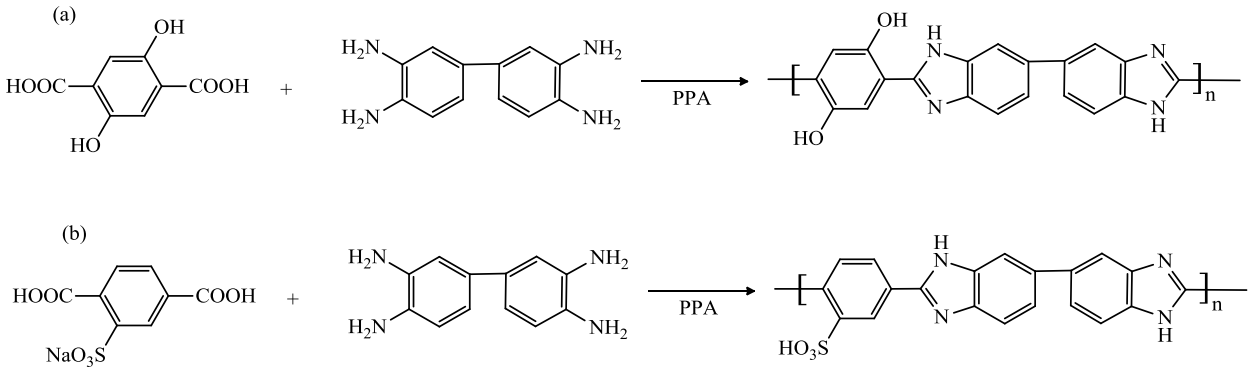

Figure 1.20: Synthesis of substituted PBIs using the sol-gel process: (a) 2OH-PBI. (b) sulfonated PBI (*s*-PBI).

1.2.1.3 Sulfonated copolymers based on aliphatic backbones

The Gemini space missions employed a sulfonated polystyrene membrane as the electrolyte for their fuel cell stacks. However, these systems could only be operated at low temperatures (below 70^{o}F) and they had weak mechanical properties and short performance

lifetimes.[3] Thus, because of these short-comings, these systems were not used on further NASA and Apollo missions. In order to overcome these issues, systems were developed by Ballard Advanced Materials that used fluorinated backbones in a α,β,β-trifluorostyrene sulfonated copolymer membrane. The membranes were patented and trademarked as BAM® (Fig. 1.21).[51]

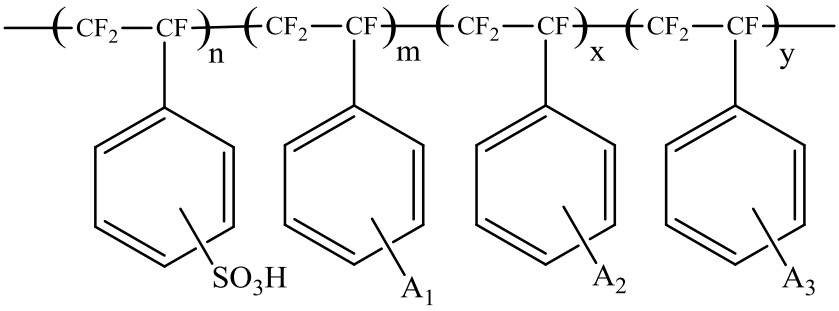

n,m,x,y > 2

A_1,A_2,A_3 = CF=CF_2, CN, NO_2, OH, alkyl halogen, alkyl ether

Figure 1.21: Chemical Structure of BAM® α,β,β-trifluorostyrene sulfonated copolymer

Holdcraft et al. compared BAM® membrane and a sulfonated polystyrene system against a poly(perfluorosulfonic acid) Nafion® membrane.[52] The BAM® membranes showed high chemical stability and the lower equivalent weight (EW) systems showed superior performance to the PSFA Nafion® membranes. However, at these lower EWs the membranes swelled too much in water and this affected their mechanical integrity. The sulfonated polystyrene showed similar performance to the BAM® membrane but also experienced similar swelling issues. Although the BAM® showed good fuel cell performance, the high cost (similar to the PFSA's) due to the highly fluorinated backbone associated with these membranes was a deterrent. In the case of the sulfonated polystyrene, the low mechanical properties and chemical instability

associated with the aliphatic backbone inhibited any possible applications for use as PEMs, though the price would have been favorable.[8]

One potential benefit of the sulfonated polystyrene PEM is that the aliphatic backbone seemed to drastically reduce the oxygen and fuel permeability of the fuel cell.[53] This was explored in an article by Carretta et al. who proposed that reduced gas and fuel permeability could be useful in direct methanol fuel cells (DMFCs).[54] Even with a highly sulfonated polystyrene system (up to 20% of chains sulfonated), methanol permeability was 70% lower than through Nafion®. The proton conductivities for these membranes were also good as compared to the PFSA's films. However the mechanical properties and durability were not discussed in the article. The mechanical properties and chemical stability is a limiting factor in most of the linear sulfonated copolymers based on aliphatic backbones.

1.2.2 Membranes for gas separation

1.2.2.1 Linear wholly Aromatic high performance materials

Matrimid® and Kapton® are examples of current state-of-the-art membranes used for gas separation (Fig. 1.22). These types of wholly aromatic polyimides along with polybenzimidazoles and aromatic polyamides have been heavily studied due to their high T_g's, stiffness, strength, and exceptional stability (Fig. 1.23).[55-68] Polymerization of these materials occur through similar mechanisms with initial attack on the carbonyl by the amine in a nucleophilic acryl substitution, however polybenzimidazoles and aromatic polyimides have a second cyclization and dehydration step.[69] The formation of the cyclic ring makes polybenzimidazoles and aromatic polyimides amorphous polymers, while sulfone or isopropylidene groups are added to aromatic polyamides to prevent crystallinity.[64-65] Aramids such as Nomex® and Kevlar® are excellent high performance materials, but the high crystallinity

and chain packing in these polymers results in very low permeability.[68] Thus, incorporation of bulky pendent groups not only decreases density from disruption of crystallinity, but also increases chain stiffness (Fig. 1.24).

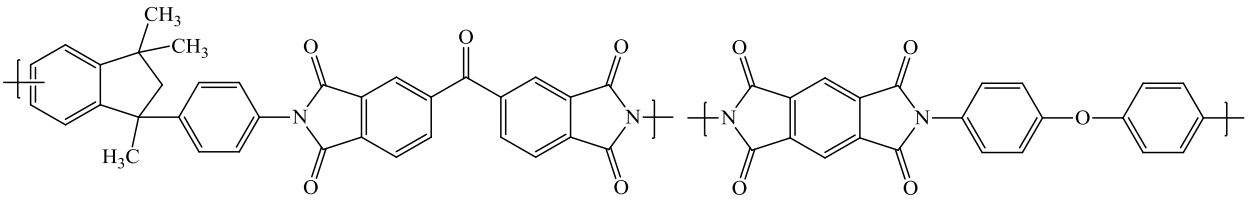

Figure 1.22: Polymeric structures of the aromatic polyimides Matrimid® and Kapton®

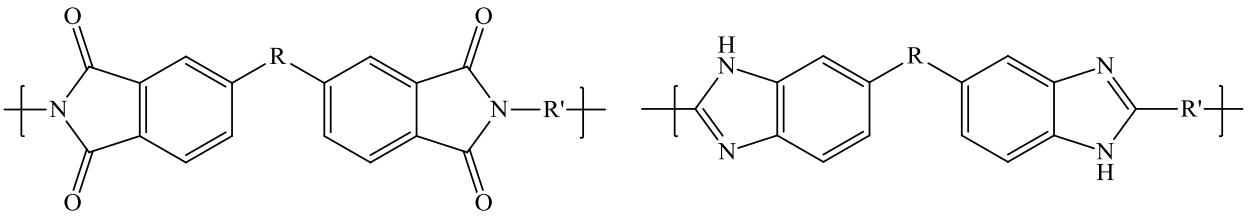

Figure 1.23: General structures of aromatic polyimides (left) and polybenzimidazoles (right)

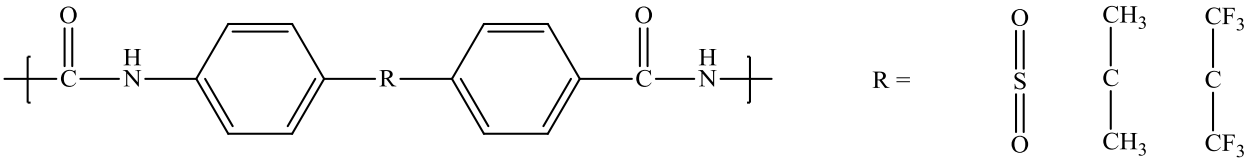

Figure 1.24: Aromatic polyamides with incorporation of bulky groups

Although polybenzimidazoles and aromatic polyimides are amorphous, incorporation of bulky groups also has the same effect on backbone mobility and gas transport properties for these membranes.[56,58-59,61] With addition of such groups in the polymer, the membranes may increase in both permeability and selectivity. This effect provides gas separation membranes with transport properties that can approach the upper bound.[65,68] Most of the research on these types of materials has focused heavily on polyimides rather than polybenzimidazoles or

polyamides. The increased backbone rigidity of the polyimides and polybenzimidazoles, along with their amorphous nature, has generally made these materials more desirable than polyamides. Additionally, polyamides are much more susceptible to plasticization than polybenzimidazoles or polyimides, especially by water, which disrupts the hydrogen bonding in the polyamides.[70] However, the biggest hindrance against both polyamides and polybenzimidazoles is their limited solubility and very low gas permeability.[62,68] Dye et al. reported permeabilities less than two barrers for hydrogen and carbon dioxide gases through the PBI membranes even at 100^{o}C.[60] As mentioned previously, inclusion of bulky groups can improve the solubility and transport properties of the membranes, but the polyimides still show superior results.[22] PBI membranes with these bulky groups prepared by Kharul et al. had a two fold increase in selectivity over the polyimide membranes for H_2/CH_4 and CO_2/CH_4, but the permeabilities where far lower. In fact the polyimide membranes had 10-15 times higher permeability for the H_2/CH_4 gas pair and over 200 times higher for the CO_2/CH_4 gas pair.[61] However, polybenzimidazoles have recently received renewed interest for high temperature gas separations (temperatures greater than 150^{o}C) due to their enhanced stability at elevated temperatures.[71-72]

Bulky functional groups can be included in either the bridging group between aromatic moieties or the bridging group between the two imide segments. Figure 1.25 shows some examples of bulky groups than have been used to enhance gas transport properties. Kapton® was the first polyimide to be produced commercially and it contained pyromellitic dianhydride (PMDA), but further research in gas separation membranes found that anhydrides with bridging groups were superior. These bridging groups were proposed to limit chain torsional movement, as well as disrupt chain packing.[56] In a study looking at the effect of the bridging group on the gas transport properties, the polymers saw the best results with the hexafluoro bridging group

(6FDA). The polyimide with the 6FDA exhibited both increased density and d-spacing. This lead to an increase in permeability and selectivity.[56] This observation has been reported with many other types of polyimide membranes with the incorporation of the 6FDA as the bridging group.[55,59,73-74] Between the bridging groups of the polyimide shown in Figure 1.25 (excluding BPADA), 6FDA was found to have the highest permeability due to the free volume brought on by the fluorine groups, and BTDA the highest selectivity.[75] The increased chain stiffness and decrease in chain mobility brought on by the carboxyl group of the BTDA was suggested as the reason for the higher selectivity. In looking at the series of polyimides plotted on the upper bound, the 6FDA containing polyimide had the best combination of transport properties.[75] Highly permeable polyimide membranes incorporating structures such as BPADA (Ultem® is a commercially available polyimide using the anhydride) have been successfully made with transport properties comparable to or exceeding that of 6FDA.[59]

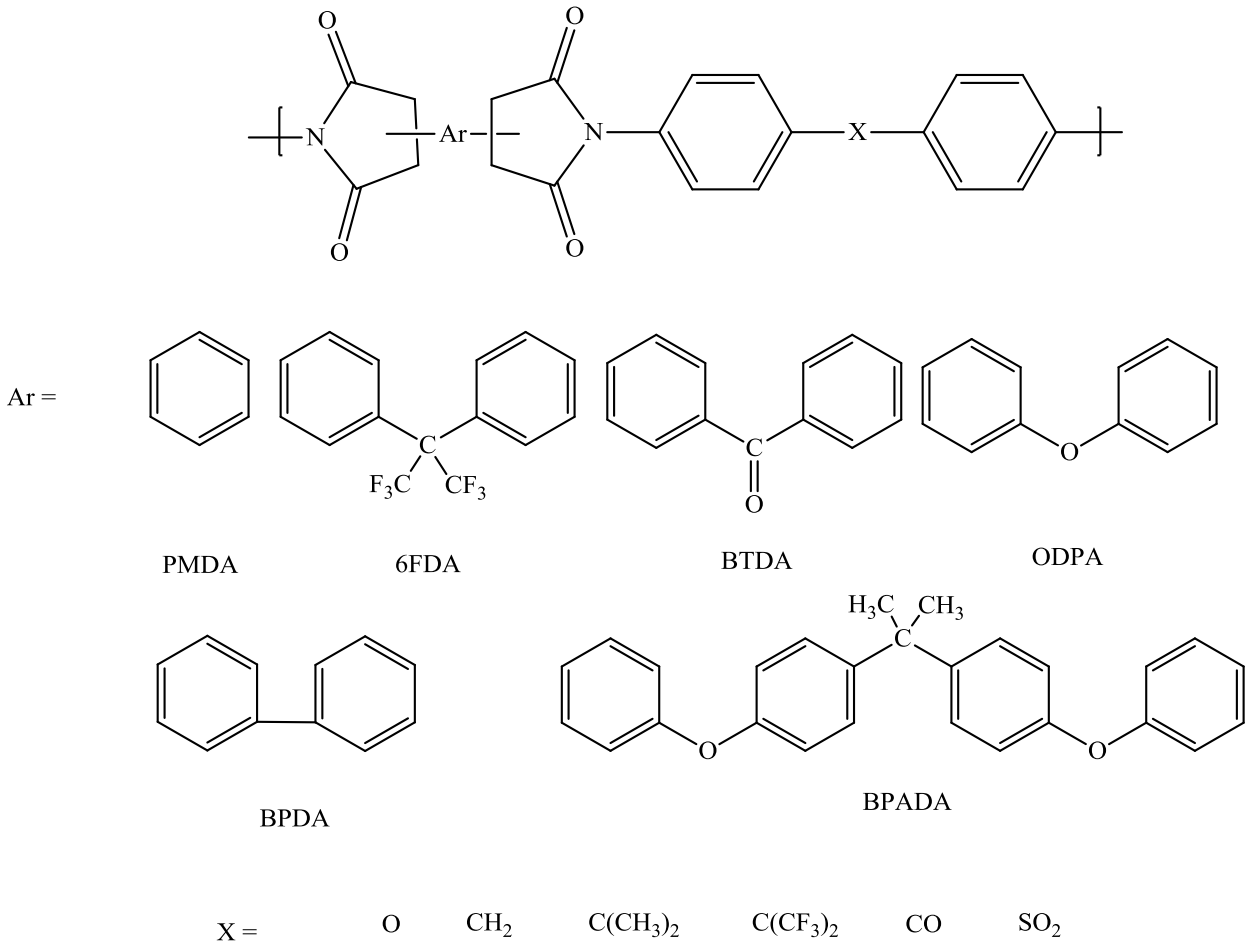

Figure 1.25: Examples of bulky groups added into polyimides to improve transport properties

The bridging group of the polyimides has a huge effect on the transport properties of polyimides, and in the case of some groups (e.g. 6FDA) can cause an increase in both the selectivity and permeability. However, this is not observed in the bridging groups of the diamine monomer, which experiences a tradeoff between permeability and selectivity. As the functional groups become bulkier and produce higher free volumes, the permeability subsequently increases and the selectivity decreases.[56,75] This is the typical trade-off associated with gas separation membranes. Thus, recent efforts have focused on making highly sterically hindered and very rigid polymer backbones to improve transport properties.[76] Matrimid® and polymers of intrinsic microporosity (denoted as PIM membranes in the literature) are two such examples of

polyimides incorporating the highly rigid backbones. Matrimid® has become an industrial standard polyimide used in many of the gas separation processes and modules, while many of the PIM membranes have transport properties that surpass even the revised upper bound.[76]

1.2.2.2 Thermally rearranged and crosslinked high performance materials

The major technical problems associated with wide scale use of membranes for gas separation are their low selectivities and stability in the gas feed matrix.[17] While membranes can show great transport results for a certain gas pair, gas feeds can have a multitude of gases present in the matrix.[77] Thus transport results can vary greatly depending on the various gases present in the matrix, with the other gas components altering the permeability and selectivity of the membrane.[77-78] The most common problem is a plasticization effect from more condensable gases such as carbon dioxide or water. Such gases can be absorbed by the membrane, increasing the volume and lowering the glass transition temperature of the membrane. The dual effect of increased chain mobility and higher free volume can significantly lower the selectivity of the membranes.[79-80] Since very high selectivity is needed for some gas separation processes the membranes would have to be continually replaced and possibly have to go through a second purification step in order to obtain the targeted purity. One solution that has been explored to counteract this problem is to create an insoluble polymer network, either through a chemical process or crosslinking. Results reported by several research groups have showed that creation of a polymer network resulted in not only higher selectivities, but also increased resistance to plasticization.[81-89] Effects of crosslinking gas separation membranes based on poly(arylene ether)s will be discussed in section 1.4.

As was the case for the linear non-arylene ether polymers, most of the crosslinking investigations have focused on polyimide systems.[83,86-91] The chemical crosslinking of

polyimides has used primarily two approaches. One is to introduce a trifunctional (or greater functionality) monomer. The second is to add a diamine monomer after polymer formation to open the imide ring. Figure 1.26 shows synthetic approaches using these crosslinking methods.

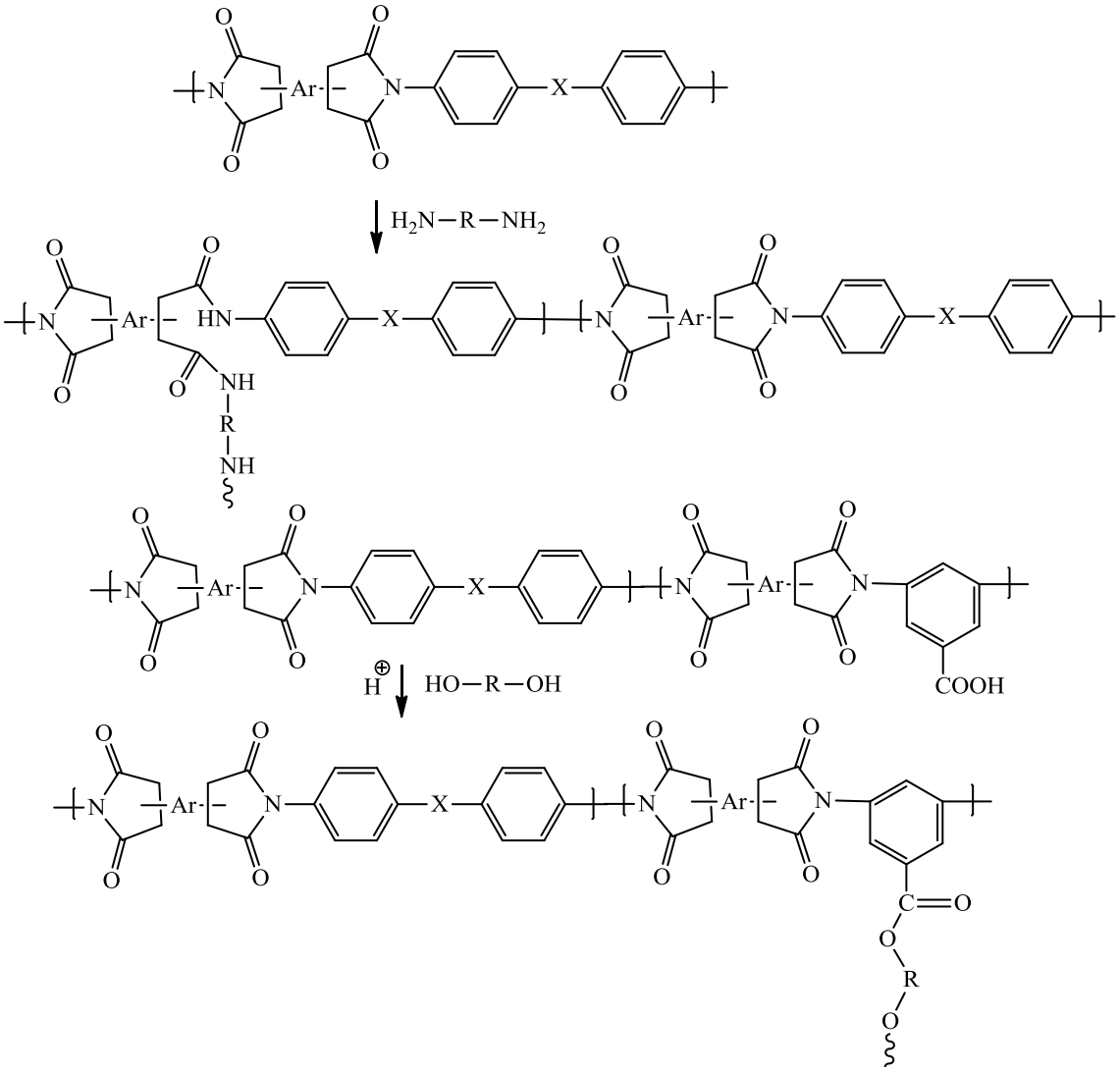

Figure 1.26: Chemically crosslinking of polyimides

Multifunctional monomers that have been used to accomplish crosslinking have included diaminobenzoic acids or triamine species. Diaminobenzoic acid monomers introduced a carboxylic acid group on the backbone, which was then crosslinked through esterification with a dihydroxy functional molecule.[85,87,91] Crosslinking results from either multifunctional monomers

or ring opening, showed increased resistance against plasticization in the membranes, and a decrease in permeability for all gases. With the exception of the He/N_2 gas pair, neither crosslinking method showed a significant increase in gas selectivity. The increase in selectivity for this gas pair was most likely brought on by a decrease in pore size or membrane densification via the chemical crosslinking.[86,90]

Unlike the chemical crosslinking, thermally annealing of polyimides and similar high performance materials has been reported to have a drastic change in transport properties for a wide range of gas pairs.[81-82,92-93] The most renowned membranes that use this technique are referred to as "Thermally Rearranged" or TR polymers. These polymers are synthesized by the same route as polyimides, except that the diamine monomer has a functional group that is ortho to the amine on the monomer.[81] Once the polyimide precursor is formed, annealing at 350-450^{o}C creates the insoluble polybenzoxazole or polybenzithiazole (if sulfur is used instead of oxygen) (Fig. 1.27). The rearrangement results in a mass loss for the polymer, with the removal of carbon dioxide. This elution of gas creates increased free volume, with comparatively uniform pore sizes that are continuous throughout the membrane. The resulting morphology creates membranes with exceptional gas transport properties that are close to or even surpass the 2008 upper bound for most common gas pairs.[94] In the first reported TR polymers, the conversion was tracked at 350^{o}C, 400^{o}C, and 450^{o}C. Conversion at each stage caused a drastic increase in gas permeability, with only a slight drop in the selectivity.[81] Further research correlated TR conversion to both temperature and structure, with higher TR conversion found for more flexible backbones and increased temperature.[93] However, while the more flexible structures yielded polymers with one hundred percent gel fraction at much lower temperatures, the transport properties were not as good.[92] Additionally, it was found that when ortho groups such as acetates

with higher masses were used, permeability was further increased, and some of these membranes had higher selectivities than the precursor polymers.[82,93] Figure 1.27 depicts some of the different ortho functional groups examined in TR polymers. Interestingly, the acetyl group produced the best results and the authors suggested that this might have been due to evolved acetic acid having a catalytic effect on the TR conversion of the polymer.[93]

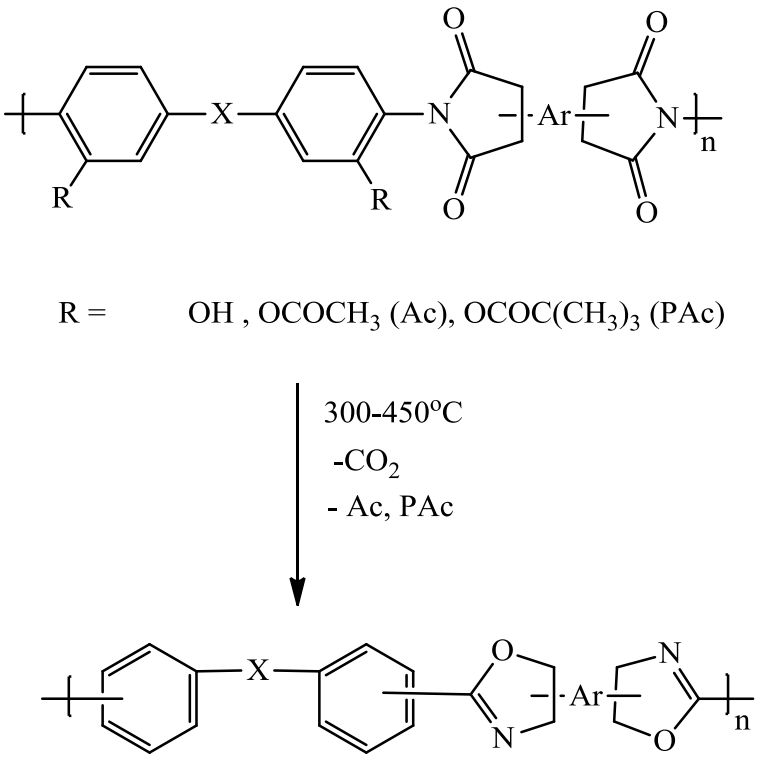

Figure 1.27: Synthesis of thermally rearranged (TR) polymers

1.3 Linear Poly(arylene ether) Membranes

Poly(arylene ether)s are generally synthesized via step-growth polymerization using a nucleophilic aromatic substitution.[95] The first reported synthesis of poly(arylene ether)s using this method was in 1967 by the Union Carbide Corporation, who reported that this reaction could be done quickly and efficiently using aromatic dihalide and bisphenol monomers. The

substitution mechanism, which occurs through a Meisenhiemer complex intermediate, is shown in Figure 1.28 and a typical synthetic scheme is shown in Figure 1.29.[96-97] The electron withdrawing bridge, usually either a sulfone or ketone, on the aromatic dihalides facilitates attack and subsequent substitution on the aromatic halide, which is otherwise less reactive toward nucleophilic substitution. For nucleophilic aromatic substitution of poly(arylene ether)s, only polar aprotic solvents were found to be applicable, since under the basic conditions necessary for the reaction, other solvents can compete with the aromatic phenoxide. Since high temperatures are typically used in these reactions, solvents such as dimethyl sulfoxide (DMSO), *N*,*N*-dimethylacetamide (DMAc), *N*-methyl-2-pyrrolidone (NMP), and *N*,*N*-dimethylformamide (DMF) are generally used.[95]

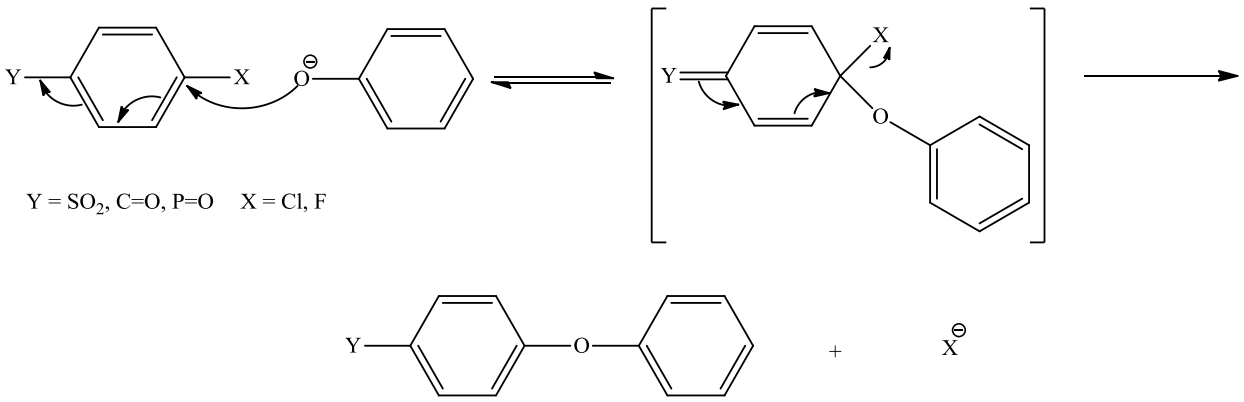

Figure 1.28: Mechanism of SnAr nucleophilic aromatic substitution

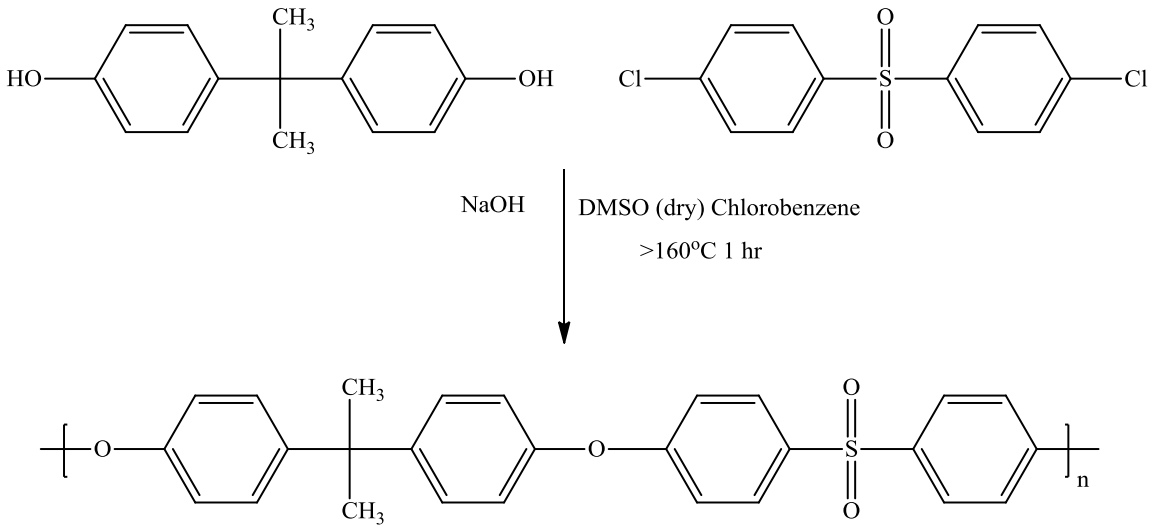

Figure 1.29: Synthesis scheme for Bisphenol A based poly(arylene ether sulfone) developed by Union Carbide

1.3.1 Sulfonated poly(arylene ether)s for use as PEMs

One of the major problems with the state of the art PFSA membranes and other PEMs is the weak mechanical and poor thermal/chemical properties arising from the aliphatic backbone of the polymers. Thus, an approach has been taken to use partially or wholly aromatic backbone copolymers as proton exchange membranes in fuel cells.[8] Poly(arylene ether)s have been shown to exhibit strong thermomechanical properties, with most glass transitions temperatures above 180°C.[98-99] The excellent thermal and chemical stability along with the high T_g and melting temperature (T_m) (if applicable) could allow for poly(arylene ether)s to have excellent fuel cell stability. Because of these properties a number of sulfonated aromatic copolymers have been suggested as alternative membranes that include, sulfonated poly(arylene ether sulfone)s,[100-101] sulfonated poly(arylene ether ketone)s ,[102-104] sulfonated polyimides,[105-106] sulfonated polybenzimidazoles (discussed earlier), sulfonated poly(arylene ether nitrile)s,[107-110] and sulfonated poly(phenylene)s.[111]

1.3.1.1 Sulfonated poly(arylene ether sulfone)s

The most widely studied of the poly(arylene ether)s for use as proton exchange membranes has been the sulfonated poly(arylene ether sulfone)s. This is due to the ease of fabrication, excellent thermal and mechanical properties, resistance to oxidation and acid-catalyzed hydrolysis, flexibility in design/modification, and low crystallinity of these copolymers, all of which tend to allow for prolonged use and improved durability of fuel cells.[8,100-101] These copolymers are generally prepared by either one of two widely used procedures. One is by synthesis of the polysulfone by polycondensation to form a high molecular weight product followed by a post-sulfonation reaction to produce the acidic sites. The other method uses a pre-sulfonated monomer to form the sulfonated copolymer directly by polycondensation.

Post-sulfonation reactions can be accomplished relativity easily via electrophilic aromatic substitution using either chlorosulfonic acid or sulfur trioxide (SO_3) as an electrophile.[112-113] Noshay and Robeson reported a modified product in 1976 using a SO_3/TEP (triethyl phosphate) complex to sulfonate the bisphenol A-based polysulfone developed a few years earlier. Figure 1.30 shows the reaction scheme.[112] Because of the electron withdrawing nature of the sulfone group, which deactivates the aromatic rings toward electrophilic aromatic substitution, sulfonation preferentially occurred on the diphenol monomer typically in the ortho position to the ether linkage. However, the sulfonic acid groups on those positions were found to be less acidic and generally unstable due to the adjacent ether bonds. Thus, other approaches have been investigated to afford sulfonation on positions on the aromatic rings of the deactivated sulfone component where the sulfonic acid groups would be more stable. These approaches have

included using lithiation to form both pendent sulfonic acid chains and sulfonic acid groups directly on the carbon atom adjacent to the carbon with the sulfone bond (Fig. 1.31).[114-115]

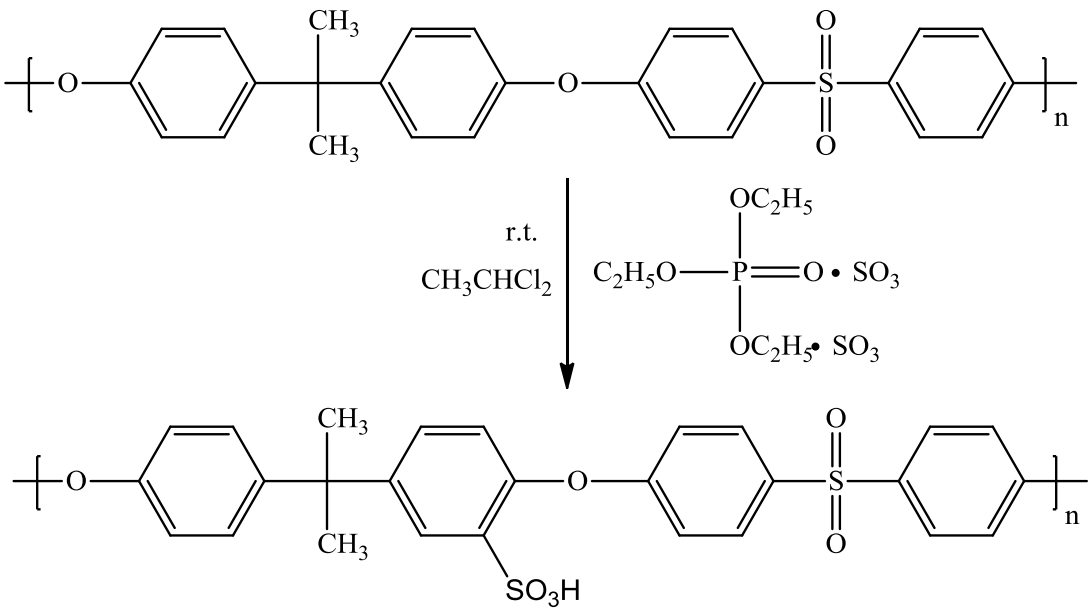

Figure 1.30: Sulfonation using a SO3/TEP complex[77]

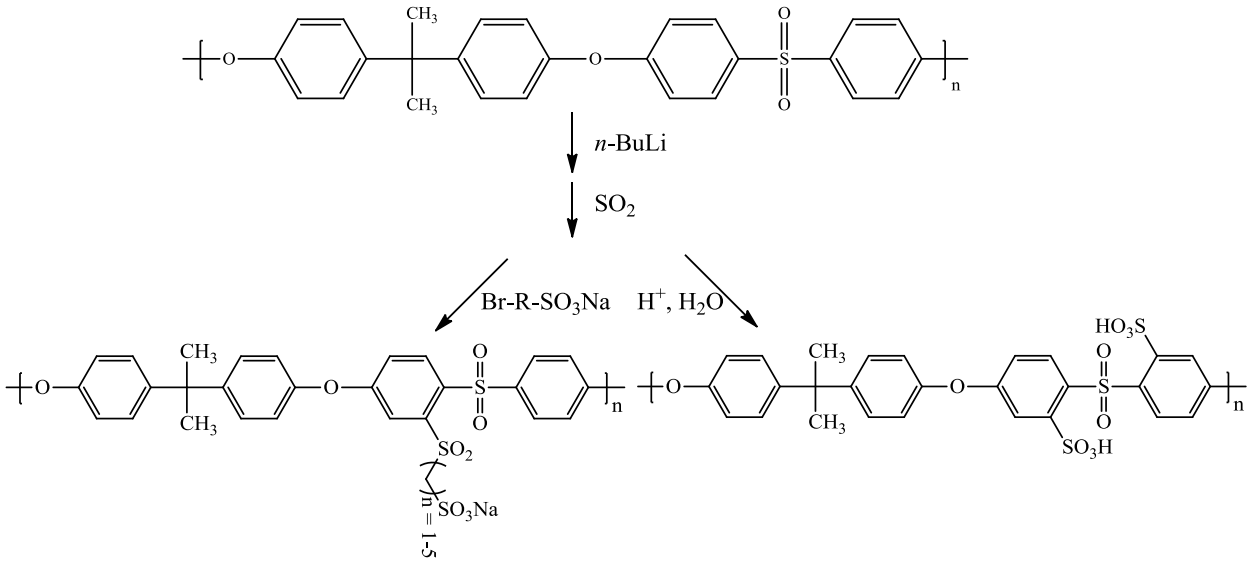

Figure 1.31: Chemical structures of sulfonated polysulfones, post-sulfonation using lithiation.

The pre-sulfonation method is also effective at solving this problem and can be used to synthesize the copolymer directly by polycondensation. All of the reactions using the pre-sulfonation method for the synthesis of sulfonated poly(arylene ether sulfone)s use the monomer 3,3'-disulfonated-4,4'-dichlorodiphenyl sulfone (SDCDPS) which was first developed as a flame retardant material by Lloyd Robeson for Union Carbide.[116] Ueda et al. was the first to report the use of the monomer for polymer synthesis, with the McGrath group further developing the polycondensation reaction and studying the directly disulfonated poly(arylene ether sulfone) membranes for fuel cell applications.[100,117]

The SDCDPS monomer was prepared 4,4'-dichlorodiphenyl sulfone by reacting it with fuming sulfuric acid to form the disodium salt (Fig.1.32).[100] Because this sulfonation reaction occurs by electrophilic aromatic substitution, the preferred position for the acid group is meta to the sulfonyl group and ortho to the chlorine substituent. The resultant product required extensive purification, including multiple recrystallizations from an isopropanol/water mixture, since there is a large amount of salt (NaCl) produced from the reaction and the subsequent neutralization

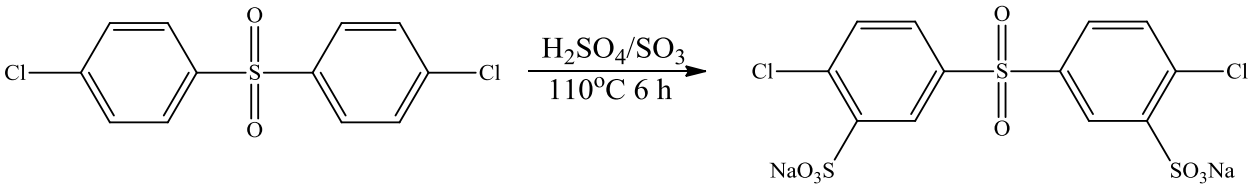

Figure 1.32: Synthesis scheme of the disulfonated monomer SDCDPS from the sulfone precursor. The product was neutralized with sodium chloride and then with sodium hydroxide to obtain the sodium salt form.

A UV-vis spectroscopy technique was developed by the McGrath group to accurately measure the amount of residual sodium chloride in the SDCDPS monomer.[118] This was developed because although the recrystallization was effective at removing the salt impurity, it was not feasible for mass production since it would require a substantial amount of extra time and solvent. In addition, recrystallization results in loss of monomer, and therefore decreased yield. If the known salt impurity can be calculated, the crude monomer can be used directly as is. Once the impurity percentage was taken into account for the monomer, high molecular weight copolymers can be achieved regardless of the amount of salt present in the SDCDPS monomer.[118]

The use of the pre-sulfonated monomer provides many advantages for the sulfonated poly(arylene ether sulfone) membranes over the post-sulfonated materials. Most notably, the degree of sulfonation, the microstructure of the disulfonated units along the chain, and the position of the acid groups can be controlled using this method by simply changing the relative concentrations of the sulfonated and non-sulfonated monomers, i.e. SDCDPS and dichlorodiphenylsulfone. In addition, the position of the sulfonic acid group, ortho to the chlorine, can only be achieved by using the pre-sulfonated route. This is significant because it has been demonstrated that when the sulfonic acid group is at this position it is more acidic and thermally stable than having the sulfonic acid groups on the other available positions.[101,119] Moreover, the directly polymerized method allows for random placement of the disulfonate groups along the chains, and thus provides for a random, but homogeneous, copolymer.

The first disulfonated poly(arylene ether sulfone) synthesized by the McGrath group via this method was a copolymer comprised of 4,4’-biphenol instead of the Bisphenol A monomer. A series of materials were investigated with a systematically varied ratio of the disulfonated and

non-sulfonated monomers. The disulfonated monomer was significantly less reactive toward nucleophilic aromatic substitution relative to dichlorodiphenyl sulfone. Thus, higher temperatures and longer reaction times were required relative to some of the more traditional poly(arylene ether sulfone) polymerizations. *N*-Methyl-2-pyrrolidone (NMP) was used as the solvent for the reactions to dissolve the copolymers and to accommodate the high temperatures required for the reactions. The reaction was refluxed with toluene prior to polymerization in order to azeotropically remove water from the system. Thus, by using the reflux step and a high reaction temperature, high molecular weight was achieved for the polymer using the direct polymerization method. In addition, by varying the relative compositions of the SDCDPS and dichlorodiphenyl sulfone monomers, the IECs of the copolymers could be easily controlled to the desired values. The resultant polymers were denoted as BPS-XX, with XX referring to the mole percent of the SDCDPS monomer as compared to the dichlorodiphenyl sulfone.[101,119-120]

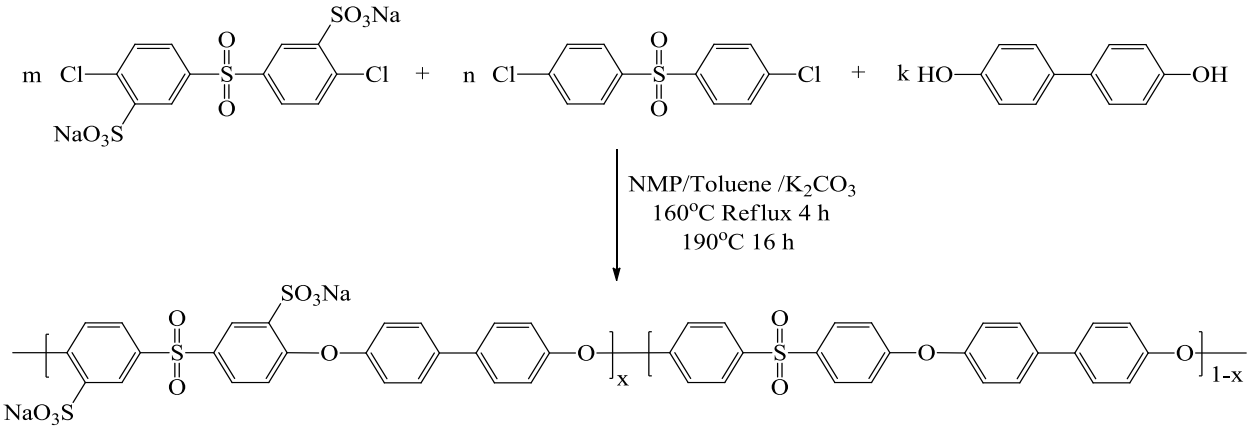

Figure 1.33: Synthesis of BPS-XX with SDCDPS, dichlorodiphenyl sulfone, and biphenol. The copolymers were denoted as BPSH-XX when in the acidified form.[84]

For the series of linear biphenol sulfone (BPS-XX) polymers, fifty percent disulfonation (BPS-50) was the maximum disulfonation level that could be used for fuel cell membranes. Any

copolymers that had disulfonation degrees above this level either swelled excessively in water or were water soluble. In the acidified form, the water uptake increased from 56% to 148% for BPSH-50 to BPSH-60. The proton conductivity and water uptake all increased as the degree of disulfonation was increased, with conductivities reaching as high as 0.17 S/cm (in liquid water at 30^{o}C) for the BPSH-60 membrane, although this membrane swelled excessively in water and lost all mechanical integrity. The BPSH-40 and BPSH-50 membranes swelled considerably less (water uptake less than 70 wt%) and had conductivities above 0.08 S/cm.[101]

Further enhancements of related membrane systems were explored by McGrath et al. that included introducing a partially fluorinated and a benzonitrile hydrophobic component to improve the durability and performance of the PEMs (Fig. 1.34).[108-110,121-122] The nitrile groups reduced the water uptake and provided slight increases in the water conductivities in liquid water, while the partially fluorinated component decreased the high frequency resistance in the membrane electrode assemblies. These components were found to be particularly useful for direct methanol fuel cell systems.[121,123] However, a major drawback of these membranes was that they required a high level of hydration for effective proton transport. Because of this dependence on the hydration level, the performance of the membrane significantly decreased at lower levels of relative humidity.[8] One approach to improve upon the performance of such membranes at lower humidities was to use the post-sulfonation method to create highly sulfonated membranes (Fig.1.35). Unfortunately, these membranes suffered from excessive swelling and poor mechanical properties.[124]

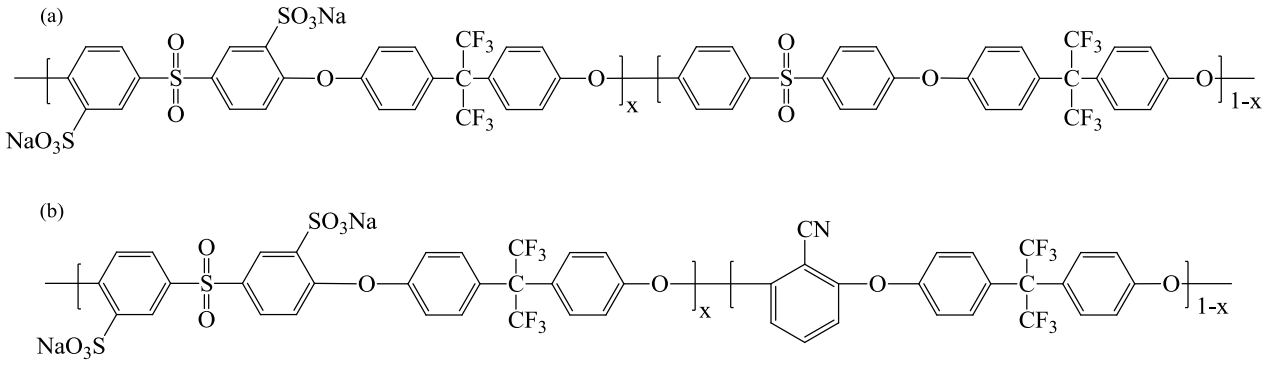

Figure 1.34: Chemical structures of disulfonated poly(arylene ether sulfone)s using the direct polymerization synthesis method (a): Partially fluorinated sulfone based upon hexafluorobisphenol A, and (b): disulfonated poly(arylene ether sulfone)s with nitrile and partially fluorinated groups.

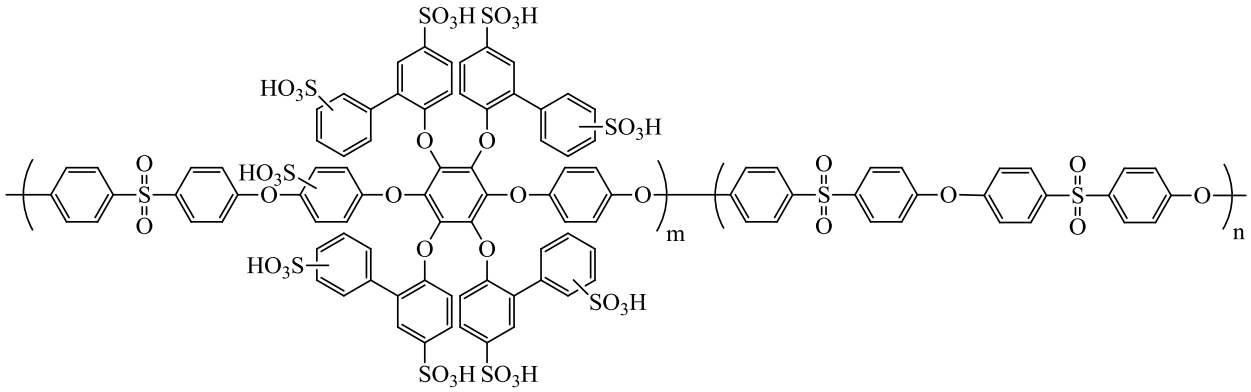

Figure 1.35: Highly sulfonated poly(arylene ether sulfone)s using a post-sulfonation method

1.3.1.2 Sulfonated poly(arylene ether ketone)s

Poly(arylene ether ketone)s, like the polysulfone-based membranes, exhibit excellent mechanical and thermal properties. In addition, many of these materials are semi-crystalline and this contributes to good properties at elevated temperatures. Their semi-crystallinity, which is not

typically associated with poly(arylene ether)s, is due to strong dipolar interactions between the ketone groups and the rigid and linear structure of the poly(arylene ether ketone) backbone. However, the semi-crystalline poly(arylene ether ketone)s generally have low solubility in most organic solvents, and this can be challenging when synthesizing high molecular weight polymers.[8] Thus, although the post-sulfonation method can be used to obtain sulfonated poly(arylene ether ketone)s[125-127] the most utilized method is the direct synthesis from pre-sulfonated monomers based upon the technique used for the sulfonated poly(arylene ether sulfone)s.

Early syntheses of poly(arylene ether ketone)s by Marvel et al. used Friedel-Crafts polyacylation. However, synthesis via nucleophilic aromatic substitution is currently the favored method.[125,127] The development of sulfonated ketone monomers was important for direct synthesis of sulfonated poly(arylene ether ketone)s and it was found that the sulfonic acid groups often disrupted chain packing, and hence any potential for crystallization.[8,102] In addition, direct synthesis utilizing pre-sulfonated monomers avoided potential crosslinking and degradation reactions associated with the harsh conditions required for post-sulfonation of poly(arylene ether ketone)s.[126] Because of the lower reactivity of the aromatic ketone halide relative to an aromatic sulfone halide toward nucleophilic aromatic substitution, a difluorinated monomer is often used instead of a dichloride monomer. This is because for nucleophilic aromatic substitution, fluorine-substituted monomers are more reactive than chlorine-substituted monomers. Furthermore, addition of sulfonic acid groups on the aromatic ketone, further decreases the reactivity, and high molecular weight copolymers have only been reported using the fluorinated dihalide monomers.[128-129] An example of a synthetic scheme to produce a pre-sulfonated monomer is shown in Figure 1.36, and examples of sulfonated poly(arylene ether ketone) copolymers

(SPAEKs) that have been prepared by both direct polymerization and post-sulfonation are shown in Figure 1.37.[102-104,128-129]

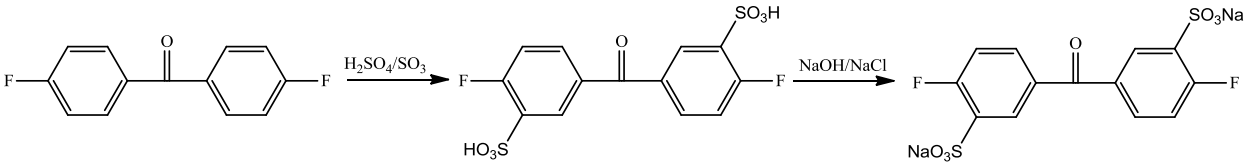

Figure 1.36: Synthesis of a disulfonated monomer, sodium 5,5'-carbonylbis(2-fluorobenzene sulfonate)

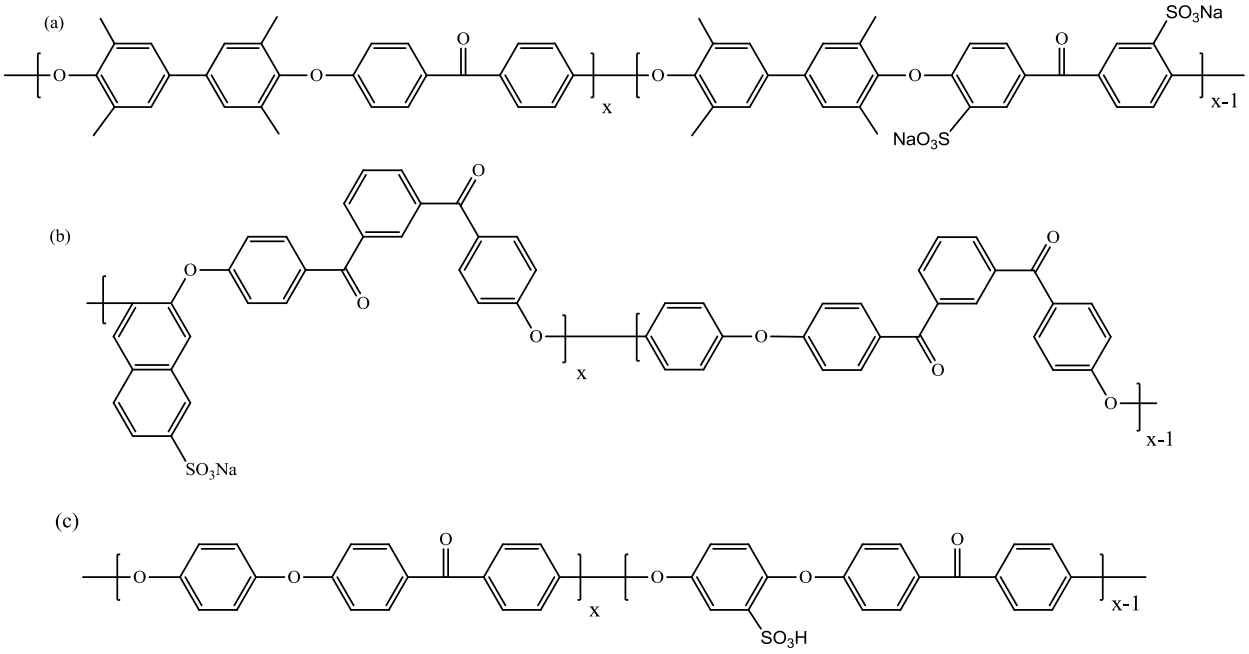

Figure 1.37: Chemical Structures of various sulfonated poly(arylene ether ketone)s (SPEAKs): (a) Direct synthesis of SPEAK with tetramethyl biphenol, (b) Direct synthesis of a SPEAK with a diketone and hydroquinone, (c) SPEAK prepared by post-sulfonation with sulfuric acid.

As was the case for the polysulfones, the direct synthesis method allowed for placement of the sulfonic acid groups on the deactivated ring which formed a more stable and acidic site.[8] SPEAK membranes that had been prepared by direct copolymerization of disulfonated

monomers had high conductivities as compared to post-sulfonated membranes with comparable IECs and degrees of sulfonation.[130] Guiver et al. reported proton conductivities as high 0.18 S/cm at 100^{o}C for an eighty percent sulfonated membrane (an eight to two ratio for sulfonated and non-sulfonated monomers), with relatively minimal water uptake of 27.2%. However, the performance was not nearly as high at lower temperatures. A sulfonated poly(arylene ether ketone) based upon tetramethyl biphenol with an IEC = 1.52 had a conductivity of 0.07 S/cm at 25^{o}C and 0.134 S/cm at 80^{o}C. This is comparable to that of the poly(perfluorosulfonic acid) Nafion® membrane.[102] An interesting effect on conductivity observed by Robertson et al., was that casting membranes from solvents such as DMF (dimethylformamide), DMAc (dimethylacetamide), and NMP (N-methyl-2-pyrrolidone) produced membranes with different conductivities.[131] The membranes cast from NMP produced the best results, with DMF leading to membranes with the lowest conductivities. This was attributed to interactions between the solvents and the sulfonic acid groups of the sulfonated poly(arylene ether ketone), which had different morphologies depending on the casting solvent. Interaction between DMF and the sulfonated copolymer resulted in the change in morphology, and decreased proton conductivity. These results were further confirmed and explored by Kim et al., who showed that membranes cast from NMP had better performance and reduced methanol crossover, in addition to increased proton conductivity.[130]

1.3.1.3 Other poly(arylene ether)s and wholly aromatic sulfonated copolymers

Although sulfonated poly(arylene ether ketone)s and sulfonated poly(arylene ether sulfone)s (SPAESs) have been the most extensively studied sulfonated membranes, many other poly(arylene ether)s and wholly aromatic sulfonated copolymers have been explored as possible proton exchange membranes. Some of these include sulfonated polyimides, sulfonated

poly(arylene ether benzonitrile)s and sulfonated poly(phenylene)s. The sulfonated polyimides and poly(arylene ether benzonitrile) membranes have been synthesized via polycondensation reactions, similar to both the sulfonated polysulfone and polyketones. However, this synthesis route is not available for poly(phenylene)s since they do not contain an ether linkage.[8,132] Reactions such as Suzuki[133-134] and nickel[135] coupling have been investigated for polymerization of the polyphenylenes, and Diels-Alder polymerization has also been performed.[111] The unique structure of sulfonated polyphenylenes with a wholly aromatic backbone and no functional linkage produces an extremely durable membrane that is very resistant to oxidation and hydrolysis. However, this can be very problematic for synthesis since poly(phenylene)s have low solubility in most organic solvents, and thus high molecular weights can be difficult to achieve.[8] Conversely, this unique structure also allows for high levels of sulfonation while retaining only modest levels of water uptake. Ohira et al. recently reported a highly sulfonated polyphenylene membrane (IEC = 2.65) with a conductivity of 0.28 S/cm at 95% RH and a water uptake of 56% (structure shown in Figure 1.38). The performance however at lower hydration levels was still not as high as that of the Nafion®.[136] Nevertheless, sulfonated polyphenylenes could provide a potentially interesting alternative to the poly(perfluorosulfonic acid)s and the sulfonated poly(arylene ether)s for use as proton exchange membranes.

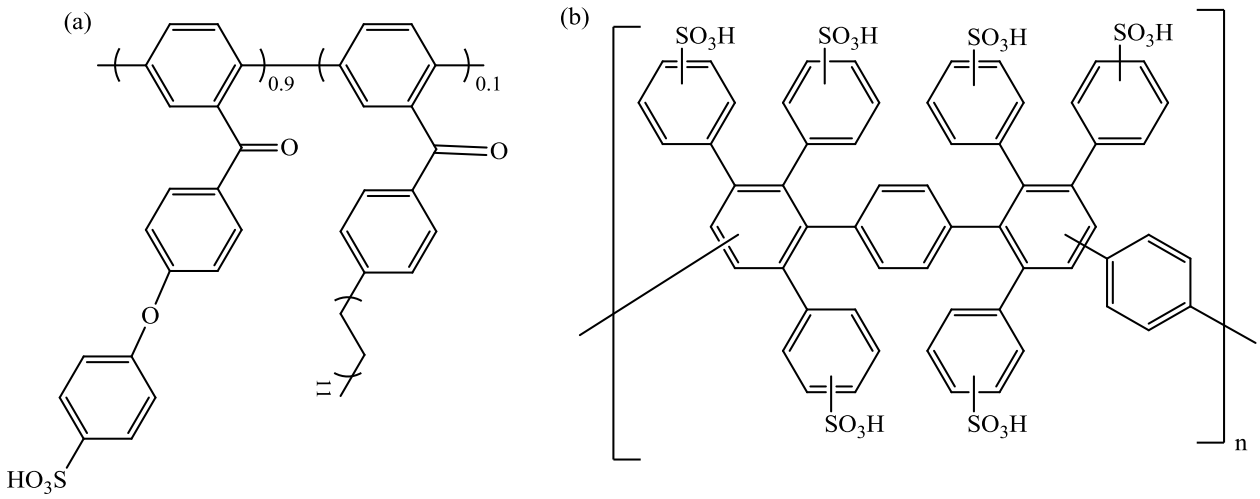

Figure 1.38: Chemical structures of sulfonated polyphenylenes: (a) Synthesized via Nickel (0) catalyzed coupling, and (b) Synthesized via Diels-Alder polymerization and post-sulfonated.

Sulfonated poly(arylene ether benzonitrile)s have a meta linkage in their backbone on the aromatic ring containing the nitrile group (Fig. 1.39). SPAESs that contain the benzonitrile groups have reduced water uptake and swelling compared to other sulfonated polysulfones with similar IEC values, and the copolymers with the benzonitriles also have low methanol permeabilities. In addition, these materials lead to fuel cells with greater power density and improved cell performance, with >1000 h of operation in direct methanol fuel cells.[121] The nitrile groups can provide better adhesion of the polymer membranes to the electrodes, and this has been attributed to polar interactions between different functional groups. Unfortunately, the nitrile group and the meta-linkage of the copolymers reduces the mechanical strength of the membrane, and has been proposed to potentially compromise long term durability.[8,121] Incompatibility between the Nafion® electrodes and the sulfonated poly(arylene ether benzonitrile)s, and this could also affect long term performance.[120]

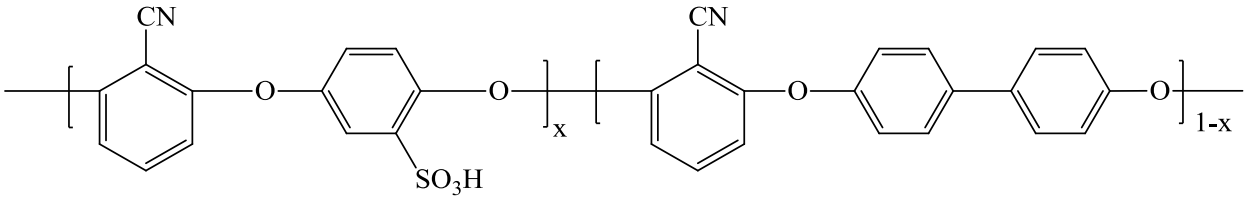

Figure 1.39: Chemical structure of a random sulfonated poly(arylene ether benzonitrile) synthesized via direct polymerization.[108]

Sulfonated polyimides offer many benefits as potential PEMs, such as good mechanical strength, low liquid and gas permeability, high thermal stability, and relatively easy film forming capabilities.[8] These polymers can consist of either a five (phthalic) or six (naphthalenic) membered imide ring (Fig. 1.40). They are synthesized from the two step polymerization of a dianhydride and a diamine. Although phthalimide structures were initially used, they were found to be more susceptible to hydrolysis and produced membranes with lower conductivities.[106,137-138] Therefore the six membered naphthalimide structures have been investigated as sulfonated PEMs, although hydrolytic stability is still an issue for these membranes.[139-140] Direct polymerization of the polyimides using the pre-sulfonated monomer approach allows for good control over the degree of sulfonation and positions of the sulfonic acid groups. Conductivities of the copolymers are similar to those of the sulfonated polysulfones with values reported above 0.1 S/cm at 30^{o}C with IEC values around 2.00 similar to those of other copolymers.[141] However, like the sulfonated poly(arylene ether sulfone)s and sulfonated poly(arylene ether ketone) membranes, the conductivities drop significantly as the relative humidity level is decreased. This is attributed to the dependence of the membranes on water for proton transport and the weaker acidity of the sulfonic acid groups as compared to Nafion® membranes.

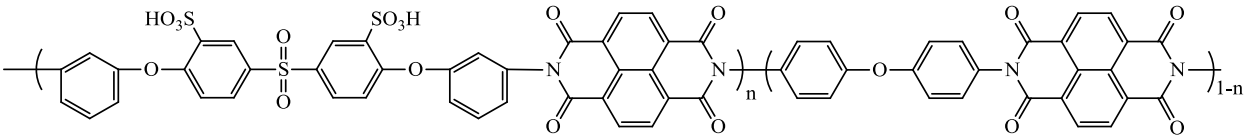

Figure 1.40: Chemical structure of a six membered naphthalenic sulfonated polyimide

1.3.2 Poly(arylene ether)s for use as gas separation membranes

Poly(arylene ether)s and polyimides are typically glassy thermoplastic polymers that are renowned for their mechanical properties and thermal stability. They are often spun to form hollow fibers and fabricated into hollow fiber modules for separations of gases. The most studied poly(arylene ether) membranes for gas separations include: poly(arylene ether sulfone)s, poly(arylene ether ketone)s, and poly(phenylene oxide)s.[142-149] In fact, polysulfone and polyphenylene oxide hollow fibers are currently used as the principle membrane materials for gas separation by Air Products and Aquilo.[150] Unlike poly(arylene ether sulfone)s and poly(arylene ether ketone)s, poly(phenylene oxide) is usually synthesized through an oxidation polymerization method (Fig. 1.41 depicts this mechanism). In this reaction, oxygen (O_2) abstracts a hydrogen from the phenolic monomer to create a radical that can then combine in two ways. Carbon-carbon coupling results in a "dead" quinone, while carbon-oxygen coupling forms a dimer which can then react in another step reaction with another radical phenolic species.[151] The choice of an amine catalyst and solvent can limit the carbon-carbon coupling and lead to ultra-high molecular weight polymers.[152-155]

Poly(arylene ether)s were some of the first materials studied as potential membranes for gas separation in the early 1980's. The commercial availability of poly(2,6-dimethylphenylene oxide) and polysulfone, along with their high T_g's and the amorphous nature of these materials, were part of the reasons for the interest in these polymers.[142,145] Some of the commercial

poly(arylene ether ketone)s and aromatic polyamides are semi-crystalline and the crystalline regions have low gas permeabilities. However, studies have been done on gas transport through substituted poly(arylene ether ketone)s where the crystalline phase has been suppressed by bulky groups.[149,156]

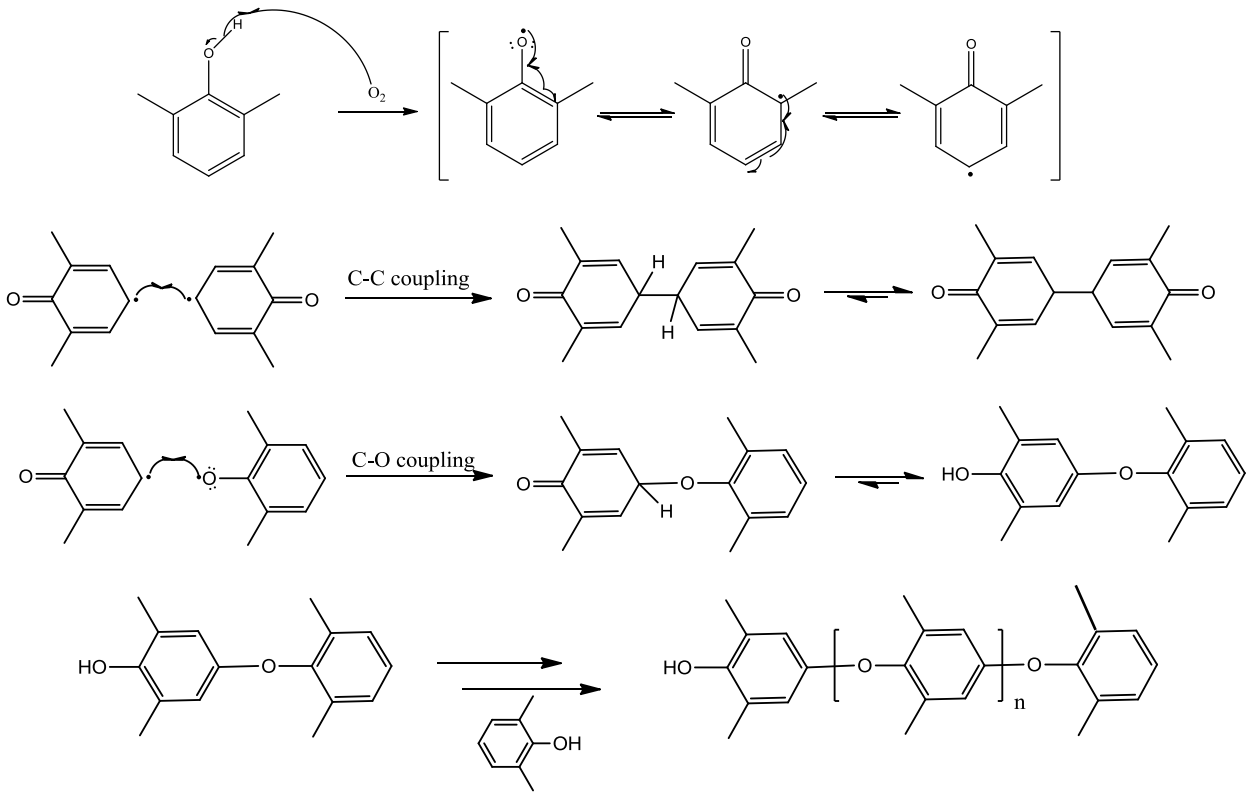

Figure 1.41: Mechanism of oxidation polymerization used to synthesize poly(phenylene oxide)

Backbone structure, along with pendant groups, has been shown to have an effect on the gas transport properties of PAEs. Backbone structure can be altered for polysulfone with the choice of the bisphenol or biphenol monomer that is polymerized with the sulfone. Generally the bisphenol monomer is preferred due to the presence of the isopropylidiene groups which increases free volume and reduces chain packing. As shown with a study by Paul et al., the bridging group had little effect on gas transport properties except for the case of incorporating hexafluorobisphenol A. This polymer had over twice the permeability relative to the other

polymers with only a small drop in selectivities for both CO_2/CH_4 and O_2/N_2 gas pairs.[146] Further studies by Paul et al. investigated effects of symmetry and pendent group placement on the bisphenol monomer. Figure 1.42 shows structural variations for polysulfones.[157-158]

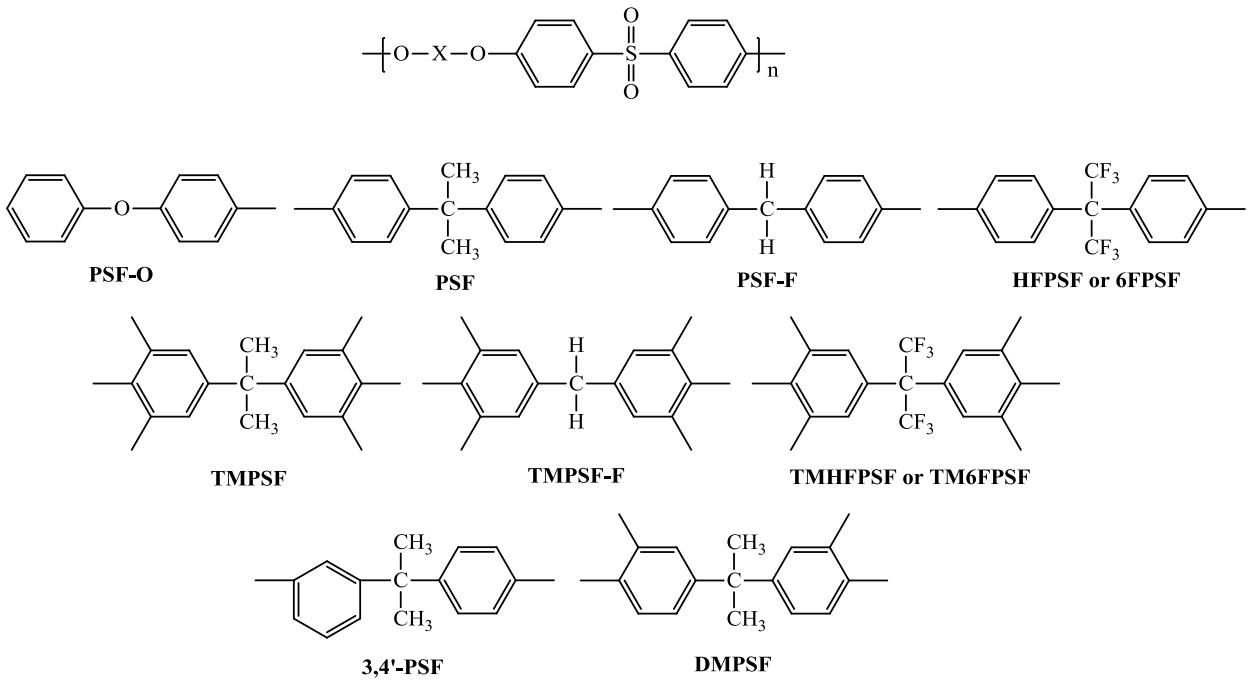

Figure 1.42: Structural variations of polysulfone: (a) isopropylidiene group, (b) pendent groups, (c) asymmetrical bisphenols

Addition of the tetramethyl groups on the bisphenol caused a greater increase in permeability of the polysulfones than using a hexfluoroisopropylidene bridging group, with only a minimal decrease in the selectivity. Combination of the hexafluoroisopropylidene bridging groups with the tetramethyl substituents produced a poly(arylene ether sulfone) that was ten times more permeable than the polysulfone that contained bisphenol A.[158] This same trend was found for methyl substituted poly(arylene ether ketone)s. However, disruption of the crystallinity caused a noticeable decrease in selectivities.[156] The methyl groups caused constrained the mobility and reduced packing efficiency, and this led to a dramatic increase in permeability. For polymers

containing asymmetric bisphenols, higher selectivity and lower permeability were observed, and this was proposed to be a result of increased constraints on mobility and better packing efficiency.[157]

Substitution with bulky and highly polar groups has been the major focus of investigations with poly(phenylene oxide)s, but poly(arylene ether sulfone)s and poly(arylene ether ketone)s with such groups have also been studied. Most of the substitutions on poly(phenylene oxide)s have been done in post-modification reactions, since the oxidative polymerization is very sensitive to the ortho functional group on the phenol. Steric hindrance from bulky groups leads to a high amount of carbon-carbon coupling and quinone formation, while polar groups inhibit oxidation due to increased oxidation potential of the phenol.[154] Transport of gases through poly(2,6-diphenyl phenylene oxide) decreased in both permeability and selectivity relative to the dimethyl analogue, while poly(phenylene oxide) without any substituents is semi-crystalline and therefore unsuitable for gas separation membranes.[159] Post-modification of poly(2,6-dimethylphenylene oxide) has been accomplished on both the open aromatic positions and also on the methyl groups.[144,160-163] In the cases of poly(arylene ether sulfone)s and poly(arylene ether ketone)s, the polymers are usually directly synthesized with the substitution performed on the monomers before polymerization.[59,147,149] These substituent groups have included trimethylsilyl, triphenylsilyl, nitro, bromo, carboxylic acid, and amines (Fig. 1.43).[143-144,147,161,163-168]

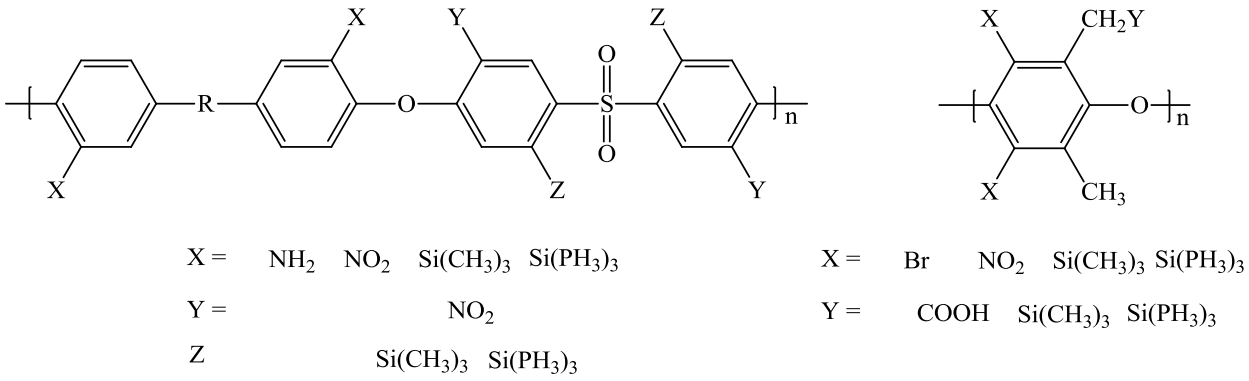

Figure 1.43: Examples of substituent groups on poly(arylene ether sulfone)s and poly(phenylene oxide)s

Substitution with amines, nitro groups, and carboxylic acids all lead to polymer derivatives with slightly increased selectivity and decreased permeability.[147,160,163-164] These substitutions seem to follow the "traditionally" observed trend with gas separation membranes, which is a trade-off relationship between permeability and selectivity. Introduction of polar groups in these polymers decreased free volume, which caused the observed results with both the polyarylene ether and poly(phenylene oxide) membranes. However, the nonpolar trimethylsilyl and bromine substituents led to different results. In the poly(phenylene oxide) series, when trimethylsilyl or bromine substituents were on the polymer backbone, a large increase in permeability was observed. Bromination of poly(2,6-dimethylpolyphenylene oxide) caused a two-fold rise in permeability with no decrease in selectivity. While the trimethylsilyl substitution on the backbone resulted in a 4-fold increase in permeability, with selectivity maintained for all gas pairs except CO_2/CH_4.[144,163] Trimethylsilyl groups produced similar effects on transport properties of the polysulfones with substitution on the bisphenol producing more permeable polymers than substitution on the sulfone moiety.[165,167] Substitution of triphenylsilyl groups on both the polysulfones and poly(phenylene oxide)s produced similar results as the polar groups, with only slightly better selectivity and reduced permeability for gas separation.[163,165] The

introduction of aromatic substitute groups in triphenylsilyl most likely increased packing density and efficiency, causing the observed change in gas transport properties.

1.4 Nonlinear Based Poly(arylene ether) Membranes

1.4.1 Nonlinear sulfonated poly(arylene ether)s for use as PEMs

1.4.1.1 Crosslinked sulfonated poly(arylene ether)s

The proton conduction through most charged polymer membranes depends on water to enhance transport of the protons. Most of these polymers have strongly acidic sulfonic acid substituents on aromatic rings to provide sites for protons as well as hydrophilicity of the polymer. The general trend observed for transport of protons through sulfonated polymers is that higher concentrations of acid groups on the polymer result in higher proton conductivity. However, if the degree of sulfonation is too high, the membranes do not have sufficient mechanical integrity when they absorb water and they can even become water-soluble. One possible solution to this problem is to synthesize crosslinked polymers, because this could allow for high sulfonation levels with improved mechanical properties.[169]

Many different approaches to chemically crosslink sulfonated polymer systems have been described in the literature with various different chemical structures.[170-174] A relatively easy approach that has been explored to achieve crosslinked networks is to endcap a linear polymer with unsaturated end groups, and then cure the material using a crosslinking reaction. Some representative systems are shown in Figures 1.44 and 1.45, and these produced highly crosslinked materials. Figure 1.44 was thermally cured via heating at 250^{o}C, while Figure 1.45 was cured with the addition of a free-radical. The networks had lower water uptake as compared

to their linear analogues with similar IECs and good proton conductivity (~ 0.13 (S/cm) in liquid water at 30°C). [172,175]

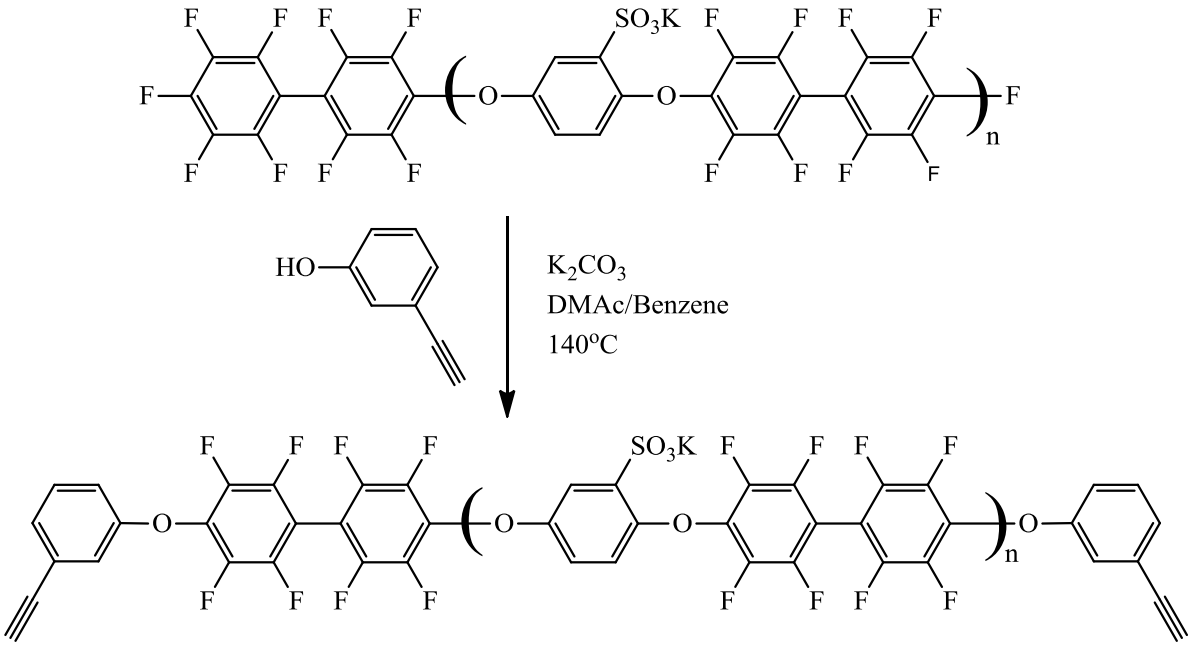

Figure 1.44: Alkyne endcapped poly(arylene ether)

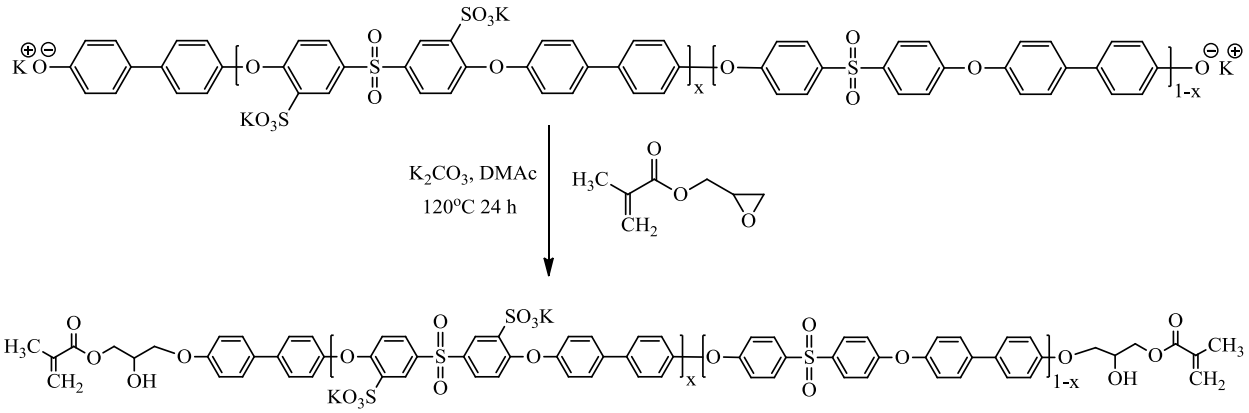

Figure 1.45: Acrylate endcapped random poly(arylene ether sulfone)

Interestingly for the crosslinked polysulfone, when the ratio of hydrophilic to hydrophobic repeat units was varied, there was little effect on the proton conductivity. However a significant

influence on the water uptake was observed. In a later paper by Lee et al., an ethynyl-terminated copolymer was crosslinked via thermal annealing, in the same fashion as Figure 1.44. Three ethynyl end groups reacted forming a new aromatic ring, connecting the three polymer chains. However due to the mono sulfonated monomer used, even with 95% of the repeat units belonging to the hydrophilic segment the IEC could only reached 1.96 meq/g.[173] Upon crosslinking the 95% hydrophilic crosslinked copolymers had water uptake and conduction almost identical to the BPSH-45 copolymer. However the crosslinked copolymer only slightly outperformed the BPSH-45 random copolymer at reduced humidity conditions, with the Nafion® 212 membrane being far superior to both at these conditions.

Crosslinkable sulfonated polymers can also be obtained by including a crosslinkable site in the repeat unit of the polymer. Sulfonated poly(arylene ether ketone)s with crosslinkable sites in the backbone have been investigated due to their good thermal stability, mechanical strength, and high proton conductivities.[8,170,174] Guiver et al. used glycerol derivatives to crosslink the polymer chains via the pendent sulfonic acid groups on the aromatic backbone using a condensation reaction (Fig. 1.46).[170] The crosslinking resulted in a substantial decrease in water uptake by the membranes (79 wt% uptake for a linear polymer to 32 wt% for the analogous crosslinked network) and improved mechanical properties. Most of the membranes became completely insoluble with only a small mole percent of the crosslinking agent added (1-3 mol percent). However since the crosslinks involved the sulfonic acid groups, the proton conductivity was unsurprisingly very low, with the highest conductivity value of only 0.06 S/cm and most around 0.02 S/cm. A benzoxazine linking agent was also investigated, but those reactions also involved reaction of the sulfonic acid groups.[174]

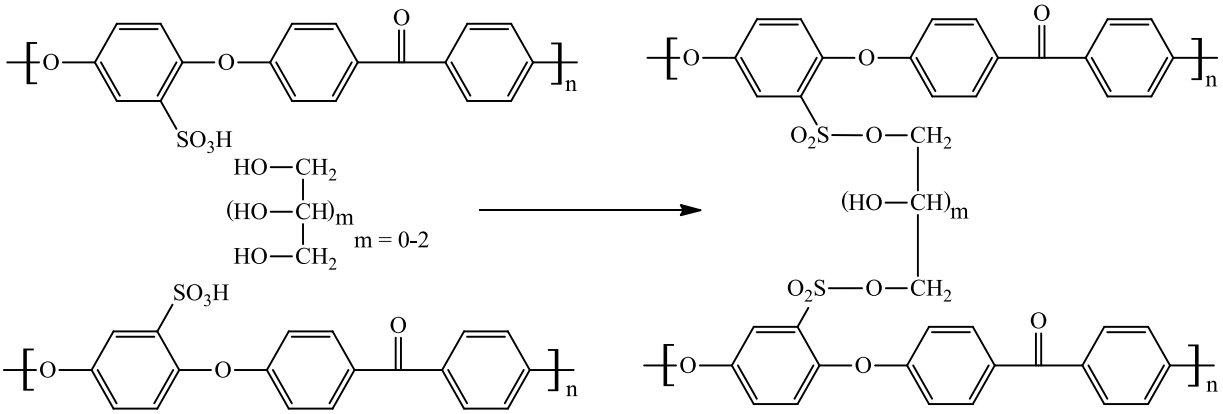

Figure 1.46: Crosslinking reaction of a sulfonated poly(arylene ether ketone)

1.4.1.2 Highly Branched and Grafted Poly(arylene ether)s

Highly branched and other specialty polymers like the crosslinked polymers allow for increased mechanical properties due to higher achievable molecular weights and increased chain entanglements. Also highly branched copolymers and unique architectures have been used to achieve many different morphologies using a variety of synthetic approaches. By grafting an oligomer onto an existing polymer backbone, distinct phase separated morphologies were observed.[176-177] Guiver et al. developed a comb-shaped copolymer with a hydrophobic backbone and a hydrophilic chain that was grafted onto the main chain.[178-179] Initially the hydrophobic backbone in these systems was based on a partially fluorinated polymer using decafluorobiphenyl as one of the monomers with a sulfonated polystyrene grafted onto the backbone to form the comb-shaped polymer. However, the polystyrene aliphatic component was found to be too chemically unstable, and a fully aromatic system was made by using a similar approach to improve the polymer stability (Fig. 1.47).[176] Another fully aromatic polymer that was investigated used a poly(phenylene oxide) oligomer that was bound to the hydrophobic backbone via a Cu-catalyzed coupling reaction. Post-sulfonation was then used to substitute sulfonic acid groups on the poly(phenylene oxide) side chains. These polymers, like the block

copolymers to be discussed later in this dissertation, had phase separated morphologies and these were imaged by transmission electron microscopy (TEM). The phase separated morphologies allowed for a continuous proton channel that was most likely responsible for the excellent conductivities (> 10^{-2} S/cm at 30% RH) that these materials exhibited.

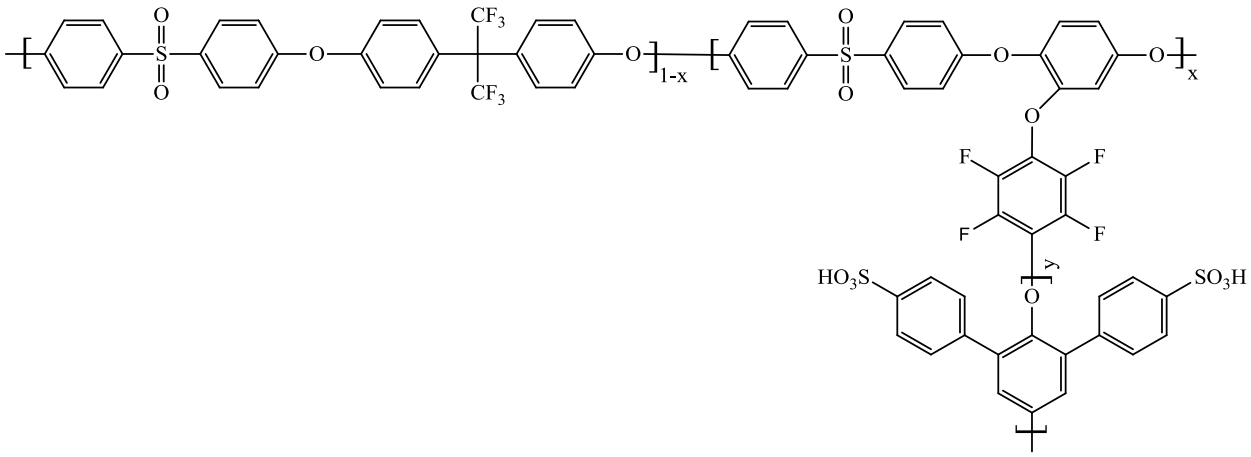

Figure 1.47: Comb-shaped fully aromatic sulfonated branched poly(arylene ether sulfone)

Jannasch et al. utilized a similar approach to the design of sulfonated branched copolymers with poly(phenylene oxide) comprising the backbone and poly(4-fluoro polystyrene) grafts (Fig. 1.48).[177,180] To synthesize these copolymers, benzylic methyl groups on poly(phenylene oxide) were lithiated to form macroinitiator sites, then 4-fluorostyrene was polymerized anionically from those sites. These graft copolymers were post-sulfonated in a relatively mild sulfonation reaction with trimethylsilylchlorosulfonate via electrophilic aromatic substitution. The electron donating effects of the ether and methyl substituents on the poly(phenylene oxide) backbone activated these polymers toward electrophilic aromatic substitution. An additional benefit of using this method is that it permitted a more homogeneous disruption of the sulfonic acid groups on the backbone, creating copolymers with some block-like character as opposed to the random distribution acquired with direct sulfonation using

sulfuric acid. Depending on the copolymer composition, either lamellar or cylindrical self-assembled morphologies were observed with distinct phase separation confirmed by both DSC and TEM. The proton conductivities of these graft copolymers were similar to or exceeded that of Nafion® at room temperature, however no data was reported for conductivities at lower relative humidities.

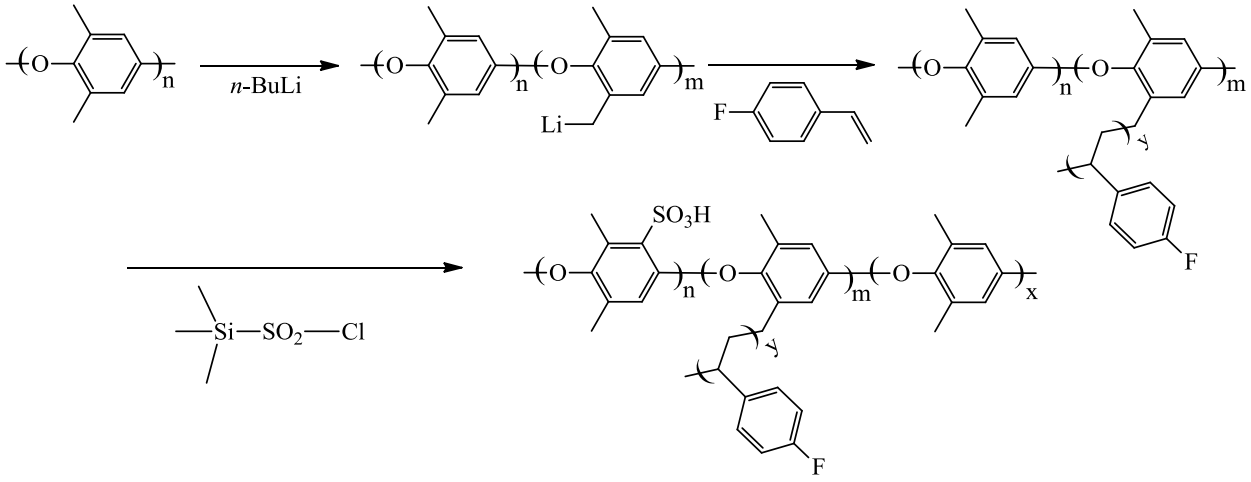

Figure 1.48: Partially sulfonated poly(phenylene oxide) with poly(4-fluorostyrene) grafts

Guiver and Jannasch, and many other research groups, designed membranes that had clearly defined hydrophobic and hydrophilic domains. The phase separated morphologies provided many desirable properties for proton exchange membranes. These materials usually consisted of an aromatic hydrophilic segment which was sulfonated, and either an aliphatic or aromatic backbone that the sulfonated segment was attached to. Two more examples are shown in Figures 1.49 and 1.50.[181-182]

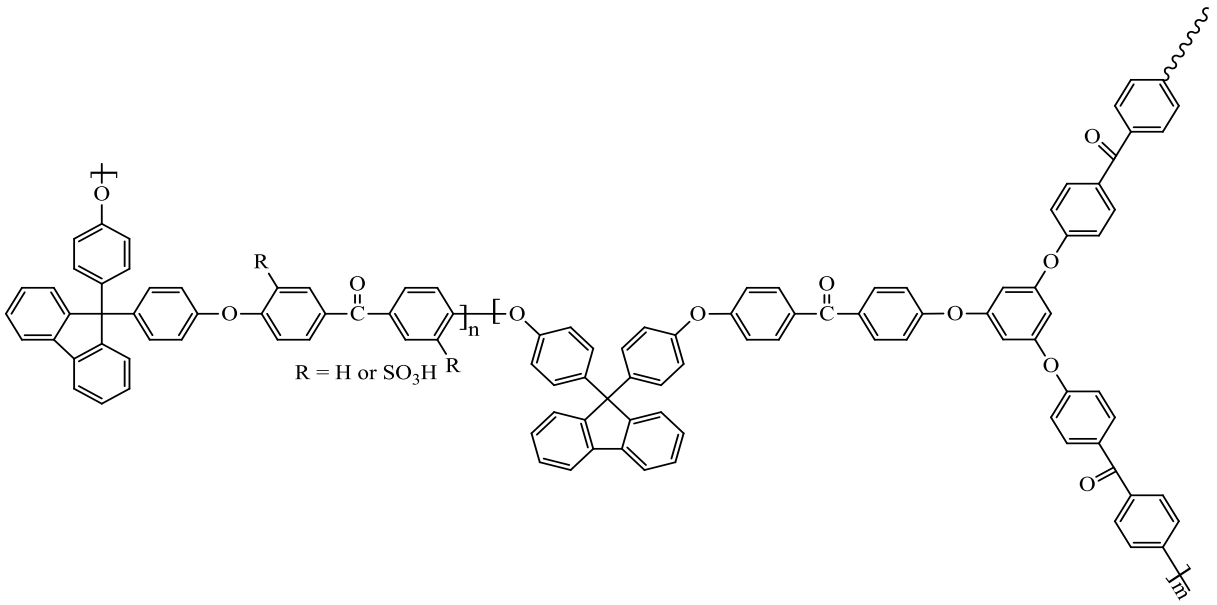

Figure 1.49: Highly branched wholly aromatic copolymer with a poly(arylene ether ketone) backbone

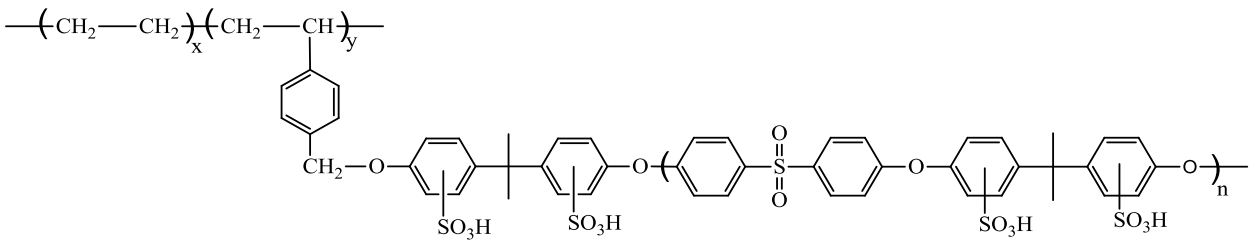

Figure 1.50: Post-sulfonated polysulfone grafted onto a polyethylene backbone

1.4.2 Nonlinear poly(arylene ether)s for gas separation membranes

Poly(arylene ether)s and their substituted derivatives have been shown to produce highly permeable gas separation membranes, but their selectivity and transport properties are inferior to many of the state-of-the-art polyimide and carbon sieving membranes.[77-78] In addition, like the polyimides, gas transport through these membranes can also suffer from plasticization effects. However, these materials are of great interest due to their economics, commercial availability, and excellent chemical/hydrolytic resistance. Thus, investigations of means to produce insoluble

poly(arylene ether) networks to improve transport properties and plasticization resistance have been conducted.[183-188]

Only a few studies have been reported on gas transport properties of crosslinked poly(arylene ether)s. However, some polyarylates and poly(arylene ether)s have been successfully crosslinked and gas transport properties through these materials have been reported. Paul et al. crosslinked poly(phenylene oxide) using a 100-W high intensity ultraviolet light with exposure time varied between 1.5 and 4 h. Benzylic hydrogens were abstracted and the resultant radicals crosslinked the polymer via radical combination.[187] The polymer was also blended with benzophenone, then the blend was crosslinked upon irradiation and the transport properties were compared to those of the crosslinked homopolymer. In both networks, the permeability of gases decreased and the selectivity increased upon crosslinking, thus corresponding to a decrease in free volume and increase in density. The transport rates through the material that had been blended with benzophenone were somewhat slower and selectivity was not as good as through the crosslinked poly(phenylene oxide) homopolymer. Interestedly, the polymer showed no increase in selectivity and decreased in permeability for the CO_2/CH_4 and O_2/N_2 gas pairs when higher intensity UV sources were used.[187] Subsequent studies by Paul et al. were conducted on polyarylates that contained both aromatic ketone groups and benzylic methyls. These materials were crosslinked by irradiation with UV light (Fig.1.51).[189-191] The crosslinked polymers exhibited reduced effects from physical aging, thus indicating that crosslinking was effective at reducing plasticization from carbon dioxide of the membranes.

In a series of patents to Zampini et al., polysulfone and poly(phenylene oxide) were chemically crosslinked by brominating the polymers, then treating them with ammonia (Fig. 1.52).[184-185] The bromination was a post-modification reaction of the benzylic methyl groups.

Films were then placed in an ammonia solution for various lengths of time. The crosslinked membranes had increased permeabilities with no significant change in selectivity for the O_2/N_2 gas pair and increased selectivity for the CO_2/CH_4 gas pair. This method increased both the permeability and selectivity for poly(phenylene oxide), however, the polysulfone didn't have the same results. While higher selectivities were observed for the polysulfone, the membranes experienced a decrease in permeability upon crosslinking. No mention of plasticization resistance of the crosslinked polymers was included in the patents.

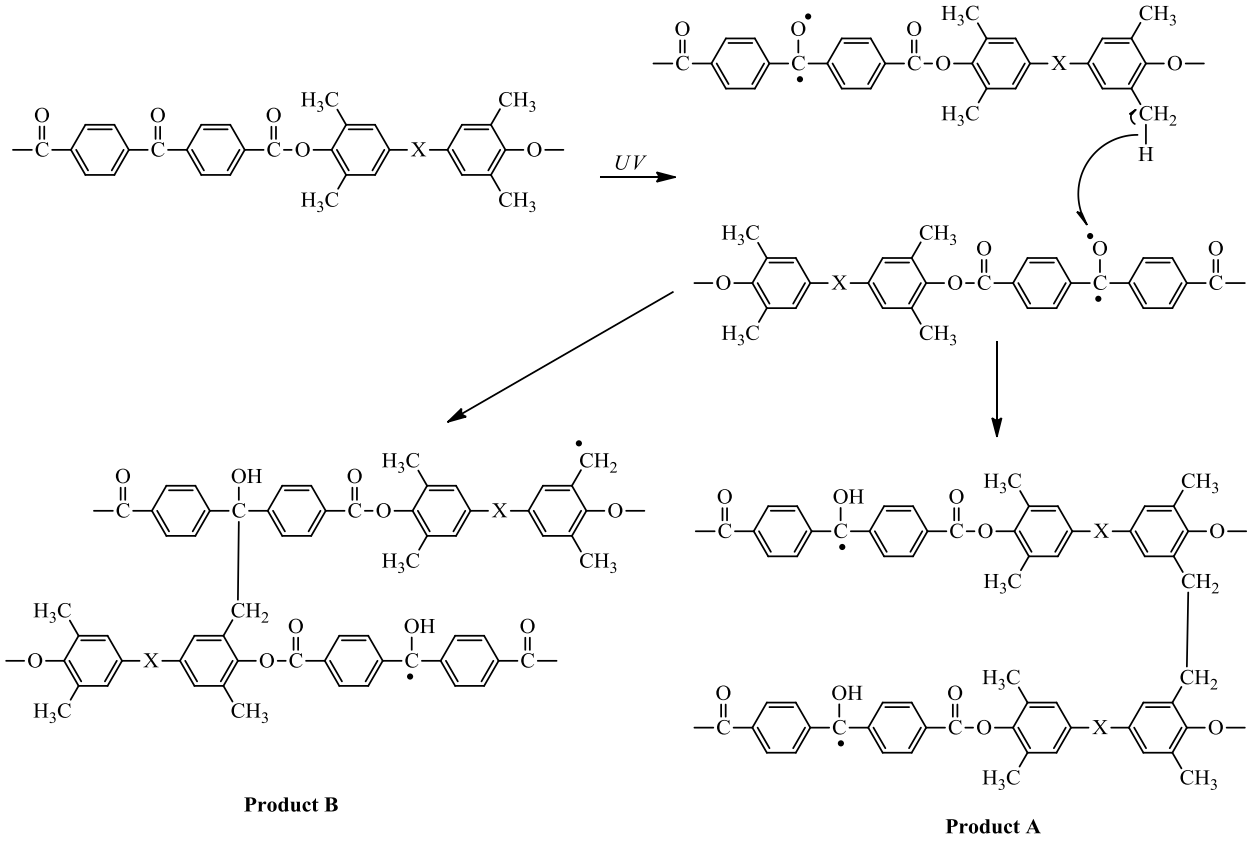

Figure 1.51: Proposed crosslinking mechanism with benzylic hydrogens in ketone based polyarylates

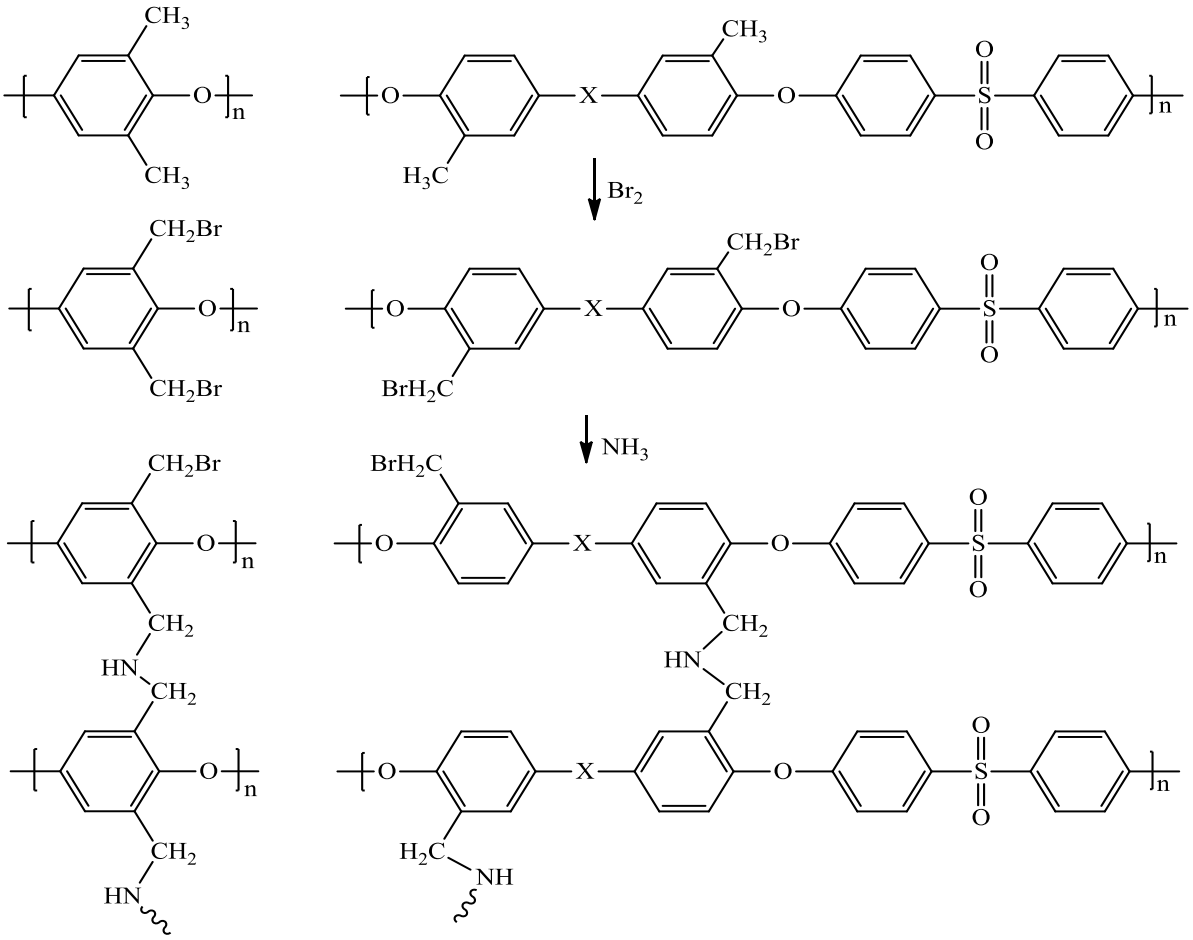

Figure 1.52: Crosslinking reaction using benzylic bromination and ammonia

1.5 Sulfonic Acid Containing Linear Poly(arylene ether) Hydrophilic-Hydrophobic Multiblock Copolymers

It has been proposed that the morphology of sulfonated random poly(arylene ether sulfone) copolymers could be one of the reasons for the poor conductivity at low humidity conditions. Although the sulfonated copolymers contained both hydrophilic and hydrophobic segments, the short random chain segments prevented the polymer from developing a well-defined phase-separated morphology.[192] However, multiblock copolymers have been widely demonstrated to form well-defined self-assembled phase separated morphologies. When the lengths (or volumes) of the two blocks are close to one another, the polymer will self-assemble

into a lamellar like morphology.[193] It has been suggested that this morphology would allow for faster water diffusion at reduced hydration levels, and that such morphologies should therefore lead to increased proton conductivities and performance under lower relative humidity conditions. Thus, sulfonated block copolymers have been studied as possible replacements for poly(perfluorinated sulfonic acid)s for use as proton exchange membranes.[8]

1.5.1 Sulfonated block copolymers based on aliphatic or partially aromatic backbones

The block copolymers that have been studied in this area are similar to the graft and branched polymers discussed earlier, and predominately include sulfonated polystyrene as the hydrophilic segment. Although, the block copolymers explored for these PEMs differ in the fact that the polymer backbones are completely linear. Both di and triblock copolymers have been synthesized, with the sulfonated poly(styrene-*b*-[ethylene-*r*-butylene]-*b*-styrene) (S-SBES)[194-196] and sulfonated poly(styrene-*b*-isobutylene-*b*-styrene) (S-SIBS)[197-200] being by far the most extensively studied (Fig. 1.53).

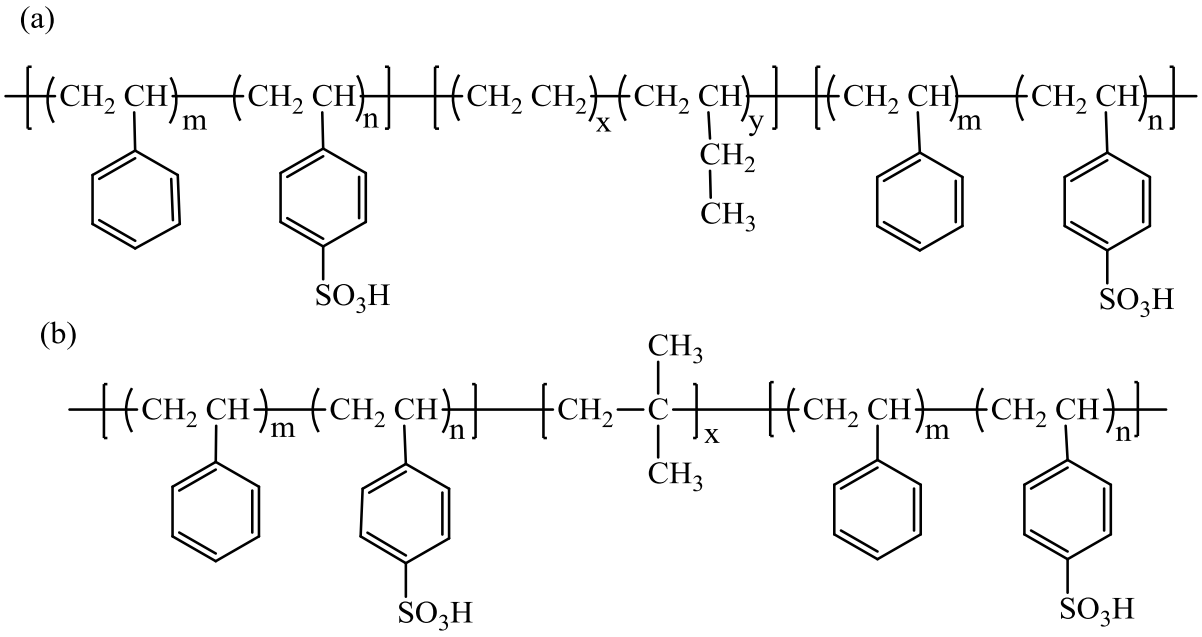

Figure 1.53: Chemical structures of (a) S-SBES, (b) S-SIBS

The S-SBES triblock copolymer, which was developed by Dais Analytic Corp., is prepared from the precursor poly(styrene-*b*-butadiene-*b*-styrene) which is reduced via hydrogenation, then sulfonated to form the targeted block copolymer.[8] The final product S-SBES is commercially available and can be cast from various organic solvents such as tetrahydrofuran (THF).[195] As was the case for the sulfonated poly(arylene ether ketone) membranes, the solvent choice appeared to affect the morphology of the S-SBES membranes. When cast from THF, the block copolymer exhibited a well-defined lamellar morphology (Fig. 1.54), as compared to a film cast from an 80:20 THF/methanol mixture which had a relatively disordered morphology.[196] As the percentage of methanol was increased in the casting solvent, the morphologies became increasingly more disordered, which indicated that the polar protic solvent (methanol) disrupted the assembly of the block copolymer into the lamellar structure. Water uptake and methanol permeability were found to substantially increase as the degree of sulfonation was changed from 20 to 30%, and both of these block copolymers had a proton conductivity >0.03 S/cm.[195]

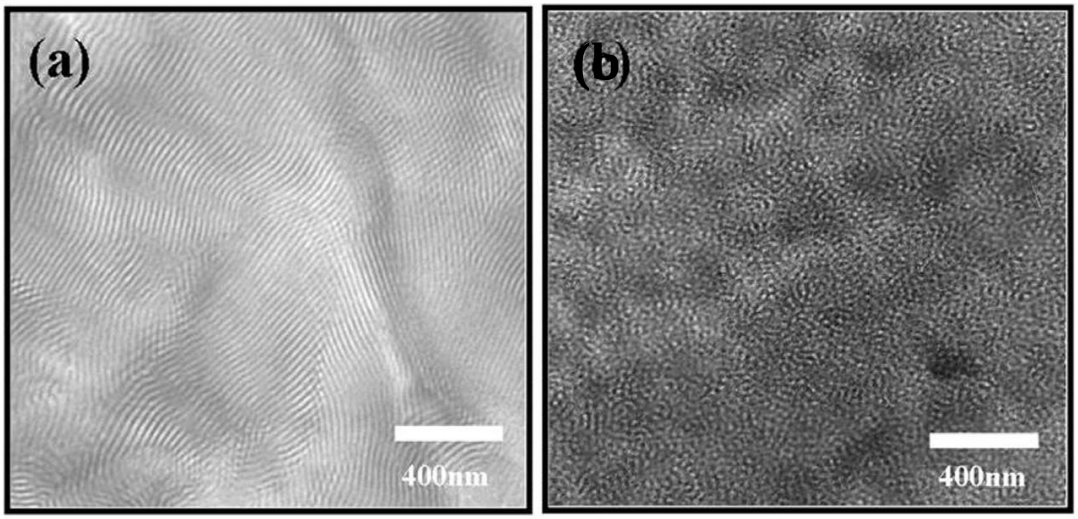

Figure 1.54: TEM images of S-SBES cast from (a) THF, (b) 20:80 methanol/THF. "Kim, J.; Kim, B.; Jung, B.; Kang, Y. S.; Ha, H. Y.; Oh, I. H.; Ihn, K. J., *Macromolecular Rapid*

Communications **2002,** *23*, 753" Reprinted with permission of John Wiley and Sons, 2014, Copyright "2002" John Wiley and Sons.

The S-SIBS that was developed by Elabd et al.,[197] was prepared by sulfonating a commercial poly(styrene-isobutylene-styrene) triblock copolymer with acetyl sulfate to form the sulfonated membrane. A degree of sulfonation as high as 82.41% was achieved for the S-SIBS membranes, which corresponded to an IEC of approximately 2.04, and this copolymer also had a well-developed phase separated morphology when cast from THF. The highly sulfonated S-SIBS membranes had conductivities near or above 0.1 S/cm. However, not surprisingly, at this high degree of sulfonation the membranes swelled excessively in water, with water uptake values exceeding 200%.[200]

One major issue regarding the sulfonated block copolymer membranes with aliphatic backbones as candidates for PEMs is their weak mechanical properties.[201-205] Although these block polymers have conductivities similar to or greater than Nafion® membranes, the degree of sulfonation required to achieve this conductivity produced very swollen and mechanically weak membranes. Therefore in order to increase the mechanical properties and decrease water uptake of these types of membranes, efforts have been undertaken to include partially fluorinated and aromatic segments (Fig.1.55, 1.56) into the polymer.[201,203,206] However, even with inclusion of the fluorinated and aromatic segments, the mechanical integrity of the aliphatic segment remains an issue. One appealing aspect of the S-SBES and S-SIBS membranes, however, is that they exhibit very low methanol permeability due to the lack of aromatic and fluorinated groups.[200] Therefore one possible application for these membranes would be in direct methanol fuel cells, where the fuel cell environment is milder compared to the hydrogen PEM fuel cell systems and low methanol permeability is critical.

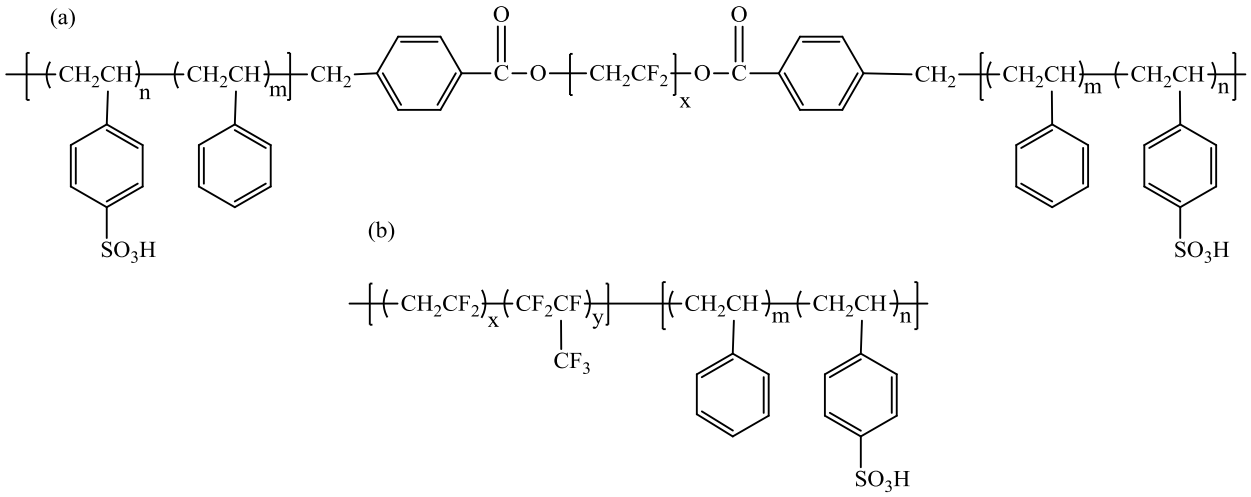

Figure 1.55: Chemical structures of partially fluorinated aliphatic backbone block copolymers: (a) Sulfonated polystyrene-b-poly(vinylidene difluoride)-b-polystyrene (S-PS-b-PVDF-b-PS), and (b) Sulfonated poly([vinylidene difluoride-co-hexafluoropropylene]-b-styrene) (P[VDF-co-HFP]-b-SPS).

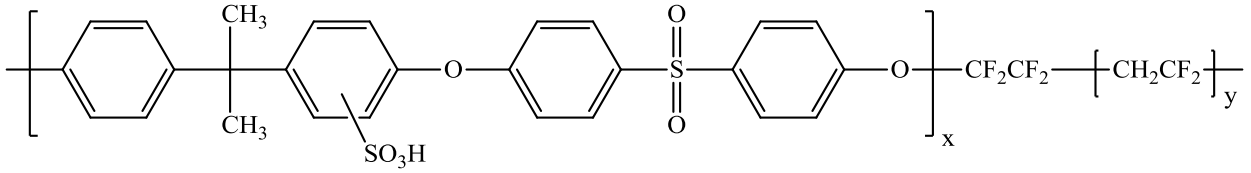

Figure 1.56: Structure of partially fluorinated and aromatic sulfonated polysulfone-b-poly(vinylidene difluoride).

1.5.2 Sulfonated block copolymers based on wholly aromatic backbones

The research in this area, as was the case for the random copolymers, is mostly focused on poly(arylene ether)s to form hydrophilic-hydrophobic block copolymers. These block copolymers have been designed to take advantage of the strong mechanical properties and chemical stabilities of the sulfonated poly(arylene ether)s, while improving the water diffusion rates at low relative humidities due to the phase separated morphologies. It has been shown that

when these types of block copolymers form a lamellar morphology, the hydrophilic and hydrophobic segments each self-assemble to form their own interconnected domains. These domains would likely be present under all humidity levels, and this is beneficial for PEMs since the hydrophilic segment provides the well-connected channels necessary for proton transport, and the hydrophobic segment improves the mechanical and chemical stability of the membrane.[8,26,192,207]

Sulfonated block copolyimides were the first to be investigated as proton exchange membranes for potential use in fuel cells. Genies et al. conducted a two-step synthesis with a naphthalenic dianhydride and a sulfonated diamine in the first step, then a non-sulfonated diamine in the second step of the synthesis (Fig.1.57).[139] The block copolymers had higher water uptake and conductivities as compared to the statistical copolymers with similar ion-exchange capacities. This showed that the block copolymer structure was effective at improving the performance of the membranes. However, performance as a function of relative humidity was not reported for these membranes.

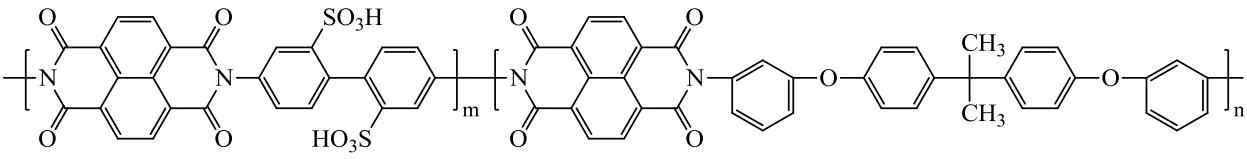

Figure 1.57: Chemical structure of a sulfonated block copolyimide.

1.5.2.1 Sulfonated block copolymers based on disulfonated poly(arylene ether sulfone) hydrophilic segments

Ghassemi et al. was the first to report sulfonated multiblock poly(arylene ether)s wherein the block copolymer was synthesized from two corresponding hydrophobic and hydrophilic

oligomers via a coupling reaction.[208] The hydrophilic oligomer was synthesized from the disulfonated monomer SDCDPS, and the hydrophobic oligomer consisted of a highly fluorinated poly(arylene ether) synthesized from decafluorobiphenyl and hexafluoroisopropylidene bisphenol A (6F-Bis A) (Fig. 1.58). A highly fluorinated segment was used for the hydrophobic block to increase the phase separation between the two different domains of the block copolymers. In addition to achieving enhanced phase separation, the increased hydrophobicity provided by the fluorines resulted in decreased water uptake of the hydrophobic regions.

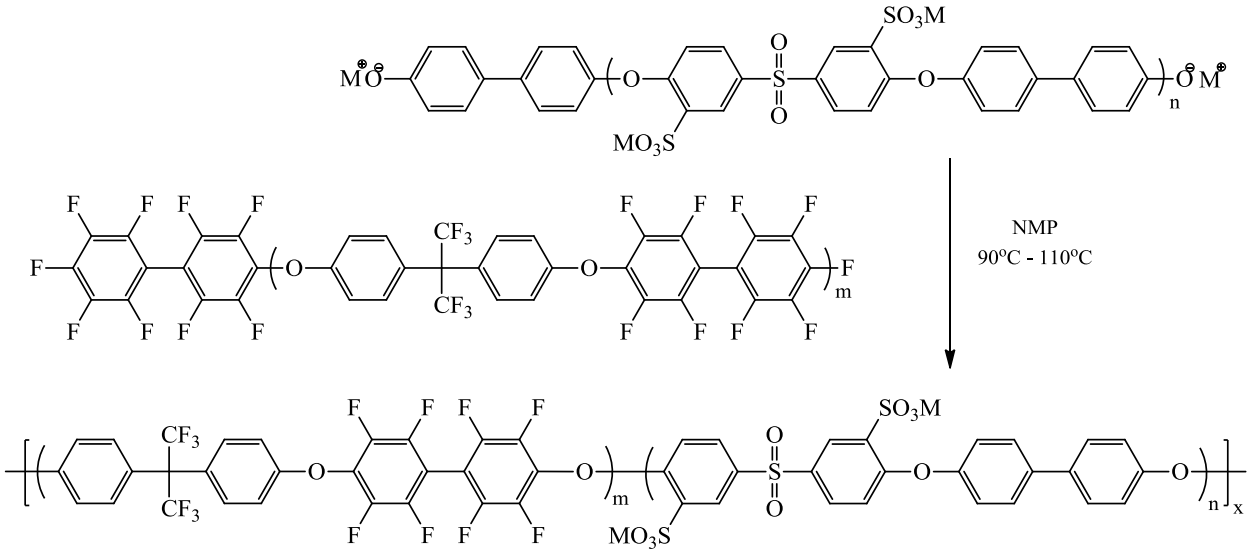

Figure 1.58: Synthesis of hydrophobic and hydrophilic oligomers to form a multiblock copolymer

The block lengths of the oligomers were designed using the Carothers equation to obtain the desired molecular weights, and then the oligomers were reacted together to form the multiblock copolymer. The molecular weights of each block ranged from 2 – 5 K (K = kg/mol), with equal and uneven molecular weights of the blocks being examined. When proton conductivities of the 5K–5K multiblock copolymer shown in Figure 1.58 were compared to Nafion® 112, the block copolymer membrane had better relative humidity performance than the

poly(perfluorinated sulfonic acid) membrane in low levels of relative humidity.[208] Following the success of the sulfonated poly(arylene ether sulfone) multiblock copolymer, further research was conducted by the McGrath group and others to study effects of different block lengths, casting solvents, and hydrophobic block structure on proton transport and conductivities.[12-13,122,209-216]

A large number of hydrophobic oligomer compositions with systematically varied block lengths were reacted with the hydrophilic segment based upon the SDCDPS and 4,4' biphenol monomers to optimize the performance of the sulfonated block copolymer membranes. Figure 1.59 shows some examples SPAES block copolymer structures. While decafluorobiphenyl was effective for creating a highly hydrophobic block, its cost prevents its use as a practical monomer for PEMs.[8] However, the partially fluorinated 6F-Bisphenol A monomer in combination with sulfone, nitrile, or ketone monomers was found to produce effective hydrophobic blocks.[122,211,213,215] In order to achieve high molecular weight for some of the systems, end-capping/chain extension of the phenolic terminated biphenol with the highly reactive decafluorobiphenol or hexafluoro biphenol was necessary due to low reactivity of the end groups. Unfortunately this chain extension resulted in the block copolymers being randomized when the coupling reaction was performed. Instead of the desired alternating multiblock copolymer structure, the block copolymer had a random arrangement of the hydrophilic and hydrophobic blocks. The alternating multiblock copolymers that were acquired had better performance and conductivity compared to the random multiblock copolymers due to the enhanced phase separation achieved by the controlled alternating structure.[211]

Effects on proton transport and conductivities were also observed with the multiblock copolymer membranes when the block lengths were changed at the same overall compositions. As the block lengths were increased for the hydrophobic and hydrophilic components, phase-

separation observed by transmission electron microscopy (TEM) became sharper and resulted in an increase in the inter-ionic-domain distance and lamellar ordering.[212,217] Figure 1.60 shows TEM images of two different block copolymers (the hydrophobic block was synthesized from biphenol and dichlorodiphenyl sulfone, and the hydrophilic block was synthesized from biphenol and disulfonated dichlorodiphenyl sulfone), one with a 10k-10k set of block lengths and the other with a 15k-15k set. The images show a clear distinct difference in morphology between the two different block copolymers. With creation of the longer hydrophilic channels in the membranes caused by the increase in block lengths, the membranes showed a notable increase in proton conductivity and water uptake for the PEMs as compared to the shorter block length block copolymers.[212]

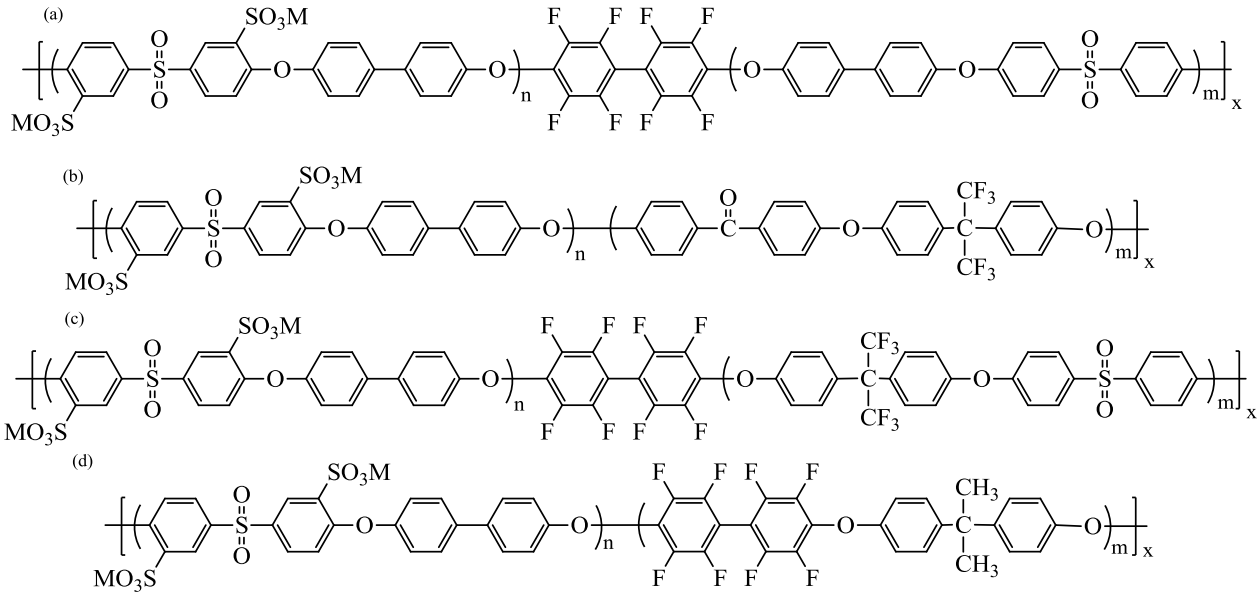

Figure 1.59: Chemical structures of aromatic multiblock copolymers based upon a disulfonated poly(arylene ether sulfone) hydrophilic segment: (a) With sulfone hydrophobic segment BPSH-BPS0, (b) Using a ketone hydrophobic segment BPSH-6FK, (c) Using chain extension to

produce a 6F-Bis A sulfone hydrophobic block, and (d) Decafluorobiphenyl based poly(arylene ether), BPSH-Bis AF.

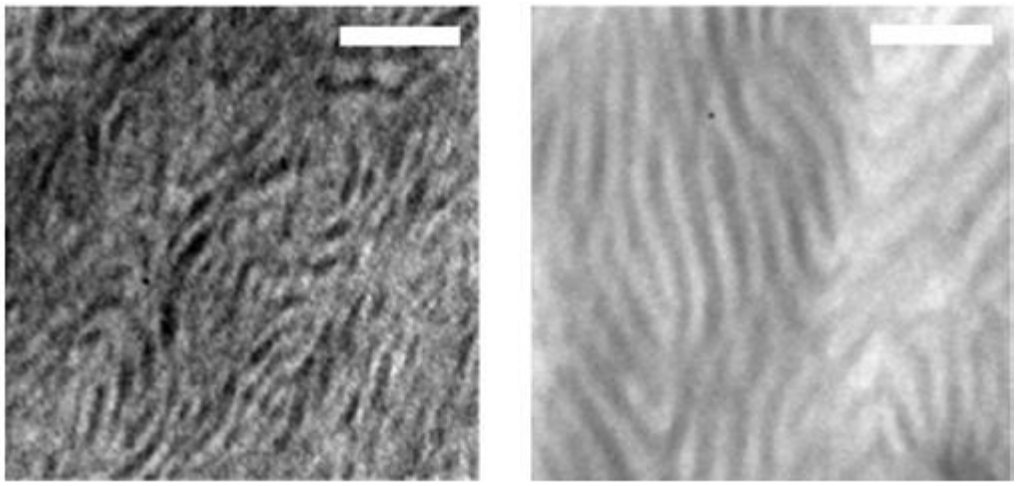

Figure 1.60: TEM images of 10k-10k (left) and 15k-15k (right) BPSH-BPS0 block copolymer films cast from NMP and dried at room temperature. Scale bar is equal to 100 nm. "Lee, M.; Park, J. K.; Lee, H.S.; Lane, O.; Moore, R. B.; McGrath, J. E.; Baird, D. G., *Polymer* **2009,** *50*, 6129" Reprinted with permission of Elsevier, 2014, Copyright "2009" Elsevier.

It was also observed that the casting solvent and the drying temperature for the block copolymer membranes had a profound effect on the transport properties of the block copolymers. McGrath et al. reported that when the block copolymer membranes were dried above the T_g of the hydrophobic segment but below the T_g of the hydrophilic segment, the block copolymers self-assembled into a more defined lamellar like morphology.[122,215-216] This rearrangement via the thermal treatment produced a drastic decrease in the water uptake for the copolymers that had longer block lengths, and did not compromise the IECs of the polymers. Prior to the annealing, the longer block caused excessive swelling in water which compromised the mechanical properties of the membranes. However by thermally annealing the block copolymer films, the

dependence on block length of water uptake diminished and the copolymers had greatly enhanced mechanical properties. In addition, the annealed membranes exhibited anisotropic swelling behavior unlike that of the random or non-annealed block copolymers, which showed isotropic swelling. It has been proposed that anisotropic swelling can potentially be beneficial for preventing premature failure of membrane electrode assemblies in wet-dry cycling conditions.

1.5.2.2 Other sulfonated poly(arylene ether) multiblock copolymers

Although most of the investigations of multiblock sulfonated poly(arylene ether) membranes have been conducted on polymers with hydrophilic segments comprised of disulfonated dichlorodiphenyl sulfone and 4,4'-biphenol, alternate hydrophilic components have been investigated to optimize performance of the PEMs (Fig. 1.61).[214,218-222] These have included sulfonated poly(arylene ether ketone)s, polyphenylenes, polyimides, and other arylene ethers. Preparations for these membranes have included both the pre-sulfonated monomer method and post-sulfonated polymer method since some of the block copolymers allowed for sulfonation even under the harsh sulfonation reaction conditions. Sulfonated multiblock copolymers based upon polysulfone segments in combination with ketone and phenylene functional groups have been recently reported. Sulfonated was performed with chlorosulfonic acid and produced block copolymers with high IECs with selective sulfonation on the hydrophilic blocks.[218-219]

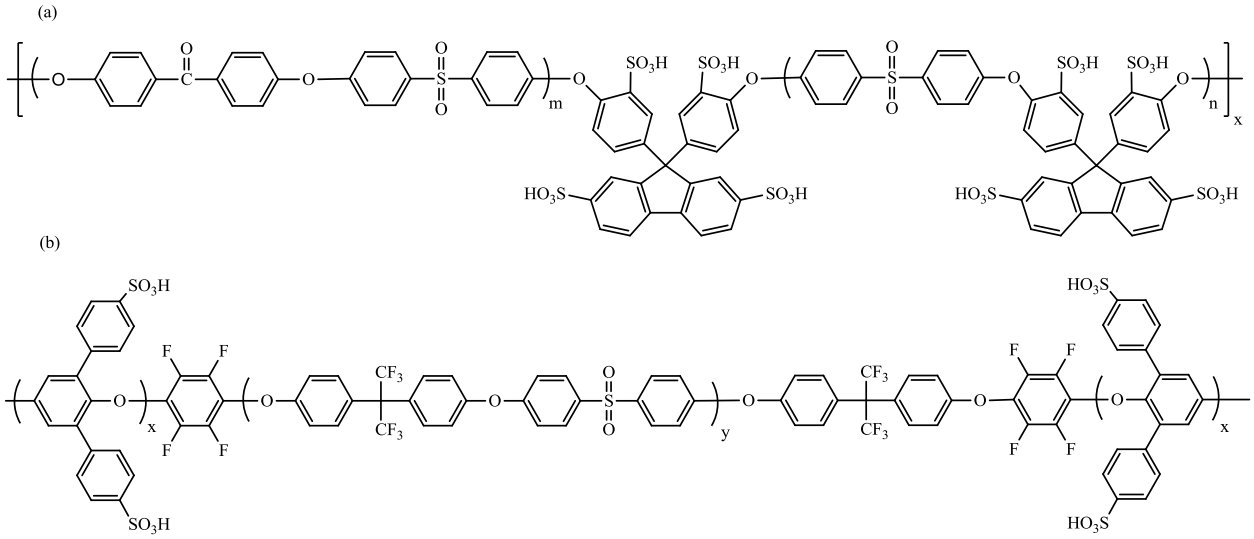

Figure 1.61: Block copolymer chemical structures prepared via postsulfonation: (a) Sulfonated poly(arylene ether sulfone ketone), and (b) A triblock copolymer.

The multiblock copolymers showed well-developed phase separation under both high and low relative humidity conditions, with conductivities reported for the sulfonated poly(arylene ether sulfone ketone) membranes of 0.03 S/cm at 40% RH and 80^{o}C (comparable to a Nafion® NRE211 membrane). In addition, the post-sulfonation did not appear to affect the mechanical stability of the film, indicating that minimal degradation occurred during the sulfonation process. As observed with the annealed block copolymer membranes, the tri-block polyphenylene copolymers swelled anisotropically with low in-plane swelling behavior for the PEMs. Both films also showed strong oxidative, thermal, and hydrolytic stability similar to that of directly polymerized disulfonated block copolymers and random copolymers.[218-219]

As was the case for the random copolymers, the presulfonated monomers can be used to create the sulfonated sulfonated polyimides and sulfonated polyimide hydrophilic oligomers.[219,221-222] The sulfonated polyimide multiblock copolymers were prepared by reacting with the sulfonated polyimide oligomers with the analogous non-sulfonated oligomers. Similar to

the random copolymers, the multiblock copolymers showed lower conductivity as compared to the copolymers with sulfonated polysulfone segments, although the block copolymers showed improved conductivity over the random copolymers.[221] although the block copolymers showed improved conductivity over the random copolymers.[221] Li et al. synthesized a sulfonated naphthalenic block copolyimide with a high IEC and investigated effects of block length on the membranes.[219] The block lengths were varied from 0-50 repeat units and the properties were measured as a function of the length. Proton conductivity under both liquid and partially hydrated conditions vastly improved as the block lengths were increased, as was the case for the sulfonated poly(arylene ether sulfone) multiblock copolymers. However, this effect seemed to level off as the number of repeat units exceeded 20. The sulfonated block copolyimide membrane with the highest IEC (2.61 meq/g) had conductivity which slightly exceed that of the Nafion® 117 for over a range of temperatures (20-100^{o}C). However the membrane also swelled greatly (>100%), and neither the mechanical properties nor the relative humidity performance of the membranes were reported.

Similar to the other strategies for increasing the IECs of block copolymers for PEMs, the McGrath group synthesized a sulfonated poly(arylene ether sulfone) hydrophilic segment based on hydroquinone.[220] Reaction of hydroquinone instead of biphenol with sulfonated dichlorodiphenyl sulfone resulted in an approximately twenty percent increase in the IEC as compared to the previous fully disulfonated oligomers. The highly disulfonated hydroquinone-based block copolymer (Fig. 1.62) self-assembled into well-developed morphologies, and AFM images indicated the presence of well-connected ion-channels. High proton conductivity was observed for the membranes with values as high as 0.21 S/cm reported for the PEMs. It was proposed that the highly hydrophilic nature of the hydroquinone block would improve the

conductivity at lower humidity levels due to the more defined phase separation of the copolymers. Highly sulfonated block copolymers such as these offer promising alternatives to the poly(perfluorosulfonic acid) membranes.[220]

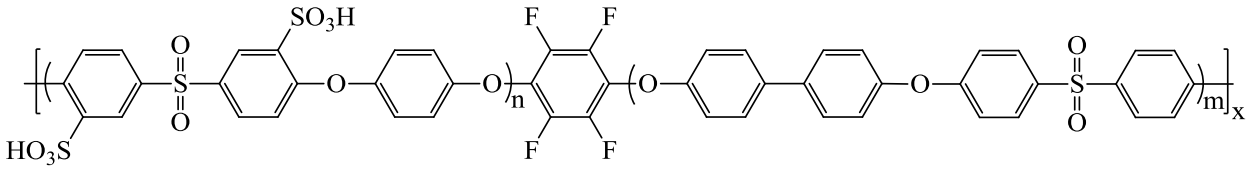

Figure 1.62: Chemical structure of hydroquinone based multiblock copolymer

Chapter 2: Multiblock Poly(arylene ether nitrile) Disulfonated Poly(arylene ether sulfone) Copolymers for Proton Exchange Membranes: Part 1 Synthesis and Characterization

Used with permission of Elsevier, 2014, as
"Chapter 2: Multiblock Poly(arylene ether nitrile) Disulfonated Poly(arylene ether sulfone) Copolymers for Proton Exchange Membranes: Part 1 Synthesis and Characterization Rowlett, J. R.; Chen, Y.; Shaver, A. T.; Lane, O.; Mittelsteadt, C.; Xu, H.; Zhang, M.; Moore, R. B.; Mecham, S.; McGrath, J. E., *Polymer* **2013,** *54*, 6305."

2.1 Introduction

Over the past few decades fuel cells have been extensively studied as an environmentally favorable alternative method for generating energy. These electrochemical devices work by converting chemical energy into electrical energy, and only water is produced as a by-product when hydrogen (H_2) gas is used as the fuel source. Among the various types of fuel cells, polymer electrolyte membrane fuel cells (PEMFC)s are considered promising candidates due to their high efficiency, high energy density, quiet operation, and elimination of carbon dioxide emission.[192] In these fuel cells the electrolyte is a solid polymer membrane known as the proton exchange membrane (PEM). The PEM is responsible for the transport of protons, forming a gas/fuel barrier for the electrodes, and electronic insulation.[6]

Currently, the state-of-the-art material used in PEMFCs is the poly(perfluorosulfonic acid) membrane Nafion®, produced by DuPont. The highly fluorinated Nafion® membrane has strong mechanical properties and chemical resistance along with high proton conductivity. However, the high cost and reduced conductivity at low relative humidities of these membranes are problematic.[10,24] Ideally a PEM material should exhibit high proton conductivity, good mechanical strength, high oxidative and hydrolytic stability, low fuel and oxidant permeability, ease of fabrication, and low cost.[6]

Sulfonated poly(arylene ether) statistical copolymers have been comprehensively investigated as potential alternatives to Nafion® for use in PEMFCs due to their strong membrane properties, and well-established oxidative, hydrolytic and chemical stability.[101-104,107,112,121,123,223-224] Although these copolymers showed high conductivity under well hydrated conditions, like Nafion® the conductivity significantly decreases at lower relative humidity (RH). The randomly distributed sulfonic acid groups on these membranes resulted in isolated morphological domains, which limited the conductivity at low RH. One solution to this issue is to use hydrophilic-hydrophobic multiblock copolymers based on sulfonated poly(arylene ether sulfone) hydrophilic regions and fluorinated poly(arylene ether) hydrophobic regions.[13,208-210,212,216,219-220,225-226] These polymers showed well-defined phase separated morphology, with a network of hydrophilic and hydrophobic domains.[225,227] The well-connected hydrophilic channels of the block copolymers allowed for significantly enhanced proton conductivity even under partially hydrated conditions.[208] It has also been suggested that partially fluorinated hydrophobic blocks may further enhance the hydrophilic/hydrophobic nanophase separation as well as provide better adhesion of the PEM with Nafion-bonded electrodes.[108,228]

In this paper we report the synthesis and characterization of a novel multiblock copolymer series based on a partially fluorinated poly(arylene ether benzonitrile) (6FPAEB) hydrophobic segment and two different poly(arylene ether sulfone) (BPSH, HQSH) hydrophilic segments. This is the first report using a benzonitrile based hydrophobic block in combination with a sulfonated poly(arylene ether sulfone) hydrophilic segment. Using a combination of these systems will deepen the understanding between block copolymer composition and PEM performance. This is further explored by comparing both hydroquinone and biphenol based block copolymers against Nafion® 212.

2.2 Experimental

2.2.1 Materials

2,6-Difluorobenzonitrile (DFBN), anhydrous dimethyl sulfoxide (DMSO), *N*-Methyl-2-pyrrolidinone (NMP), *N*,*N*-dimethylacetamide (DMAc), cyclohexane, and toluene were purchased from Sigma-Aldrich. DFBN, DMSO, and toluene were used as received, and NMP and DMAc were distilled from calcium hydride before use. 4,4′-Hexafluoroisopropylidenediphenol (6F-BPA), received from Ciba, was sublimed and then recrystallized twice from toluene. Monomer grade 4,4′-biphenol (BP) and hydroquinone (HQ) were provided by Eastman Chemical Company, and dried under vacuum at 80^{o}C prior to use. Hydroquinone was also recrystallized from ethanol prior to drying. 3,3'-Disulfonated-4,4'-dichlorodiphenylsulfone (SDCDPS) was received from Akron Polymer Systems and dried under vacuum at 150^{o}C for 3 days prior to use. A previously reported method was used to determine purity of the SDCDPS monomer from UV-Vis spectroscopy.[118] Potassium carbonate (K_2CO_3), acetone, and methanol were purchased from Fisher Scientific. Potassium carbonate was dried under vacuum at 180^{o}C prior to use, while acetone and methanol were used without further purification.

2.2.2 Synthesis of the 6FPAEB hydrophobic oligomer

All oligomers were synthesized via nucleophilic aromatic substitution with different block lengths being achieved by using a molar off-set of one of the monomers. An example synthesis of an 6FPAEB oligomer with a targeted 7,000 g/mol molecular weight is as follows: 6FBPA (10.279 g, 30.57 mmol) and DMAc (70 mL) were placed into a three neck round bottom flask equipped with a stir bar, condenser, nitrogen inlet, and Dean-Stark trap. The mixture was heated to 140^{o}C and stirred until 6FBPA was completely dissolved. Once a clear solution was

obtained, K_2CO_3 (3.45 g, 24.96 mmol) and toluene (35 mL) were added into the flask. The reaction was allowed to reflux at 140^oC for 4 h to azeotropically remove water from the system, and then slowly heated to 170^oC to remove toluene from the system. After removal, the reaction temperature was decreased to 80^oC and DFBN (4.53 g, 32.57 mmol) was added to the flask. The reaction was allowed to proceed for 8 h at 125^oC (w/o nitrogen gas), then cooled to room temperature and filtered to remove any excess K_2CO_3 or by-product salts. Once filtered, the oligomer was precipitated in methanol (1000 mL), stirred overnight, filtered and then dried in *vacuo* at 110 ^oC for 48 h.

2.2.3 Synthesis of the BPS100 hydrophilic oligomer

To synthesize a BPS100 hydrophilic oligomer with a targeted molecular weight of 9,000 g/mol, BP (1.788 g, 9.60 mmol), SDCDPS (4.435 g, 9.03 mmol), and DMAc (28 mL) were placed into a three neck round bottom flask, equipped with a mechanical stirrer, a condenser, a nitrogen inlet and a Dean-Stark trap. The mixture was stirred until dissolved, then K_2CO_3 (1.53 g, 11.09 mmol) and toluene (14 mL) were added. The reaction bath was heated to 145^oC for 4 h to azeotropically remove water from the system, and then slowly raised to 180^oC by the controlled removal of toluene. The reaction was allowed to proceed at 180^oC for 72 h. The mixture was cooled to room temperature and filtered to remove salts, then coagulated in acetone (1000 mL). The precipitated oligomer was stirred overnight in acetone, filtered and then dried in *vacuo* at 160^oC for 48 h.

2.2.4 Synthesis of the HQS100 hydrophilic oligomer

A representative synthesis of a desired 7,000 g/mol HQS100 oligomer is as follows: SDCDPS (10.183 g, 20.73 mmol), HQ (2.395 g, 21.75 mmol), and DMSO (35 mL) were placed into a three neck round bottom flask equipped with a mechanical stirrer, condenser, nitrogen

inlet, and Dean-Stark trap. The mixture was heated to 140°C and stirred until dissolved, then K_2CO_3 (3.45 g, 24.96 mmol) and toluene (15 mL) were added. The reaction was allowed to reflux for 4 h to azeotropically remove water from the system. After 4 h the toluene was drained and the reaction was allowed to proceed at 140°C for 72 h. The mixture was cooled to room temperature and filtered to remove any salts. The oligomer was coagulated in acetone (1000 mL), stirred overnight, filtered and then dried in *vacuo* at 160°C for 48 h.

2.2.5 Synthesis of hydrophobic-hydrophilic multiblock copolymers

Both multiblock copolymer systems were synthesized with equal block lengths of the hydrophobic and hydrophilic segments to form a series of multiblock copolymers. For the biphenol based block copolymers, BPS100 (4.500 g, 0.500 mmol), K_2CO_3 (0.150 g, 1.087 mmol), NMP (44 mL) and cyclohexane (15 mL) were added to a three-necked 100-mL flask equipped with a mechanical stirrer, condenser, nitrogen inlet and Dean-Stark trap. The reaction bath was heated to 120 °C and refluxed for 6 h to remove water from the system. After removing cyclohexane, the reaction bath was cooled to 90°C, and 6FPAEB oligomer (4.600 g, 0.510 mmol) was added. The bath temperature was raised to 135°C and kept at this temperature for 48 h. The reaction mixture was precipitated into acetone (1000 mL) affording a fibrous polymer. The product was stirred in acetone for 12 h, in deionized (DI) water at 90°C for 12 h, filtered and then dried in *vacuo* at 150°C for 24 h. The copolymers based on the hydroquinone hydrophilic segments were synthesized in the same fashion, except that DMSO was used as the solvent for the reaction.

2.2.6 Membrane preparation and acidification

The potassium salt form block copolymers were dissolved in DMAc (~7% w/v), after drying at 150°C for 24 h, and filtered through a 0.45 μm Teflon syringe filter. The solution was

cast onto a dry, clean glass substrate and dried for 24 h under an infrared lamp at ~80°C. Furthermore, the membranes were annealed under vacuum at 220°C, about 30°C higher than the T_g of the 6FPAEB blocks. The membranes were converted to the acid form by boiling in 0.5 M sulfuric acid for 2 h, followed by boiling in DI water for 2 h.

2.2.7 Characterization

^{1}H and ^{19}F NMR analyses were conducted on a Varian Unity Plus spectrometer operating at 400 MHz (376 MHz for ^{19}F). The spectra of BPS100 and HQS100 oligomers along with their corresponding block copolymers were obtained from a 10% (w/v) 1 mL solution in DMSO-d_6. The spectra of 6FPAEB hydrophobic oligomers were obtained from a solution in $CDCl_3$. ^{13}C NMR analyses were conducted on a Varian Unity spectrometer, operating at 100.58 MHz with DMSO-d_6 as the solvent. Intrinsic viscosities of all oligomers and block copolymers were obtained via size exclusion chromatography (SEC). Values for the 6FPAEB oligomers were obtained from an Alliance Waters 2690 Separations Module using chloroform as the mobile phase (25^{o}C), with a Viscotek T60A dual viscosity detector and laser refractometer equipped with a Waters HR 0.5 + HR 2 + HR 3 + HR 4 styragel column set. The hydrophilic oligomers and block copolymer intrinsic viscosities were obtained from Agilent 1260 Infinity Multi-Detector SEC using NMP with 0.05 M LiBr as the mobile phase (50^{o}C) with 3 PLgel 10 μm mixed-B 300 x 7.5 mm columns in series and a Viscostar II Viscometer. Glass transition temperatures (T_g's) were determined by differential scanning calorimetry (DSC) with a TA Instruments DSC Q-1000 at a heating rate of 10^{o}C/min under a stream of nitrogen.

2.2.8 Morphology

Small angle x-ray scattering (SAXS) was performed using a Rigaku S-Max 300 3 pinhole SAXS system. The x-ray source was Cu Kα radiation with a wavelength of 0.154 nm. The sample-to-

detector distance was 1600 mm. SAXS two-dimensional images were obtained using a fully integrated 2D multiwire proportional counting gas-filled detector, with an exposure time of 1 h. All the membranes were characterized in the potassium salt form. The measured intensity values were corrected for thickness, sample transmission and background scattering. The bulk morphologies of the membranes were characterized by transmission electron microscopy (TEM). Electron density contrast between hydrophilic and hydrophobic segments within the membrane samples was enhanced by quantitatively exchanging the acidic protons on the sulfonic acid moieties with cesium ions. Acidified membranes were immersed in DI water and titrated with aqueous CsOH solution until the solution became neutral. The cesium stained membranes were then embedded in epoxy and ultramicrotomed into 50–70 nm thin sections with a diamond knife. Transmission electron micrographs were obtained using a Philips EM 420 transmission electron microscope (TEM) operating at an accelerating voltage of 47 kV.

2.2.9 Tensile testing

Uniaxial load tests were performed using an Instron 5500R universal testing machine equipped with a 200-lb load cell. The crosshead displacement rate was 5 mm/min and gauge the length was 26.5 mm. The tensile test specimens were prepared with dimensions of 50 mm length and a minimum width of 4 mm per ASTM D638-03. Prior to testing, salt form membrane specimens were dried in the vacuum oven at 150^{o}C and tested at room temperature. All specimens were mounted in pressure locking pneumatic grips.

2.2.10 Proton conductivity and water uptake

Proton conductivities of the 6FPAEB-BPSH and 6FPAEB-HQSH membranes in the fully hydrated state were determined at 30^{o}C in liquid water. Before the measurement, the membranes were equilibrated in DI water at 30^{o}C for 24 h. A Solartron (1252 + 1287) impedance/gain-phase

analyzer over the frequency range of 10 Hz to 1 MHz was used for the measurements following a previously reported method.[229] A humidity-temperature oven (ESPEC, SH240) was used for proton conductivity measurements of the membranes. The conductivity was calculated by using equation 2.1.

(2.1) $$\sigma = L/(R \cdot S)$$

Where σ (S/cm) is proton conductivity, L (cm) is the distance between the two electrodes, R (Ω) is the resistance of the membrane and S (cm^2) is the surface area available for proton transport though the membrane. The water uptake of all membranes were determined gravimetrically. The membranes were equilibrated in DI water at room temperature for 2 days after acidification. Wet membranes were removed from DI water, blotted dry to remove surface droplets, and quickly weighed. The membranes were dried at 120^{o}C under vacuum for 24 h and re-weighed. The water uptake of the membranes was calculated according to equation 2, where W_{dry} and W_{wet} refer to the mass of the dry and wet membrane, respectively.

(2.2) $$\text{Water Uptake (\%)} = (W_{wet} - W_{dry})/W_{dry} \times 100$$

2.2.11 Relative humidity

A controlled humidity-temperature oven (ESPEC, SH240) was used to measure proton conductivity as a function of relative humidity of the membranes. Samples were cut and thickness of the membranes where measured in the wet state. Membranes were equilibrated in the cell at 95% relative humidity overnight prior to testing. Samples were equilibrated at each new humidity level for 30 minutes prior to measuring the proton conductivity. The range was from 95% to 30% relative humidity. To account for changes in sample thickness at different humidities the wet thickness and dry thickness were measured and these were extrapolated as a function of relative humidity. The conductivities of the samples were first measured starting

from 95% relative humidity then systematically decreased to 30% relative humidity and then systematically increased back to 95% humidity. This gave two plots, one from high to low and another from low to high humidity. The oven temperature was held constant at 80^{o}C.

2.2.12 Fuel cell testing

The MEA was assembled into the single cell fuel cell from fuel cell technology. The AvCrab GDL (EP40T) was used for all experiments. Fuel cell test station model 850e from scribner associate Inc. was used all all experiments. Cells were conditioned for 12 h prior to experiments. For conditioning or breaking process, the anode and cathode humidity was set at 95 and 80% relative humidity at 80^{o}C with the cell potential set at 0.6 V. The current was significantly increased during the first 10 h, with stability achieved after 11-12 h. Polarization curves were performed at lowest humidity condition (low to high). After finishing of the polarization curve, the cell was set to the next humidity condition and held for 1 h in order to stabilize the fuel cell. The cell potential and current were collected during polarization curve, and high frequency resistance was collected during the experiment at 1000 hertz.

2.3 Results and Discussion

2.3.1 Synthesis of telechelic hydrophilic and hydrophobic oligomers

All of the fully disulfonated hydrophilic (Fig. 2.2) and the unsulfonated hydrophobic oligomers (Fig. 2.1) were synthesized via step-growth polycondensation reactions. While the synthesis of the biphenol based poly(arylene ether sulfone) hydrophilic segments has been heavily studied in our research group,[122,208-210,215-216] the higher ion-exchange capacity (IEC) hydroquinone has been relatively unexplored.[220] Targeted molecular weights were achieved by off-setting the monomer ratio based upon the Carothers equation. The hydroquinone and

biphenol monomers were used in excess for the synthesis of the sulfonated oligomers and the difluorobenzonitrile monomer for the unsulfonated oligomers.

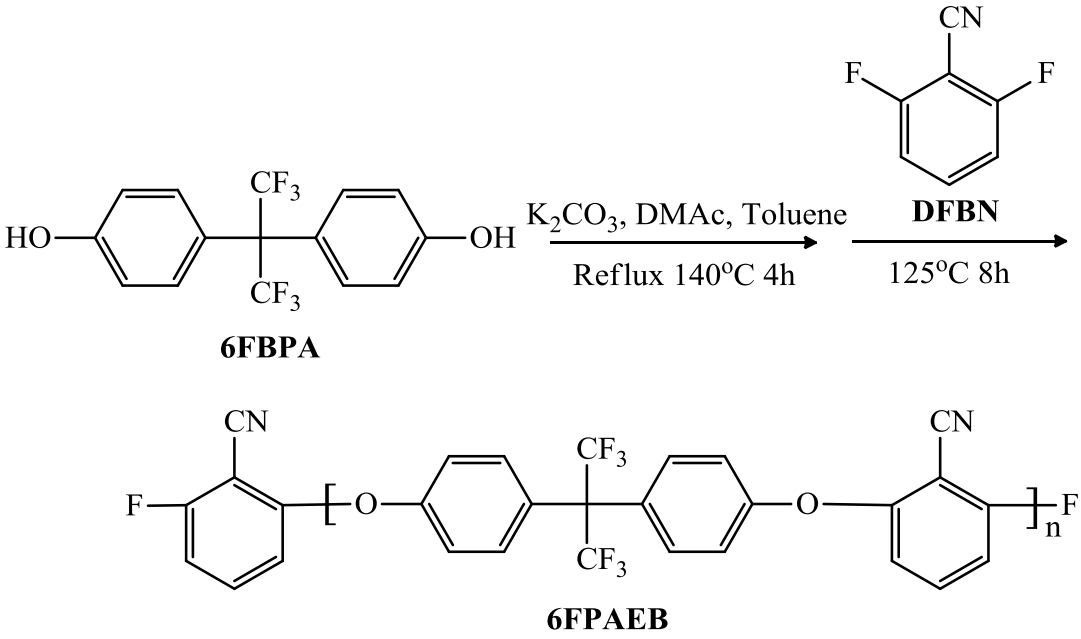

Figure 2.1: Synthesis of fluorine terminated poly(arylene ether benzonitrile) (6FPAEB) hydrophobic oligomer

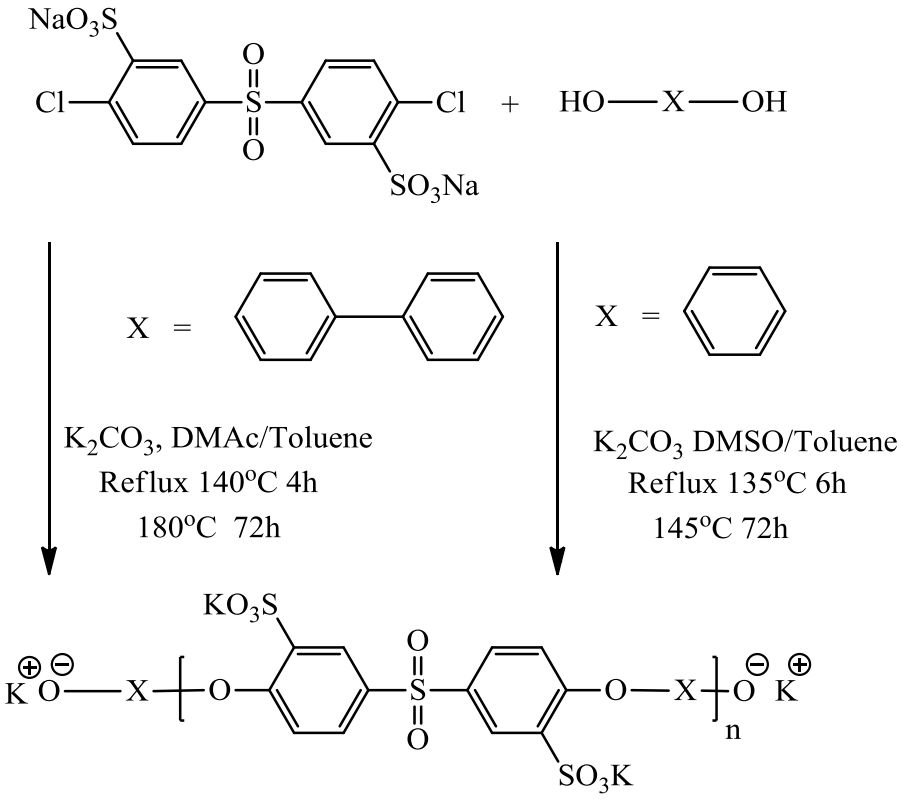

Figure 2.2: Synthesis of the phenoxide terminated disulfonated poly(arylene ether sulfone) oligomers

The number-average molecular weights (M_n) of the hydrophilic oligomers were determined by ^{1}H NMR using end-group analysis. In the spectrum of the HQS100 the small peaks at 6.75 and 6.85 ppm were attributed to the phenoxide end-groups, while the peaks at 6.95, 7.10, 7.85, and 8.25 ppm were assigned to the protons on the backbone of the main chain (Fig. 2.3). By comparing the integration values between the end-groups and the main chain polymers the number average molecular weight was determined. The same procedure was used to calculate the M_n of the biphenol hydrophilic oligomer BPS100.[122,215-216] Analysis of a ^{19}F NMR spectrum was used to determine the number average molecular weight (M_n) of the unsulfonated hydrophobic oligomer. Figure 2.4 shows the ^{19}F NMR spectrum of a 6FPAEB oligomer, with the peak at -63.4 ppm attributed to the fluorines in the backbone and the peak at -105.9 ppm

attributed to the end-group aromatic fluorines. The two kinds of fluorine in the spectra have a mole ratio of 6n/2, where n is the number of the repeat units or the oligomer. The number of repeat units was calculated based upon this ratio to obtain the M_n of the 6FPAEB oligomers. Molecular weights ranging from 4 to 15 kg/mol were obtained for all of the oligomers. However, for hydroquinone based oligomers greater than 10 kg/mol, long reaction times were required for completion of the reaction. Thus, the fluorine terminated disulfonated monomer was used in order to successfully synthesize these moieties.

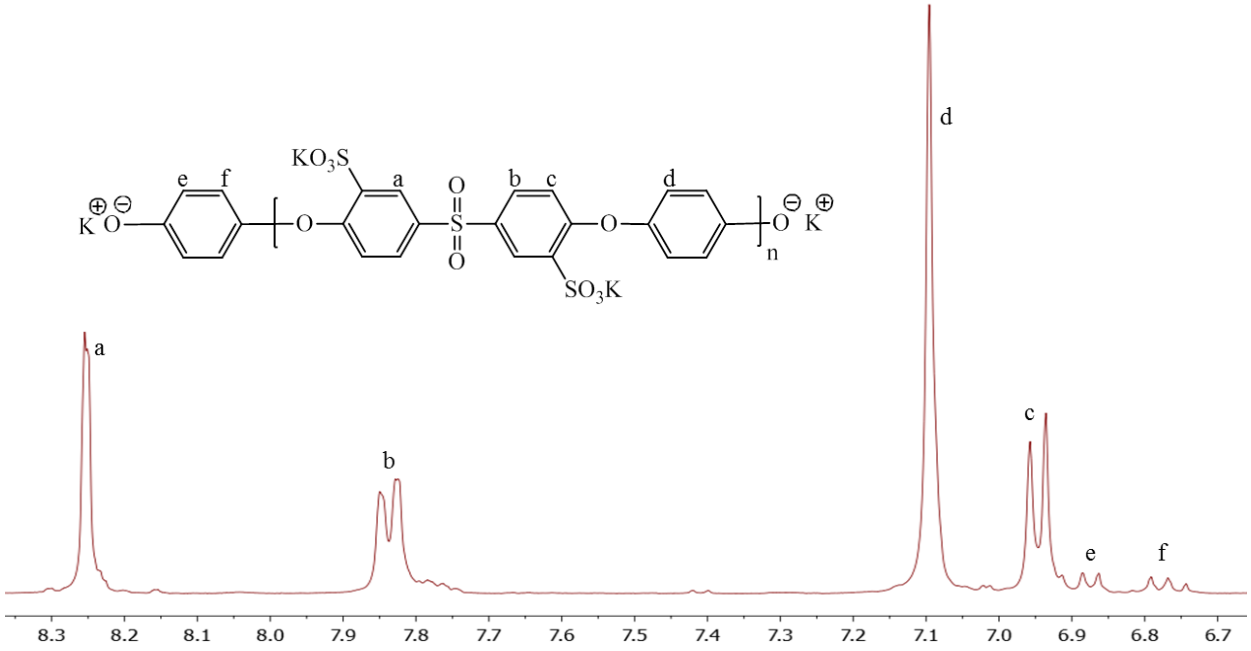

Figure 2.3: ^{1}H NMR of phenoxide terminated HQS100 oligomer.

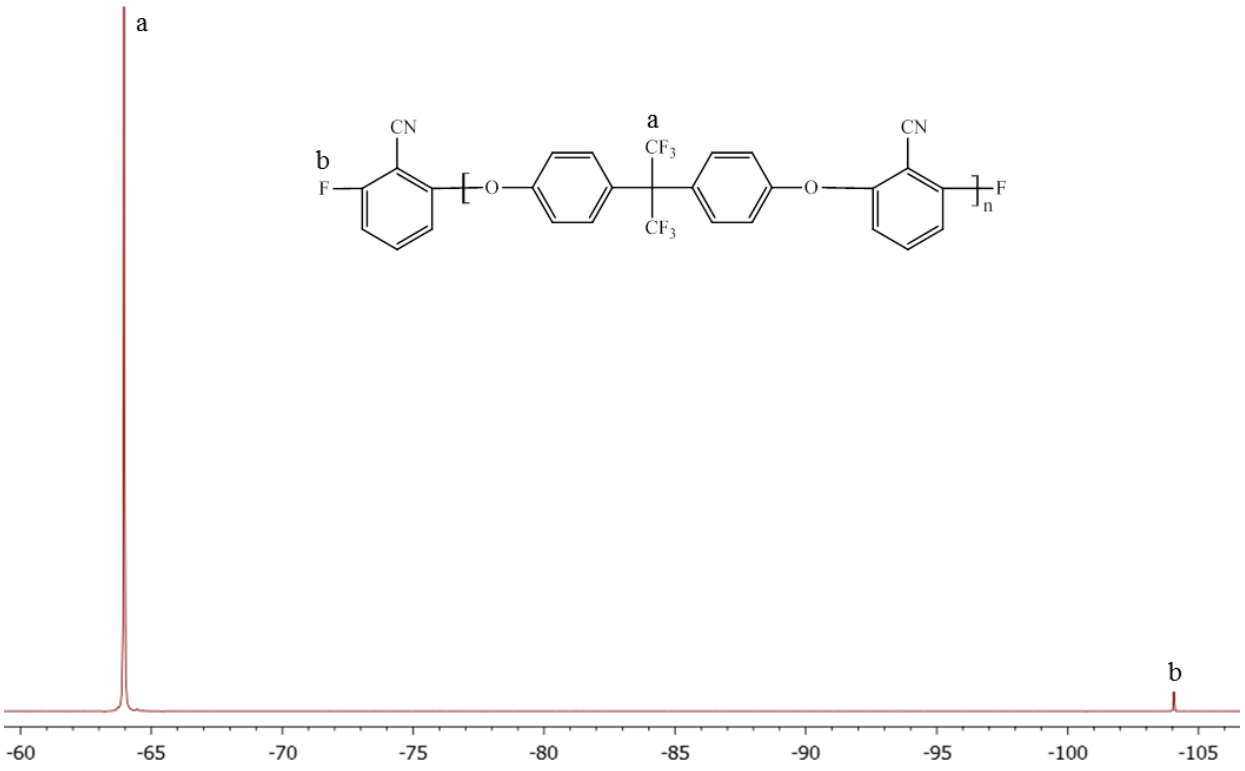

Figure 2.4: ^{19}F NMR of 6FPAEB oligomer

2.3.2 Synthesis of 6FPAEB-BPSH and 6FPAEB-HQSH multiblock copolymers

Two series of equal block length hydrophilic-hydrophobic multiblock copolymers were synthesized via nucleophilic aromatic substitution using relatively mild reaction temperatures (Fig. 2.5). The acronyms 6FPAEB-BPS100 and 6FPAEB-HQS100 were used to denote that the polymers were in the salt form. When converted to the proton form they were referred to as 6FPAEB-BPSH and 6FPAEB-HQSH. Only equal block lengths of the hydrophilic and hydrophobic segments were synthesized and the lengths were denoted after the acronym as xK-xK, where x referred to the number average molecular weight of the blocks. In both systems the hydrophobic segment was used in slight excess, thus the completion of the reaction was judged by the disappearance of the phenoxide end-groups on the hydrophilic segments in ^{1}H NMR spectra (Fig. 2.6). The reaction temperature was maintained at mild conditions to avoid possible

ether-ether interchange side reactions that would disrupt the alternating multiblock copolymer structure. To confirm that these side reactions were minimized, the ^{13}C NMR spectra of both systems were compared with the analogous random copolymer, denoted as 6FPAEB-35 (Fig. 2.7). The spectrum of the random 6FPAEB-35 copolymer had more than four sets of multiplets associated with the ether bonds, which indicates a random sequence. However, in the spectra of the multiblock copolymers only four narrow singlet peaks were visible in this region, which suggested that ether-ether interchange reactions had been minimized in the coupling reactions. In addition, the ^{1}H NMR spectra were used to calculate the ion-exchange capacity of the polymers by taking the integration ratio between the hydrophobic and hydrophilic peaks.

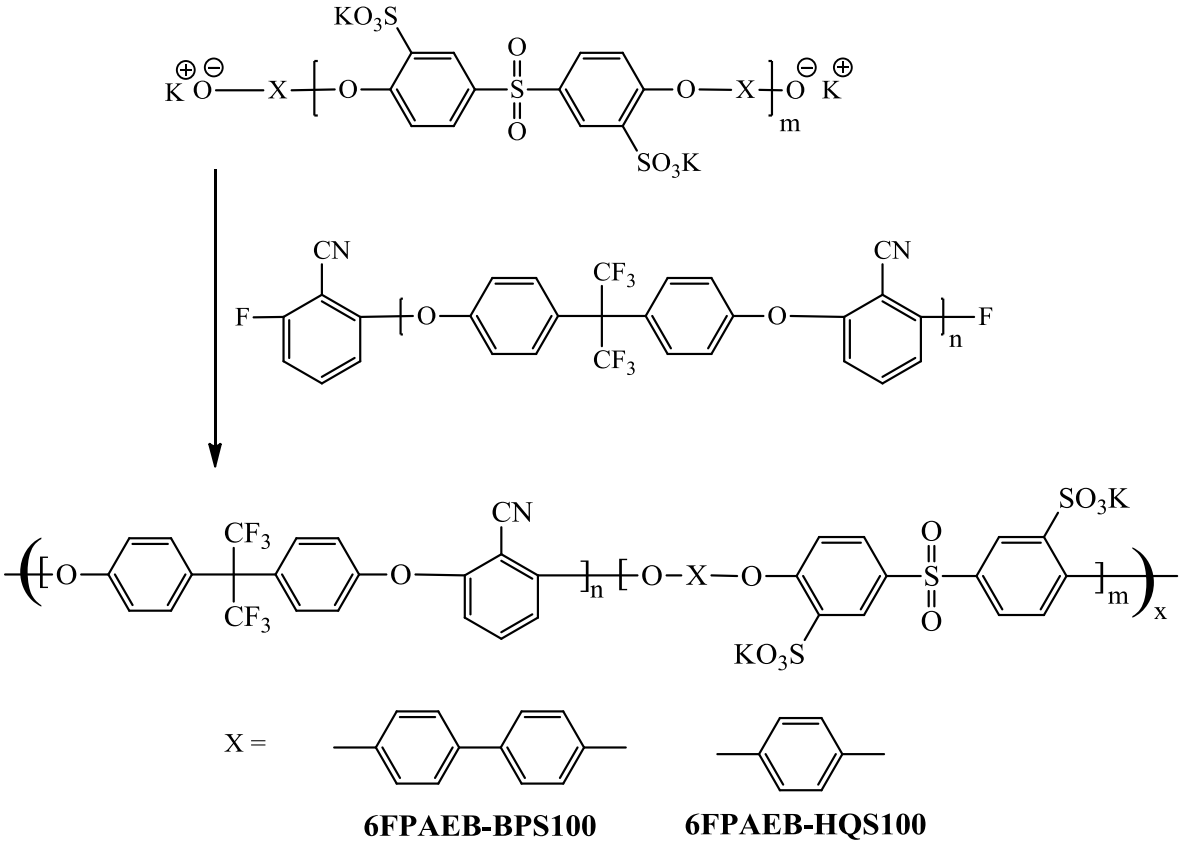

Figure 2.5: Synthesis of biphenol and hydroquinone multiblock copolymers 6FPAEB-BPS100 and 6FPAEB-HQS100

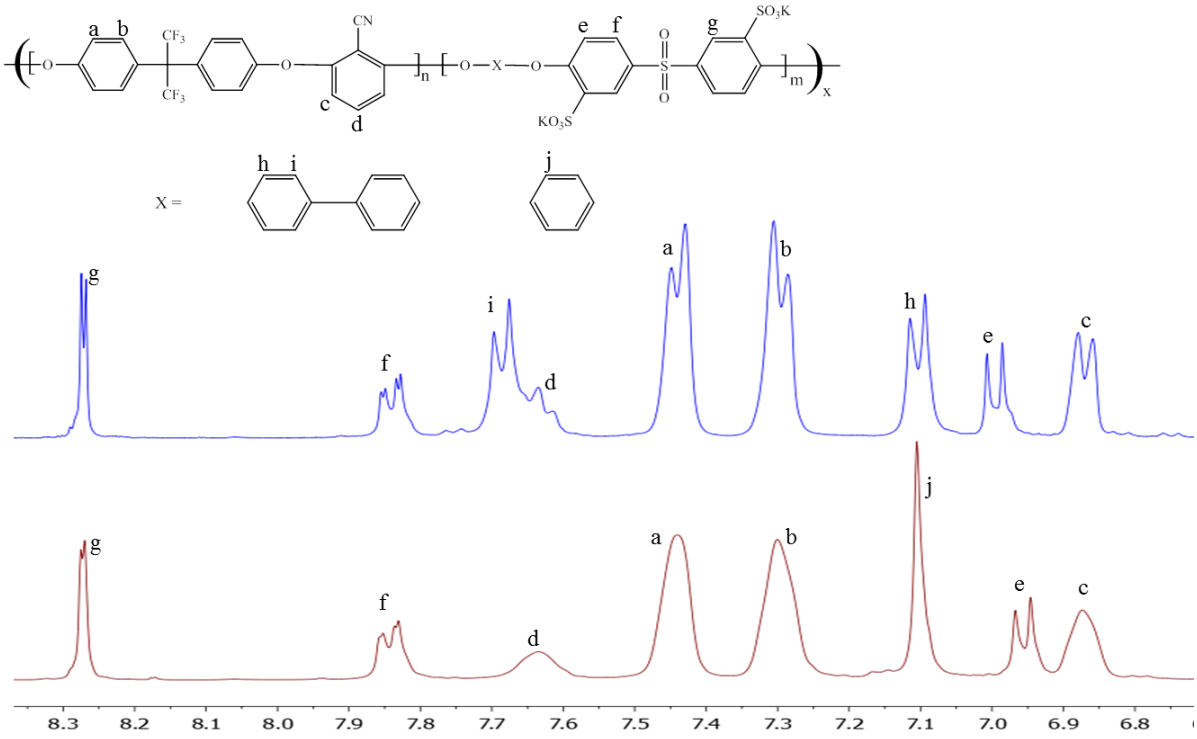

Figure 2.6: ^{1}H NMR spectra of biphenol and hydroquinone multiblock copolymers 6FPAEB-BPS100 and 6FPAEB-HQS100

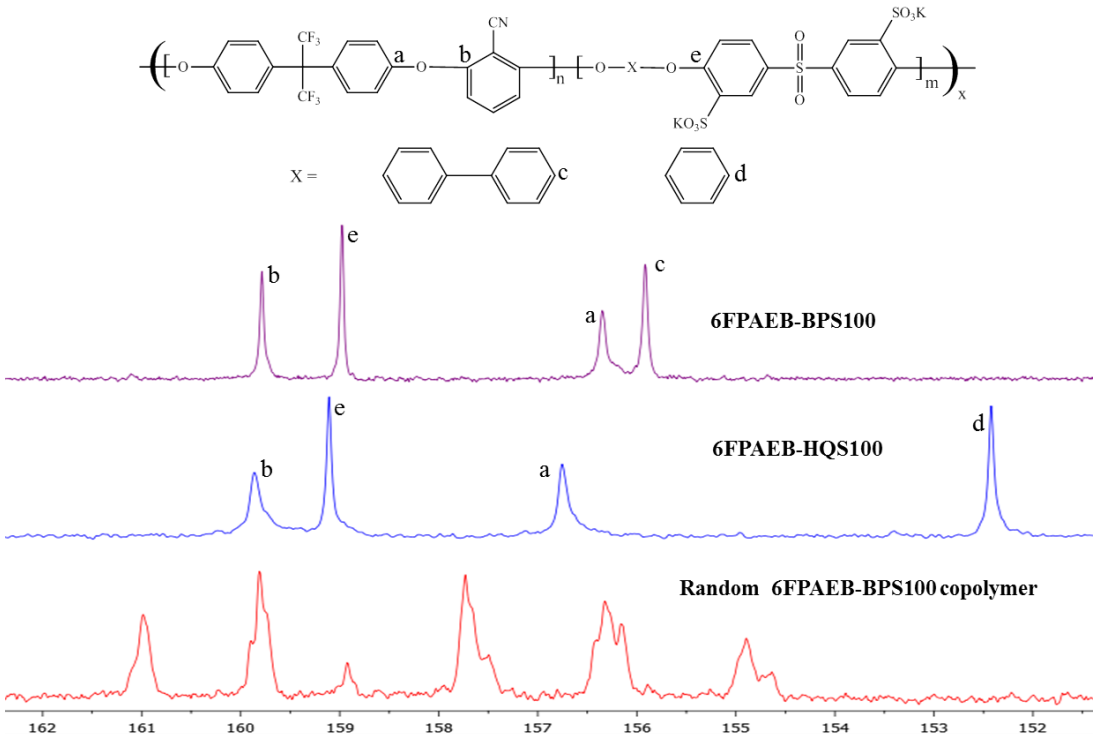

Figure 2.7: ^{13}C NMR spectra of a 6FPAEB-BPS100 15k-15k multiblock copolymer (top), 6FPAEB-HQS100 5k-5k multiblock copolymer (middle), and 6FPAEB-35 random copolymer (bottom).

2.3.3Membrane properties

The hydroquinone based multiblock copolymers were directly compared against the biphenol analogs in order to investigate how polymer structure and sulfonation level affected the proton exchange membrane microstructure and properties. The membrane properties are summarized in Table 2.1 as a function of both polymer structure and block length. All the membranes listed in the table were annealed at 220^{o}C in the potassium salt form, a temperature between the T_g of the hydrophobic and the T_g of the hydrophilic segments. The glass transition temperatures of the block copolymers were measured by DSC. The T_g of the 6FPAEB hydrophobic phase was approximately 190^{o}C, while the T_g of the disulfonated poly(arylene ether

sulfone) regions appeared as a broad transition above 250°C. This annealing method has been shown previously to produce block copolymers with moderate water uptake, good hydrated mechanical properties and improved conductivity relative to the non-annealed films.[122,215-216]

Table 2.1. Properties of 6FPAEB-BPSH and 6FPAEB-HQSH multiblock copolymers

6FPAEB-BPSH (Block Length)	IEC (meq/g)[a]	M_w (kDa)[b]	Water Uptake (%)[c]	Conductivity (S/cm)[d]
7K-7K	1.57	57	46	0.13
9K-9K	1.53	63	44	0.13
13K-13K	1.63	104	51	0.14
15K-15K	1.57	92	46	0.14
6FPAEB-HQSH				
5K-5K	1.69	49	46	0.14
7K-7K	1.80	45	64	0.17
9K -9K	1.65	97	84	0.15
15K -15K	1.67	100	75	0.15
Nafion® 212	1.00	-	22	0.12

a. Measured from ^{1}H NMR
b. Measured by SEC in NMP with 0.05 M LiBr at 50°C
c. Values were obtained for membranes in the acid form
d. Measured in liquid water at 30°C

For each series equal block lengths of the hydrophilic and hydrophobic segments were used to synthesize the multiblock copolymers. In both series a small excess of the hydrophobic oligomer was used to monitor the completion of the reaction via disappearance of the end groups with NMR spectroscopy. This resulted in a target IEC of 1.6 meq/g for the 6FPAEB-BPSH, and 1.8 meq/g for the 6FPAEB-HQSH multiblock copolymers. The difference in the theoretical IECs was due to the difference in molecular weight between the biphenol and hydroquinone

monomers in the hydrophilic segments. Thus, the oligomers that contained the lower molecular weight hydroquinone monomer contained more sulfonic acid groups per gram of material. By comparing the two different block copolymers we were able to examine how ion-exchange capacity in the hydrophilic phase and polymer structure changed the membrane properties without changing the ratio between the hydrophilic and hydrophobic segments.

All of the multiblock copolymers formed tough, durable, and ductile membranes when cast from solution, with stress-strain performance (Fig. 2.8) and SEC confirming that high molecular weight was achieved (M_w ranged from 45 – 104 kDa). In addition, the measured IEC values for the copolymers were close to the targeted values, which further indicated that a high degree of coupling was achieved. The hydroquinone based block copolymers, as expected, had higher IECs and water uptake values than the 6FPAEB-BPSH block copolymers. However, while the water uptake values increased with longer block lengths for the 6FPAEB-HQSH systems, this trend was not observed for the biphenol-based copolymers. Nevertheless, only moderate water uptake values were observed for all of the sulfonated membranes, with the highest being 84%. This is a stark decrease in water uptake from an earlier reported system that incorporated the hydroquinone monomer in the hydrophilic phase.[220] For those multiblock copolymers, high water swelling (> 110%) was observed for copolymers with all of the block lengths that were studied, even as low as 3K-3K. The reduced swelling ratios found in the present study, compared to random copolymers and other block copolymer systems with similar IECs, were attributed to the annealing step that was used in the fabrication of the membranes. It was hypothesized that the annealing allowed for development of the phase-separated morphology. Also it should be noted that both of the sulfonated multiblock copolymer membranes had improved proton conductivity compared with the Nafion® 212 control, with the

6FPAEB-HQSH membranes having higher conductivities relative to the copolymers with biphenol in the hydrophilic phase. In addition, the conductivities of both membrane systems were on par or higher than other reported poly(arylene ether sulfone) multiblock copolymer systems.[122,215,230]

The yield stresses for these membranes were between 50-60 MPa, with the elongation at break increasing as the block lengths of the membranes were increased. The hydroquinone based PEMs with the higher IECs in the hydrophilic phases had slightly increased yield stresses compared to membranes where biphenol was in the hydrophilic phases that had similar block length. The chemical structure and IEC seemed to have only a small effect on the performance. Nevertheless, both systems showed good mechanical properties and produced tough and ductile membranes. To provide consistency for testing the materials, the membranes were dried in a vacuum oven prior to mechanical testing to remove any water from the systems.

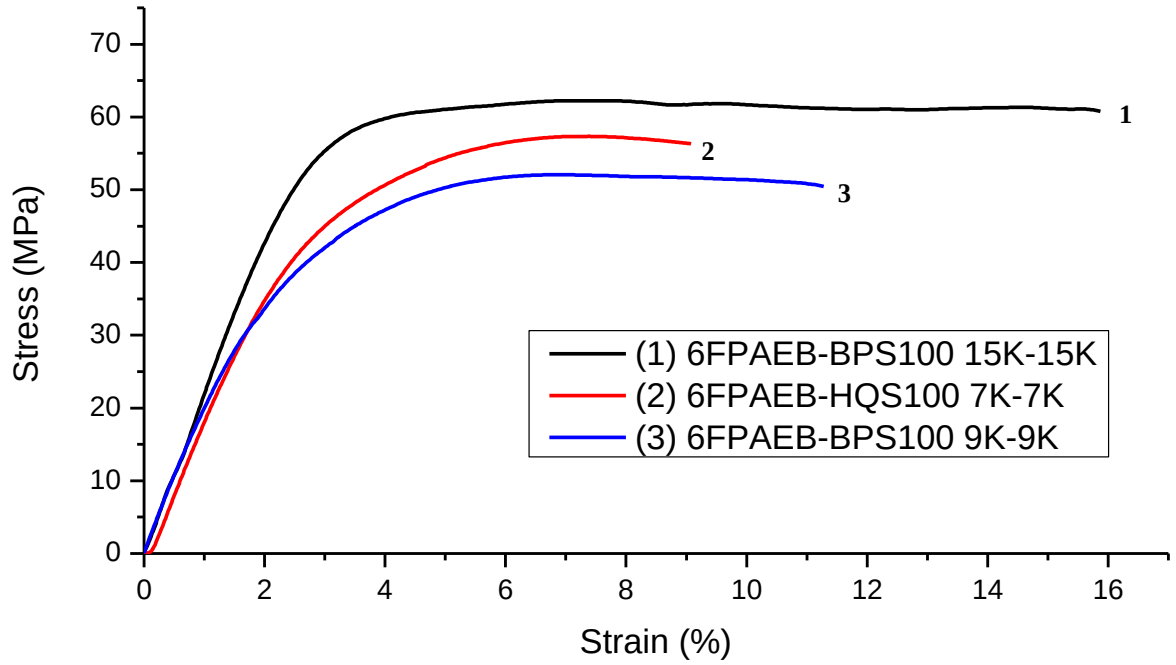

Figure 2.8: Stress-strain behavior of sulfonated multiblock copolymers. Samples were dried in the potassium salt form prior to testing, with the tensile experiment being performed at room temperature and 5 mm/min.

2.3.4 Small angle X-Ray scattering (SAXS)

Small angle X-Ray scattering (SAXS) can be used to determine the lamellar structure in semicrystalline polymers, dimensions of phase-separation in block copolymers and heterogeneities in ionomers. The scattered intensity versus the magnitude of the scattering vector q profile is often used to represent the patterns of SAXS. The profiles of the multiblock copolymer membranes cast with DMAc and annealed are presented in Figure 2.9. In the investigated range of scattering wave vectors, the profiles of the multiblock copolymer membranes exhibit scattering maxima, while the SAXS profile of the 6FPAEB-35 random copolymer membrane is featureless. The observed scattering maxima in the profiles of the 6FPAEB-BPS100 and 6FPAEB-HQS100 membranes are attributed to the aggregated nanophase

separated ionic domains. In addition, as the block length increased in the biphenol based multiblock copolymers the scattered intensity also increased, which suggests that the longer blocks induced an enhanced degree of phase separation. The SAXS profiles of these three multiblock copolymers had a primary peak at q_{max}, and also a secondary peak at $2q_{max}$, which is consistent with the scattering behavior of similar multiblock copolymer systems in our previous studies.[212] This may suggest that multiblock copolymers with longer block lengths in the 6FPAEB-BPS100 series exhibit lamellar morphologies. Additionally when comparing the copolymers of the two different systems with 7K-7K block lengths, the hydroquinone based multiblock copolymer had a clear secondary peak. This indicates that the copolymers with the higher IECs in the hydrophilic phases had enhanced phase separation at lower block lengths relative to the biphenol analogs. TEM micrographs (Figure 2.10) further confirmed these two trends observed in the SAXS profiles and the existence of a lamellar morphology for the 6FPAEB-BPS100 15K-15K multiblock copolymer. In the SAXS profile of the 6FPAEB-BPS100 7K-7K copolymer, the 2^{nd} order peak is weaker and broader than those of the longer block lengths. This suggests that the short block lengths with ionic domain aggregation could not form well-ordered lamellar structures. This is consistent with the TEM study that showed a disordered morphology in the 6FPAEB-BPS100 7K-7K copolymer (Figure 2.10). Enhanced phase separation yields more distinct and ordered ionic domains. It was also observed that as the block length and charge density of the multiblock copolymers increased, the main scattering peak shifted to lower *q* values. This indicates that the interdomain distance increased as block length increased.

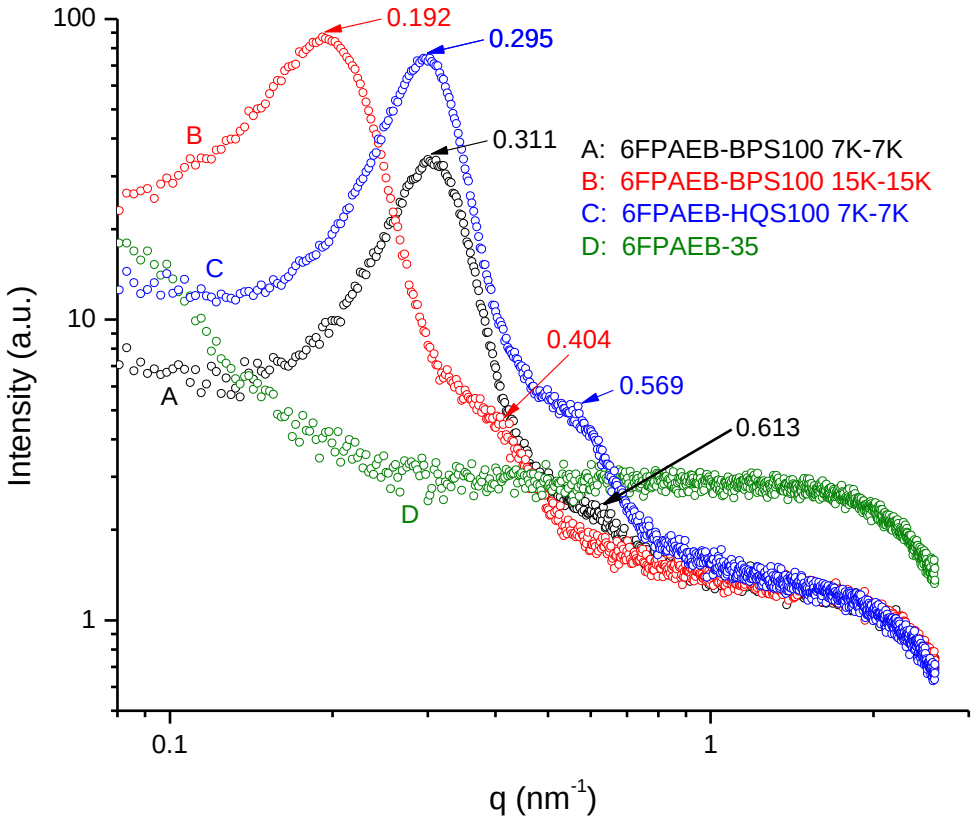

Figure 2.9: SAXS profiles of 6FPAEB-BPS100 and 6FPAEB-HQS100 multiblock copolymers and a 6FPAEB35 random copolymer membrane.

2.3.5 Transmission electron microscopy (TEM)

It has been observed that hydrophilic-hydrophobic multiblock copolymers can exhibit well-ordered nanophase separation.[210] This separation is believed to provide a co-continuous hydrophilic phase and facilitate proton transport. The sharp phase separated morphology accounts for heightened performance of PEMs under low relative humidity conditions. Figure 2.10 shows the TEM images of the 6FPAEB-BPSH and 6FPAEB-HQSH multiblock copolymer membranes with different block lengths. The bright and dark regions in the images correspond to un-stained hydrophobic domains and cesium ion stained electron-rich hydrophilic domains,

respectively. As block length was increased, the images of the multiblock copolymer membranes showed enhanced connectivity of the hydrophilic and hydrophobic domains. However, the 6FPAEB-HQSH showed greater connectivity and lamellar formation at lower block lengths over the 6FPAEB-BPSH membranes. The higher IECs in the hydrophilic phases of the hydroquinone based membranes over the biphenol analogs may have allowed for sharper phase separation and accounted for the more defined morphology.

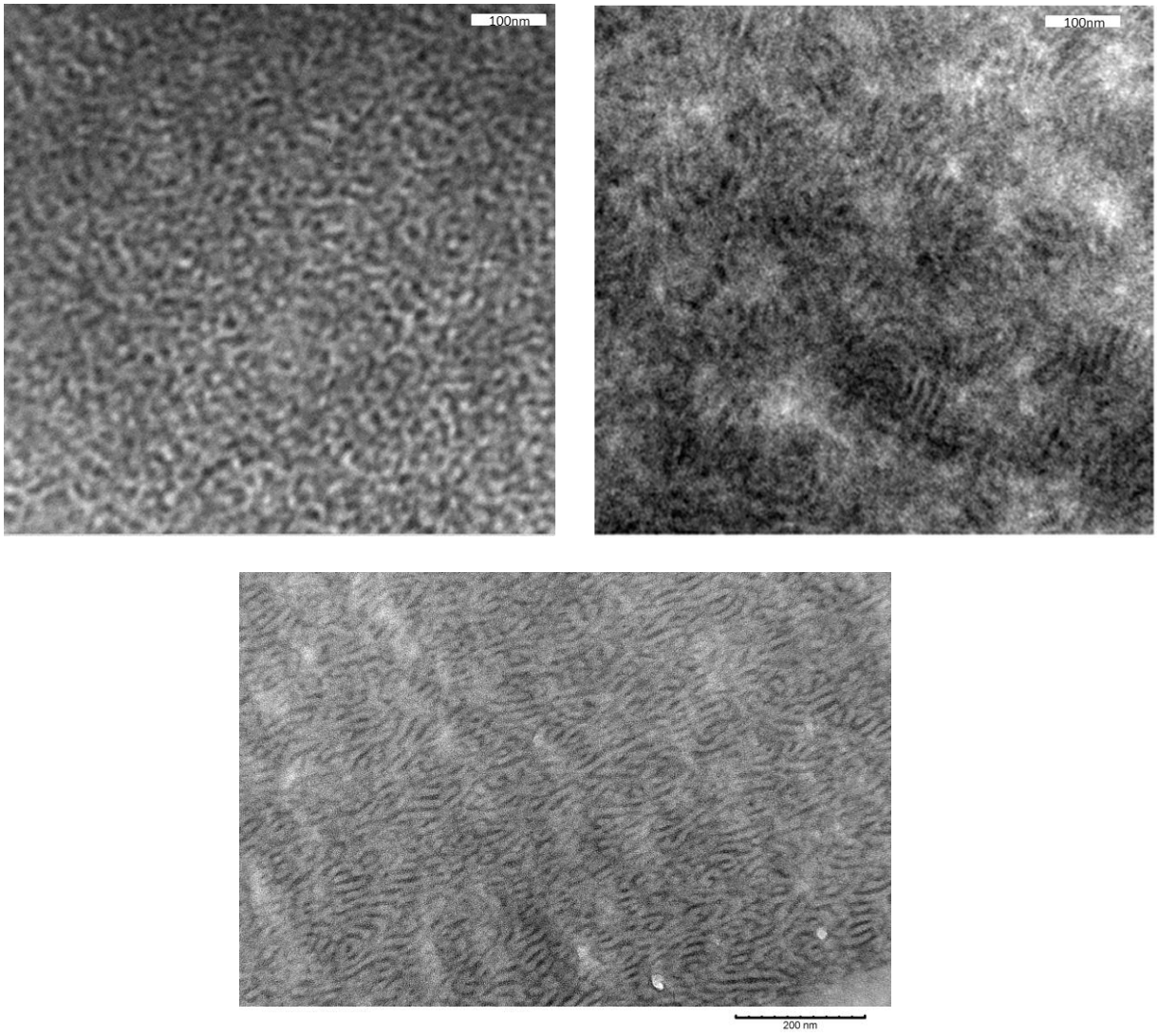

Figure 2.10: TEM images of 6FPAEB-BPSH (top left: 7K-7K, top right: 15K-15K) and 6FPAEB-HQSH (bottom 7K-7K) multiblock copolymer membranes.

2.3.6 Relative humidity and fuel cell testing

Figures 2.11 and 2.12 show how proton conductivities vary with relative humidity of the multiblock copolymers compared against Nafion® 212. The method used for these measurements differed from the method used in the past in our group for measuring relative humidity performance. Previously, the membrane was removed from the controlled-humidity oven and the thickness was measured at each humidity level. However, this method was controversial due to the fact that opening the oven most likely ruined the equilibrium present in the oven. Thus, in the method presented herein, the membranes were not removed from the oven during the entire experiment. However, the thickness of the membrane still needed to be accounted for because at lower humidities the membrane swelled less than at higher humidity levels. To account for the thickness variation, thickness in the wet and dry states were used to simulate the thickness at 30% and 95% relative humidity. The values were then extrapolated to estimate the thickness at the other relative humidity levels.

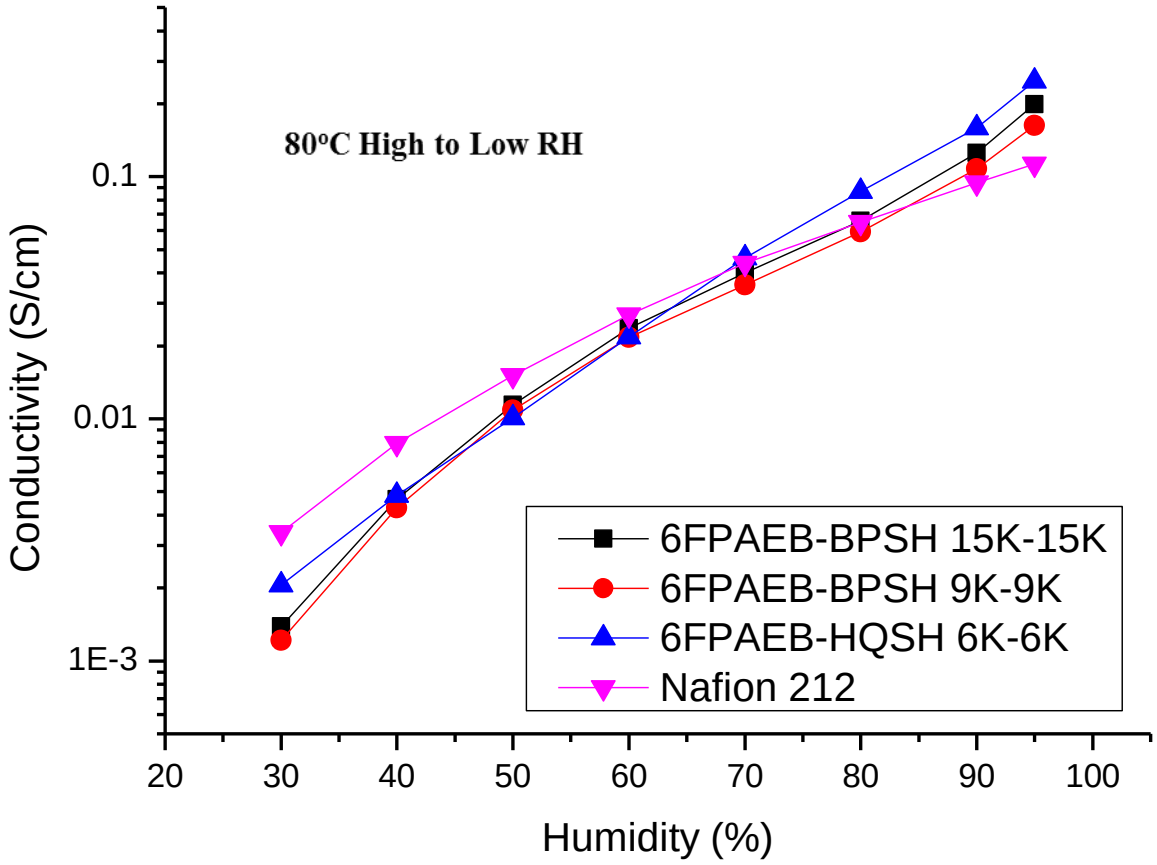

Figure 2.11: Proton conductivity as a function of relative humidity from high to low humidity for the multiblock copolymer membranes compared against Nafion® 212.

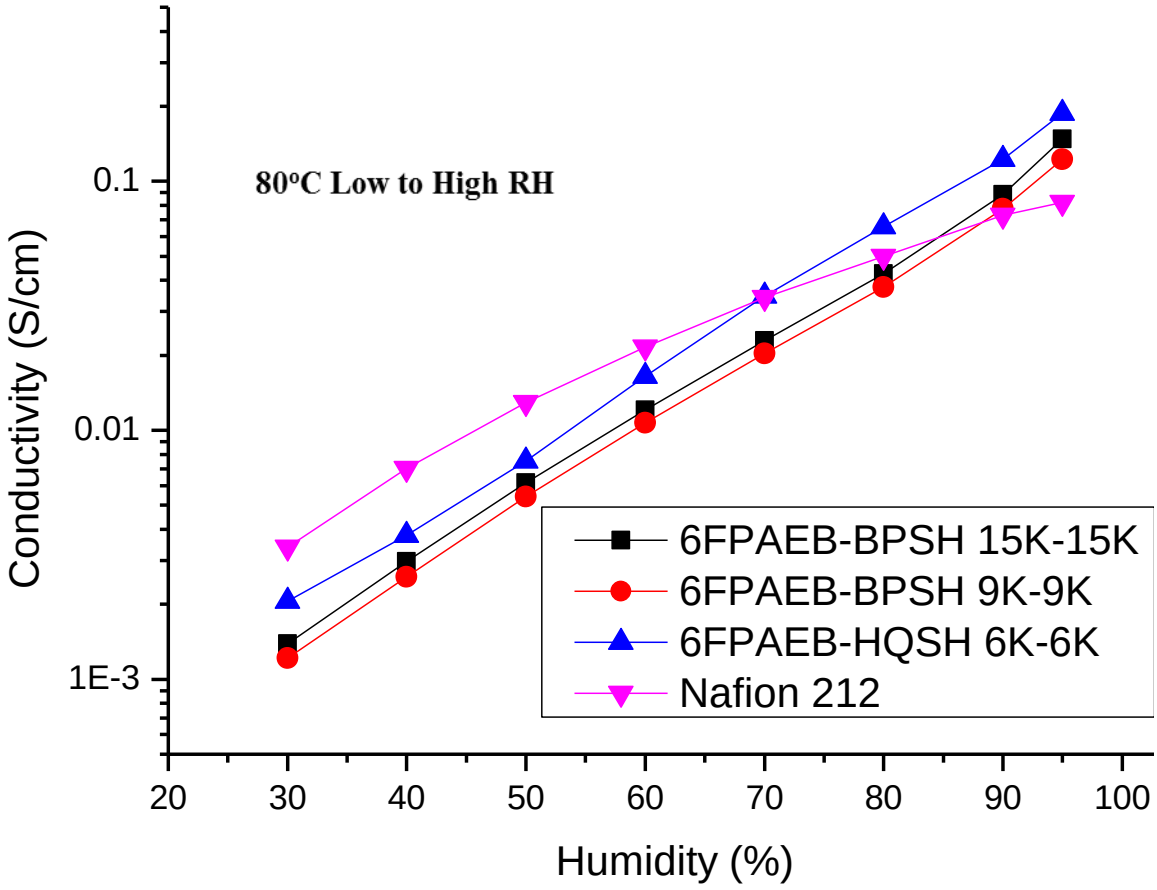

Figure 2.12: Proton conductivity as a function of relative humidity from low to high humidity for the multiblock copolymer membranes compared against Nafion® 212.

In both Figure 2.11 and 2.12 the hydroquinone based multiblock copolymer had higher conductivity than the biphenol based analog over the entire humidity range. The higher IEC and increased phase separation is the most likely reason for the increased conductivity experience by the hydroquinone membrane. While the conductivity was closer for the membranes in the high to low humidity plot, this gap was slightly widened in the low to high humidity plot. This indicates that the hydroquinone membrane experienced less hysteresis than the biphenol membranes. An offset plot showing the difference in conductivities going from low to high and high to low humidity for the membranes is shown in Figure 2.13. As can be seen in Figure 2.13, the gap

between the high to low and low to high curves is larger for the biphenol based membranes. For the multiblock copolymers this gap, or hysteresis, is most likely related to phase separation. The hysteresis slightly decreases as the block lengths are increased from 9K to 15K for the biphenol based multiblock copolymers, and further decreases for the hydroquinone based multiblock copolymer. As swelling and deswelling of the membrane occurred the more defined phase separation seemed to prevent a loss in the conductivities.

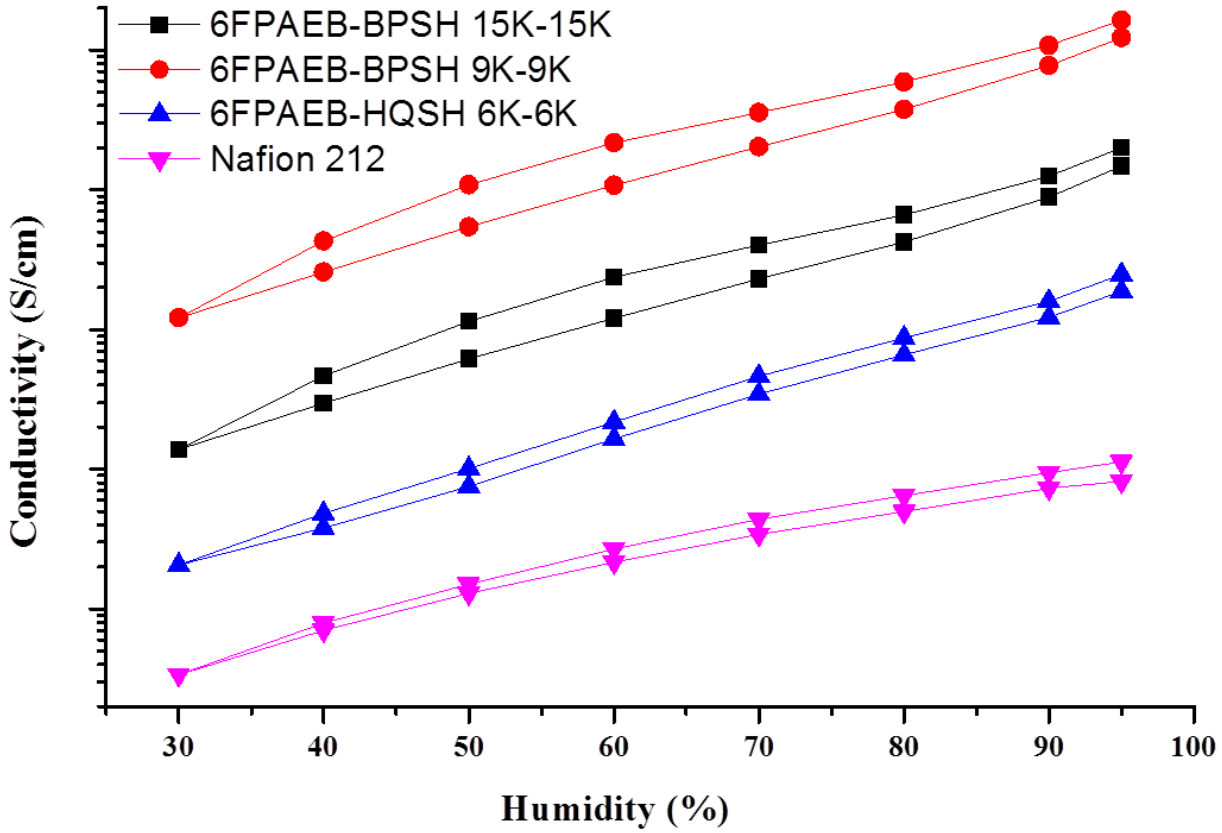

Figure 2.13: Plot of multiblock copolymer membranes and Nafion® 212 comparing conductivies going from high to low and low to high relative humidity.

However, both the biphenol and hydroquinone based membranes had the same trend when compared to the Nafion® 212 membrane. The multiblock copolymers had higher conductivities at the higher humidity levels while the perfluorinated membrane had higher

conductivities at lower relative humidities. This is consistent with the fuel cell performance shown in Figure 2.14.

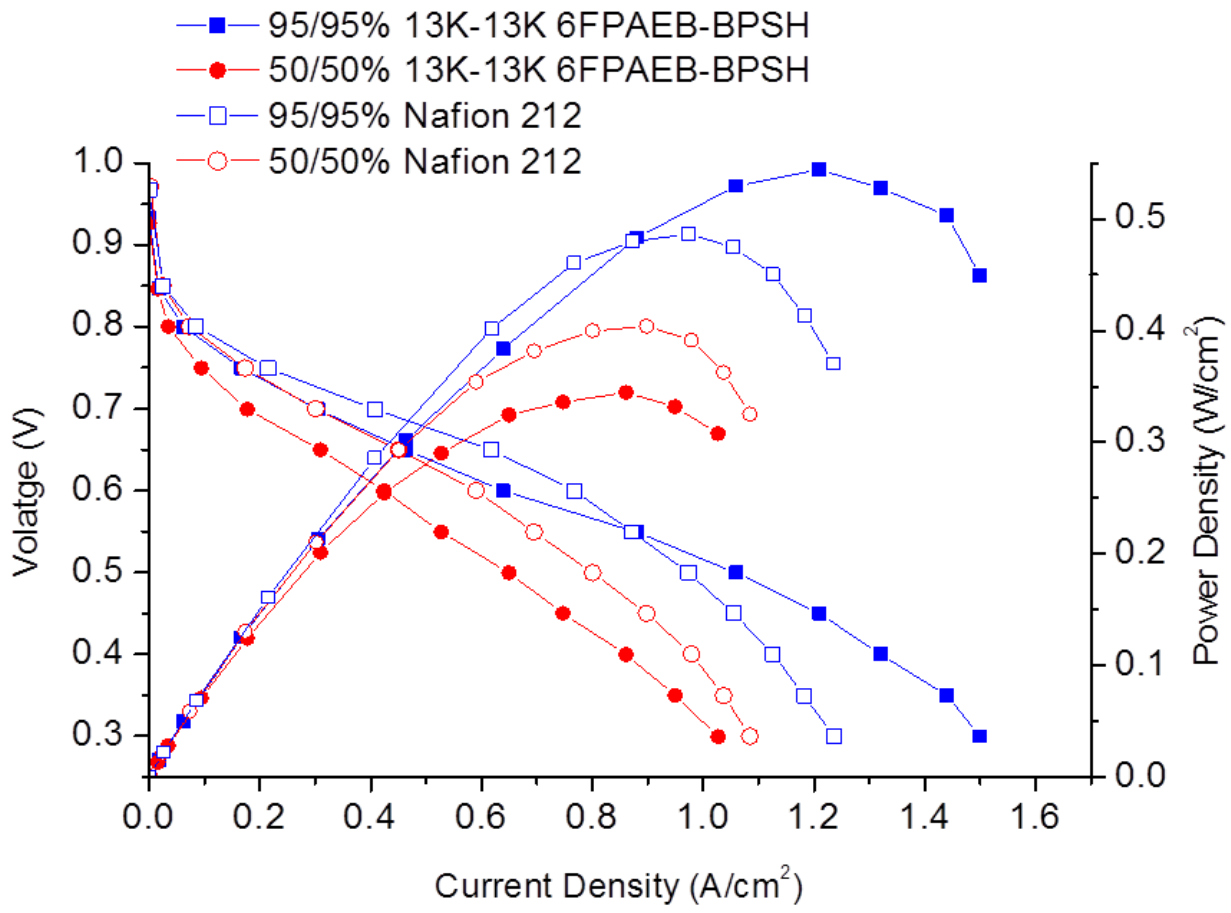

Figure 2.14: Fuel cell performance of multiblock copolymer and Nafion® 212 at 50% and 95% relative humidity at the electrodes. Testing was conducted in air at 101 kPa from 25 cm^2 MEAs.

The numbers in the legend refer to the humidity of the electrodes. Thus 95/95% means that both the anode and cathode where controlled at 95% relative humidity. Although not shown, these levels do not have to be equal, and testing can take place at 95/50% or 50/95% for instance. When tested at 95/95% relative humidity the multiblock copolymer had a higher power density maximum than the Nafion® 212 membrane. However, when the relative humidity was at 50/50%

the Nafion® 212 membrane had a higher maximum power density than the multiblock copolymer membrane. This is the same result that was observed when conductivity was measured as a function of relative humidity. Nevertheless, the results are encouraging due to the fact that conductivity and performance of the multiblock copolymers are very close to that of the perfluorinated membrane at low relative humidities. In fact, the conductivity of the hydroquinone based membrane at 30% relative humidity is within fifty percent of the Nafion® 212 membrane. With this testing method (which is generally the accepted method in the literature) most sulfonated copolymer membrane conductivities at 30% relative humidity are not within an order or magnitude relative to the Nafion membranes.[192,231-232]

2.4 Conclusions

Two series of hydrophobic-hydrophilic multiblock copolymers were successfully synthesized based on the combination of fluorine terminated poly(arylene ether benzonitrile) (6FPAEB) hydrophobic oligomers and phenoxide terminated disulfonated poly(arylene ether sulfone) hydrophilic oligomers (BPS100, HQS100). The alternating multiblock copolymer structures and compositions were confirmed by NMR spectroscopy, with SEC and stress-strain results confirming that high molecular weights were achieved. The 6FPAEB-HQSH series with the higher IEC in the hydrophilic phase showed increased proton conductivity and water uptake over the 6FPAEB-BPSH multiblock copolymers. However, by treating the membranes at a temperature between the T_g of the hydrophilic and hydrophobic regions, only moderate water uptake values were observed even at long block lengths. The fabricated membranes exhibited strong phase-separated morphology with well-defined hydrophobic and hydrophilic regions. Furthermore, the increased hydrophilicity of the hydrophilic phases in the hydroquinone series resulted in enhanced lamellar formation at similar block lengths over that of the biphenol based

block copolymers. The morphological dependence on block length observed in TEM images was confirmed with SAXS for the sulfonated membranes. The hydroquinone based membranes showed better conductivity as a function of relative humidity than the biphenol based membranes, indicating a positive effect with the change to a more hydrophilic phase. Furthermore, the fact that the multiblock copolymer membranes had high conductivity over a range of relative humidities, along with strong mechanical properties suggests that these materials may be promising membranes for H_2/Air proton exchange membranes.

Chapter 3: Multiblock Copolymers Based On Increased Hydrophobicity Bisphenol A Moieties for Proton Exchange Membranes

Used with permission of The Electrochemical Society, 2014, as
"Chapter 3: Multiblock Copolymers Based On Increased Hydrophobicity Bisphenol A Moieties for Proton Exchange Membranes Rowlett, J. R.; Chen, Y.; Shaver, A. T.; Fahs, G. B.; Sundell, B. J.; Li, Q.; Kim, Y. S.; Zelenay, P.; Moore, R. B.; Mecham, S.; McGrath, J. E., *J. Electrochem. Soc.* **2014,** *161*, F535."

3.1 Introduction

Wholly aromatic polymeric materials have been extensively shown to be viable candidates for use as proton exchange membranes (PEMs) in polymer electrolyte fuel cells (PEMFCs) due to their high proton conductivity, strong mechanical properties, and excellent thermal, chemical and oxidative stability.[6,26,100-101,207,233-234] The major focus of these studies has been based on sulfonated poly(arylene ether sulfone)s (SPAESs) and sulfonated poly(arylene ether ketone)s (SPEAKs).[102-103,120] The use of a pre-sulfonated monomer allowed these materials to be synthesized without the need to post-sulfonate the resultant membranes. Copolymers produced from this pre-sulfonation method were found to be more stable plus the low methanol permeability of these wholly aromatic membranes made these materials even more attractive in direct methanol fuel cells (DMFCs), as low methanol permeability increases fuel efficiency and cell performance.[119,224,231] High fuel crossover is a critical problem associated with the highly fluorinated Nafion® and similar poly(perfluorosulfonic acid) membranes, which are traditionally used as the PEMs in DMFCs.

Recently, sulfonated poly(arylene ether) copolymers containing nitrile groups have been shown to further improve performance by reducing membrane swelling compared to analogous copolymers that have similar ion-exchange capacities (IEC)s.[107-110,121,235-236] The membrane

electrode assemblies (MEAs) of these copolymer membranes showed superior performance to both Nafion® and the biphenol based SPAES statistical copolymer (BPSH-40) membranes. The reduction in water uptake caused by introduction of the nitrile group has been proposed to allow for better interfacial adhesion between the PEM with Nafion-bonded electrodes, decreasing the high frequency resistance (HFR) and increasing the performance of the MEAs.[236-238] Additionally, studies conducted on the non-fluorinated systems suggested that elimination of the fluorine moiety resulted in delamination between the membrane and the Nafion®.[239-240]

While nitrile-containing copolymer systems showed promising electrode compatibility and low methanol permeability with statistical copolymer architecture, further improvement can be made with multiblock copolymers.[237] Two major advantages were expected with multiblock copolymers: i) enhanced proton conductivity and ii) better mechanical properties. Enhanced proton conductivity arises due to the self-assembled morphology of the multiblock copolymer, with the increases in conductivity allowing for the use of a membrane with reduced resistance.[226] The less resistant multiblock copolymer membranes then consequently reduce cell resistance. Additionally, improved mechanical properties due to hydrophilic-hydrophobic phase separations can allow for the use of higher IEC membranes (high IEC membranes are usually less mechanically stable) as well as improve fuel cell stability. Our previous results showed that the cell using high IEC multiblock copolymers exhibited substantially reduced cell resistance that had been hard to obtain with the cell using statistical copolymers. However, using high IEC multiblock copolymer membranes often requires further structure control since membranes with higher IEC absorb more water.[13,122,208,215-217,220] One approach taken to attempt to control the water uptake and mechanical properties of these multiblock copolymers is by control of the hydrophobic segment in the design of the multiblock copolymer. Investigation of SPAES using

different sized hydrophobic components and varying block lengths in the multiblock copolymer have been reported.[217,230] However, very little research has been explored involving a change in hydrophobic nature via chemical structure control of the non-sulfonated segment.

In this work we report novel multiblock copolymers that have extremely low water uptake. The multiblock copolymer series was synthesized with a SPAES hydrophilic phase and a poly(arylene ether benzonitrile) hydrophobic phase. A partial mole percent of the fluorinated monomer was replaced with a series of non-fluorinated bisphenol A moieties with increasing hydrophobicity as a result of added benzyl methyl groups. The electrochemical properties of these copolymers were examined to elucidate the structural effect on membrane properties. Further DMFC testing and performance will be discussed in a second corresponding publication.

3.2 Experimental

3.2.1 Materials

2,6-Difluorobenzonitrile (DFBN), *N*-Methyl-2-pyrrolidinone (NMP), *N*,*N*-dimethylacetamide (DMAc), cyclohexane, and toluene were purchased from Sigma-Aldrich. DFBN and toluene were reagent grade and used as received, NMP and DMAc were distilled from calcium hydride before use. 4,4′-Hexafluoroisopropylidenediphenol (6F-BPA), received from Ciba, was sublimated and then recrystallized twice from toluene. Monomer grade 4,4′-biphenol (BP) was provided by Eastman Chemical Company, and dried under vacuum at 80^{o}C prior to use. Monomer grade 3,3'-disulfonated-4,4'-dichlorodiphenylsulfone (SDCDPS) was received from Akron Polymer Systems and dried under vacuum at 150^{o}C for 3 days prior to use. A previously reported method was used to determine purity of the SDCDPS monomer from UV-Vis spectroscopy.[118] 2,2-Bis(4-hydroxy-3-methylphenyl)propane (dimethyl bisphenol A, DMBPA), and 2,2-bis(4-hydroxy-3,5-dimethylphenyl)propane (tetramethyl bisphenol A,

TMBPA) were both reagent grade, purchased from TCI America and used as received. 4,4'-(Propane-2,2-diyl)diphenol (Bisphenol A, Bis A) was kindly provided by Solvay and recrystallized from toluene prior to use. Reagent grade potassium carbonate (K_2CO_3), acetone, and methanol were purchased from Fisher Scientific. Potassium carbonate was dried under vacuum at 180^oC prior to use, while acetone and methanol were used without further purification.

3.2.2 Synthesis of the nitrile-containing hydrophobic oligomers

All oligomers were synthesized via nucleophilic aromatic substitution with different block lengths being achieved by using a molar excess of the benzonitrile monomer. An example synthesis of a hydrophobic oligomer with a targeted 10,000 g/mol molecular weight (M_n) is as follows: 6FBPA (5.14 g, 15.29 mmol), Bis A (3.49 g, 15.29 mmol) and DMAc (70 mL) were placed into a three neck round bottom flask equipped with a stir bar, condenser, nitrogen inlet, and Dean-Stark trap. The mixture was heated to 140^oC and stirred until 6FBPA was completely dissolved. Once a transparent solution was obtained, K_2CO_3 (4.86 g, 35.17 mmol) and toluene (35 mL) were added into the flask. The reaction was allowed to reflux at 140^oC for 4 h to azeotropically remove water from the system, and then slowly heated to 170^oC to remove toluene. The reaction temperature was decreased to 80^oC and DFBN (4.42 g, 31.79 mmol) was added to the flask (added after dehydration to prevent any possible DFBN monomer loss). The reaction was allowed to proceed for 8 h at 125^oC (in a closed system to prevent loss of DFBN monomer), then cooled to room temperature and filtered to remove any excess K_2CO_3 or by-product salts. The oligomer was precipitated in methanol (1000 mL), stirred overnight, filtered and then dried *in vacuo* at 110 ^oC for 48 h. All other hydrophobic oligomers were synthesized in the same fashion.

3.2.3 Synthesis of hydrophobic-hydrophilic multiblock copolymers

All multiblock copolymer systems were synthesized with equal block lengths of the hydrophobic and hydrophilic segments to form a series of multiblock copolymers. The hydrophilic oligomers (BPS100) were synthesized as reported previously.[13,122,211,213] An example synthesis of the multiblock copolymer is as follows: BPS100 (4.500 g, 0.500 mmol), K_2CO_3 (0.150 g, 1.087 mmol), and NMP (45 mL) were added to a three-necked 100-mL flask equipped with a mechanical stirrer, condenser, nitrogen inlet and Dean-Stark trap. The reaction bath was heated to 120 ^oC, then cyclohexane (15 mL) was added and the mixture was refluxed for 6 h to remove water from the system. After removing cyclohexane, the reaction bath was cooled to 90^oC, and the hydrophobic oligomer (4.600 g, 0.510 mmol) was added. The bath temperature was raised to 135^oC and kept at this temperature for 48 h. The reaction mixture was precipitated into isopropanol (1000 mL) and stirred for 12 h. The product was filtered then washed in deionized (DI) water at 90^oC for 12 h, filtered again and then dried in vacuo at 150^oC for 24 h. The copolymers based on the different hydrophobic segments were synthesized in the same fashion as the procedure described above.

3.2.4 Synthesis of a hydrophobic-hydrophilic statistical copolymer 6FTMPAEB-50

A statistical copolymer was synthesized with similar molar ratios to the hydrophobic-hydrophilic multiblock copolymers. 6F-BisA (1.681 g, 5.000 mmol), 2,6-DCBN (1.720 g, 10.000 mmol), TMBPA (1.422 g, 5.000 mmol), SDCDPS (5.039 g, 10.000 mmol), BP (1.862 g, 10.000 mmol) and NMP (50 mL) were added to a three-necked 100 mL flask equipped with a mechanical stirrer, condenser, nitrogen inlet and Dean-Stark trap. The reaction bath was heated to 150^oC, then K_2CO_3 (3.870 g, 28.000 mmol) and toluene (25 mL) were added and refluxed for 3 h to dehydrate the system. Toluene was drained from the system and the reaction was heated to

190^{o}C and maintained at this temperature for 72 h. The viscous solution was hot filtered using an aspirator to remove salts, and then precipitated dropwise in isopropanol (1600 mL) and stirred overnight. The fibrous white solid was filtered using an aspirator, washed with additional isopropanol and then dried in vacuo at 150^{o}C for 24 h.

3.2.5 Membrane preparation and acidification

The potassium salt form segmented block copolymers were dissolved in DMAc (~7% w/v), after drying at 150^{o}C for 24 h, and filtered through a 0.45 μm Teflon syringe filter. The solutions were cast onto a dry, clean glass substrate and dried for 24 h under an infrared lamp at ~80°C. Additionally, the membranes were annealed under vacuum at 220°C in the potassium salt form, about 30°C higher than the T_g of the nitrile based hydrophobic blocks. The membranes were converted to the acid form by boiling in 0.5 M sulfuric acid for 2 h, followed by boiling in DI water for 2 h.

3.2.6 Characterization

^{1}H, ^{19}F, and ^{13}C NMR analyses were conducted on a Varian Unity Plus spectrometer operating at 400 MHz (376 MHz for ^{19}F and 100.58 MHz for ^{13}C). The spectra of the BPS100 hydrophilic oligomers along with their corresponding block copolymers were obtained from a 10% (w/v) 1 mL solution in DMSO-d_6. The spectra of the hydrophobic oligomers were obtained from a solution in $CDCl_3$. ^{13}C NMR analyses were conducted on a Varian Unity spectrometer, operating at 100.58 MHz with DMSO-d_6 as the solvent. Weight average molecular weights (M_ws) of all block copolymers were obtained via multi-detector size-exclusion chromatography (SEC) using NMP with 0.05 M LiBr as the mobile phase (50^{o}C) with 3 PLgel 10 μm mixed-B 300 x 7.5 mm columns in series with a Wyatt Viscostar II Viscometer, a Wyatt Heleos II multi

angle light scattering detector, and a Wyatt T-rex refractive index detector. M_ws were reported for these systems as this is an accurate measured value using this technique.

3.2.7 Tensile testing

Uniaxial load tests were performed using an Instron 5500R universal testing machine equipped with a 200-lb load cell. The crosshead displacement rate was 5 mm/min and the gauge length was 26.5 mm. The tensile test specimens were prepared with dimensions of 50 mm length and a minimum width of 4 mm per ASTM D638-03. Prior to testing, acid form membrane specimens were dried *in vacuo* at 100^{o}C and tested at room temperature. All specimens were mounted in pressure locking pneumatic grips.

3.2.8 Proton conductivity and water uptake

Proton conductivities of the multiblock copolymer membranes in the fully hydrated state were determined at 30^{o}C in liquid water. Measurements were made in-plane with a four electrode configuration. Before the measurement, the membranes were equilibrated in DI water at 30^{o}C for 24 h. A Solartron (1252 + 1287) impedance/gain-phase analyzer over the frequency range of 10 Hz to 1 MHz was used for the measurements following a previously reported method.[241] The conductivity was calculated by using equation 3.1.

(3.1) $$\sigma = \frac{L}{R \cdot S}$$

Where σ (S/cm) is proton conductivity, L (cm) is the distance between the two electrodes, R (Ω) is the resistance of the membrane and S (cm^2) is the surface area available for proton transport though the membrane. The water uptake of all membranes was determined gravimetrically. The membranes were equilibrated in DI water at room temperature for 2 days after acidification. Wet membranes (in acid form) were removed from DI water, blotted dry to remove surface droplets, and quickly weighed. The membranes were dried at 120^{o}C under vacuum for 24 h and re-

weighed. The water uptake of the membranes was calculated according to equation 3.2, where W_{dry} and W_{wet} refer to the mass of the dry and wet membrane, respectively.

(3.2) $$Water\ Uptake\ (\%) = \frac{W_{wet} - W_{dry}}{W_{dry}} \times 100$$

3.2.9 Membrane electrode assembly and fuel cell testing

Membrane electrode assemblies (MEAs) using multiblock copolymers were prepared by using the gas diffusion electrode (GDE) method. For the GDE method, commercial GDEs with carbon-supported PtRu (75% metal loading, HiSPEC® 12100, Johnson Matthey) and Pt (60% metal loading, HiSPEC® 9100, Johnson-Matthey) were used for anode and cathode catalyst layers, respectively. The catalyst loading for the anode and cathode were 2.7 and 2 mg/cm^2, respectively. Multiblock copolymer membranes were inserted between anode and cathode GDE with a glass fiber reinforced Teflon gasket to assemble the MEAs. H_2/air and DMFC polarization curves with high frequency resistance (HFR) were obtained using a fuel cell test station equipped with an internal AC impedance analyzer (Fuel Cell Technology Inc). Cell performance was obtained after 3 h break-in under H_2/air conditions at a cell voltage of 0.7 V at 75°C. For DMFC mode operations, 0.5, and 1 M aqueous methanol solutions were supplied to the anode with a flow rate of 1.8 mL/min; fully humidified air was supplied at 500 sccm without back pressure (high humidification and stoichiometry were used to minimize ohmic and mass transfer effects). HFR was measured by applying a sinusoidal wave perturbation of 2 kHz where capacitive contributions to cell impedance were found to be minimized.

3.2.10 Morphology

The membranes were tested in the potassium salt form after annealing at 220^{o}C using the same method as listed for the membrane preparation. Additionally the membranes were dried in a vacuum oven at 100^{o}C for 12 h prior to being tested to ensure that no water was present in the

membranes. SAXS experiments were performed using a Rigaku S-Max 3000 3 pinhole SAXS system, equipped with a rotating anode emitting X-rays with a wavelength of 0.154 nm (Cu Kα). The q-range was calibrated using a silver behenate standard. Two-dimensional SAXS patterns were obtained using a fully integrated 2D multiwire, proportional counting, gas-filled detector, with an exposure time of 1 hour. All the SAXS data were analyzed using the SAXSGUI software package to obtain radially integrated SAXS intensity versus scattering vector q, where $q = (4\pi/\lambda)\sin(\theta)$, where θ is one half of the scattering angle and λ is the wavelength of the X-ray. Interdomain distance (d_x) was calculated from the scattering vector peaks (q_x) based on equation 3.3, which was derived from Bragg's law.

(3.3) $$d_x = \frac{2\pi}{q_x}$$

3.3 Results and Discussion

3.3.1 Synthesis of fluorine terminated nitrile-containing hydrophobic oligomers

Figure 3.1 shows the synthesis scheme used for the fluorine terminated hydrophobic oligomers. For each of the oligomers the difluorobenzonitrile (DFBN) monomer was used in excess according to the Carothers equation in order to obtain a targeted number average molecular weight (M_n) of approximately 10 kg/mol.[242] In each of the oligomers synthesized equal molar amounts were used of the fluorinated and non-fluorinated phenolic monomers to afford statistical copolymer oligomers with a 50/50 ratio. The oligomers were denoted as $6F_{50}X_{50}$PAEB where X referred to either bisphenol A (Bis A), dimethyl bisphenol A (DM), or tetramethyl bisphenol A (TM) monomers.

The progress of the reactions was monitored by ^{1}H NMR spectroscopy, where the completion of the reaction was judged by the disappearance of the phenyl protons next to the

phenoxide endgroups. Molecular weight of the hydrophobic oligomers were then determined by ^{19}F NMR spectroscopy by comparing the ratio of the fluorines on the benzonitrile terminated chain to the fluorines on the backbone of the main chain. Figure 3.2 shows the ^{19}F spectra with the peak at -64 ppm attributed to the backbone and -105 ppm to the endgroups. Molecular weights of 10 kg/mol were achieved for each of the hydrophobic oligomers.

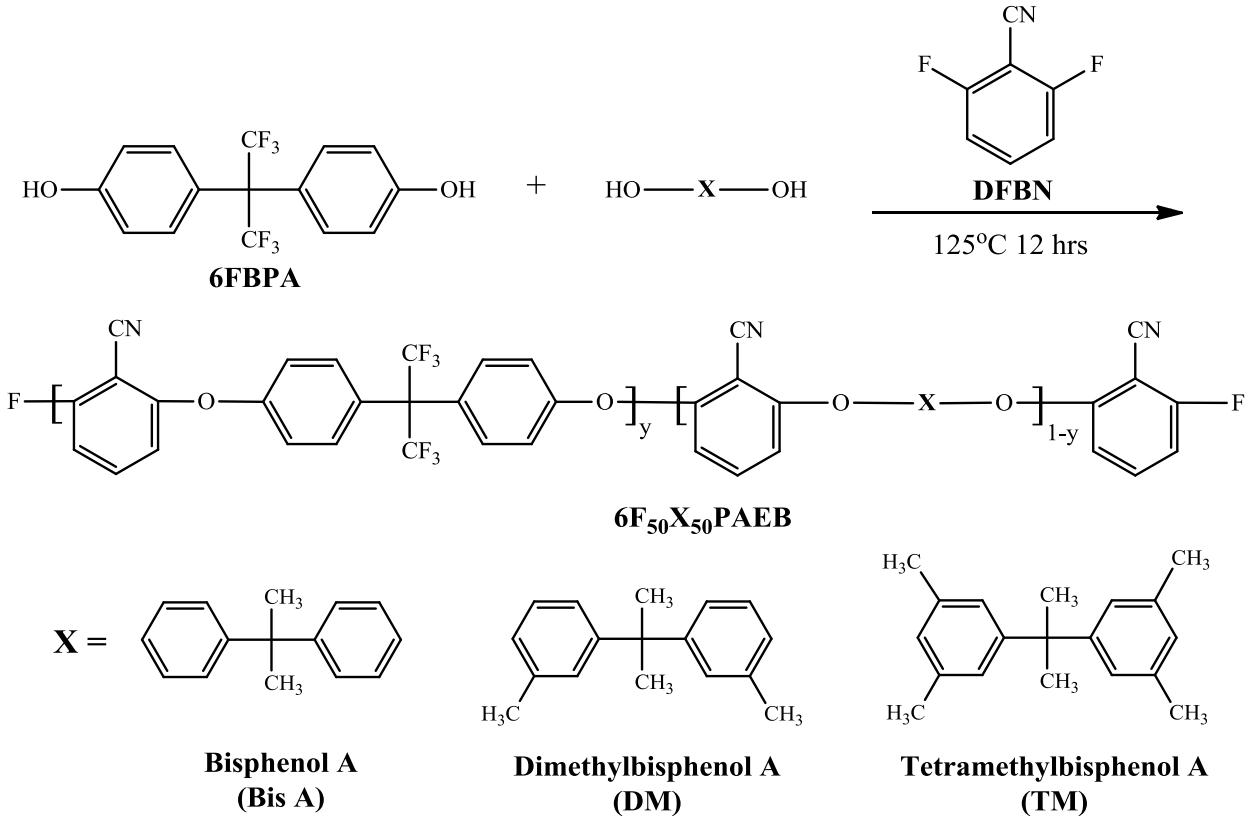

Figure 3.1: Synthesis of the fluorine terminated benzonitrile-containing hydrophobic oligomers

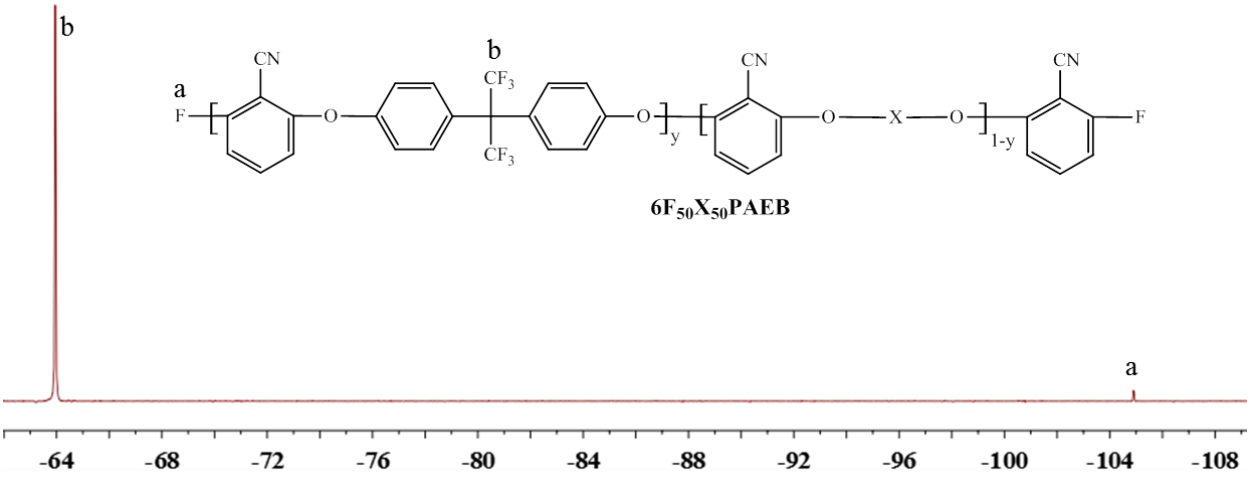

Figure 3.2: ^{19}F NMR of benzonitrile terminated hydrophobic oligomer

3.3.2 Synthesis of BPS100 hydrophilic oligomers and corresponding multiblock copolymers

Synthesis of the disulfonated hydrophilic oligomer, (BPS100), has been well established and was performed according to previous reported procedures.[13,122,211,213,215-216,220] Phenol terminated oligomers of 10 kg/mol were synthesized for the BPS100 hydrophilic segments, which were then reacted with the different activated halide terminated hydrophobic segments (also 10 kg/mol) to form a series of 10K-10K (K is used to represent kg/mol) multiblock copolymers with increasing hydrophobicity. The hydrophobicity was increased via the introduction of methyl groups on the bisphenol A based diol monomer. Addition of two methyl groups on the bisphenol A unit afforded the dimethyl multiblock copolymer, while the four methyl groups gave the tetramethyl multiblock copolymer. Nomenclature for the multiblock copolymers was referred to as $6F_{50}X_{50}$PAEB-BPS100 when in the potassium salt form, and $6F_{50}X_{50}$PAEB-BPSH when in the acid form. Figure 3.3 shows the synthesis scheme for the multiblock copolymers. Similar to the previous multiblock copolymers produced in our group, relatively mild reaction temperatures where used in order to reduce any possible ether-ether

interchange reactions, which have been shown to occur at elevated temperatures.[96] By using this method an alternating multiblock copolymer composition was achieved and confirmed by ^{13}C NMR spectroscopy. Figure 3.4 shows the region of the ^{13}C spectrum associated with the carbons of ether bonds in the multiblock copolymers and the structures of the multiblock versus the statistical copolymer. The top three spectra represent the multiblock copolymers while the bottom is a statistical copolymer with the same composition as the tetramethyl containing multiblock copolymer. The top three spectra show sharp and clearly defined peaks associated with the ether bonds of the three different multiblock copolymers, while the bottom statistical spectrum shows many jagged and uneven peaks. This is because the statistical copolymer has many more possible ether bonds in its structure. Comparison of the ^{13}C spectra indicate that ether-ether interchange reactions were minimized for the reactions and that an alternating multiblock copolymer morphology was maintained.

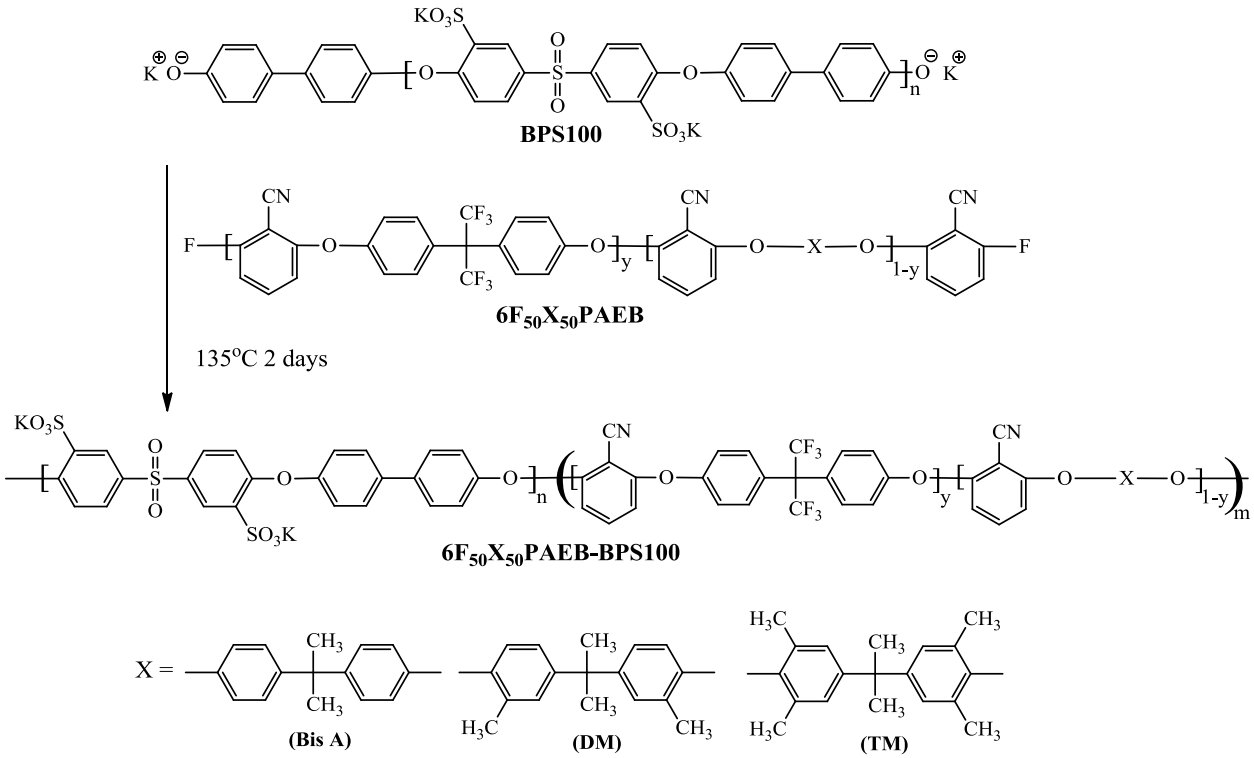

Figure 3.3: Synthesis scheme for benzonitrile-containing hydrophilic-hydrophobic multiblock copolymers

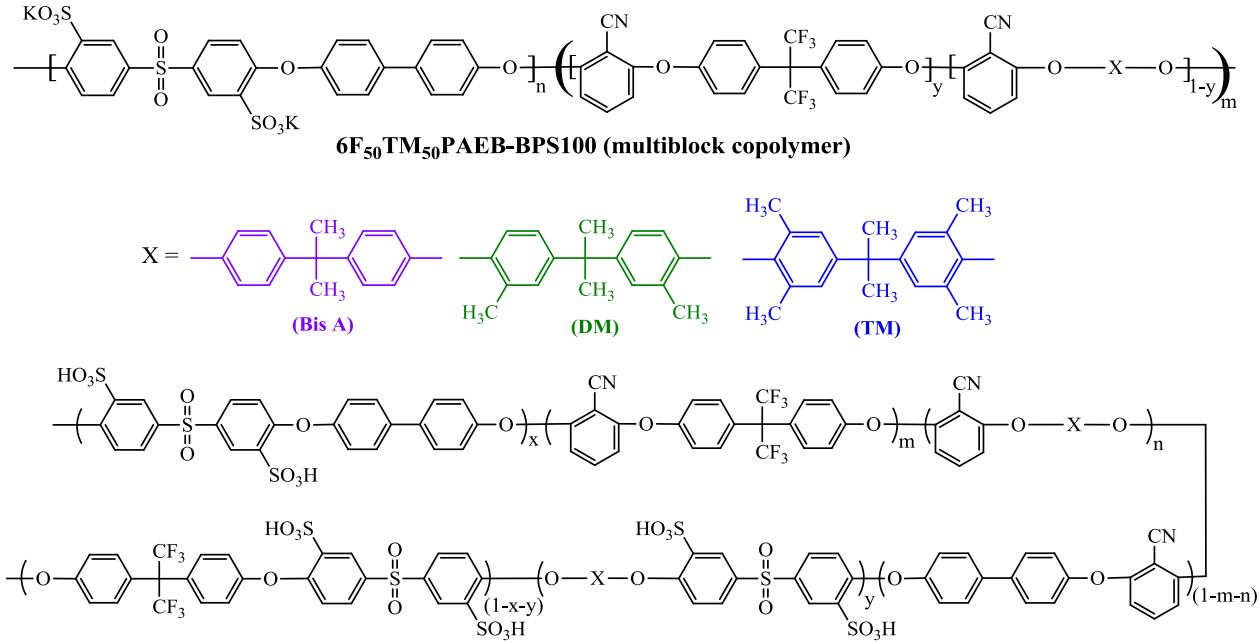

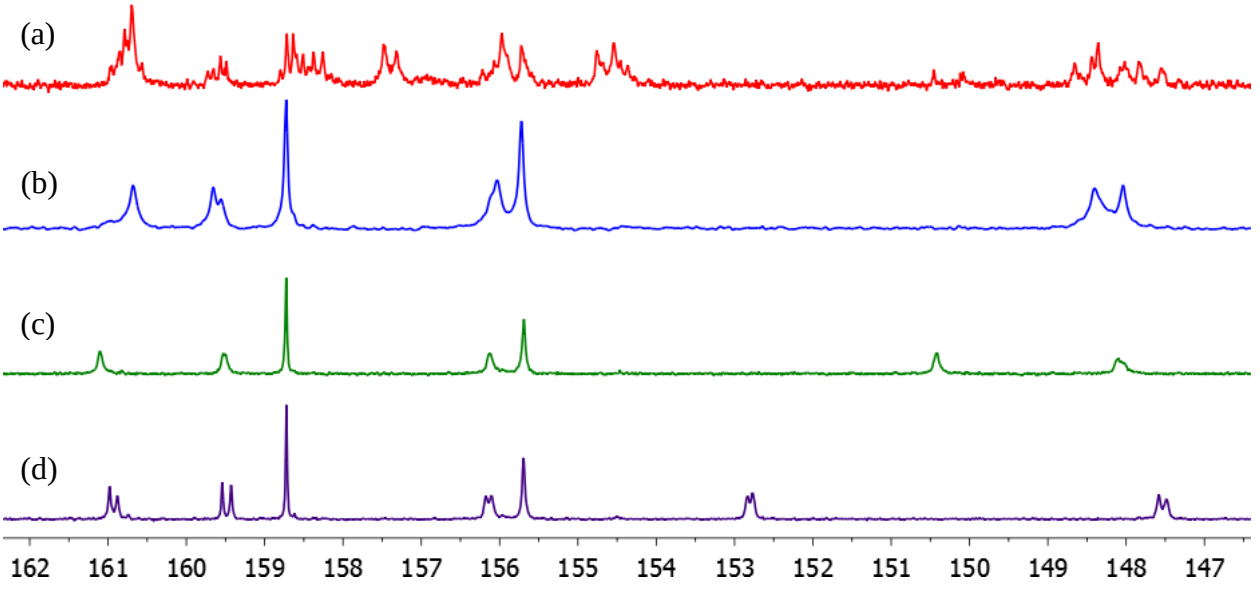

Figure 3.4: ^{13}C NMR and structures of multiblock copolymers $6F_{50}X_{50}$PAEB-BPS100 and a random copolymer 6FTMPAEB-BPS-50 focused in the ether region of the spectra: (a) statistical copolymer 6FTMPAEB-50, (b) $6F_{50}TM_{50}$PAEB-BPS100, (c) $6F_{50}DM_{50}$PAEB-BPS100, and (d) $6F_{50}BisA_{50}$PAEB-BPS100.

Additionally to gauge the progress of the reaction a small mole percent excess of the hydrophobic oligomer was used and the disappearance of the phenyl protons next to the phenoxide endgroups was followed by ^{1}H NMR spectroscopy (Fig. 3.5). After 48 h the viscosity of the reactions significantly increased and showed no presence of the biphenol endgroup moieties in the spectra, thus the reactions were deemed complete. The ratio between the hydrophilic and hydrophobic peaks in the ^{1}H NMR spectrum was used to calculate the resulting IEC of the multiblock copolymers. To calculate this, the ratio between the peak at 8.3 ppm, which corresponds to the proton adjacent to the sulfonate group, and the bisphenol A bridging methyl groups at 1.7 ppm were used for all of the multiblock copolymers.

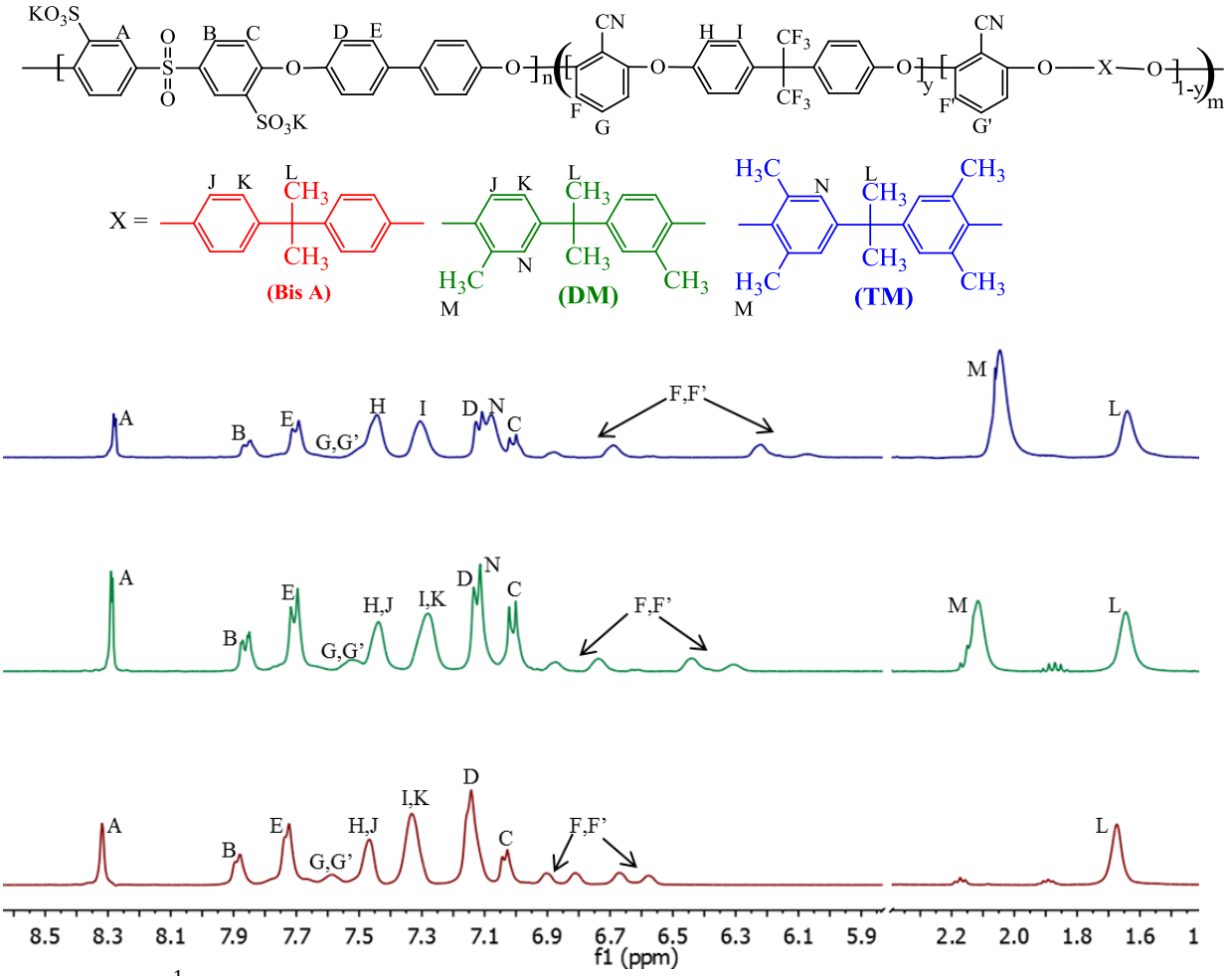

Figure 3.5: ^{1}H NMR of $6F_{50}X_{50}$PAEB-BPS100 series: top tetramethyl bisphenol A, middle dimethyl bisphenol A, and bottom bisphenol A.

3.3.3 Characterization of membrane properties for $6F_{50}X_{50}$PAEB-BPSH series

The series of multiblock copolymer membranes were characterized in regards to ion-exchange capacity, water uptake, and proton conductivity. These membrane properties are listed in Table 3.1 as a function of polymer structure. All membranes listed in Table 3.1 were annealed at 220^{o}C in their potassium salt forms, a temperature between the glass transitions of the hydrophobic and hydrophilic segments, which has been shown to facilitate the formation of phase-separated morphological structure and reduce water swelling.[122,215-216] The T_g of the hydrophilic phase appears as a very broad transition around 250^{o}C and can be hard to

distinguish, as shown in previous publications.[216] However, the glass transition temperatures (T_gs) of the hydrophobic oligomers can be seen in Figure 3.6, which indicate that 220°C is in between the T_g of the hydrophilic and hydrophobic phase for the multiblock copolymers.

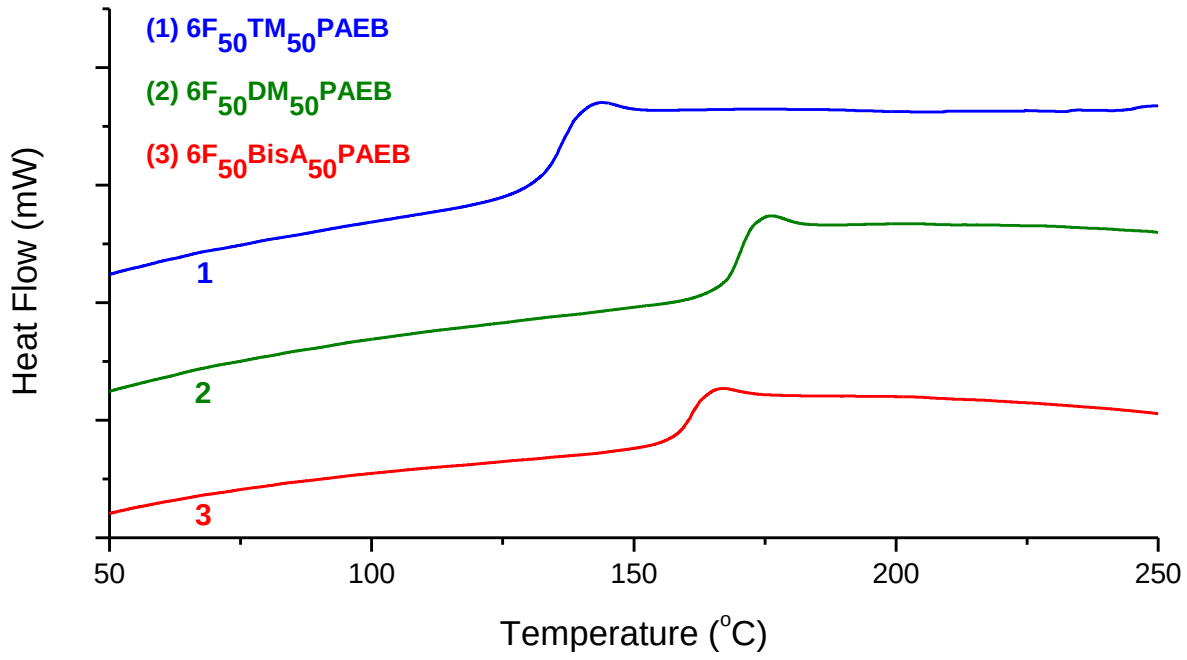

Figure 3.6: DSC of hydrophobic oligomers

Table 3.1: Properties of 10K-10K $6F_{50}X_{50}$PAEB-BPSH PEMs (1.0 M MeOH)

$6F_{50}X_{50}$ PAEB-BPSH	IEC (meq/g)[a]	IEC (meq/g)[b]	M_w (kg/mol)	Water Uptake (wt%)	Proton Conductivity (S/cm)	Methanol Permeability (cm^2/s)[c]	Relative Selectivity[d]
TM	1.50	1.50	50	20	0.10	1.28 E-07	1.4
DM	1.65	1.75	80	35	0.15	1.50 E-07	1.8
Bis A	1.74	1.65	75	40	0.12	1.38 E-07	1.6
Nafion® 212	1.00	-	-	22	0.12	2.20 E-07	1.0

a. Measured from ^{1}H NMR
b. Measured by titration with 0.01 M NaOH
c. Measured from limiting current method using fuel cell hardware in 1.0 M MeOH
d. Selectivity = proton conductivity/methanol permeability, relative selectivity is normalized with Nafion® selectivity

All multiblock copolymers tested were of equal block length between the hydrophobic and hydrophilic segments to enhance consistency between different compositions. Block lengths of 10 kg/mol were chosen to provide long enough lengths to allow for phase-separation between the two segments. Fifty mole percent of the fluorinated monomers were replaced with the various bisphenols for each of the PEMs in order to reduce the methanol permeability and to gauge the effect of the different comonomers. Fluorination level has been shown to have an increasing effect on methanol permeability, however only fifty percent was replaced due to previous studies in which pure non-fluorine containing membranes were found to be incompatible with the Nafion-bounded electrodes.[14-15]

As seen in Table 3.1 the inclusion of increasingly hydrophobic bisphenol moieties had a drastic effect on the properties of the multiblock copolymers. Notably, the IEC and water uptake of the membranes were significantly decreased as the comonomer was changed to dimethyl and

tetramethyl-substituted bisphenols. The lower IEC and M_w of the tetramethyl membrane indicates a slightly lower degree of hydrophilic block incorporation in the segmented multiblock copolymer. Although the IEC for the multiblock copolymer containing tetramethyl bisphenol A was less than for the other two systems, the ratio of the drop in water uptake was much greater than the ratio for the decrease in the IEC. For example the TM had half the water uptake than the Bis A multiblock but the TM multiblock was only about 10% higher in IEC. This indicates that the four pendant benzylic methyl groups are responsible for the stark decline in water uptake in the PEMs. This was most evident from the change to the dimethyl to tetramethyl bisphenol with a decrease from 35 to only 20 percent water uptake for the membranes. To further quantify this point the volume based parameters are presented in Table 3.2. The values from IEC_v wet and dry were calculated according to a previous reported procedure.[243] As was the case for the weight based values, the tetramethyl system had a lower volume water uptake which resulted in less of a drop in IEC_v going from the dry to wet state. The dimethyl membrane had a swelling characteristic comparable to that of the Nafion® membrane, while the tetramethyl was considerably less than the other membranes.

Table 3.2: Volume based properties for multiblock copolymers

$6F_{50}X_{50}$PAEB-BPSH	**Density (g/cm^3)**	**Water Uptake (vol%)**	**IEC_v(dry) (cm^3/meg)**	**IEC_v(wet) (cm^3/meg)**
TM	1.21	24	1.82	1.46
DM	1.24	43	2.05	1.43
Bis A	1.24	50	2.16	1.44
Nafion® 212	2.0	40	1.84	1.31

Even with the lower water uptake and IEC, the tetramethyl system still had a respectable proton conductivity in liquid water of 0.10 S/cm. Thus, the tetramethyl system produced the most desirable system due to the very low water adsorption of the membrane. The conductivity range for the membranes was from 0.10-0.15 S/cm, which is in the expected range for the disulfonated poly(arylene ether sulfone) multiblock copolymers. In addition, all of the membranes showed greatly reduced methanol permeability in 1M MeOH as compared to Nafion® 212, with the tetramethyl based membrane having once again the lowest value in the membrane series. Due to this reduction in methanol adsorption, the bisphenol based multiblock copolymers also exhibited greater relative selectivity than the perfluorosulfonic acid based membrane. These results suggest that these membranes would have excellent performance in fuel cell operation and may allow for higher methanol concentrations.

SEC and tensile testing confirmed that multiblock copolymer structures were formed, and the molecular weights of the copolymers are sufficient to provide transparent ductile membranes when cast from DMAc solution. Weight average molecular weights (M_ws), shown in table 3.1, were between 50 kg/mol and 80 kg/mol. The stress-strain behavior of the membranes verified that ductile materials were acquired, with mechanical properties very representative of SPAESs (Fig. 3.7). The stress-strain performance of the bis A and dimethyl multiblock copolymers were very similar to each other, with the dimethyl system having a longer elongation at break. The yield stress for the tetramethyl system was less than that of the other two multiblock copolymers, but it exhibited the longest elongation at break of the membranes.

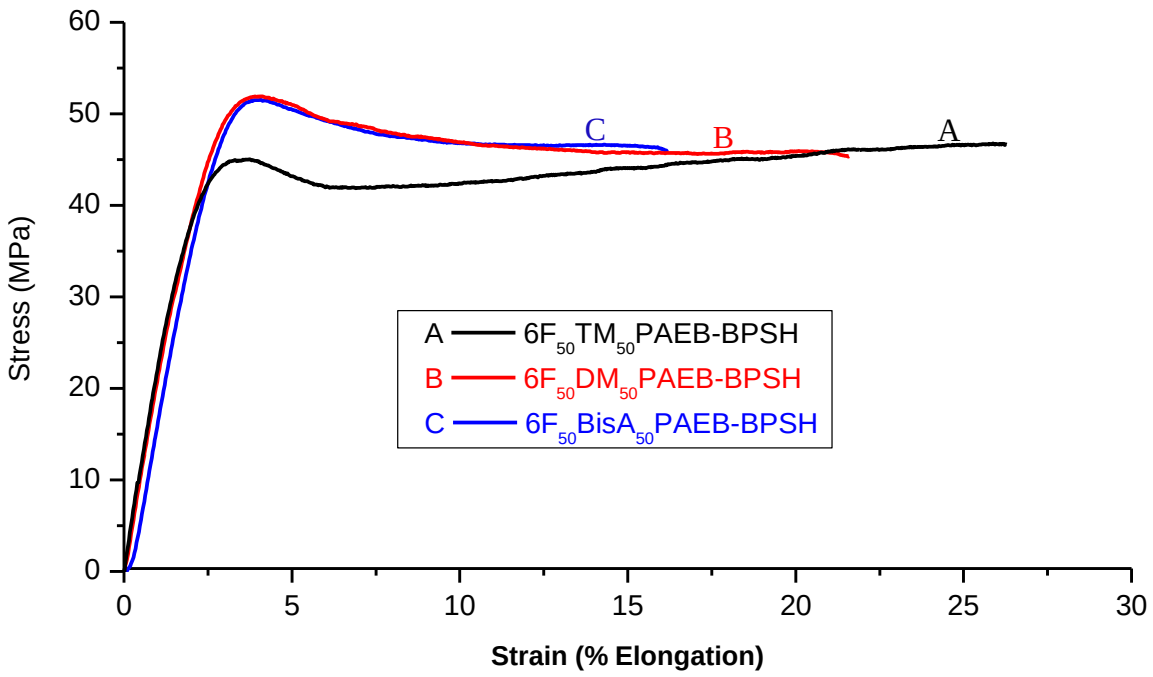

Figure 3.7: Stress-strain curves for acid form membranes, samples dried prior to testing with rate of 5mm/min: (a) $6F_{50}BisA_{50}$PAEB-BPS100, (b) $6F_{50}DM_{50}$PAEB-BPS100, and (c) $6F_{50}TM_{50}$PAEB-BPSH.

SAXS was performed in order to investigate the effects of bisphenol A methyl substitution on the morphological features of multiblock copolymer membranes (Fig. 3.8). All of the SAXS profiles showed a primary peak at q_{max} (Table 3.3) and also a secondary peak at $2q_{max}$, which is consistent with a lamellar organization of the phase-separated domains in these mutliblock copolymers.[212] The most significant difference between these profiles was the smaller domain spacing (larger q_{max}) observed for the tetramethyl multiblock copolymers. In addition, the primary SAXS peak for the tetramethyl series was found to be significantly sharper compared to the dimethyl and bisphenol A based multiblock copolymers (see FWHM, Table 3.3). Similarly, the secondary peak for the tetramethyl series was also observed to be more prominent and well-resolved. This scattering behavior suggests that the phase separated

morphology of the tetramethyl based multiblock copolymers exhibits a more refined order in comparison to the dimethyl and bisphenol A based multiblock copolymers.

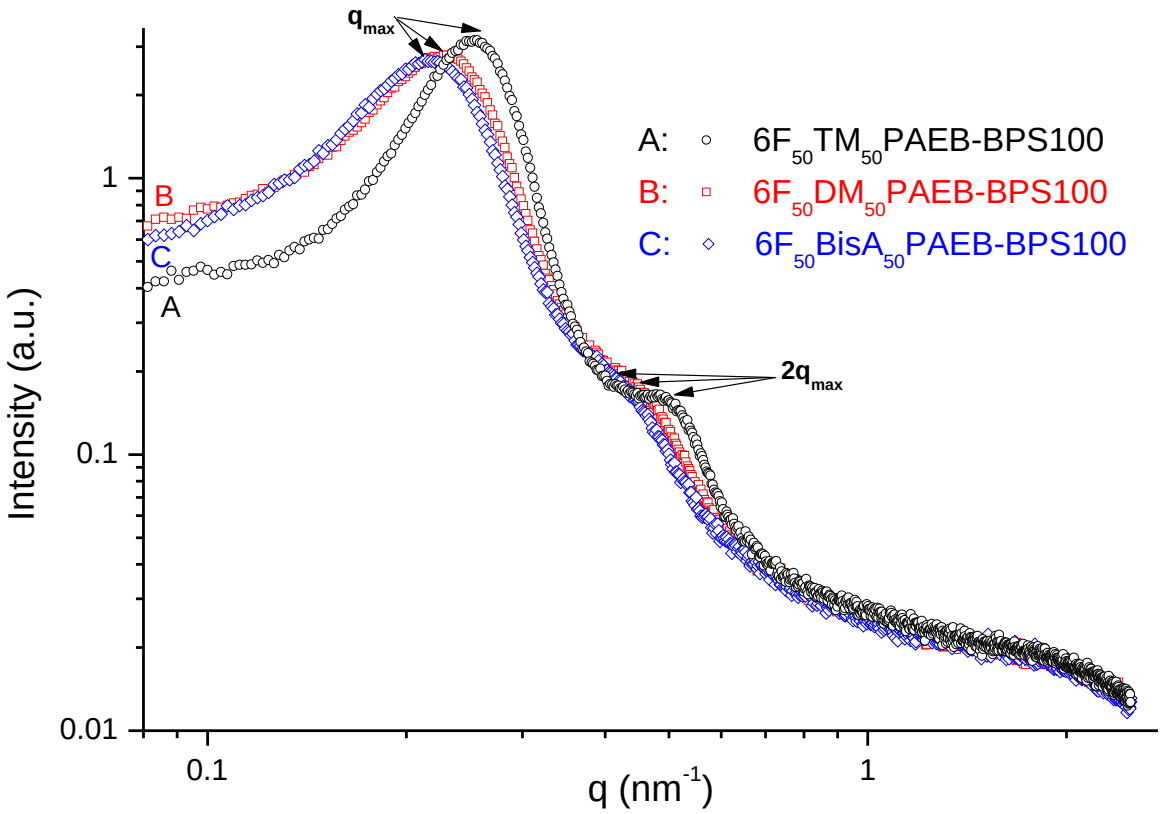

Figure 3.8: SAXS profiles of bis A based multiblock copolymers

Table 3.3: Interdomain distance for SAXS profiles

Sample	D-spacing q_{max} (nm)	FWHM (q_{max})	χ_{eff}
$6F_{50}TM_{50}$PAEB-BPS100	24.5	0.090	0.283
$6F_{50}DM_{50}$PAEB-BPS100	27.3	0.114	0.541
$6F_{50}BisA_{50}$PAEB-BPS100	28.2	0.107	0.701

Based upon self-consistent mean-field theory (SCFT), the Bragg spacing for the primary scattering peak (d_1) for a lamellar phase-separated block copolymer may be correlated to the effective segment-segment interaction parameter (χ_{eff}) by the following relationship:

(3.4) $$d_1 = 1.10aN^{2/3}\chi_{eff}^{1/6}$$

where a is the statistical segment (Kuhn) length, and N is the number of Kuhn segments within a diblock sequence.[244-245] For the multiblock copolymers studied here, the statistical segment length was approximated using the Kuhn segment length of polycarbonate, with a = 2.94 nm and the Kuhn length of each multiblock assumed to be identical based on studies of bisphenol A and tetramethyl bisphenol A polycarbonates.[246] The value for N was computed by considering the segment length to correspond to two adjacent polycarbonate monomers, resulting in a value of N = 29 segments within a single 10K-10K AB diblock sequence.[247] These assumptions have been used for simplicity due to the structural similarity between each multiblock copolymer considered. Following these calculations, the observed increase in q_{max} with increasing methyl group content corresponds to a decrease in the effective interaction parameter between the blocks of the multiblock copolymers (Table 3.3). With increasing hydrophobicity (and likely an increase in steric constraints) imposed by the addition of methyl substituents, the driving force for phase separation increases, leading to a more ordered phase separated morphology. This increase in lamellar organization of the highly hydrophobic tetramethyl multiblock copolymers may also be a factor in the observed increase in elongation over that of the bis A and dimethyl systems (Fig. 3.7). Future studies will focus on morphological transformations during in-situ tensile/SAXS experiments. Similarly the more ordered morphology could have restricted the swelling of the

hydrophilic domain, thus contributing to the observed reduction in water uptake of the multiblock copolymer membranes.

Fig. 3.9 shows the polarization curves of MEAs using the multiblock copolymers. The MEAs were prepared using similar thickness membranes (~30 μm thick) and Nafion-bonded electrodes. Under H_2/air conditions, all three MEAs exhibited a comparable performance (Fig. 3.9a). The MEAs using $6F_{50}DM_{50}$PAEB-BPSH and $6F_{50}BisA_{50}$PAEB-BPSH exhibited notably reduced high frequency resistance (HFR), ca. ~0.05 Ω cm^2 compared to the MEA using $6F_{50}TM_{50}$PAEB-BPSH. This is consistent with the conductivity of the stand-alone membranes shown in Table 1. Under 0.5 M methanol feed conditions, all MEAs exhibited comparable performance. In the low methanol feed conditions, the amount of crossover methanol is minimal and the samples performed comparably, similar to the H_2/air fuel cell. Under 1 M methanol feed conditions, on the other hand, the MEA using $6F_{50}TM_{50}$PAEB-BPS1H showed better performance than the other MEAs. The relatively low methanol permeability of $6F_{50}TM_{50}$PAEB-BPSH likely contributed to the better performance, as the measured methanol limiting current for this cell was 0.2 A/cm^2 which is ~ 50% lower than the other MEAs.

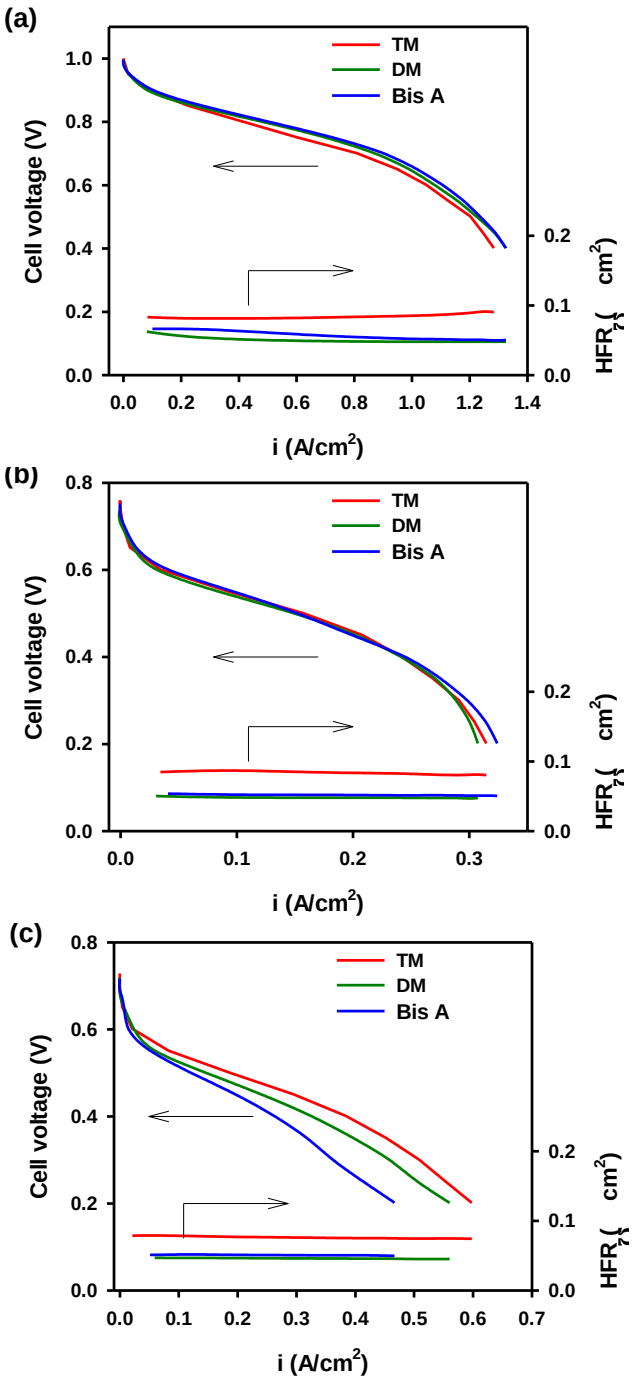

Figure 3.9: i-V polarization curves (a) H_2/air (b) 0.5 M DMFC and (c) 1 M DMFC at 80°C; Membrane thickness: $6F_{50}TM_{50}$PAEB-BPSH: 28 μm, $6F_{50}DM_{50}$PAEB-BPSH: 31 μm and $6F_{50}BisA_{50}$PAEB-BPSH: 25 μm.

3.4 Conclusions

A series of multiblock copolymers were synthesized with a disulfonated hydrophilic phase and a partially fluorinated hydrophobic phase. Fifty mole percent of the fluorine was removed in the hydrophobic segments and replaced with a series of biphenol A moieties with increasing amount of benzylic methyl groups. The characterization results showed that, there is a strong correlation between the addition of the methyl groups and the phase separation, the resulting morphology, and the membrane properties. It is hypothesized that the addition of the methyl groups results in higher hydrophobicity of the otherwise comparable membranes and this is the driving force leading to increased phase separation and improved MEA membrane properties. Addition of the methyl groups on the corresponding multiblock copolymers effectively reduced the IEC, resulting in lower water adsorption, and a decreased interdomain distance. This was most evident in the tetramethyl system, which had a water adsorption nearly half that of the dimethyl and Bis A PEMs. As expected when fabricated into MEAs the tetramethyl system showed the lowest methanol permeability and cross-over current, even over that of the Nafion® 212 membrane. The lower methanol permeability was the reason attributed to the improved performance of the tetramethyl membrane over the other two block copolymers at higher methanol concentration conditions. The control over backbone structure along with the reduction in fluorine content should allow for PEMs with superior performance and reduced methanol permeability at higher methanol concentrations in DMFC applications.

Chapter 4: Gas Transport Properties and Characterization of UV Cross-linked Poly(phenylene oxide)-Poly(arylene ether ketone) Copolymers

4.1 Introduction

Poly(2,6-dimethylphenylene oxide) (PPO) and its derivatives have been extensively studied as potential membranes for CO_2/CH_4 separation systems.[142,150] This class of polymers, like many other glassy polymers, is of interest for gas separation applications because of their good transport properties.[20-22] The rigidity and stiffness of the glassy polymer backbone, along with disruption of chain packing by the methyl substituents, are considered the primary reasons for the strong transport results. The increased free volume caused by the methyl groups on PPO are related to the highly permeable nature.[248]

Derivatives of PPO have included modifications of the polymer by electrophilic aromatic substitution with bromine, nitration, and sulfonation on the open ortho position of the aromatic backbone.[143-144,161,168,249] Additionally, effects of side chain substitution have been investigated with carboxylation and esterification of the methyl substituent, and also replacement of the methyl group with aromatic rings.[155,159-160,162] Bromination of PPO caused a stark increase in permeability over that of the unmodified PPO, and there was relatively little decrease in gas selectivity. The nitrated and sulfonated PPO polymers had increased selectivities but gas permeability decreased. However, these systems have some potential issues with sufficient thermal and oxidative stability due to the presence of the aromatic methyl groups. PPO derivatives such as poly(2,6-diphenyl phenylene oxide) with increased stability have been synthesized by oxidative polymerization. However these polymers suffered from significantly reduced transport properties.[154-155,159,248]

While significant work has been done on PPO modifications, relatively little research has been performed on copolymers containing PPO.[250-252] The primary reason for the lack of investigation is that PPO is synthesized by a conventional oxidative polymerization process, which produces monofunctional polymers.[151-153,253] To obtain difunctionality, the 2,6-dimethyl phenol monomer needs to be copolymerized with a difunctional monomer such as a tetramethyl-substituted bisphenol derivative e.g. (2,2',6,6'-tetramethyl-4,4'-biphenol), 4,4'-methylenebis(2,6-dimethylphenol), or 2,2-bis(4-hydroxy-3,5-dimethylphenyl)propane).[254-256] These reactions require precise conditions with low oxygen flow rates and longer reaction times to ensure inclusion of the difunctional comonomer. This may be due to reduced reactivity of the *ortho*-substituted bisphenol moiety over the 2,6-dimethyl phenol monomer. Difunctionality can also be achieved by using a quinone coupling reaction with low molecular weight PPO.[257] Once synthesized, the difunctional oligomers can be used to produce copolymers from various polymerization reactions.[250-251] However, the authors could find very few reports of gas transport properties of PPO copolymers.[258-259] Therefore, a study of the effect of copolymerization of PPO on the gas transport properties could be an important addition to the gas separation membrane field. Furthermore, membranes that are cross-linkable, such as some aromatic polyimides, are of particular interest because of their increased selectivity and resistance to CO_2 plasticization after crosslinking.[80-81,83-85] Thus, designing a crosslinked PPO copolymer could provide a new class of membranes with outstanding gas transport properties.

This manuscripts reports the synthesis, characterization, crosslinking, and gas transport properties of novel poly(2,6-dimethylphenylene oxide)-poly(arylene ether ketone) (PPO-PAEK) copolymers. These can be cast into thin films, then crosslinked *in situ* with UV light. The copolymers were synthesized by polycondensation of a difunctional PPO oligomer with

difluorobenzophenone. A PPO-PAEK copolymer was compared against PPO and other PPO derivatives, and a poly(arylene ether ketone) prepared from tetramethyl bisphenol A and difluorobenzophenone to elicit effects of polymer structure on the membrane and transport properties. In addition, effects of crosslinking and ketone concentration for the membranes on gas transport properties were investigated.

4.2 Experimental

4.2.1 Materials

Difunctional poly(phenylene oxide) (PPO) oligomers were purchased from Sabic and had a molecular weight of ~1,650 g/mol. 2,6-Dimethyl phenol (2,6-xylenol, 99+%), *N*,*N*-dimethylacetamide (DMAc), and toluene were purchased from Sigma-Aldrich. DMAc was distilled from calcium hydride before use. 4,4'-Difluorobenzophenone and 2,2-bis(4-hydroxy-3,5-dimethylphenyl)propane (tetramethyl bisphenol A, TMBPA 99+%) were purchased from TCI America. Reagent grade potassium carbonate (K_2CO_3) was purchased from Fisher Scientific and dried under vacuum at 180^{o}C prior to use. Toluene and Isopropanol were obtained from Fisher Scientific and used as received.

4.2.2 Synthesis of poly(phenylene oxide)-poly(arylene ether ketone) copolymers (PP0-PAEK) and the tetramethylbisphenol A-based poly(arylene ether ketone) homopolymer (TMBPA-BP)

The copolymers were synthesized via nucleophilic aromatic substitution. A representative synthesis is provided. A difunctional PPO oligomer of ~1,650 g/mol (8.70 g, 5.27 mmol), difluorobenzophenone (1.15 g, 5.27 mmol), and DMAc (50 mL) were charged into a 100-mL, 3-neck, round-bottom flask equipped with a mechanical stirrer, nitrogen inlet and Dean-Stark trap. The mixture was heated to 140^{o}C and stirred until the monomers were completely dissolved. Once dissolved, K_2CO_3 (1.10 g, 7.96 mmol) and toluene (25 mL) were added into the flask. The

reaction was allowed to reflux at 140^{o}C for 4 h to azeotropically remove water from the system and then it was slowly heated to 160^{o}C to remove toluene. The reaction was allowed to proceed at 160^{o}C for 12 h and then cooled to room temperature. After 12 h the solution was very viscous, and was diluted with 50 mL of DMAc. Filtration of the solution to remove the by-product salt was difficult. Therefore, the product was precipitated into boiling DI water to afford a white fibrous product. Afterwards, the copolymer was stirred in DI water (~80^{o}C) overnight to remove any residual salt or solvent, filtered, and then dried *in vacuo* at 180^{o}C for 24 h. The tetramethylbisphenol A containing poly(arylene ether ketone) (TMBPA-BP) was synthesized in exactly the same fashion, except that tetramethylbisphenol A was used instead of the PPO oligomer.

4.2.3 Membrane preparation

Copolymers were dissolved (~4% w/v) and filtered using a high-pressure, 0.45-μm filter with a nitrogen pressure of 1500 psi. The resultant solution was cast onto a clean glass substrate, dried *in vacuo* at 80^{o}C for 12 h, and then *in vacuo* at 150^{o}C for an additional 12 h. Membranes were removed from the glass substrates by immersion into a DI water bath. Films were dried at 150^{o}C *in vacuo* prior to testing to remove any absorbed water or residual solvent.

4.2.4 UV crosslinking

UV crosslinking was done via a high-intensity, mercury longwave UV lamp (UVP, Model B-100) equipped with a 365-nm light filter at room temperature with an intensity of 19.7 mW/cm^2. Each sample was irradiated at a distance of 3.5 cm from the UV lamp for 1 h per side.

4.2.5 Characterization

^{1}H NMR analysis was performed on a Varian Inova spectrometer operating at 400 MHz. Spectra were obtained from 1 mL of a 15% (w/v) solution in CD_2Cl_2. The PPO-PAEK

copolymers had limited solubility in $CDCl_3$ so CD_2Cl_2 was used instead. Glass transition temperatures (T_g's) were determined by differential scanning calorimetry (DSC) with a TA Instruments DSC Q-200 under nitrogen gas and a heating rate of 10°C/min. DSC spectra were conducted in the temperature range 150°C-350°C, which were first held isothermally at 150°C for 5 min to remove any possible residual solvents left in the samples. Glass transition temperatures were determined from the second heats. Thermal gravimetric analysis (TGA) was performed on a TA Instruments TGA Q-5000 under air atmosphere with a heating rate of 10°C/min. Fourier Transform Infrared Spectroscopy with attenuated total reflectance (FTIR-ATR) was performed to observe carbonyl groups in the PPO-PAEK copolymer and the TMBPA-BP homopolymer. The FTIR-ATR spectra were recorded on an FTIR spectrometer (Thermo Scientific Nicolet 8700 FTIR) equipped with an ATR attachment with a horizontal diamond crystal. The resolutions of the spectra were 4 cm^{-1} and 128 background scans were collected. A small amount of polymer was placed on the diamond crystal and the FTIR spectra were collected with 128 scans. Spectra were normalized using the peak at ~2736 cm^{-1} since intensity was similar for both spectra at the indicated peak. Number average molecular weights (M_n's) of all polymers were obtained via multi-detector size-exclusion chromatography (SEC) using chloroform or THF as the mobile phase (30°C) with 3 PLgel 10 μm mixed-B 300 x 7.5 mm columns in series with a Wyatt Viscostar II Viscometer, a Wyatt Heleos II multi-angle light scattering detector, and a Wyatt T-rex refractive index detector.

4.2.6 Gel fractions

Gel fractions of the crosslinked samples were measured using a Soxhlet extractor (Wilmad-LabGlass, Vineland, NJ, USA) with chloroform. The initial mass of the film was weighed before the sample was extracted. Crosslinked polymers were extracted with refluxing

chloroform. After 6 h, the crosslinked samples were heated to 100°C for 12 h under vacuum, and then the final film mass was recorded. Gel fractions were calculated by Equation 4.1:

(4.1) $$Gel\ Fraction = \frac{W_{initial} - W_{final}}{W_{initial}} \times 100$$

4.2.7 Density calculations

Density was measured using a Mettler-Toledo balance equipped with a density measurement kit. Ethanol was chosen as the reference liquid because the samples showed low ethanol uptake over the time scale of the density measurement.

4.2.8 Pure gas permeability measurements

Pure gas permeabilities of H_2, N_2, CH_4, CO_2 and O_2 were measured using a constant volume, variable pressure method. The film sample was housed in a stainless steel Millipore filter holder (Millipore, Billerica, MA, USA).[260] Upstream pressure was measured with a Honeywell Super TJE 1500 psi transducer (Honeywell Sensotec, Columbus, Ohio, USA), and downstream pressure was measured using a MKS Baratron 626 transducer (MKS, Andover, MA, USA). Pressure readings were recorded using National Instruments LABVIEW software. All of the permeation experiments were done at 35°C.

4.3 Results and Discussion

4.3.1 Synthesis of PPO-PAEK copolymers

Figure 4.1 displays the reaction scheme employed for the PPO-PAEK copolymers. Difunctional PPO oligomers were reacted with difluorobenzophenone via step growth polycondensation to form high molecular weight copolymers (Table 4.1). The difunctional PPO oligomer obtained from Sabic was believed to be synthesized via the introduction of 2,2-bis(4-

hydroxy-3,5-dimethylphenyl)propane (tetramethylbisphenol A) into the PPO copolymer. This was confirmed with ^{1}H NMR of the final copolymer that showed the bridging methyl groups in the upfield region of the spectrum (Fig. 4.2). A 1:1 mole ratio was used between the oligomers and the difunctional ketone monomer in order to achieve high molecular weight, with the progress of the reaction being analyzed by NMR spectroscopy. Two reactions were conducted with the difunctional PPO oligomer, one with the oligomer used as received and the other after purification by dissolution in toluene and precipitation into isopropanol. Purification removed low molecular weight and monofunctional oligomer impurities (Fig. 4.3), and subsequently increased the molecular weight of the oligomer. Molecular weight was calculated by the ratio of the integration of the tetramethylbisphenol A to the PPO hydrogen peaks which were approximately 1650 g/mol and 2650 g/mol. The copolymer produced from the lower molecular weight oligomer is referred to as PPO-PAEK (1) and the copolymer with the higher molecular weight oligomer is referred to as PPO-PAEK (2). The difference in molecular weight produced two copolymers with different compositions. PPO-PAEK (1) had approximately 10 wt% of the copolymer corresponding to the ketone moieties, 15 wt% to the tetramethylbisphenol A moieties, and 75 wt% to the PPO. The higher molecular oligomer resulted in a copolymer with less ketone and tetramethylbisphenol A moieties, and a higher concentration of PPO (~ 6% ketone, 10% tetramethylbisphenol A, 84% PPO). To make a comparison series with the different compositions, tetramethylbisphenol A was also polymerized with difluorobenzophenone to produce the poly(arylene ether ketone) homopolymer (Fig. 4.1). This homopolymer polymerization was conducted using a previously reported procedure and had the highest value of ketone inclusion with ~ 39 wt% of the composition corresponding to the ketone containing monomer (Table 4.1).[261] The compositions of the polymers were confirmed with ^{1}H NMR

spectroscopy. In the NMR spectra in Figure 4.2, the ketone and benzylic methyl peaks drop dramatically in the middle spectrum, with a further decrease in the bottom spectrum.

Table 4.1: Composition and molecular weights of TMBPA-BP and PPO-PAEK

Sample	PPO wt%	TMBPA wt%	Ketone wt%	Benzylic Methyl to Ketone Ratio
TMBPA-BP	-	61	39	4:1
PPO-PAEK (1)	75	15	10	28:1
PPO-PAEK (2)	84	10	6	43:1

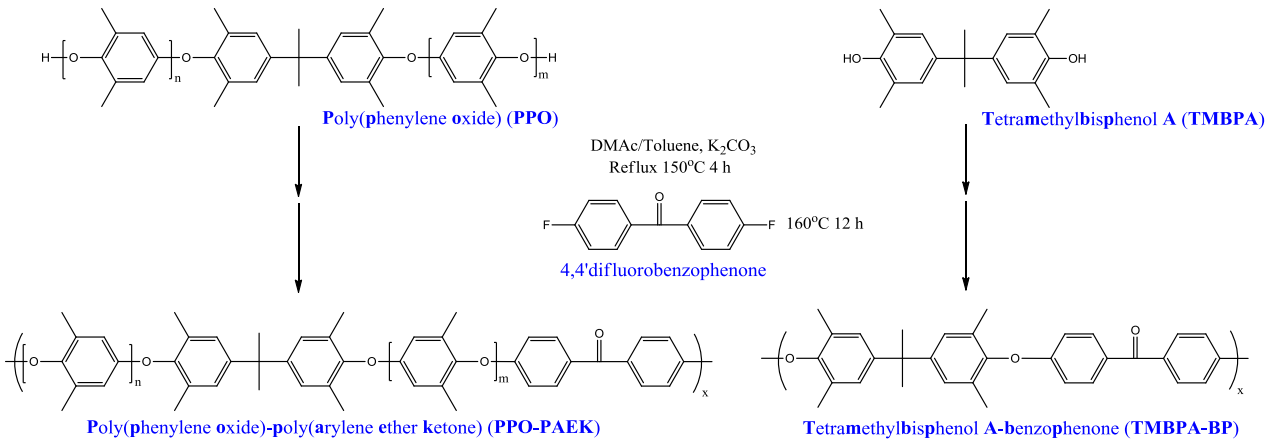

Figure 4.1: Synthesis of PPO-PAEK copolymers and TMBPA-BP homopolymer

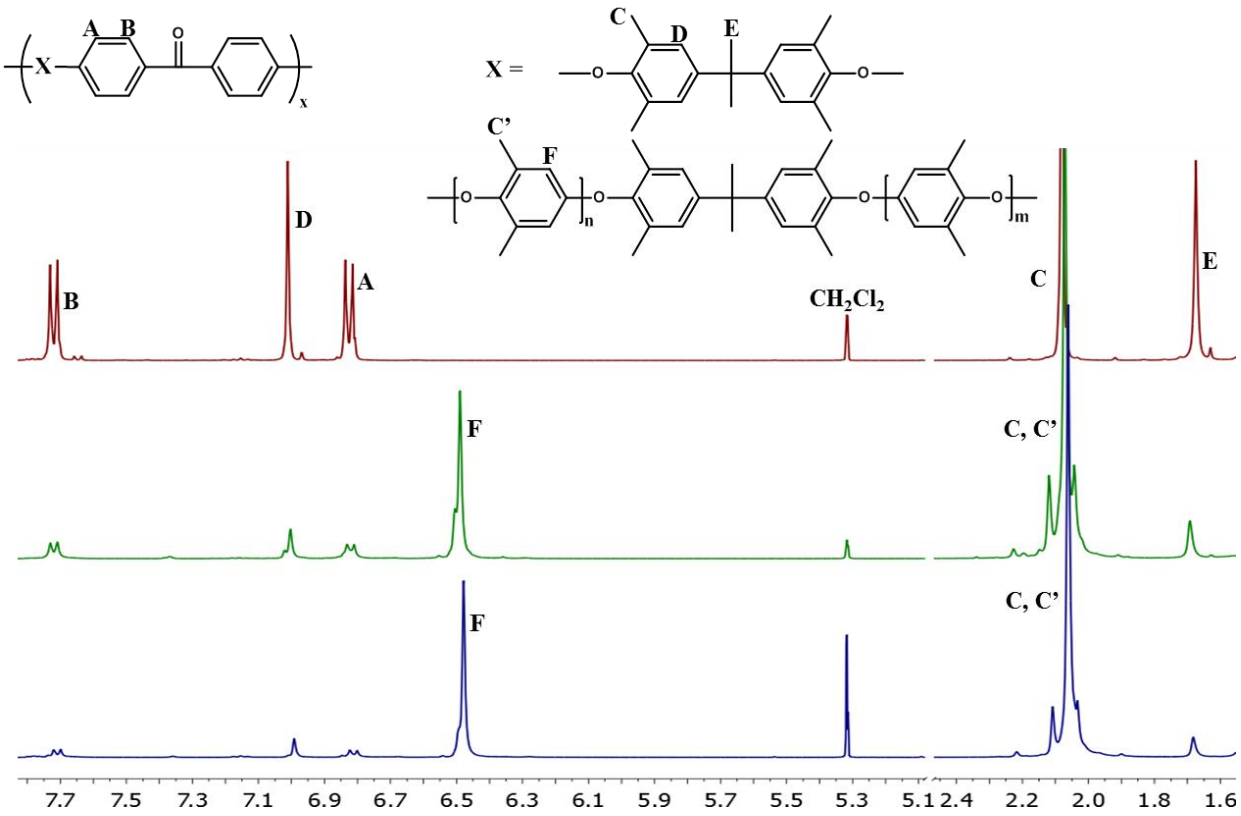

Figure 4.2: ^{1}H NMR spectra of the copolymers and homopolymer: (top) TMBPA-BP, (middle) PPO-PAEK (1), and (bottom) PPO-PAEK (2).

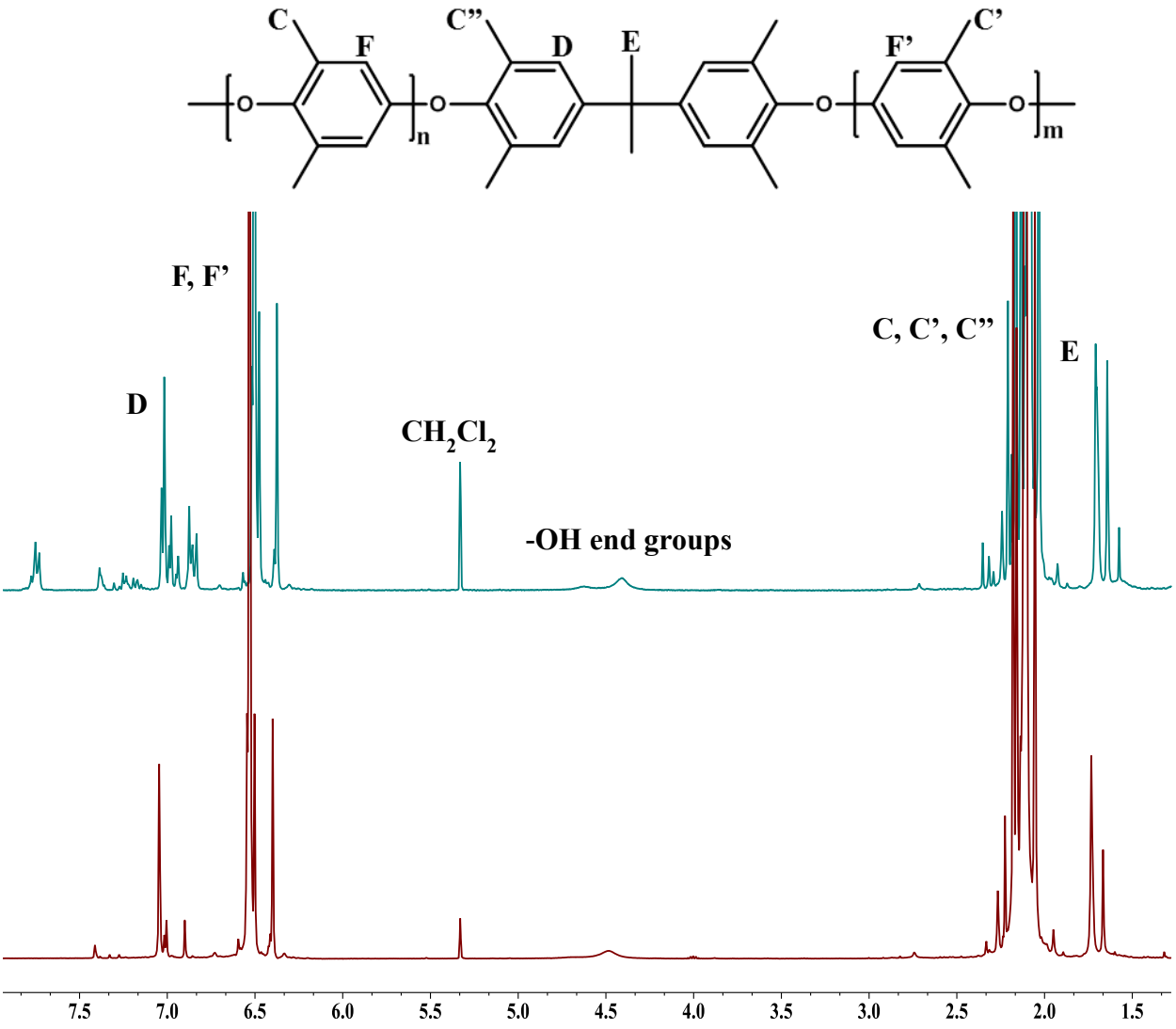

Figure 4.3: ^{1}H NMR comparison of PPO difunctional oligomer before (top) and after (bottom) purification.

4.3.2 Crosslinking and characterization

The PPO-PAEK copolymers and TMBPA-BP homopolymer were crosslinked using a UV light to produce films with high gel fractions (Table 4.2). The UV crosslinking most likely occurred through excitation of the carbonyl group from the singlet to triplet state and then intermolecular hydrogen abstraction of a benzylic hydrogen.[262] Figure 4.4 depicts a scheme of the proposed mechanism for the UV crosslinking. To designate that the films were in the

crosslinked form they are referred to as PPO-PAEK (1)/(2) XL and TMBPA-BP XL, with XL being the acronym indicating crosslinking. Support for this mechanism of crosslinking is shown in the IR spectrum of the crosslinked (XL) and non-crosslinked PPO-PAEK copolymer (Fig. 4.5). The two spectra were normalized by the peak at ~2736 cm^{-1} to compare the two different films, with the crosslinked film showing a reduction in the carbonyl peak (~ 1700 cm^{-1}). Additionally a hydroxyl peak (~ 3700 – 3200 cm^{-1}), which was absent in the non-crosslinked film, was present in the crosslinked film suggesting crosslinking through the carbonyl group producing a tertiary alcohol in what had been the ketone position.

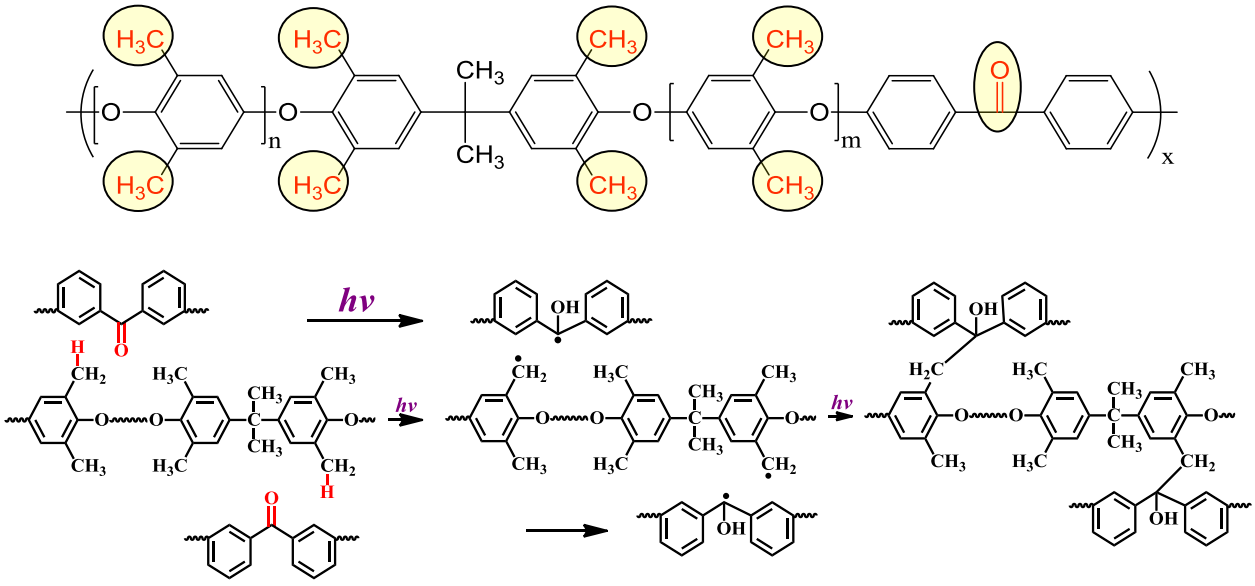

Figure 4.4: A scheme of the proposed UV crosslinking mechanism for PPO-PAEK copolymer

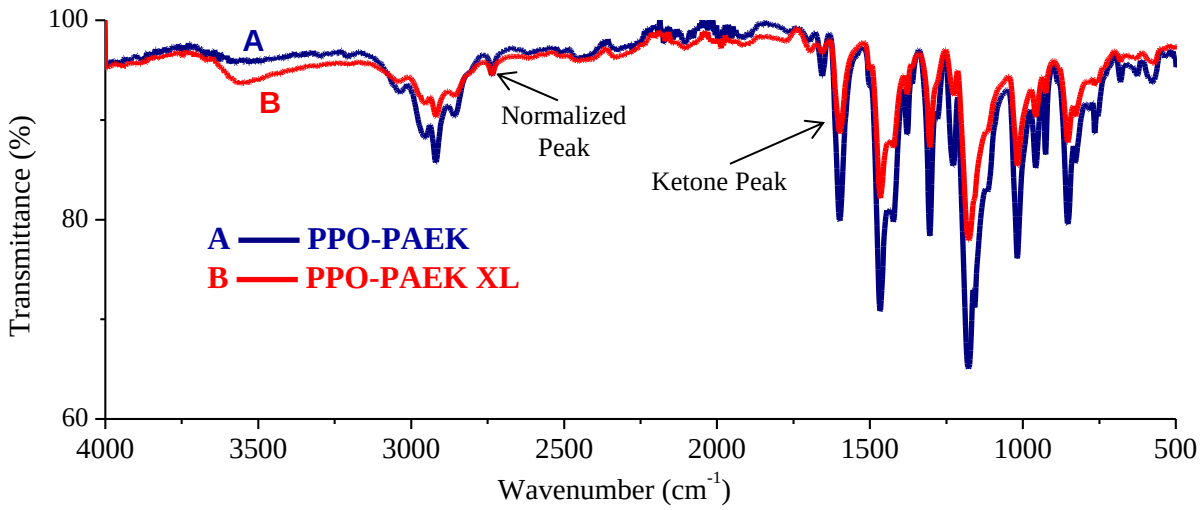

Figure 4.5: Normalized IR spectrum of a crosslinked and non-crosslinked PPO-PAEK copolymer

Table 4.2 shows the gel fractions and glass transition temperatures (T_g's) for the non-crosslinked and crosslinked films compared against those of PPO and PPO-NO_2. The glass transition temperatures (T_g's) for PPO and PPO-NO_2 were obtained from literature.[161] This PPO-NO_2 copolymer was included in the comparison because the percentage of PPO that was nitrated was 15% (~ 6 wt%), which was close to the wt% of the ketone groups in the PPO-PAEK (1) and (2) copolymers. Additionally, the properties of the PPO-PAEK copolymers would also have a slight effect from the isopropylidene groups of the tetramethylbisphenol A in the copolymer.

Although the TMBPA-BP had the same gel fraction as PPO-PAEK (1), it would be expected that the crosslink density would be much higher for the TMBPA-BP polymer. Since the proposed crosslinking mechanism requires both methyl and ketone moieties, the small amount of ketone may be a limiting factor for the crosslinking reaction. Thus, the higher amount of ketone in the TMBPA-BP polymer should allow for more crosslinking sites. Figure 4.6 shows evidence for this as the crosslinking only caused a slight rise in the glass transition temperatures of the PPO-PAEK (1) and PPO-PAEK (2) copolymers, while the T_g increased significantly for the

TMBPA-BP polymer. This large increase in T_g is a good indication that the TMBPA-BP had a higher density of crosslinks. PPO-PAEK (1) and PPO-PAEK (2) increased by about the same amount after crosslinking, but both had very low ketone content so crosslink density might not have been largely affected. However, PPO-PAEK (1) had a higher T_g than both the PPO and TMBPA-BP homopolymers. This rise in T_g could have been brought on by the impurities contained in the unpurified PPO oligomer used to synthesize the PPO-PAEK (1) copolymer. Although, no weight loss occurred before 400^{o}C in the TGA of the PPO-PAEK (1) and XL membranes (Fig. 4.7). This might be a strong indication of good stability in air. However, while crosslinking did not seem to drastically improve thermally and oxidative stability, crosslinking should provide resistance against plasticization for the membranes.

Table 4.2: Comparison of crosslinked and non-crosslinked PPO-PAEK and TMBPA-BP

Sample	**Gel Fraction (%)**	**T_g (^{o}C)**
PPO	-	~ 207
PPO-NO_2 (15%)	-	~ 233
PPO-PAEK (1)	94	~ 213
PPO-PAEK (1) XL	-	~ 218
PPO-PAEK (2)	-	~ 207
PPO-PAEK (2) XL	-	~ 212
TMBPA-BP	-	~ 210
TMBPA-BP XL	94	~ 224

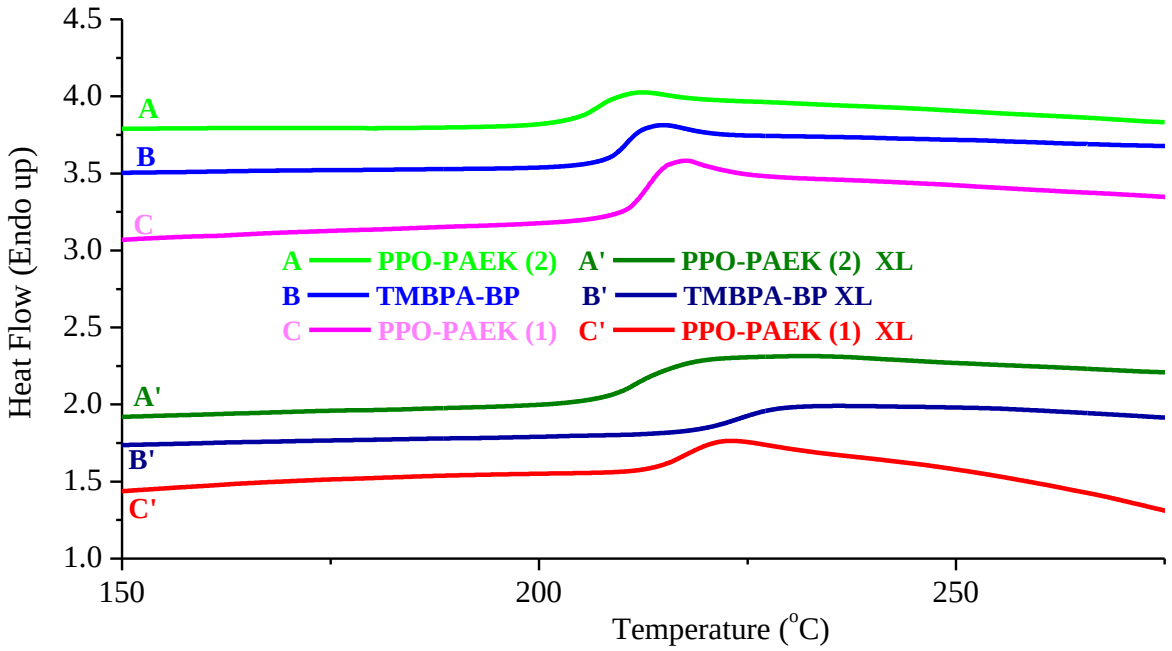

Figure 4.6: Glass transition temperatures of the copolymers and TMBPA-BP homopolymer and their crosslinked networks. DSC was performed under nitrogen with a heating rate of 10°C/min.

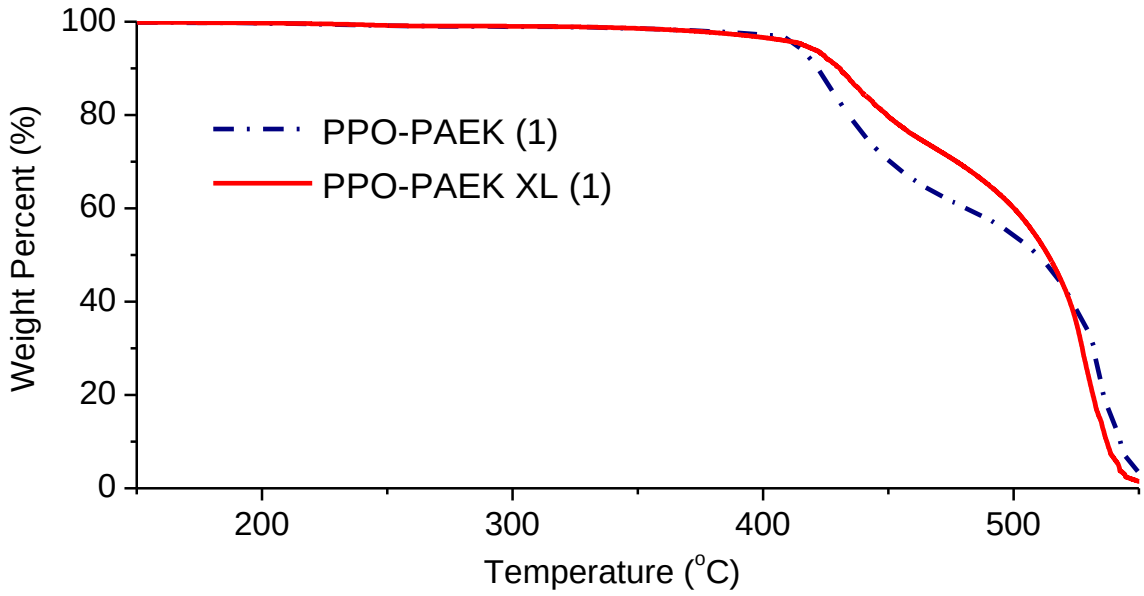

Figure 4.7: TGA of the PPO-PAEK and PP0-PAEK XL films performed in air with a heating rate of 10°C/min

4.3.3 Gas transport properties

Pure gas transport properties are displayed in Table 4.3. PPO-PAEK (1), TMBPA-BP, and the crosslinked membranes are compared with literature values for PPO, PPO derivatives, polysulfone (PSF), and Matrimid membranes that were tested under the same conditions.[161,263] Addition of the ketone into the the PPO to make the copolymer resulted in a decrease in permeability for all the gases and an increase in the selectivity for CO_2/CH_4 and O_2/N_2 gas pairs. Interestingly, the change in gas transport properties between PPO and PPO-PAEK (1) was very close to that of the nitrated PPO (PPO-NO_2), with the ketone-based copolymer having slightly better selectivity. Although the nitro groups are on the PPO ring for the PPO-NO_2, the addition of polar groups has a similar effect for both systems. After crosslinking, both the PPO-PAEK (1) and TMBPA-BP polymers showed a significant increase in selectivities, and a corresponding decrease in the gas permeabilities (Fig. 4.8). TMBPA-BP XL had a higher selectivity and a lower permeability than PPO-PAEK (1) XL. The larger increase in selectivity and decrease in permeability is also a strong indication that the TMBPA-BP XL polymer has a higher crosslink density than the PPO-PAEK (1) XL. In comparing the ketone-based polymers to the Matrimid and PSF, both the PPO-PAEK and TMBPA-BP (and the XL derivatives) showed better performance than the PSF and comparable results to Matrimid for O_2/N_2 and CO_2/CH_4 separation. While PPO and UV crosslinked systems have traditionally been explored as gas separation membranes for CO_2/CH_4 gas pairs, the performance of the PPO-PAEK (1) material was better relative to the upper bound for O_2/N_2 separation.

The PPO-PAEK copolymer and TMBPA-BP polymer systems could easily be synthesized and produced in the same method as PSF. In addition, like the unmodified PPO, these copolymer and polymers could be formed into hollow fibers or bulk membranes for gas

separation applications. By crosslinking, the membrane or hollow fiber may provide the additional benefits of increased durability, operation time, mechanical properties, and resistance to CO_2 induced plasticization.[83,85] Furthermore, crosslinking would most likely result in reduced swelling and water uptake, which might be advantageous in vapor/gas separation applications that currently use unmodified PPO.[150]

Table 4.3: Gas transport properties of PPO, PPO derivatives, and standards in pure gases at 35°C and 10 atm.

Polymer	P_{CO_2}	P_{CH_4}	P_{N_2}	P_{O_2}	P_{H_2}	P_{CO_2}/P_{CH_4}	P_{O_2}/P_{N_2}
PPO	58.00	4.00	3.60	16.00	-	14.3	4.4
PPO-PAEK (1)	43.20	2.66	2.42	11.30	92.0	16.2	4.7
PPO-PAEK (1) XL	19.60	0.89	0.95	5.00	52.4	22.0	5.3
TMBPA-BP	-	-	1.16	5.50	-	-	4.7
TMBPA XL	-	-	0.42	2.61	-	-	6.2
PPO-NO_2 (15%)	40.50	2.60	2.50	11.50	-	15.6	4.6
Polysulfone	5.50	0.24	0.22	1.29	-	22.9	5.7
Matrimid	10.00	0.28	0.32	2.12	23.7	35.3	6.6

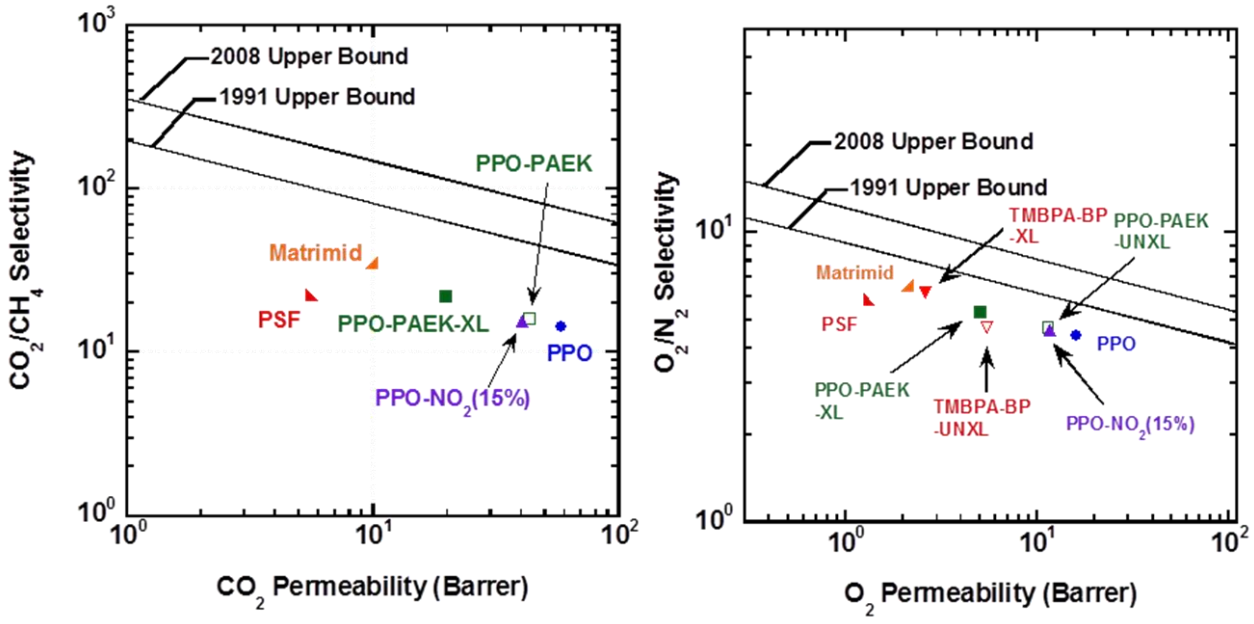

Figure 4.8: Upper bound plots for O_2/N_2 and CO_2/CH_4 gas pairs of PPO, PPO derivatives, TMBPA-BP, and industrial PSF and Matrimid membranes. Values used for PPO-PAEK, PPO-PAEK XL, TMBPA-BP, TMBPA-BP XL are for pure gases at 35°C and 10 atm, with other membrane values being obtained from literature with the same testing conditions.[22,161,263]

4.4 Conclusions

The inclusion of a ketone comonomer into difunctional PPO resulted in a copolymer that showed increased selectivity and reduced permeability relative to unmodified PPO. Glass transition temperatures and transport properties were shown to be related to ketone content in the membranes, with the TMBPA-BP polymer having the largest change. Transport properties of the PPO-PAEK (1) copolymer were very close to that of the nitrated PPO, with the inclusion of the polar groups increasing the glass transition temperature and density of the PPO derivatives. Additionally, the higher ketone content TMBPA-BP polymer showed higher selectivity and lower permeability the PPO-PAEK (1) copolymer. This crosslinking reaction was conducted in the solid state at room temperature, and thus, the cast membrane remained intact. Crosslinking

produced an increase in T_g along with continuing the trend in reduced permeability and enhanced selectivity for both the PPO-PAEK polymers and the highly crosslinked TMBPA-BP polymer. Transport properties of PPO derivatives and TMBPA-BP were parallel to unmodified PPO relative to the upper-bound, indicating no loss in performance. Further testing of these systems to include different molecular weights of PPO oligomers, would elicit a better understanding of crosslink density on membrane and transport properties for these systems. This control over structure and crosslinking would allow for a system of PPO based membranes with tunable gas transport properties.

Chapter 5: Effect of Charge Density on Membrane Properties of Multiblock Copolymers

5.1 Introduction

The ion exchange capacity (IEC) is the most frequent parameter used denote the charge density of ion-containing polymers. This is defined as the moles of ionic groups per gram of polymer (meq/g). The charge density has a major impact on membrane properties for many different applications that utilize charged polymers.[6,123,264-265] For proton exchange or electrodialysis membranes, this can result in a change in conductivity, water uptake, mechanical properties, and morphology. The use, however, of IEC to describe the charge densities of hydrophobic-hydrophilic block copolymers is too simplistic because it does not take into account the phase-separated morphologies of such systems.

Previous reports along with results on multiblock copolymers described in chapter 2 showed that a change in charge density brought on by variations in backbone structure can significantly alter membrane properties.[217,220,266-267] Conductivity and fuel cell performance could be improved with higher ionic character in the hydrophilic phase of the multiblock copolymer, such as with the change from a bisphenol monomer with two rings to hydroquinone with lower mass (each polymerized with disulfonated dichlorodiphenylsulfone). With higher ionic character the multiblock copolymer showed enhanced phase separation. Thus, we proposed that switching to a hydrophilic phase with even higher ionic character might allow for even further advancements in membrane performance. Moreover, the series of controlled fluorinated multiblock copolymers that were discussed in chapter 3 ($6F_{50}X_{50}$PAEB-BPSH) showed that by adding methyl substituents onto a bisphenol A moiety in the hydrophobic phase, a sharper phase separation was obtained, mechanical properties were improved, and water uptake and methanol permeability decreased. However, the multiblock copolymer that had the tetramethylbisphenol A

moieties incorporated had a lower IEC than the multiblock copolymers that had the dimethylbisphenol A and bisphenol A moieties in the hydrophobic phase of the multiblock copolymers. This raised the question of whether the improved properties were a result of steric considerations and corresponding increases in free volume caused by the methyl substituents on the bisphenol, or were simply a result of the reduced charge density compared to the two other multiblock copolymers. Therefore delineation of the benefits obtained by including benzylic methyl groups on the bisphenol monomers in the hydrophobic phase required investigations of multiblock copolymers with higher IECs.

This chapter presents two novel multiblock membranes with further increased charge density. In one block copolymer, the charge density of the hydrophilic block was increased to by using trisulfonated system with monosulfonated hydroquinone and disulfonated dichlorodiphenylsulfone to increase the overall IEC. In the other block copolymer, the length of the disulfonated hydrophilic block relative to the hydrophobic block was increased to increase the overall IEC. The performance and properties of the membranes are compared to analogous membranes with lower IECs to gauge the effects of backbone structure, the density of sulfonic acids in the hydrophilic phase, and block lengths.

5.2 Experimental

5.2.1 Materials

2,6-Difluorobenzonitrile, hydroquinonesulfonic acid potassium salt (sulfonated hydroquinone), anhydrous dimethyl sulfoxide (DMSO), *N*-Methyl-2-pyrrolidinone (NMP), *N*,*N*-dimethylacetamide (DMAc), cyclohexane, and toluene were purchased from Sigma-Aldrich. Difluorobenzonitrile, DMSO, and toluene were used as received. NMP and DMAc were vacuum distilled from calcium hydride before use. 4,4′-Hexafluoroisopropylidenediphenol, received from

Ciba, was sublimed and recrystallized twice from toluene. Reagent grade 2,2-bis(4-hydroxy-3,5-dimethylphenyl)propane (tetramethylbisphenol A) was purchased from TCI America and used as received. Monomer grade 4,4′-biphenol and hydroquinone were provided by Eastman Chemical Company and 4,4'-biphenol was dried under vacuum at 80^{o}C prior to use. Hydroquinone and sulfonated hydroquinone were recrystallized from ethanol and dried at 110^{o}C prior to use. 3,3'-Disulfonated-4,4'-dichlorodiphenylsulfone (SDCDPS) was received from Akron Polymer Systems and dried under vacuum at 150^{o}C for 3 days prior to use. 3,3'-Disulfonated-4,4'-difluorodiphenylsulfone (SDFDPS) was synthesized from 4,4'-difluorodiphenylsulfone via a previously reported procedure.[100,118] SDFDPS was recrystallized twice from an 80:20 isopropanol/water solution and dried under vacuum at 150^{o}C for 3 days prior to use. Potassium carbonate (K_2CO_3), acetone, methanol, and isopropanol were purchased from Fisher Scientific. Potassium carbonate was dried under vacuum at 180^{o}C prior to use, while acetone, methanol, and isopropanol were used without further purification.

5.2.2 Synthesis of difunctional oligomers

Synthetic methods for preparing 6FPAEB, $6F_{50}TM_{50}$PAEB, BPS100, and HQS100 oligomers were discussed in chapters 2 and 3. Their structures are detailed in Figure 5.1. A more highly sulfonated oligomer with phenolic endgroups (SQS100) and a number average molecular weight of ~5 kg/mol was prepared from monosulfonated hydroquinone and disulfonated difluorodiphenylsulfone. Disulfonated difluorodiphenylsulfone (5.06 g, 11.04 mmol), monosulfonated hydroquinone (2.70 g, 11.83 mmol), and DMSO (40 mL) were charged into a 3-neck round bottom flask equipped with a mechanical stirrer, condenser, nitrogen inlet, and Dean-Stark trap. The mixture was heated to 125^{o}C and stirred until all the monomers were completely dissolved. Once dissolved, K_2CO_3 (1.9 g, 13.74 mmol) and cyclohexane (12 mL) were added

into the reaction flask. The solution was refluxed with cyclohexane at 125°C for 4 h in order to azeotropically remove water from the system, and then heated to 135°C. The reaction was allowed to proceed for 24 h, then diluted with DMSO and allowed to cool to room temperature. The solution was filtered to remove salts using a Buchner funnel, and precipitated into isopropanol (1000 mL). The precipitated oligomer was stirred overnight and then dried *in vacuo* at 110 °C for 48 h.

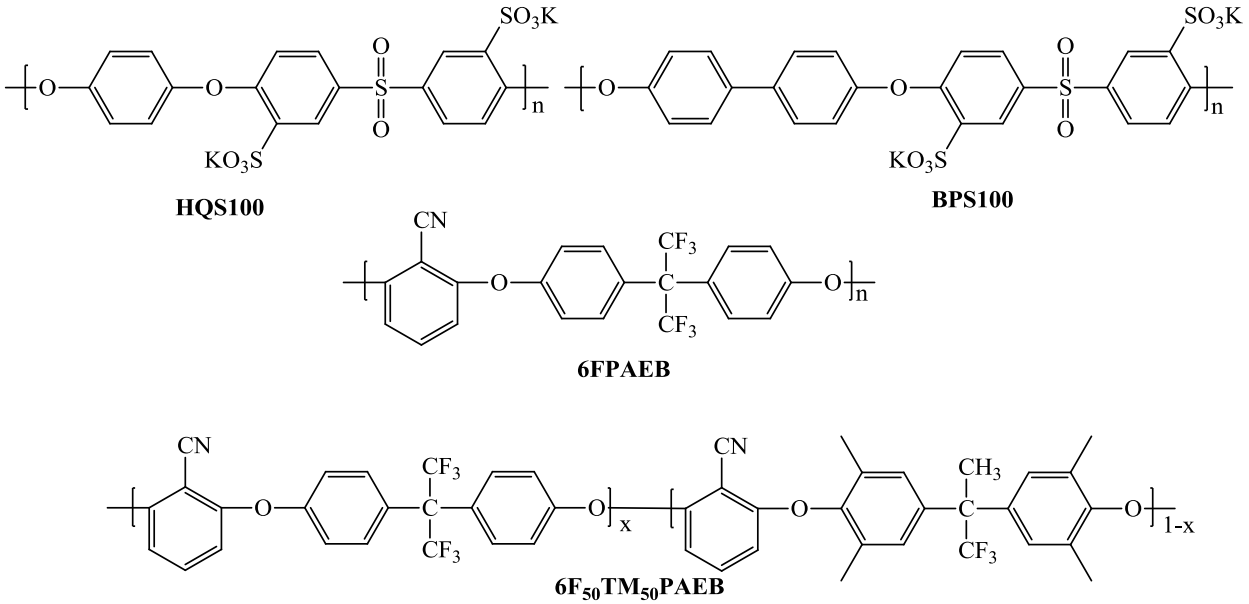

Figure 5.1: Structures of previously discussed hydrophobic and disulfonated hydrophilic oligomers

5.2.3 Synthesis of hydrophilic-hydrophobic multiblock copolymers

The multiblock copolymers 6FPAEB-BPS100, 6FPAEB-HQS100, and $6F_{50}TM_{50}$PAEB-BPS100 were synthesized according to the methods reported in chapters 2 and 3. Their structures are shown in Figure 5.2. The copolymer that contained monosulfonated hydroquinone in the hydrophilic phase was synthesized according to the following procedure. SQS100 (4.22 g, 0.74 mmol) and DMSO (45 mL) were added to a three-neck, 100-mL round bottom flask equipped

with a mechanical stirrer, condenser, nitrogen inlet and Dean-Stark trap. The solution was heated to 120 ^{o}C, then cyclohexane (15 mL) and K_2CO_3 (0.2 g, 1.45 mmol) were added and the mixture was refluxed for 6 h to remove water from the system. The cyclohexane was drained from the reaction and then the mixture was cooled to 90^{o}C. After cooling, a 6FPAEB hydrophobic oligomer (5.20 g, 0.61 mmol) was added. The bath temperature was raised to 135^{o}C and kept at this temperature for 48 h. The reaction mixture was diluted with DMSO and allowed to cool to room temperature. The multiblock copolymer was precipitated into isopropanol (1000 mL) and stirred for 12 h. The product was filtered then washed in deionized (DI) water at 90^{o}C for 12 h, filtered again, and then dried *in vacuo* at 150^{o}C for 24 h.

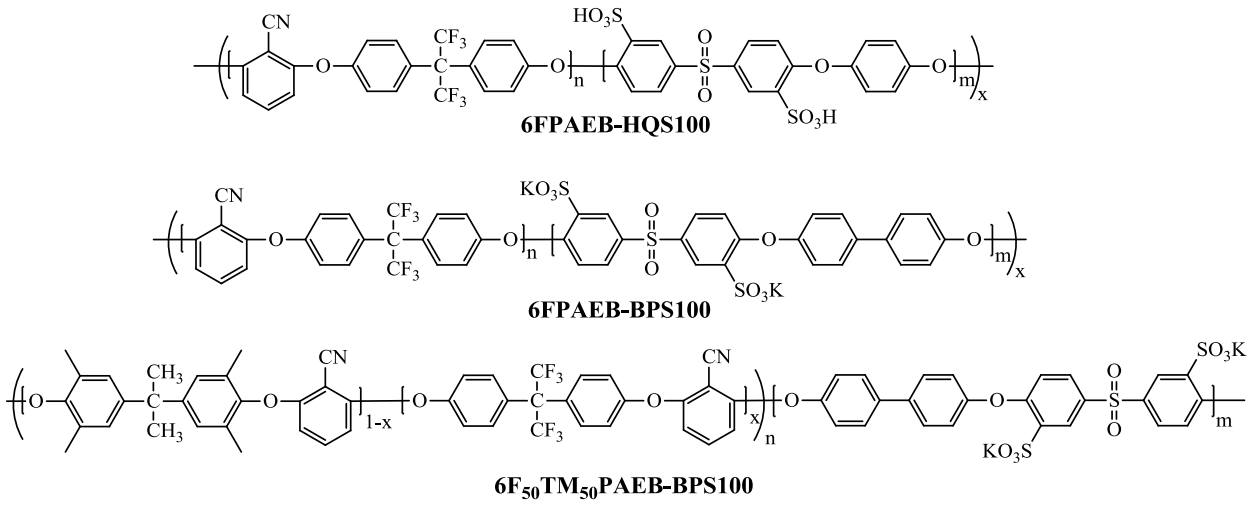

Figure 5.2: Structures of previously synthesized multiblock copolymers

5.2.4 Membrane preparation and acidification

The potassium salt forms of the multiblock copolymers were dried at 150°C for 24 h, then they were dissolved in DMAc (~5% w/v) and filtered through a 0.45 μm Teflon syringe filter. The solutions were cast onto a dry, clean glass substrate and dried for 24 h under an infrared lamp at ~80°C. Then the membranes were annealed under vacuum at 220°C (about 30°C

higher than the T_g of the nitrile-based hydrophobic blocks). The membranes were removed from the glass plate by placing them in a water bath, and then converted to the acid form by boiling in 0.5 M sulfuric acid for 2 h, followed by boiling in DI water for 2 h. The 6FPAEB-SQS100 multiblock copolymer was cast from a (~5% w/v) DMF solution due to insolubility in DMAc, and utilized the same drying conditions.

5.2.5 Characterization

^{1}H NMR, and ^{19}F NMR analyses were conducted on a Varian Unity Plus spectrometer operating at 400 MHz (376 MHz for ^{19}F). The spectra of the hydrophilic oligomers along with their corresponding block copolymers were obtained from a 10% (w/v) 1 mL solution in DMSO-d_6. The spectra of the hydrophobic oligomers were obtained from a solution in $CDCl_3$. Ion-exchange capacities was obtained via titration of the membranes with a 0.01 M NaOH solution and from the ^{1}H NMR spectra of the multiblock copolymers. For titration, the membranes were acidified, dried and weighed, then stirred in a 1.0 M NaCl solution at 50^{o}C overnight prior to titrating. Weight average molecular weights (M_w's) of the block copolymers were obtained via multi-detector size-exclusion chromatography (SEC) using NMP with 0.05 M LiBr as the mobile phase (50^{o}C) with 3 PLgel 10-μm mixed-B 300 x 7.5 mm columns in series with a Wyatt Viscostar II Viscometer, a Wyatt Heleos II multi-angle light scattering detector, and a Wyatt T-rex refractive index detector.

5.2.6 Tensile testing

Uniaxial load tests were performed using an Instron 5500R universal testing machine equipped with a 100 Newton load cell. The crosshead displacement rate was 1 mm/min and the gage length was 22 mm. The tensile test specimens were prepared with dimensions of 50 mm length and a minimum width of 3.2 mm per ASTM D1708-13. Prior to testing, the salt forms of

membrane specimens were dried in the vacuum oven at 150°C and tested at room temperature. All specimens were mounted in pressure locking pneumatic grips. Samples were run in triplicate with the median being used for representation for the mechanical properties for all samples except the copolymer that contained monosulfonated hydroquinone, which was limited due to sample availability.

5.2.7 Proton conductivity and water uptake

Proton conductivities of the multiblock copolymer membranes in the fully hydrated state were determined at 30°C in liquid water. Measurements were made in-plane with a four electrode configuration. Before the measurement, the membranes were equilibrated in DI water at 30°C for 24 h. A Solartron (1252 + 1287) impedance/gain-phase analyzer over the frequency range of 10 Hz to 1 MHz was used for the measurements following a previously reported method.[241] The conductivity was calculated by using equation 5.1.

(5.1) $$\sigma = \frac{L}{R \cdot S}$$

Where σ (S/cm) is proton conductivity, L (cm) is the distance between the two electrodes, R (Ω) is the resistance of the membrane and S (cm^2) is the surface area available for proton transport though the membrane. The water uptake of all membranes was determined gravimetrically. The membranes were equilibrated in DI water at room temperature for 2 days after acidification. Wet membranes (in the acid form) were removed from DI water, blotted dry to remove surface droplets, and quickly weighed. The membranes were dried at 120°C under vacuum for 24 h and re-weighed. The water uptake of the membranes was calculated according to equation 5.2, where W_{dry} and W_{wet} refer to the mass of the dry and wet membrane, respectively.

(5.2) $$Water\ Uptake\ (\%) = \frac{W_{wet} - W_{dry}}{W_{dry}} \times 100$$

5.2.8 Morphology

The membranes were tested in their potassium salt forms after annealing at 220^{o}C using the same method as listed for the membrane preparation. Additionally the membranes were dried in a vacuum oven at 100^{o}C for 12 h prior to being tested to ensure that no water was present in the membranes. SAXS experiments were performed using a Rigaku S-Max 3000 3 pinhole SAXS system, equipped with a rotating anode emitting X-rays with a wavelength of 0.154 nm (Cu Kα). The q-range was calibrated using a silver behenate standard. Two-dimensional SAXS patterns were obtained using a fully integrated 2D multiwire, proportional counting, gas-filled detector, with an exposure time of 1 h. All the SAXS data were analyzed using the SAXSGUI software package to obtain radially integrated SAXS intensity versus scattering vector q, where q = $(4\pi/\lambda)\sin(\theta)$, where θ is one half of the scattering angle and λ is the wavelength of the X-ray.

5.3 Results and Discussion

5.3.1 Synthesis of difunctional oligomers

The 6FPAEB and $6F_{50}TM_{50}$PAEB hydrophobic fluorine terminated oligomers were synthesized by the protocols described in chapters 2 and 3. Hydrophilic oligomers BPS100 and HQS100, with phenolic end groups were successfully acquired using the methods reported in chapters 2 and 3 as well. It was difficult to obtain controlled molecular weights of the hydrophilic oligomer that contained sulfonated hydroquinone (SQS100) when disulfonated dichlorodiphenylsulfone was utilized as the comonomer. Substitution of a sulfonic acid group on hydroquinone lowers the nucleophilicty towards nucleophilic aromatic substitution. Low reactivity of hydroquinone itself was also problematic for synthesis of oligomers from hydroquinone and disulfonated dichlorodiphenylsulone (the HQS100 oligomer). For example, molecular weights higher than ~10 kg/mol could not be achieved using the disulfonated

dichlorodiphenylsulfone monomer. A possible reason for the decreased reactivity of the hydroquinone relative to biphenol is their pK_a difference (Fig. 5.3). While there is no difference in the pK_{a1} and pK_{a2} for 4,4'-biphenol, there is a large increase in pK_{a1} and pK_{a2} for hydroquinone (measured in water).[268] However, the mechanism with the weak base occurs with only one phenol group deprotonated at a time. Nevertheless, there is still a large difference in pKa when the first hydroxyl group is bonded, as can been seen in Figure 5.3, with 4-phenylphenol almost one order of magnitude lower than p-methoxyphenol. Thus, the hydroxyl groups of the hydroquinone deprotonate slower and the weak potassium carbonate base might not be basic enough for complete deprotonation since the pK_a of potassium carbonate is ~10. Therefore a larger excess of potassium carbonate or the use of a strong base might be required to obtain higher molecular weight oligomers for the cases of incorporating hydroquinone moieties. Nevertheless, aromatic rings substituted with fluorine are more reactive than with chlorine in nucleophilic aromatic substitution. Thus, the disulfonated difluorodiphenylsulfone monomer was used to synthesize the SQS100 oligomer within reasonable reaction times. Additionally, the highly polar nature of the oligomer that contained the monosulfonated hydroquinone polymerized with disulfonated difluorodiphenylsulfone (SQS100) compared to those without the monosulfonated hydroquinone (HQS100 and BPS100 oligomers) limited the choice of solvent for polymerization (Fig. 5.4). DMSO was a solvent for both monomers and was suitable for the nucleophilic aromatic substitution reaction. However, DMSO also degrades at high temperatures. Thus, the reaction temperature was limited to 140^{o}C to avoid side reactions. Because of this limited choice in solvent and temperature, only low oligomeric molecular weights were obtained, even with the disulfonated difluorodiphenylsulfone monomer (less than 6 kg/mol) when monosulfonated hydroquinone was the comonomer. Nevertheless, the reaction produced

oligomers with sufficiently high molecular weights for preparing multiblock copolymers (Fig. 5.5). If suitable higher temperature polar aprotic solvents could be identified, higher molecular weights for the oligomeric species would be expected. Molecular weights of the oligomer were obtained via ^{1}H NMR by comparing the integrals of the protons on the endgroups to the protons in the backbone (Fig. 5.6).

	pK_{a1}	pK_{a2}
4,4'-biphenol	9.7	9.7
Hydroquinone	10.0	11.5
4-phenylphenol	9.5	
p-methoxyphenol	10.2	

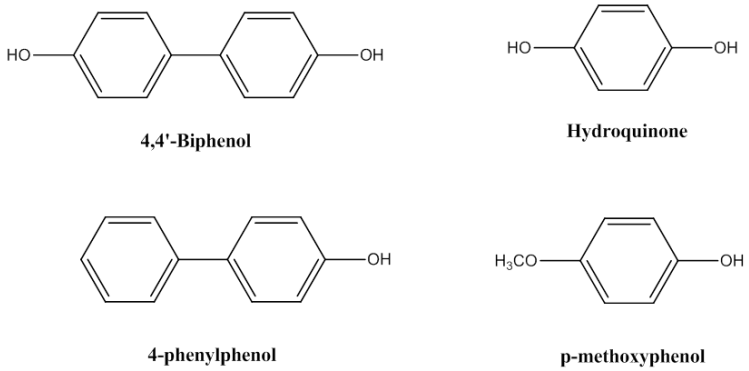

Figure 5.3: Acid constants for monomers and derivatives

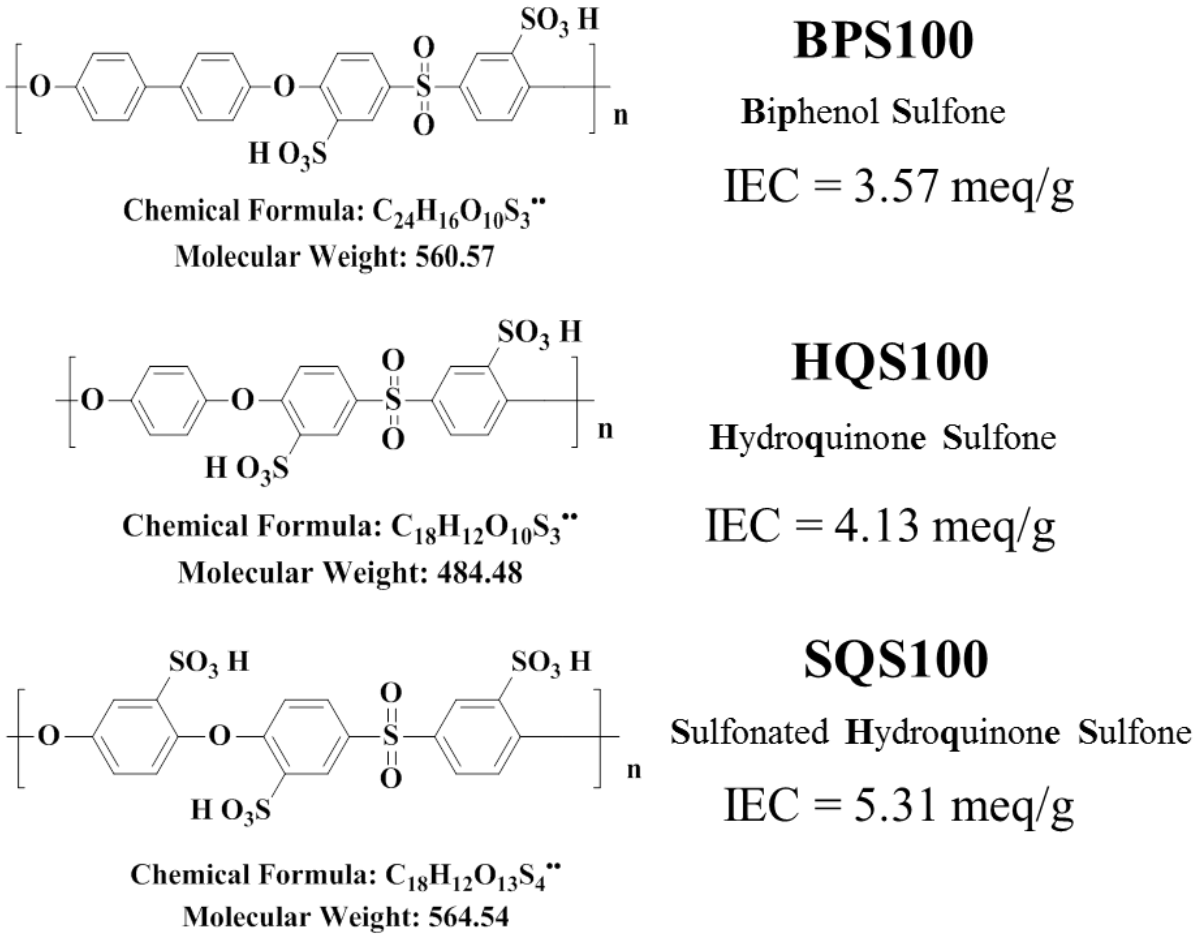

Figure 5.4: Structure and charge density of the three different sulfonated hydrophilic oligomers

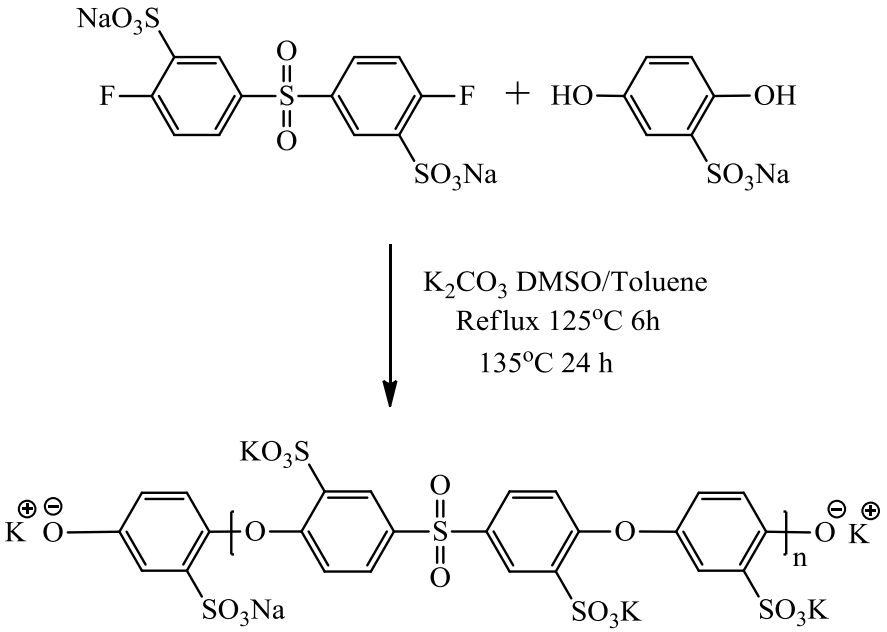

Figure 5.5: Direct polymerization of a highly sulfonated poly(arylene ether sulfone) oligomer (SQS100)

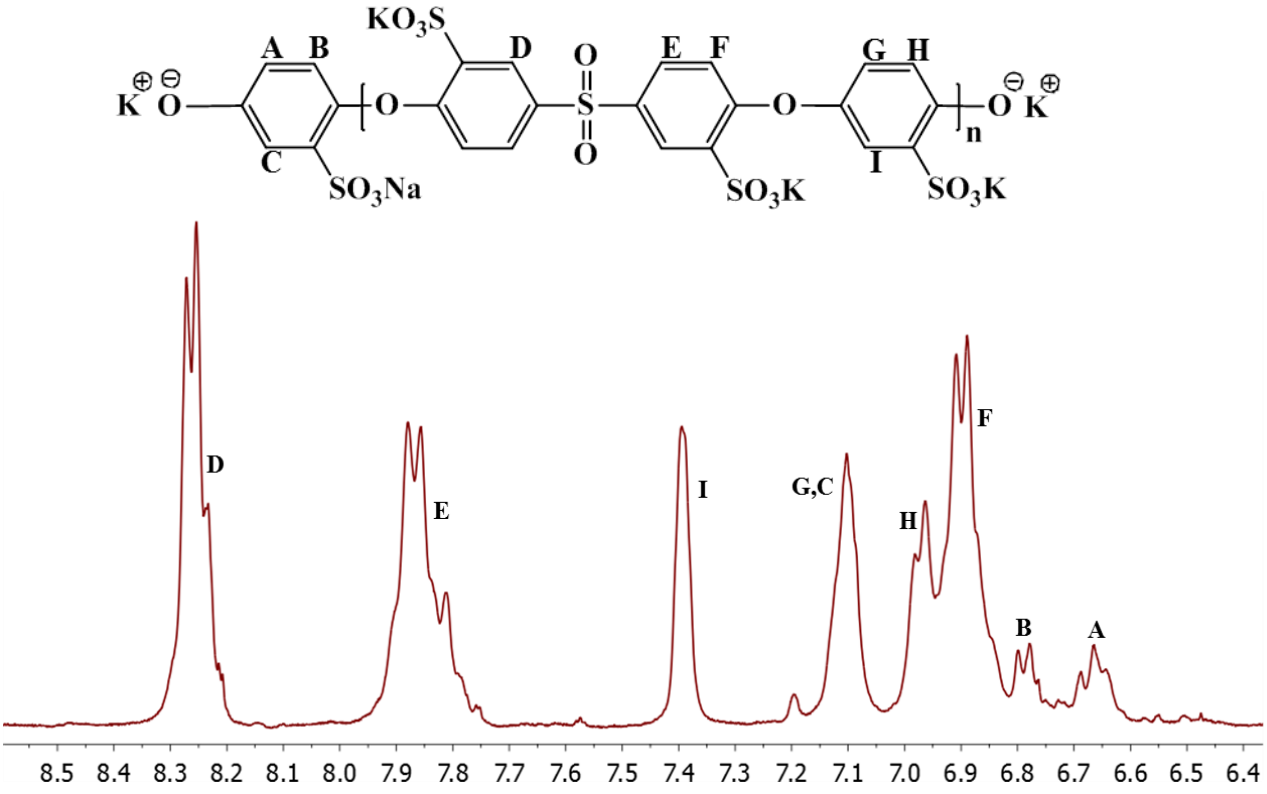

Figure 5.6: ^{1}H NMR of a SQS100 hydrophilic oligomer

5.3.2 Synthesis of hydrophilic-hydrophobic multiblock copolymers with high IECs

Synthesis of the biphenol and hydroquinone based multiblock copolymers with the poly(arylene ether benzonitrile) hydrophobic segment (6FPAEB-BPS100, and 6FPAEB-HQS100) were discussed in chapter 2. For the multiblock copolymer that contained monosulfonated hydroquinone in the hydrophilic segment (6FPAEB-SQS100), only a 5 kg/mol oligomer could be obtained. Thus this highly sulfonated oligomer was paired with a slightly higher molecular weight hydrophobic oligomer to aid in achieving a sufficiently high molecular weight multiblock copolymer. DMSO was used as the reaction solvent for the coupling reaction between the oligomers to form the multiblock copolymers (Fig. 5.7). It was found in previous multiblock copolymer reactions that the SQS100 oligomer had low reactivity towards the hydrophobic block. Thus in reasonable reaction times the oligomer only coupled a few times. Therefore to achieve high molecular weights in 48 h, a longer hydrophobic block was used. Since the hydrophilic oligomer is not fully reacting, 1:1 molar stoichiometry was no longer necessary. Thus, to compensate for the higher molecular weight of the hydrophobic block in the 6FPAEB-SQS100 multiblock copolymer, a 10 mol% excess of the hydrophilic oligomer was used in the coupling reaction. Progress of the reactions and final compositions of the multiblock copolymers were monitored by ^{1}H NMR spectroscopy. Figure 5.8 shows the comparison of the multiblock copolymers, which confirmed successful incorporation of both oligomers for all of the systems. The 6FPAEB-SQS100 multiblock copolymers showed less inclusion of the hydrophilic segment into the multiblock copolymer than was charged to the reaction. This can most likely be attributed to decreased reactivity of the phenoxide endgroups.

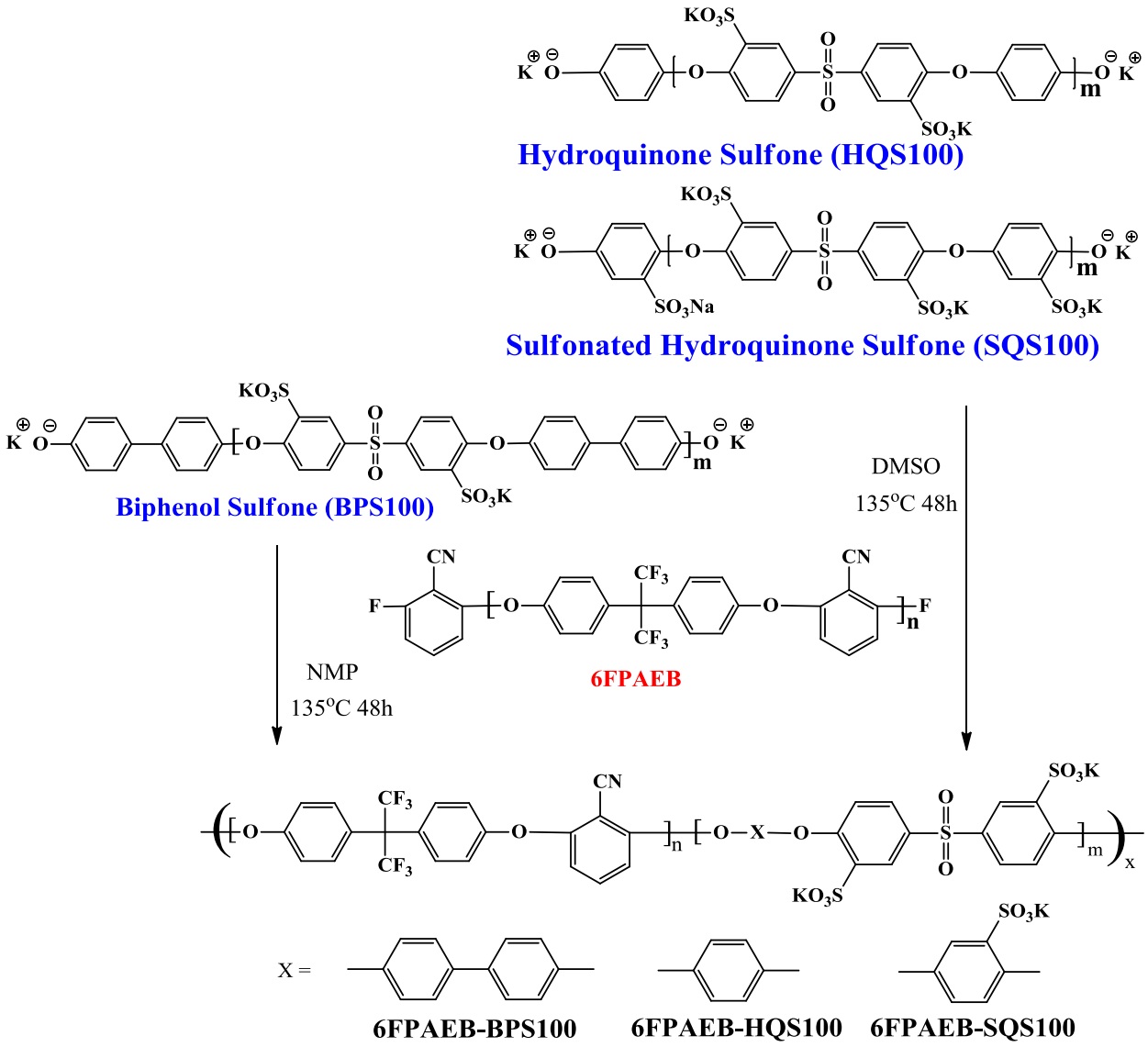

Figure 5.7: Synthesis of multiblock copolymers with controlled hydrophilicities (IECs) and block lengths

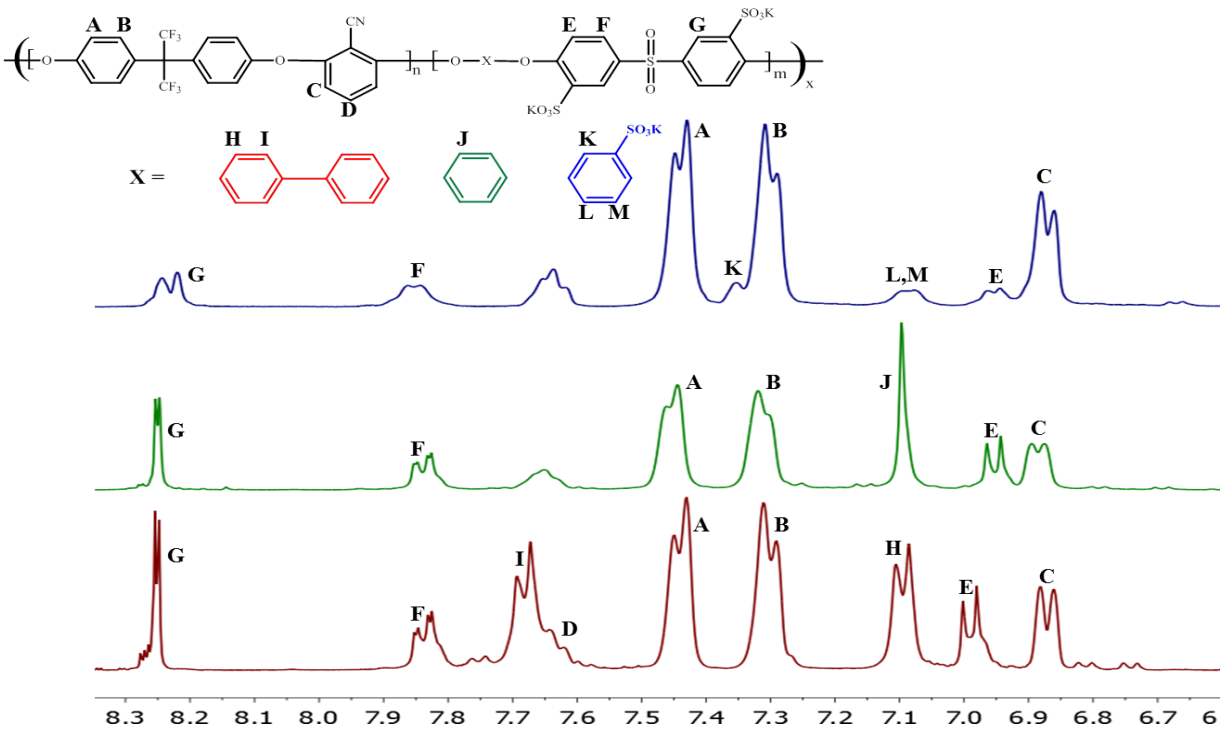

Figure 5.8: ^{1}H NMR spectra multiblock copolymers with 6FPAEB and the hydrophobic block and varied hydrophilic blocks: (top) 6FPAEB-SQS100, (middle) 6FPAEB-HQS100, and (bottom) 6FPAEB-BPS100.

The synthesis of the partially fluorinated multiblock copolymers containing tetramethyl bisphenol A ($6F_{50}TM_{50}$PAEB-BPS100) was previously discussed chapter 3. A similar $6F_{50}TM_{50}$PAEB-BPS100 multiblock copolymer but with a higher IEC was prepared by utilizing a higher molecular weight hydrophilic segment compared to the hydrophobic segment. The $6F_{50}TM_{50}$PAEB-BPS100 multiblock copolymer discussed in chapter 3 was comprised of hydrophilic and hydrophobic blocks having approximately equal block lengths. To avoid confusion the two $6F_{50}TM_{50}$PAEB-BPS100 multiblock copolymers are referred to as high and low IEC membranes. For the high IEC $6F_{50}TM_{50}$PAEB-BPS100 multiblock copolymer, equal molar stoichiometry was used for the two types of blocks. Figure 5.9 demonstrates that use of the higher molecular weight hydrophilic oligomer relative to the hydrophobic block length

successfully resulted in a block copolymer with a higher amount of sulfonation compared to the similar multiblock copolymer with equal block lengths described in chapter 3. The hydrophilic peaks were increased in intensity compared to the hydrophobic peaks, indicating a higher composition of hydrophilic moieties in the resulting multiblock copolymer. The IECs of all the multiblock copolymers were calculated from the integral ratios of the peaks corresponding to the hydrophilic versus hydrophobic blocks.

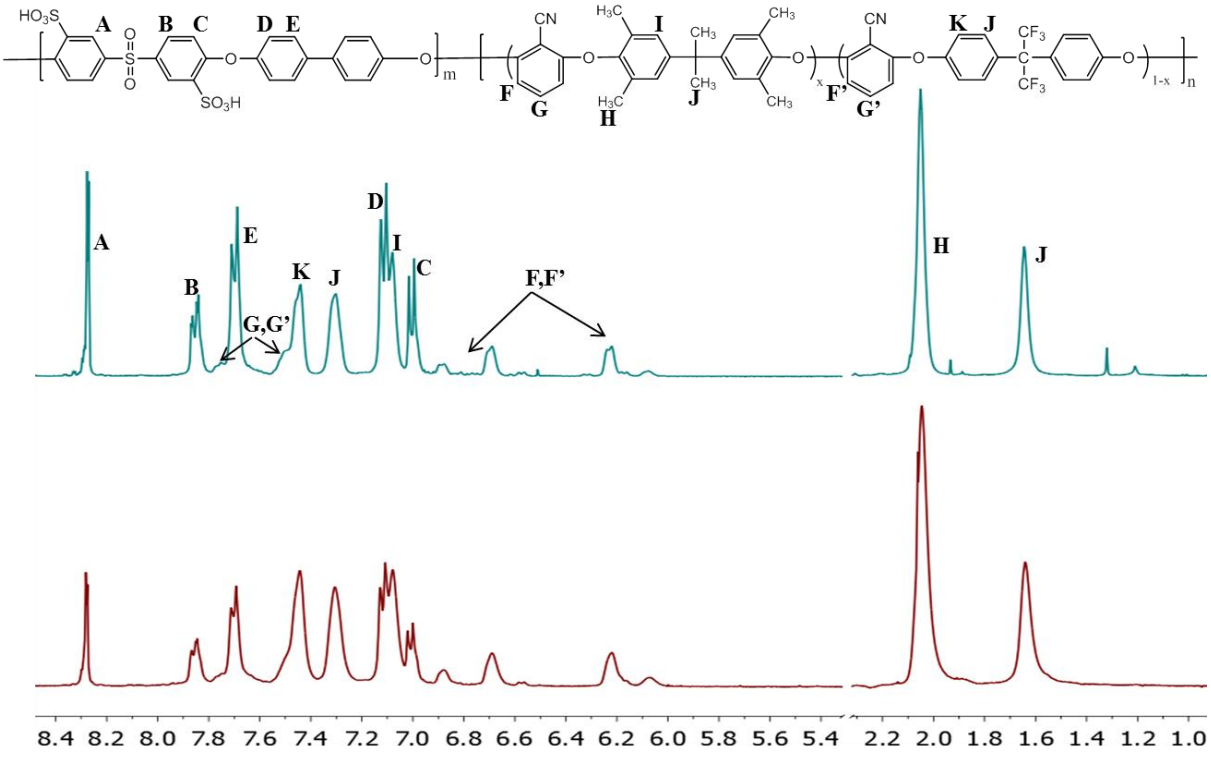

Figure 5.9: Comparison of compositions of $6F_{50}TM_{50}$PAEB-BPS100 multiblock copolymers with different IECs. Top spectrum is the higher IEC multiblock copolymer (~52 wt% hydrophilic phase) and bottom is lower IEC multiblock copolymer (~42 wt% hydrophilic phase) from chapter 3.

5.3.3 Membrane Properties

The two multiblock copolymer membranes are shown in Table 5.1 and Table 5.2 and are compared against analogous systems.

Table 5.1: Comparison of membranes with varying charge density that contain methyl substituents on rings in the hydrophobic phase ($6F_{50}X_{50}$PAEB-BPSH[a])

Sample	Block Length	IEC (meq/g)[c]	Wt% BPSH	M_w (kg/mol)	Water Uptake (wt%)
$6F_{50}TM_{50}$PAEB-BPSH	10.9 K – 10.2 K	1.50	42	50	20
$6F_{50}TM_{50}$PAEB-BPSH[b]	6.7 K – 8.0 K	1.85	52	40	42
$6F_{50}DM_{50}$PAEB-BPSH[b]	10.7 K – 10.2 K	1.65	46	80	35
$6F_{50}BisA_{50}$PAEB-BPSH[b]	11.3 K – 10.2 K	1.74	49	75	40

[a] The multiblock copolymers are denoted as XXS-100 when in the salt form and as XXSH when converted to the acid form. Thus, when $6F_{50}TM_{50}$PAEB-BPS100[a] is converted from salt to acid form the nomenclature changed to $6F_{50}TM_{50}$PAEB-BPSH.

[b] Multiblock copolymers prepared in chapter 3

[c] IEC of multiblock copolymer films via ^{1}H NMR

Table 5.2: Membrane properties of 6FPAEB based multiblock copolymers

Polymer	Block Length	IEC (meq/g)[b]	IEC (meq/g)[c]	M_w (kg/mol)	Water Uptake (wt%)	Proton Conductivity (S/cm)
6FPAEB-BPSH[a]	7K – 7K	1.57	1.64	58	39	0.13
6FPAEB-HQSH[a]	7K – 7K	1.73	1.76	46	51	-
6FPAEB-SQSH[a]	9K – 5K	1.78	1.81	59	45	-

[a] The multiblock copolymers are denoted as XXS-100 when in the salt form and as XXSH when converted to the acid form. Thus, when 6PAEB-SQS100 is converted from salt to acid form the nomenclature changed to 6FPAEB-SQSH.

[b] IEC of multiblock copolymer films via ^{1}H NMR

[c] IEC of multiblock copolymers from titration of films with 0.01 M NaOH

All the membranes were annealed at 220^{o}C prior to testing the membrane properties to enhance assembly of lamellar morphology in the multiblock copolymers. In comparing the multiblock copolymers in Table 5.1, with the use of a longer hydrophilic segment compared to the hydrophobic segment, a large increase in IEC was observed. This corresponded to increased water uptake along with the rise in IEC. However, the high IEC tetramethyl bisphenol A based membrane showed only a modest water uptake of 42 wt%. This value is only slightly higher than the water uptake of the dimethylbisphenol A and bisphenol A based multiblock copolymers reported in chapter 3, which was 35 wt% and 40 wt% respectively (Table 5.1). However the high IEC tetramethylbisphenol A based multiblock copolymer had a significantly higher IEC than the

other two samples (1.65, 1.75). This is a strong indication that the methyl substituents are responsible for the excellent water management properties.

As shown in Table 5.2 the uneven block lengths used for the 6FPAEB-SQSH multiblock copolymer combined with the higher charge density within the hydrophilic block resulted in a polymer with a similar IEC to that of the 6FPAEB-HQSH multiblock copolymer. While the IEC of the 6FPAEB-SQSH was not as high as expected, due to less incorporation of the SQSH oligomer than was charged into the reaction, the water uptake produced an interesting result. The copolymer containing the monosulfonated hydroquinone in the hydrophilic block (6FPAEB-SQSH) had a similar overall charge density relative to the 6FPAEB-HQSH membrane, but the water uptake was somewhat lower for the copolymer with the more highly sulfonated, but lower block length, hydrophilic block. Thus, it is reasoned that the morphology of the copolymer (6FPAEB-SQSH) with a higher volume fraction of the hydrophobic 6FPAEB block is probably limiting the water uptake of the highly sulfonated SQSH hydrophilic segment

All of the multiblock copolymers had weight average molecular weights ranging from 40-60 kg/mol which was consistent with previously reported results. Incorporation of tetramethylbisphenol A in the $6F_{50}TM_{50}$PAEB-BPSH membranes seemed to reduce the copolymer molecular weights slightly, while the lower block lengths (only 7K hydrophobic and hydrophilic) of the blocks in the 6FPAEB series was the most likely cause for the lower M_w. Nevertheless, the mechanical properties of all the membranes were excellent, suggesting that the entanglement molecular weight had been reached (Fig. 5.10). The membranes all had a yield stress ranging from 45-55 MPa, and except for 6FPAEB-HQS100 all reached at least 30% elongation. The lower elongation of the 6FPAEB-HQS100 could be due to the lower molecular weight of the multiblock copolymer.

Although the molecular weight was fairly low for the $6F_{50}TM_{50}$PAEB-BPS100 membrane with the higher IEC, the phase separated morphology may have accounted for the strong mechanical properties despite this limitation (Fig.5.11). The increase in charge density brought on by the uneven block lengths seemed to have little effect on the SAXS plots of the $6F_{50}TM_{50}$PAEB-BPS100 multiblock copolymers. The secondary peak ($2q_{max}$) was very prominent for both profiles, with the q_{max} being very similar between the two copolymers. Although, the profile of JR-2-39 might appear to be slightly broader than the JR-1-113 profile, it appears that the charge density has little effect on degree of phase separation of the multiblock copolymer. In the case of the 6FPAEB based multiblock copolymers, all of the SAXS profiles of the membranes appeared representative of multiblock copolymers (Fig.5.12). The 6FPAEB-BPS100 and 6FPAEB-HQS100 had a noticeable secondary q_{max}, while this was absent in the 6FPAEB-SQS100. Additionally, the 6FPAEB-SQS100 was much broader than the other two multiblock copolymers. Thus, the uneven molecular weights of the segments in the 6FPAEB-SQS100 might be preventing further phase separation or more ordered morphology. Nevertheless, the higher molecular weight of the hydrophobic oligomer allowed for excellent mechanical properties and reduced water uptake, while maintaining a high charge density.

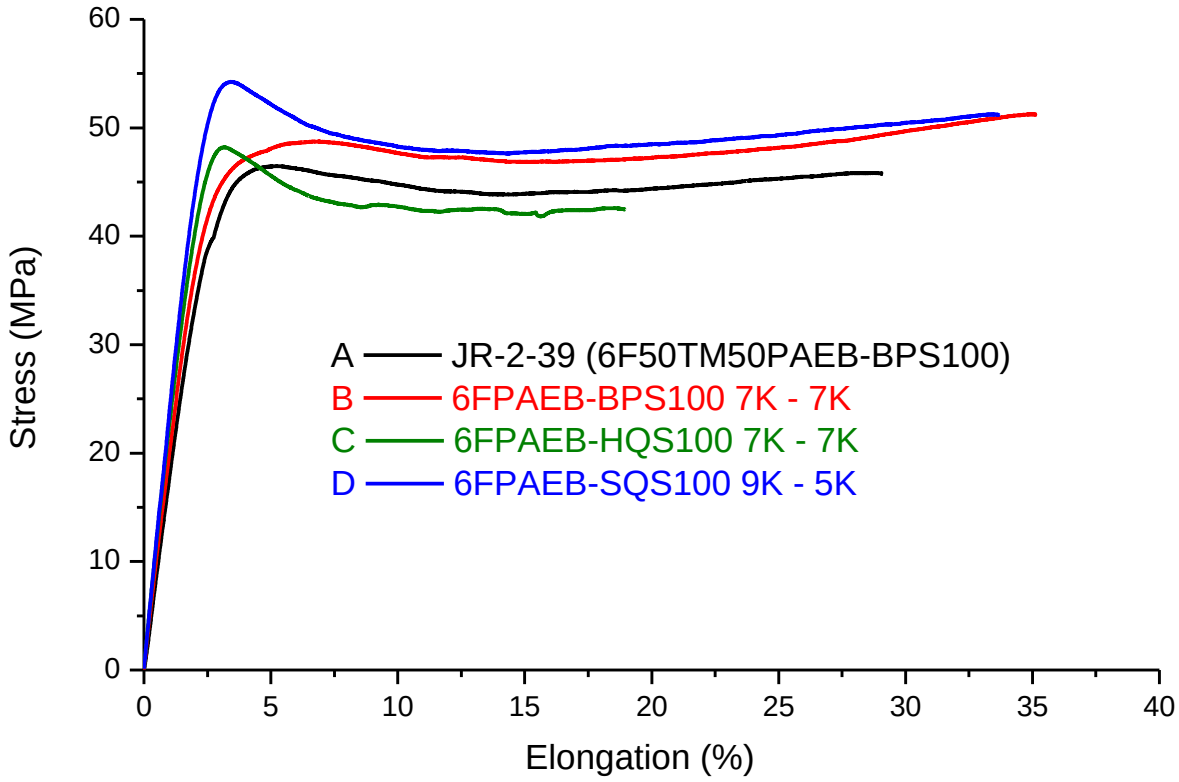

Figure 5.10: Representative tensile properties of multiblock copolymers

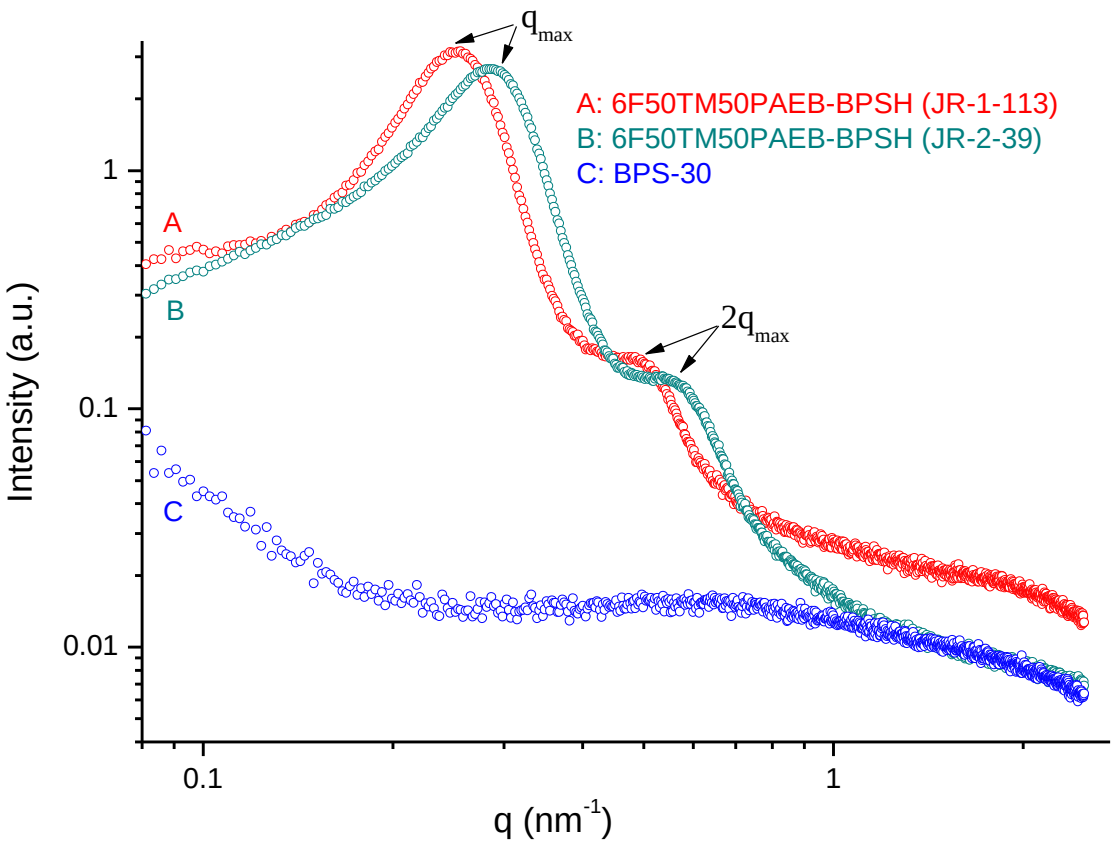

Figure 5.10: SAXS profiles comparing different charge densities of tetramethylbisphenol A based multiblock copolymers

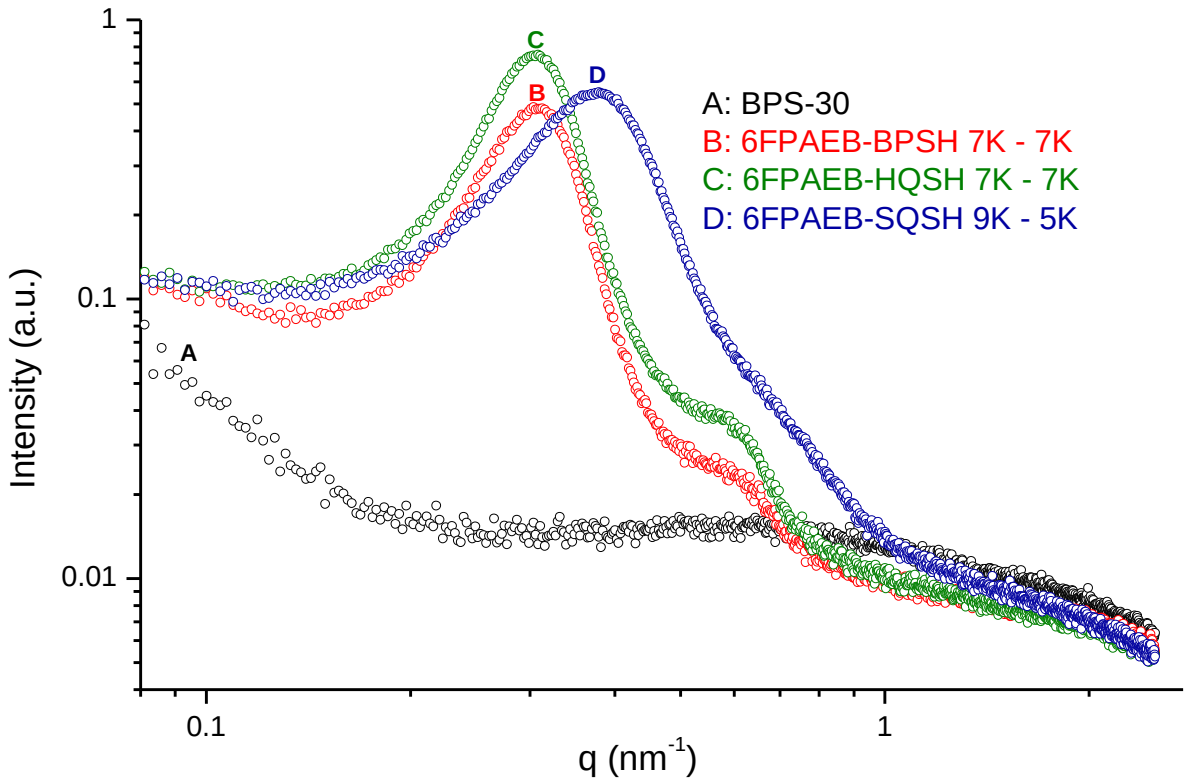

Figure 5.11: SAXS profiles of multiblock copolymers with 6FPAEB hydrophobic blocks and varied hydrophilic blocks

5.4 Conclusions

The effect of charge density and block molecular weight were investigated in two multiblock copolymers. The high charge density was accomplished via two different methods. One method employed a highly polar hydrophilic segment utilizing a monosulfonated hydroquinone monomer. The second method used uneven block lengths with a slightly higher molecular weight hydrophilic segment in combination with the hydrophobic segment. Despite the uneven block length and the higher charge density of the $6F_{50}TM_{50}$PAEB-BPSH (JR-2-39) membrane, the SAXS profile showed very little difference between the lower IEC analog. Additionally, the higher IEC membrane showed excellent mechanical properties and low water

uptake despite the increase in charge density. Thus, it can be concluded that tetramethyl substituents on the bisphenol of the hydrophobic phase are having profound effect on the morphology and membrane properties. When the trisulfonated SQS100 hydrophilic oligomer was utilized in conjugation with a higher molecular weight 6FPAEB hydrophobic oligomer, high IEC and modest water uptake values were observed. The large difference in molecular weights between the oligomeric blocks seemed to inhibit phase separation in the case of the trisulfonated multiblock copolymers. However, the high concentration of the hydrophobic component appeared to have a positive effect, as excellent mechanical properties and water management was observed.

Chapter 6: Conclusions and Recommended Future Research

6.1 Conclusions

Results from this dissertation have defined important structure-property relationships for dense membranes based on poly(arylene ether)s for fuel cell and gas separation processes. Both multiblock and random copolymers were synthesized and investigated. Relationships among backbone composition and morphology of the membranes and transport and mechanical properties were the focus of this dissertation.

Investigation of multiblock copolymers for use as proton exchange membranes in either direct methanol or H_2/air fuel cells revealed a strong dependence on both backbone structure and how the membranes were prepared. The increasing of the hydrophilicity or hydrophobicity of the oligomeric segments by incorporation of a hydroquinone monomer in the hydrophilic phase or methyl substituents in the hydrophobic phase results in membranes with increased phase separation. Annealing multiblock copolymer membranes facilitates phase separation producing multiblock copolymers with well-developed morphologies. Hydroquinone or sulfonated hydroquinone moieties can be used to produce higher charge density membranes over the biphenol analogs, with only modest increase in water uptake. Additionally, methyl substituents on the bisphenol significantly lower water uptake of the multiblock copolymers. The combination of methyl substituents with a reduction in fluorine content produces membranes with extremely low methanol permeability and excellent fuel cell performance in direct methanol fuel cells. Positive effects of adding methyl substituents on the bisphenol moiety on fuel cell performance is magnified at higher methanol concentrations, potentially creating suitable membranes that can be used at these higher concentrations.

Difunctional poly(2,6-dimethylphenylene oxide) oligomers can be chain extended with difluorobenzophenone to form high molecular weight copolymers. The use of benzylic methyl substituents in combination with benzophenone groups creates UV-crosslinkable membranes that can achieve high gel fractions. Crosslink density is dependent on ketone concentration for these polymers, with higher increases in glass transition temperatures occurring for polymers with higher ketone incorporation. Crosslinking occurs through a hydrogen abstraction mechanism from the benzylic methyls of the copolymer or homopolymer. After crosslinking, membranes show higher selectivity but lower permeability for O_2/N_2 and CO_2/CH_4 gas pairs. Control of the concentration of ketones through either backbone structure or oligomer molecular weight allows for poly(arylene ether)s with tunable gas transport properties.

6.2 Recommendations for Further Research

The results obtained for the poly(arylene ether) random and multiblock copolymers in this thesis prompt further investigation of structure-property relationships of related systems. Multiblock copolymers with excellent direct methanol fuel cell performance can be achieved by including methyl substituents on the bisphenol moiety and reducing the fluorine content. Along with this, enhanced phase separation is achievable by increasing hydrophilicity or hydrophobicity of the segments in the multiblock copolymers. To further quantify the effect of benzylic methyl groups, testing of the high IEC $6F_{50}TM_{50}$PAEB-BPSH multiblock copolymer in direct methanol fuel cell systems must be conducted. Combining ketone groups and benzylic methyl groups allows for poly(arylene ether) copolymers that are UV-crosslinkable. Crosslink density and transport properties appear to be dependent on the ketone concentration in the poly(arylene ether)s. This can be further understood by measuring gas transport properties of the PPO-PAEK (2) and PPO-PAEK (2) crosslinked membranes.

Based upon the strong performance of the $6F_{50}TM_{50}$PAEB-BPSH multiblock copolymer, the proposed next steps would be to include the benzylic groups in the whole repeating unit of the hydrophobic phase. By using a monomer that contains both fluorine and benzylic methyl groups, as shown in Figure 6.1, this would provide partial fluorination with a simplified synthesis. Additionally, use of the ketone groups in combination with the tetramethyl-substituted bisphenols could allow for UV crosslinking of the membrane, which could also reduce methanol permeability.

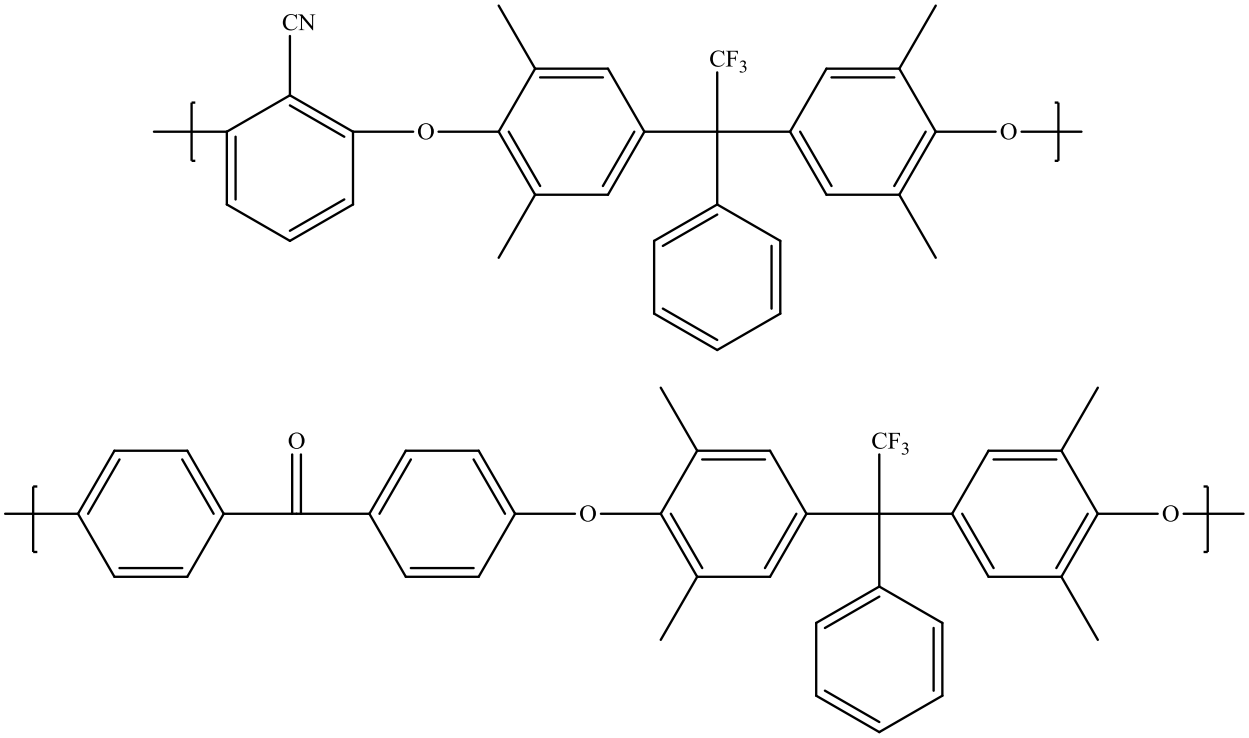

Figure 6.1: Proposed structure of a hydrophobic crosslinkable polymer having benzylic methyl substituents and a partially fluorinated backbone

Furthermore, enhanced phase separation was achieved by optimizing either the hydrophobic or hydrophilic phase. Thus by including methyl groups in the hydrophobic phase

plus replacement of biphenol with hydroquinone or sulfonated hydroquinone in the hydrophilic phase might further magnify these effects (Fig.6.2). Further increased phase separation might be beneficial for both H_2/air and methanol fuel sources, with crosslinked sites limiting any excessive swelling of the membranes. In order to get higher molecular weight disulfonated oligomers that contain hydroquinone, investigation into using different bases such as hydroxides as opposed to carbonates is recommended.

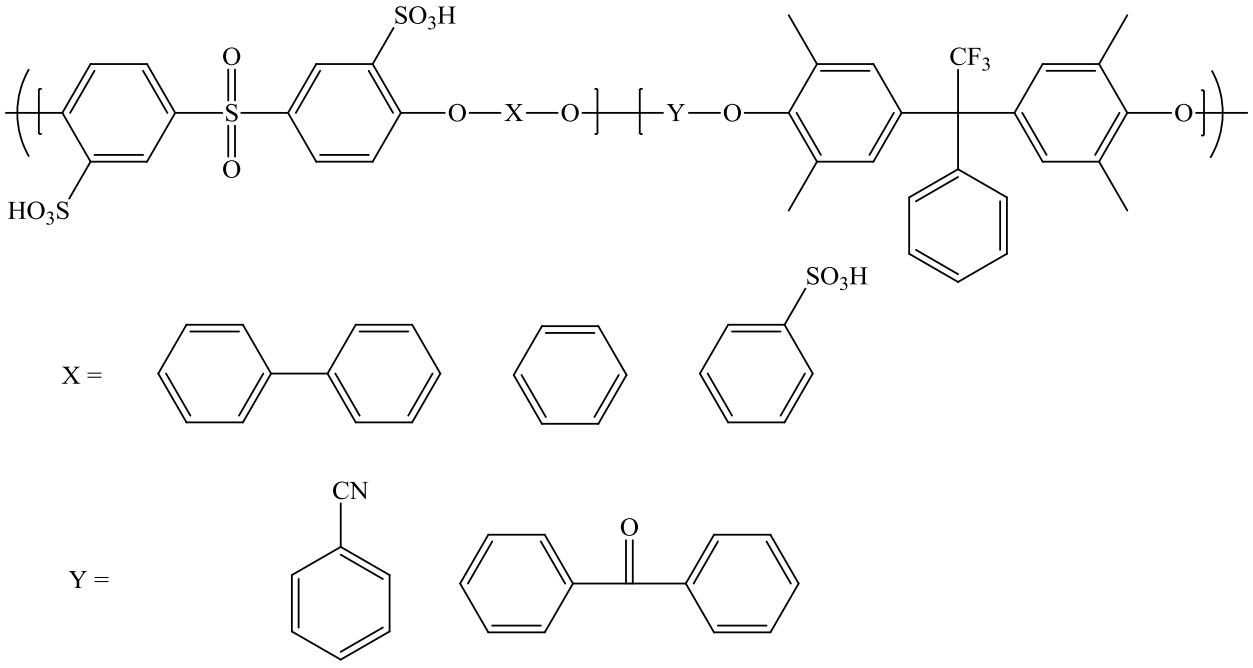

Figure 6.2: Proposed multiblock copolymers with 3F-tetramethylbisphenols in the hydrophobic segments

For poly(arylene ether)s in gas separation applications, higher crosslinking could be obtained via a methylated poly(arylene ether ketone) system. Trimethylhydroquinone is an inexpensive and commercially available molecule as it is used in the synthesis of Vitamin C. By eliminating one of the aromatic rings in comparison to the tetramethylbisphenol A-benzophenone polymer, this would provide the highest possible crosslink density in a wholly

aromatic polymer. Since the crosslink density of networks that contain benzylic methyl groups and aromatic ketones appears to be more dependent on the concentration of ketone groups than methyl groups, tetramethyl hydroquinone might not be that advantageous over the trimethyl-substituted moiety. With the system proposed in Figure 6.3 the wt% of the ketone groups would be approximately 55%, which is a significant increase over that of the tetramethylbisphenol A-benzophenone polymer. The high percentage of ketone would most likely further increase both crosslink density and selectivities of gas permeabilities.

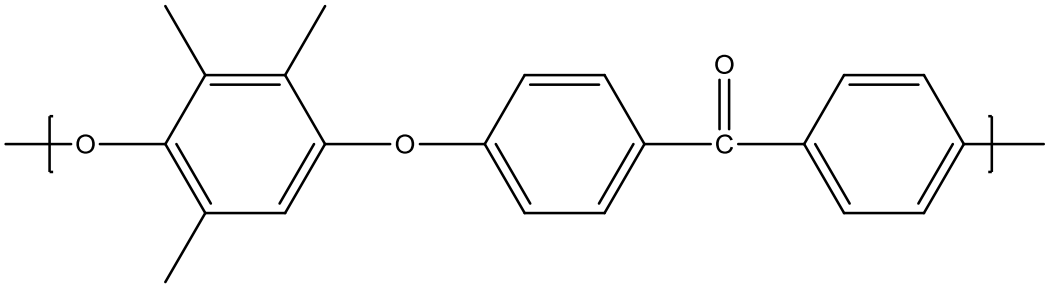

Figure 6.3: Trimethyl hydroquinone based poly(arylene ether ketone)

References:

1. Pinnau, I.; Freeman, B. D., Formation and Modification of Polymeric Membranes: Overview. In *Membrane Formation and Modification*, American Chemical Society, 1999; Vol. 744, pp 1-22.
2. Polymer Science: A Comprehensive Reference. Matyjaszewski, K.; Möller, M., (Eds). Elsevier, Oxford, UK, 2012; Vol. 8, pp 325-347.
3. Hoogers, G., *Fuel Cell Technology: Handbook*. CRC Press: Boca Raton, Fl., 2003.
4. Gasik, M., *Materials for Fuel Cells*. CRC Press: Boca Raton, Fl., 2008.
5. Bagotsky, V. S., *Fuel Cells: Problems and Solutions*. John Wiley & Sons: Hoboken, NJ, 2009.
6. Hickner, M. A.; Ghassemi, H.; Kim, Y. S.; Einsla, B. R.; McGrath, J. E., *Chem. Rev.* **2004,** *104*, 4587.
7. http://en.wikipedia.org/wiki/Fuel_cell.
8. Polymer Science: A Comprehensive Reference. Matyjaszewski, K.; Möller, M., (Eds). Elsevier, Oxford, UK, 2012; Vol. 10, pp 597-775.
9. http://www.hydrogenandfuelcells.energy.gov.
10. Mauritz, K. A.; Moore, R. B., *Chem. Rev* **2004,** *104*, 4535.
11. Ghassemi, H.; Ndip, G.; McGrath, J. E., *Polymer* **2004,** *45*, 5855.
12. Wang, H.; Badami, A. S.; Roy, A.; McGrath, J. E., *J. Polym. Sci., Part A: Polym. Chem.* **2006,** *45*, 284.
13. Li, Y.; Roy, A.; Badami, A. S.; Hill, M.; Yang, J.; Dunn, S.; McGrath, J. E., *J. Power Sources* **2007,** *172*, 30.
14. Baker, R. W.; Cussler, E. L.; Eykamp, W.; Koros, W. J.; Riley, R. L.; Strathmann, R. H., *Membrane Separation Systems*. Noyes Data Corporation: Park Ridge, NJ, 1991.
15. Noble, R. D.; Stern, S. A., *Membrane Separations Technology Principles and Applications*. Elsevier Science B.V.: Amersterdam, 1995.
16. http://en.wikipedia.org/wiki/Gas_separation.
17. Koros, W. J.; Mahajan, R., *J. Membr. Sci.* **2000,** *175*, 181.
18. Bernardo, P.; Drioli, E., *Petroleum Chemistry* **2010,** *50*, 271.
19. Paul, D. R.; Yampolskii, Y. P., *Polymeric Gas Separation Membranes*. CRC Press: Boca Raton, Fl, 1994.
20. Robeson, L. M., *J. Membr. Sci.* **1991,** *62*, 165.
21. Freeman, B. D., *Macromolecules* **1999,** *32*, 375.
22. Robeson, L. M., *J. Membr. Sci.* **2008,** *320*, 390.
23. http://www.co2crc.com.au/aboutccs/cap_membranes.html.
24. Banerjee, S.; Curtin, D. E., *J. Fluorine Chem.* **2004,** *125*, 1211.
25. GB1034197, **1966**.
26. Higashihara, T.; Matsumoto, K.; Ueda, M., *Polymer* **2009,** *50*, 5341.
27. Grot, W. G. EP66369A1, **1982**.
28. Kreuer, K. D., *Solid State Ionics* **1997,** *97*, 1.
29. Li, L.; Deng, B.; Ji, Y.; Yu, Y.; Xie, L.; Li, J.; Lu, X., *J. Membr. Sci.* **2010,** *346*, 113.
30. L.Gubler; Kuhn, H.; Scherer, G. G.; Brack, H. P.; Simbeck, K., *Fuel Cells* **2004,** *4*, 196.
31. Huang, H. S.; Chen, C. Y.; Lo, S. C.; Lin, C. J.; Chen, S. J.; Lin, L. J., *Appl. Surf. Sci.* **2006,** *253*, 2685.

32. Tsang, E. M. W.; Zhang, Z.; Shi, Z.; Soboleva, T.; Holdcroft, S., *J. Am. Chem. Soc.* **2007,** *129*, 15106.
33. Tsang, E. M. W.; Zhang, Z.; Yang, A. C. C.; Shi, Z.; Peckham, T. J.; Narimani, R.; Frisken, B. J.; Holdcroft, S., *Macromolecules* **2009,** *42*, 9467.
34. Zhang, Z.; Chalkova, E.; Fedkin, M.; Wang, C.; Lvov, S. N.; Komarneni, S.; Chung, T. C. M., *Macromolecules* **2008,** *41*, 9130.
35. Vogel, H.; Marvel, C. S., *J. Polym. Sci.* **1961,** *50*, 511.
36. Wainright, J. S.; Wang, J. T.; Weng, D.; Savinell, R. F.; Litt, M., *J. Electrochem. Soc.* **1995,** *142*, L121.
37. Mader, J.; Xiao, L.; Schmidt, T. J.; Benicewicz, B. C., *Adv. Polym. Sci.* **2008,** *216*, 63.
38. Samms, S. R.; Wasmus, S.; Savinell, R. F., *J. Electrochem. Soc.* **1996,** *143*, 1225.
39. Wang, J. T.; Savinell, R. F.; Wainright, J.; Litt, M.; Yu, H., *Electrochim. Acta* **1996,** *41*, 193.
40. Glipa, X.; Haddad, M. E.; Jones, D. J.; Roziere, J., *Solid State Ionics* **1997,** *97*, 323.
41. Asensio, J. A.; Borros, S.; Gomez-Romero, P., *J. Polym. Sci. Part A Polym. Chem.* **2002,** *40*, 3703.
42. Glipa, X.; Bonnet, B.; Mula, B.; Jones, D. J.; Rozière, J., *J. Mater. Chem* **1999,** *9*, 3045.
43. Jones, D. J.; Roziere, J., *J. Membr. Sci.* **2001,** *185*, 41.
44. Qingfeng, L.; Hjuler, H. A.; Bjerrum, N. J., *J. Appl. Electrochem.* **2001,** *31*, 773.
45. Qing, S.; Huang, W.; Yan, D., *Eur. Polym. J.* **2005,** *41*, 1589.
46. Qing, S.; Huang, W.; Yan, D., *React. Funct. Polym.* **2006,** *66*, 219.
47. Xiao, L.; Zhang, H.; Scanlon, E.; Ramanathan, L. S.; Choe, E. W.; Rogers, D.; Apple, T.; Benicewicz, B. C., *Chem. Mater.* **2005,** *17*, 5328.
48. Qian, G.; Smith Jr, D. W.; Benicewicz, B. C., *Polymer* **2009,** *50*, 3911.
49. Yu, S.; Benicewicz, B. C., *Macromolecules* **2009,** *42*, 8640.
50. Mader, J. A.; Benicewicz, B. C., *Macromolecules* **2010,** *43*, 6706.
51. Wei, J.; Stone, C.; Steck, A. E. WO9508581A1, **1995**.
52. Basura, V. I.; Chuy, C.; Beattie, P. D.; Holdcroft, S., *J. Electroanal. Chem.* **2001,** *501*, 77.
53. Ehrenberg, S. G.; Serpico, J.; Wnek, G. E.; Rider, J. N. US5468574A, **1995**.
54. Carretta, N.; Tricoli, V.; Picchioni, F., *J. Membr. Sci.* **2000,** *166*, 189.
55. Kim, T. H.; Koros, W. J.; Husk, G. R., *Sep. Sci. Technol.* **1988,** *23*, 1611.
56. Kim, T. H.; Koros, W. J.; Husk, G. R.; O'Brien, K. C., *J. Membr. Sci.* **1988,** *37*, 45.
57. Ayala, D.; Lozano, A. E.; de Abajo, J.; Garcia-Perez, C.; de la Campa, J. G.; Peinemann, K. V.; Freeman, B. D.; Prabhakar, R., *J. Membr. Sci.* **2003,** *215*, 61.
58. Park, H.; Kim, Y. K.; Lee, J. M.; Lee, S. Y.; Lee, Y. M., *J. Membr. Sci.* **2004,** *229*, 117.
59. Dhara, M. G.; Banerjee, S., *Prog. Polym. Sci.* **2010,** *35*, 1022.
60. Pesiri, D. R.; Jorgensen, B.; Dye, R. C., *J. Membr. Sci.* **2003,** *218*, 11.
61. Kumbharkar, S. C.; Karadkar, P. B.; Kharul, U. K., *J. Membr. Sci.* **2006,** *286*, 161.
62. Sadeghi, M.; Semsarzadeh, M. A.; Moadel, H., *J. Membr. Sci.* **2009,** *331*, 21.
63. Kumbharkar, S. C.; Kharul, U. K., *J. Membr. Sci.* **2010,** *357*, 134.
64. Ghosal, K.; Freeman, B. D.; Chern, R. T.; Alvarez, J. C.; de la Campa, J. G.; de Abajo, J., *Polymer* **1995,** *36*, 793.
65. Morisato, A.; Ghosal, K.; Freeman, B. D.; Chern, R. T.; Alvarez, J. C.; de la Campa, J. G.; Lozano, A. E.; de Abajo, J., *J. Membr. Sci.* **1995,** *104*, 231.

66. Singh, A.; Ghosal, K.; Freeman, B. D.; Lozano, A. E.; De la Campa, J. G.; De Abajo, J., *Polymer* **1999,** *40*, 5715.
67. Huang, S. H.; Hu, C. C.; Lee, K. R.; Liaw, D. J.; Lai, J. Y., *Eur. Polym. J.* **2005,** *42*, 140.
68. Espeso, J.; Lozano, A. E.; de la Campa, J. G.; de Abajo, J., *J. Membr. Sci.* **2006,** *280*, 659.
69. Bower, G. M.; Frost, L. W., *J. Polym. Sci.* **1963,** *1*, 3135.
70. Krizan Timothy, D.; Coburn John, C.; Blatz Philip, S., Structure of Amorphous Polyamides. In *Barrier Polymers and Structures*, American Chemical Society, 1990; Vol. 423, pp 111-125.
71. Klaehn, J. R.; Orme, C. J.; Peterson, E. S.; Stewart, F. F.; Urban-Klaehn, J. M., *Membr. Sci. Technol. Ser.* **2011,** *14*, 295.
72. Berchtold, K. A.; Singh, R. P.; Young, J. S.; Dudeck, K. W., *J. Membr. Sci.* **2012,** *415-416*, 265.
73. Kawakami, H.; Mikawa, M.; Nagaoka, S., *J. Membr. Sci.* **1996,** *118*, 223.
74. Qiu, W.; Xu, L.; Chen, C.C.; Paul, D. R.; Koros, W. J., *Polymer* **2013,** *54*, 6226.
75. Tanaka, K.; Kita, H.; Okano, M.; Okamoto, K. i., *Polymer* **1992,** *33*, 585.
76. Budd, P. M.; Msayib, K. J.; Tattershall, C. E.; Ghanem, B. S.; Reynolds, K. J.; McKeown, N. B.; Fritsch, D., *J. Membr. Sci.* **2005,** *251*, 263.
77. Baker, R. W.; Lokhandwala, K., *Ind. Eng. Chem. Res.* **2008,** *47*, 2109.
78. Bernardo, P.; Drioli, E.; Golemme, G., *Ind. Eng. Chem. Res.* **2009,** *48*, 4638.
79. Du, N.; Park, H. B.; Dal-Cin, M. M.; Guiver, M. D., *Energy Environ. Sci.* **2012,** *5*, 7306.
80. Sanders, D. F.; Smith, Z. P.; Guo, R.; Robeson, L. M.; McGrath, J. E.; Paul, D. R.; Freeman, B. D., *Polymer* **2013,** *54*, 4729.
81. Park, H. B.; Jung, C. H.; Lee, Y. M.; Hill, A. J.; Pas, S. J.; Mudie, S. T.; Van Wagner, E.; Freeman, B. D.; Cookson, D. J., *Science (Washington, DC, U. S.)* **2007,** *318*, 254.
82. Sanders, D. F.; Smith, Z. P.; Ribeiro, C. P., Jr.; Guo, R.; McGrath, J. E.; Paul, D. R.; Freeman, B. D., *J. Membr. Sci.* **2012,** *409-410*, 232.
83. Wind, J. D.; Sirard, S. M.; Paul, D. R.; Green, P. F.; Johnston, K. P.; Koros, W. J., *Macromolecules* **2003,** *36*, 6433.
84. Hayes, R. A. US4717393A, **1988**.
85. Staudt-Bickel, C.; Koros, W. J., *J. Membr. Sci.* **1999,** *155*, 145.
86. Liu, Y.; Wang, R.; Chung, T. S., *J. Membr. Sci.* **2001,** *189*, 231.
87. Wind, J. D.; Staudt-Bickel, C.; Paul, D. R.; Koros, W. J., *Ind. Eng. Chem. Res.* **2002,** *41*, 6139.
88. Cao, C.; Chung, T. S.; Liu, Y.; Wang, R.; Pramoda, K. P., *J. Membr. Sci.* **2003,** *216*, 257.
89. Shao, L.; Chung, T. S.; Goh, S. H.; Pramoda, K. P., *J. Membr. Sci.* **2004,** *238*, 153.
90. Tin, P. S.; Chung, T. S.; Liu, Y.; Wang, R.; Liu, S. L.; Pramoda, K. P., *J. Membr. Sci.* **2003,** *225*, 77.
91. Wind, J. D.; Paul, D. R.; Koros, W. J., *J. Membr. Sci.* **2004,** *228*, 227.
92. Guo, R.; Sanders, D. F.; Smith, Z. P.; Freeman, B. D.; Paul, D. R.; McGrath, J. E., *J. Mater. Chem. A* **2013,** *1*, 6063.
93. Guo, R.; Sanders, D. F.; Smith, Z. P.; Freeman, B. D.; Paul, D. R.; McGrath, J. E., *J. Mater. Chem. A* **2013,** *1*, 262.
94. Yeong, Y. F.; Wang, H.; Pallathadka Pramoda, K.; Chung, T. S., *J. Membr. Sci.* **2012,** *397-398*, 51.

95. Johnson, R. N.; Farnham, A. G.; Clendinning, R. A.; Hale, W. F.; Merriam, C. N., *J. Polym. Sci., Part A-1: Polym. Chem.* **1967,** *5*, 2375.
96. Attwood, T. E.; Newton, A. B.; Rose, J. B., *Brit. Polym. J.* **1972,** *4*, 391.
97. Attwood, T. E.; Barr, D. A.; King, T.; Newton, A. B.; Rose, J. B., *Polymer* **1977,** *18*, 359.
98. Rose, J. B., *Polymer* **1974,** *15*, 456.
99. Hale, W. F.; Farnham, A. G.; Johnson, R. N.; Clendinning, R. A., *J. Polym. Sci., Part A-1: Polym. Chem.* **1967,** *5*, 2399.
100. Wang, F.; Hickner, M.; Ji, Q.; Harrison, W.; Mecham, J.; Zawodzinski, T. A.; McGrath, J. E., *Macromol. Symp.* **2001,** *175*, 387.
101. Wang, F.; Hickner, M.; Kim, Y. S.; Zawodzinski, T. A.; McGrath, J. E., *J.Membr. Sci.* **2002,** *197*, 231.
102. Gil, M.; Ji, X.; Li, X.; Na, H.; Hampsey, J. E.; Lu, Y., *J. Membr. Sci.* **2004,** *234*, 75.
103. Xing, P.; Robertson, G. P.; Guiver, M. D.; Mikhailenko, S. D.; Wang, K.; Kaliaguine, S., *J. Membr. Sci.* **2004,** *229*, 95.
104. Shang, X.; Tian, S.; Kong, L.; Meng, Y., *J. Membr. Sci.* **2005,** *266*, 94.
105. Miyatake, K.; Zhou, H.; Matsuo, T.; Uchida, H.; Watanabe, M., *Macromolecules* **2004,** *37*, 4961.
106. Yin, Y.; Suto, Y.; Sakabe, T.; Chen, S.; Hayashi, S.; Mishima, T.; Yamada, O.; Tanaka, K.; Kita, H.; Okamoto, K. I., *Macromolecules* **2006,** *39*, 1189.
107. Sankir, M.; Kim, Y. S.; Pivovar, B. S.; McGrath, J. E., *J. Membr. Sci.* **2007,** *299*, 8.
108. Kim, D. S.; Kim, Y. S.; Guiver, M. D.; Pivovar, B. S., *J. Membr. Sci.* **2008,** *321*, 199.
109. Gao, Y.; Robertson, G. P.; Guiver, M. D.; Mikhailenko, S. D.; Li, X.; Kaliaguine, S., *Macromolecules* **2005,** *38*, 3237.
110. Gao, Y.; Robertson, G. P.; Guiver, M. D.; Mikhailenko, S. D.; Li, X.; Kaliaguine, S., *Polymer* **2006,** *47*, 808.
111. Fujimoto, C. H.; Hickner, M. A.; Cornelius, C. J.; Loy, D. A., *Macromolecules* **2005,** *38*, 5010.
112. Noshay, A.; Robeson, L. M., *J. Appl. Polym. Sci.* **1976,** *20*, 1885.
113. Quentin, J. P. DE2021383B2, **1979**.
114. Kerres, J.; Cui, W.; Reichle, S., *J. Polym. Sci., Part A: Polym. Chem.* **1996,** *34*, 2421.
115. Karlsson, L.; Jannasch, P., *J. Membr. Sci.* **2004,** *230*, 61.
116. Robeson, L. M.; Matzner, M. EP58403A2, **1982**.
117. Ueda, M.; Toyota, H.; Ouchi, T.; Sugiyama, J.; Yonetake, K.; Masuko, T.; Teramoto, T., *J. Polym. Sci., Part A: Polym. Chem.* **1993,** *31*, 853.
118. Li, Y.; VanHouten, R. A.; Brink, A. E.; McGrath, J. E., *Polymer* **2008,** *49*, 3014.
119. Takamuku, S.; Jannasch, P., *Polymer Chemistry* **2012,** *3*, 1202.
120. Harrison, W. L.; Hickner, M. A.; Kim, Y. S.; McGrath, J. E., *Fuel Cells* **2005,** *5*, 201.
121. Kim, Y. S.; Sumner, M. J.; Harrison, W. L.; Riffle, J. S.; McGrath, J. E.; Pivovar, B. S., *J. Electrochem. Soc.* **2004,** *151*, A2150.
122. Chen, Y.; Rowlett, J. R.; Lee, C. H.; Lane, O. R.; VanHouten, D. J.; Zhang, M.; Moore, R. B.; McGrath, J. E., *J. Polym. Sci. Part A Polym. Chem.* **2013,** *51*, 2301.
123. Roy, A.; Hickner, M. A.; Yu, X.; Li, Y.; Glass, T. E.; McGrath, J. E., *J. Polym. Sci. Part B: Polym. Phys.* **2006,** *44*, 2226.
124. Matsumoto, K.; Higashihara, T.; Ueda, M., *J. Polym. Sci. Part A Polym. Chem.* **2009,** *47*, 3444.
125. Lee, J.; Marvel, C. S., *J. Polym. Sci., Polym. Chem. Ed.* **1984,** *22*, 295.

126. Litter, M. I.; Marvel, C. S., *J. Polym. Sci., Polym. Chem. Ed.* **1985,** *23*, 2205.
127. Ogawa, T.; Marvel, C. S., *J. Polym. Sci., Polym. Chem. Ed.* **1985,** *23*, 1231.
128. Gao, Y.; Robertson, G. P.; Guiver, M. D.; Jian, X.; Mikhailenko, S. D.; Wang, K.; Kaliaguine, S., *J. Polym. Sci., Part A: Polym. Chem.* **2003,** *41*, 2731.
129. Gao, Y.; Robertson, G. P.; Guiver, M. D.; Mikhailenko, S. D.; Li, X.; Kaliaguine, S., *Macromolecules* **2004,** *37*, 6748.
130. Liu, B.; Kim, D. S.; Murphy, J.; Robertson, G. P.; Guiver, M. D.; Mikhailenko, S.; Kaliaguine, S.; Sun, Y. M.; Liu, Y. L.; Lai, J. Y., *J. Membr. Sci.* **2006,** *280*, 54.
131. Robertson, G. P.; Mikhailenko, S. D.; Wang, K.; Xing, P.; Guiver, M. D.; Kaliaguine, S., *J. Membr. Sci.* **2003,** *219*, 113.
132. Miyatake, K.; Zhou, H.; Watanabe, M., *Macromolecules* **2004,** *37*, 4956.
133. Child, A. D.; Reynolds, J. R., *Macromolecules* **1994,** *27*, 1975.
134. Wallow, T. I.; Novak, B. M., *J. Am. Chem. Soc.* **1991,** *113*, 7411.
135. Ogato, N.; Rikukawa, M. WO9424717A1, **1994**.
136. Seesukphronrarak, S.; Ohira, K.; Kidena, K.; Takimoto, N.; Kuroda, C. S.; Ohira, A., *Polymer* **2010,** *51*, 623.
137. Essafi, W.; Gebel, G.; Mercier, R., *Macromolecules* **2004,** *37*, 1431.
138. Guo, X.; Fang, J.; Watari, T.; Tanaka, K.; Kita, H.; Okamoto, K. i., *Macromolecules* **2002,** *35*, 6707.
139. Geniesa, C.; Merciera, R.; Silliona, B.; Cornetb, N.; Gebelb, G.; Pineric, M., *Polymer* **2001,** *42*, 359.
140. Piroux, F.; Espuche, E.; Mercier, R.; Pinéri, M., *J. Membr. Sci.* **2003,** *223*, 127.
141. Einsla, B. R.; Kim, Y. S.; Hickner, M. A.; Hong, Y.T.; Hill, M. L.; Pivovar, B. S.; McGrath, J. E., *J. Membr. Sci.* **2005,** *255*, 141.
142. Toi, K.; Morel, G.; Paul, D. R., *J. Appl. Polym. Sci.* **1982,** *27*, 2997.
143. Chern, R. T.; Sheu, F. R.; Jia, L.; Stannett, V. T.; Hopfenberg, H. B., *J. Membr. Sci.* **1987,** *35*, 103.
144. Chern, R. T.; Jia, L.; Shimoda, S.; Hopfenberg, H. B., *J. Membr. Sci.* **1990,** *48*, 333.
145. Erb, A. J.; Paul, D. R., *J. Membr. Sci.* **1981,** *8*, 11.
146. McHattie, J. S.; Koros, W. J.; Paul, D. R., *Polymer* **1991,** *32*, 2618.
147. Ghosal, K.; Chern, R. T.; Freeman, B. D.; Daly, W. H.; Negulescu, I. I., *Macromolecules* **1996,** *29*, 4360.
148. Wang, Z. Y.; Moulinie, P. R.; Handa, Y. P., *J. Polym. Sci., Part B: Polym. Phys.* **1998,** *36*, 425.
149. García, C.; Tiemblo, P.; Lozano, A. E.; de Abajo, J.; de la Campa, J. G., *J. Membr. Sci.* **2002,** *205*, 73.
150. Baker, R. W., *Ind. Eng. Chem. Res.* **2002,** *41*, 1393.
151. Hay, A. S.; Blanchard, H. S.; Endres, G. F.; Eustance, J. W., *J. Am. Chem. Soc.* **1959,** *81*, 6335.
152. Hay, A. S., *J. Polym. Sci.* **1962,** *58*, 581.
153. Finkbeiner, H.; Hay, A. S.; Blanchard, H. S.; Endres, G. F., *J. Org. Chem.* **1966,** *31*, 549.
154. Hay, A. S., *J. Polym. Sci., Part A: Polym. Chem.* **1998,** *36*, 505.
155. Hay, A. S., *Prog. Polym. Sci.* **1999,** *24*, 45.
156. Handa, Y. P.; Roovers, J.; Moulinie, P., *J. Polym. Sci., Part B: Polym. Phys.* **1997,** *35*, 2355.
157. Aitken, C. L.; Koros, W. J.; Paul, D. R., *Macromolecules* **1992,** *25*, 3424.

158. McHattie, J. S.; Koros, W. J.; Paul, D. R., *Polymer* **1992,** *33*, 1701.
159. Aguilar-Vega, M.; Paul, D. R., *J. Polym. Sci., Part B: Polym. Phys.* **1993,** *31*, 1577.
160. Story, B. J.; Koros, W. J., *J. Appl. Polym. Sci.* **1991,** *42*, 2613.
161. Ghosal, K.; Chern, R. T., *J. Membr. Sci.* **1992,** *72*, 91.
162. Story, B. J.; Koros, W. J., *J. Membr. Sci.* **1992,** *67*, 191.
163. Zhang, J.; Hou, X., *J. Membr. Sci.* **1994,** *97*, 275.
164. Ghosal, K.; Chern, R. T.; Freeman, B. D.; Savariar, R., *J. Polym. Sci., Part B: Polym. Phys.* **1995,** *33*, 657.
165. Kim, I. W.; Lee, K. J.; Jho, J. Y.; Park, H. C.; Won, J.; Kang, Y. S.; Guiver, M. D.; Robertson, G. P.; Dai, Y., *Macromolecules* **2001,** *34*, 2908.
166. Dai, Y.; Guiver, M. D.; Robertson, G. P.; Kang, Y. S.; Lee, K. J., *Macromolecules* **2003,** *36*, 6807.
167. Dai, Y.; Guiver, M. D.; Robertson, G. P.; Kang, Y. S.; Lee, K. J.; Jho, J. Y., *Macromolecules* **2004,** *37*, 1403.
168. Hamad, F.; Khulbe, K. C.; Matsuura, T., *Desalination* **2002,** *148*, 369.
169. Lee, C. H.; Park, H. B.; Chung, Y. S.; Lee, Y. M.; Freeman, B. D., *Macromolecules* **2006,** *39*, 755.
170. Mikhailenko, S. D.; Wang, K.; Kaliaguine, S.; Xing, P.; Robertson, G. P.; Guiver, M. D., *J. Membr. Sci.* **2004,** *233*, 93.
171. Paul, M.; Park, H. B.; Freeman, B. D.; Roy, A.; McGrath, J. E.; Riffle, J. S., *Polymer* **2008,** *49*, 2243.
172. Lee, K. S.; Jeong, M. H.; Lee, J. P.; Lee, J. S., *Macromolecules* **2009,** *42*, 584.
173. Lee, K. S.; Jeong, M. H.; Lee, J. P.; Kim, Y. J.; Lee, J. S., *Chemistry of Materials* **2010,** *22*, 5500.
174. Ye, Y. S.; Yen, Y. C.; Cheng, C. C.; Chen, W. Y.; Tsai, L. T.; Chang, F. C., *Polymer* **2009,** *50*, 3196.
175. Paul, M.; Roy, A.; Riffle, J. S.; McGrath, J. E., *ECS Transactions* **2008,** *6*, 9.
176. Li, N.; Wang, C.; Lee, S. Y.; Park, C. H.; Lee, Y. M.; Guiver, M. D., *Angew. Chem. Int. Ed. Engl.* **2011,** *50*, 9158.
177. Ingratta, M.; Jutemar, E. P.; Jannasch, P., *Macromolecules* **2011,** *44*, 2074.
178. Norsten, T. B.; Guiver, M. D.; Murphy, J.; Astill, T.; Navessin, T.; Holdcroft, S.; Frankamp, B. L.; Rotello, V. M.; Ding, J., *Adv. Funct. Mater.* **2006,** *16*, 1814.
179. Kim, D. S.; Kim, Y. S.; Guiver, M. D.; Ding, J.; Pivovar, B. S., *J. Power Sources* **2008,** *182*, 100.
180. Ingratta, M.; Elomaa, M.; Jannasch, P., *Polym. Chem.* **2010,** *1*, 739.
181. Wang, L.; Wang, D.; Zhu, G.; Li, J., *Eur. Polym. J.* **2011**.
182. Kim, H. K.; Zhang, M.; Yuan, X.; Lvov, S. N.; Chung, T. C. M., *Macromolecules* **2012,** *45*, 2460.
183. Holladay, H. P.; Malon, R. F.; Zampini, A. EP107636A1, **1984**.
184. Zampini, A.; Malon, R. F. US4468503A, **1984**.
185. Malon, R. F.; Zampini, A. EP130963A1, **1985**.
186. Yamada, S.; Shiro, K. EP256530A2, **1988**.
187. Wright, C. T.; Paul, D. R., *J. Appl. Polym. Sci.* **1998,** *67*, 875.
188. Nagai, K., *Kobunshi Ronbunshu* **2003,** *60*, 468.
189. Wright, C. T.; Paul, D. R., *J. Membr. Sci.* **1997,** *124*, 161.
190. Wright, C. T.; Paul, D. R., *J. Membr. Sci.* **1997,** *129*, 47.

191. McCaig, M. S.; Paul, D. R., *Polymer* **1999,** *40*, 7209.
192. Elabd, Y. A.; Hickner, M. A., *Macromolecules* **2011,** *44*, 1.
193. Bates, F. S.; Fredrickson, G. H., *Phys. Today* **1999,** *52*, 32.
194. Edmondson, C. A.; Fontanella, J. J.; Chung, S. H.; Greenbaum, S. G.; Wnek, G. E., *Electrochim. Acta* **2001,** *46*, 1623.
195. Kim, J.; Kim, B.; Jung, B., *J. Membr. Sci.* **2002,** *207*, 129.
196. Kim, J.; Kim, B.; Jung, B.; Kang, Y. S.; Ha, H. Y.; Oh, I. H.; Ihn, K. J., *Macromol. Rapid Comm.* **2002,** *23*, 753.
197. Elabd, Y. A.; Napadensky, E.; Sloan, J. M.; Crawford, D. M.; Walker, C. W., *J. Membr. Sci.* **2003,** *217*, 227.
198. Elabd, Y. A.; Walker, C. W.; Beyer, F. L., *J. Membr. Sci.* **2004,** *231*, 181.
199. Suleiman, D.; Elabd, Y. A.; Napadensky, E.; Sloan, J. M.; Crawford, D. M., *Thermochimica Acta* **2005,** *430*, 149.
200. Elabd, Y. A.; Napadensky, E.; Walker, C. W.; Winey, K. I., *Macromolecules* **2006,** *39*, 399.
201. Yang, Y.; Shi, Z.; Holdcroft, S., *Macromolecules* **2004,** *37*, 1678.
202. Chen, L.; Hallinan, D. T.; Elabd, Y. A.; Hillmyer, M. A., *Macromolecules* **2009,** *42*, 6075.
203. Xu, K.; Li, K.; Khanchaitit, P.; Wang, Q., *Chem. Mater.* **2007,** *19*, 5937.
204. Moore, H. D.; Saito, T.; Hickner, M. A., *J. Mater.Chem.* **2010,** *20*, 6316.
205. Saito, T.; Moore, H. D.; Hickner, M. A., *Macromolecules* **2010,** *43*, 599.
206. Shi, Z.; Holdcroft, S., *Macromolecules* **2005,** *38*, 4193.
207. Maier, G.; Meier-Haack, J., *Adv. Polym. Sci.* **2008,** *216*, 1.
208. Ghassemi, H.; McGrath, J. E.; Zawodzinski, T. A., *Polymer* **2006,** *47*, 4132.
209. Lee, H. S.; Roy, A.; Lane, O.; Dunn, S.; McGrath, J. E., *Polymer* **2008,** *49*, 715.
210. Lee, H. S.; Roy, A.; Badami, A. S.; McGrath, J. E., *Macromol. Res.* **2007,** *15*, 160.
211. Nakabayashi, K.; Matsumoto, K.; Ueda, M., *J. Polym. Sci. Part A Polym. Chem.* **2008,** *46*, 3947.
212. Lee, M.; Park, J. K.; Lee, H. S.; Lane, O.; Moore, R. B.; McGrath, J. E.; Baird, D. G., *Polymer* **2009,** *50*, 6129.
213. Nakabayashi, K.; Matsumoto, K.; Higashihara, T.; Ueda, M., *J. Polym. Sci. Part A Polym. Chem.* **2008,** *46*, 7332.
214. Li, N.; Lee, S. Y.; Liu, Y. L.; Lee, Y. M.; Guiver, M. D., *Energy & Environmental Sci.* **2012,** *5*, 5346.
215. Chen, Y.; Guo, R.; Lee, C. H.; Lee, M.; McGrath, J. E., *Int. J. Hydrogen Energy* **2012,** *37*, 6132.
216. Chen, Y.; Lee, C. H.; Rowlett, J. R.; McGrath, J. E., *Polymer* **2012,** *53*, 3143.
217. Roy, A.; Yu, X.; Dunn, S.; McGrath, J. E., *J. Membr. Sci.* **2009,** *327*, 118.
218. Bae, B.; Miyatake, K.; Watanabe, M., *Macromolecules* **2010,** *43*, 2684.
219. Li, N.; Liu, J.; Cui, Z.; Zhang, S.; Xing, W., *Polymer* **2009,** *50*, 4505.
220. Lee, H. S.; Lane, O.; McGrath, J. E., *J. Power Sources* **2010,** *195*, 1772.
221. Zhao, C.; Li, X.; Wang, Z.; Dou, Z.; Zhong, S.; Na, H., *J. Membr. Sci.* **2006,** *280*, 643.
222. Goto, K.; Rozhanskii, I.; Yamakawa, Y.; Otsuki, T.; Naito, Y., *Polym. J. (Tokyo, Jpn.)* **2009,** *41*, 95.
223. Cho, C. G.; Kim, Y. S.; Yu, X.; Hill, M.; McGrath, J. E., *J. Polym. Sci. Part A Polym. Chem.* **2006,** *44*, 6007.

224. Sethuraman, V. A.; Weidner, J. W.; Haug, A. T.; Protsailo, L. V., *J. Electrochem. Soc.* **2008,** *155*, B119.
225. Lee, H. S.; Badami, A. S.; Roy, A.; McGrath, J. E., *J. Polym. Sci., Part A: Polym. Chem.* **2007,** *45*, 4879.
226. Nakabayashi, K.; Matsumoto, K.; Higashihara, T.; Ueda, M., *Polym. J.* **2009,** *41*, 332.
227. Roy, A.; Hickner, M. A.; Yu, X.; Li, Y.; Glass, T. E.; McGrath, J. E., *J. Polym. Sci., Part B: Polym. Phys.* **2006,** *44*, 2226.
228. Wiles, K. B.; De, D. C. M.; De, A. J.; McGrath, J. E., *J. Membr. Sci.* **2007,** *294*, 22.
229. Springer, T. E.; Zawodzinski, T. A.; Wilson, M. S.; Gottesfeld, S., *J. Electrochem. Soc.* **1996,** *143*, 587.
230. Bae, B.; Miyatake, K.; Watanabe, M., *Macromolecules (Washington, DC, U. S.)* **2009,** *42*, 1873.
231. Park, C. H.; Lee, C. H.; Guiver, M. D.; Lee, Y. M., *Progress in Polymer Science* **2011,** *36*, 1443.
232. Dupuis, A. C., *Prog. Mater. Sci.* **2011,** *56*, 289.
233. Dobrovolsky, Y. A.; Jannasch, P.; Lafitte, B.; Belomoina, N. M.; Rusanov, A. L.; Likhachev, D. Y., *Russ. J. Electrochem.* **2007,** *43*, 489.
234. Kreuer, K. D., *J. Membr. Sci.* **2001,** *185*, 29.
235. Sumner, M. J.; Harrison, W. L.; Weyers, R. M.; Kim, Y. S.; McGrath, J. E.; Riffle, J. S.; Brink, A.; Brink, M. H., *J. Membr. Sci.* **2004,** *239*, 199.
236. Gao, Y.; Robertson, G. P.; Guiver, M. D.; Wang, G.; Jian, X.; Mikhailenko, S. D.; Li, X.; Kaliaguine, S., *J. Membr. Sci.* **2006,** *278*, 26.
237. Kim, Y. S.; Pivovar, B. S., *Ann. Rev. Chem. Biomol. Eng.* **2010,** *1*, 123.
238. Kim, Y. S.; Pivovar, B. S., *J. Electrochem. Soc.* **2010,** *157*, B1616.
239. Harrison, W. L.; Hickner, M. A.; Kim, Y. S.; McGrath, J. E., *Fuel Cells* **2005,** *5*, 201.
240. Fu, Y. Z.; Manthiram, A., *J. Power Sources* **2006,** *157*, 222.
241. Lee, C. H.; Park, H. B.; Lee, Y. M.; Lee, R. D., *Ind. Eng. Chem. Res.* **2005,** *44*, 7617.
242. Carothers, W. H., *Trans. Faraday Soc.* **1936,** *32*, 39.
243. Kim, Y. S.; Einsla, B.; Sankir, M.; Harrison, W.; Pivovar, B. S., *Polymer* **2006,** *47*, 4026.
244. Semenov, A. N., *Sov. Phys. JETP* **1985,** *61*, 733.
245. Kim, S.; Nealey, P. F.; Bates, F. S., *ACS Macro Lett.* **2012,** *1*, 11.
246. Kim, S.; Liu, J., *Korea Polym. J.* **2001,** *9*, 129.
247. Aharoni, S. M., *Macromolecules* **1983,** *16*, 1722.
248. Alentiev, A.; Drioli, E.; Gokzhaev, M.; Golemme, G.; Ilinich, O.; Lapkin, A.; Volkov, V.; Yampolskii, Y., *J. Membr. Sci.* **1998,** *138*, 99.
249. Sridhar, S.; Smitha, B.; Ramakrishna, M.; Aminabhavi, T. M., *J. Membr. Sci.* **2006,** *280*, 202.
250. Clark, R. F.; Krantz, K. W. US3696137A, **1972**.
251. Krijgsman, J.; Feijen, J.; Gaymans, R. J., *Polymer* **2004,** *45*, 4677.
252. Kuo, S. W.; Huang, C. F.; Tung, P. H.; Huang, W. J.; Huang, J. M.; Chang, F. C., *Polymer* **2005,** *46*, 9348.
253. Van, A. H. A. M.; Venderbosch, R. W.; Van, G. M. H. P.; Lemstra, P. J.; Meijer, E. W., *J. Macromol. Sci., Pure Appl. Chem.* **1995,** *A32*, 515.
254. Heitz, W.; Risse, W. DE3340493A1, **1985**.
255. Risse, W.; Heitz, W.; Freitag, D.; Bottenbruch, L., *Makromol. Chem.* **1985,** *186*, 1835.
256. Percec, V. US4665137A, **1987**.

257. White, D. M., *J. Polym. Sci., Polym. Chem. Ed.* **1981,** *19*, 1367.
258. Tran, A.; Kruczek, B., *J. Appl. Polym. Sci.* **2007,** *106*, 2140.
259. Gajbhiye, S. B., *J. Appl. Polym. Sci.* **2013,** *127*, 2497.
260. Lin, H. Q.; Freeman, B. D., Permeation and diffusion. In *Handbook for Materials Measurements Methods*, Czichos, H.; Saito, T.; Smith, L. E., (Eds). Springer 2011.
261. Wang, F.; Sylvia, J. M.; Jacob, M. M.; Peramunage, D., *J. Power Sources* **2013,** *242*, 575.
262. Guillet, J., *Polymer photophysics and photochemistry: An introduction to the study of photoprocesses in macromolecules*. Cambridge University Press: 1985.
263. Vu, D. Q.; Koros, W. J.; Miller, S. J., *J. Membr. Sci.* **2003,** *211*, 311.
264. Robeson, L. M.; Hwu, H. H.; McGrath, J. E., *J. Membr. Sci.* **2007,** *302*, 70.
265. Park, H. B.; Freeman, B. D.; Zhang, Z. B.; Sankir, M.; McGrath, J. E., *Angew. Chem., Int. Ed.* **2008,** *47*, 6019.
266. Rowlett, J. R.; Chen, Y.; Shaver, A. T.; Lane, O.; Mittelsteadt, C.; Xu, H.; Zhang, M.; Moore, R. B.; Mecham, S.; McGrath, J. E., *Polymer* **2013,** *54*, 6305.
267. Li, Q.; Chen, Y.; Rowlett, J. R.; McGrath, J. E.; Mack, N. H.; Kim, Y. S., *ACS Appl. Mater. Interfaces* **2014,** *6*, 5779.
268. Jonsson, M.; Lind, J.; Merenyi, G., *J. Phys. Chem. A* **2002,** *106*, 4758.